Modulation of T-cell alloreactivity by molecular and biochemical effects of HLA-DPB1 in haematopoietic stem cell transplantation

Inaugural-Dissertation

zur

Erlangung des Doktorgrades

Dr. rer. nat.

der Fakultät für

Biologie an der

Universität Duisburg-Essen

vorgelegt von

Thuja Meurer

aus Düsseldorf

April 2020

Die der vorliegenden Arbeit zugrundeliegenden Experimente wurden am Institut für Zelltherapeutische Forschung des Universitätsklinikums Essen durchgeführt.

1. Gutachter: Prof.‘in Dr. Katharina Fleischhauer

2. Gutachter: Prof.‘in Dr. Monika Lindemann

3. Gutachter: Prof. Dr. Johannes Schetelig

Vorsitzender des Prüfungsausschusses: Prof. Dr. Stefan Westermann

Tag der mündlichen Prüfung: 17.07.2020

DOI: 10.17185/duepublico/72357
URN: urn:nbn:de:hbz:464-20210420-111551-5

Table of contents

1. Preface

The herein presented thesis consists of a selection of two published original articles and one submitted original article.

The work presented in this thesis was carried out between December 2016 and March 2020 and was supervised by Prof. Dr. Katharina Fleischhauer at the Institute of Experimental Cellular Therapy, University Hospital Essen.

2. Zusammenfassung

Das human Leukozytenantigen (HLA)-DP gehört zu den HLA Klasse-II-Antigenen und ist Angriffspunkt für eine T-Zell-Alloreaktivität in der hämatopoetischen Stammzelltransplantation (HSZT). Geringere Toxizität und ein verbessertes klinisches Ergebnis sind assoziiert mit limitierter T-Zell-Alloreaktivität gegen gut verträgliche (permissive) Kombinationen von HLA-DP Diskrepanzen zwischen Spender und Empfänger. Zwei gegenwärtige Modelle für HLA-DP Permissivität basieren auf strukturellen Differenzen, beziehungsweise auf unterschiedlichen Expressionsniveaus. Jedoch ist die biologische Grundlage beider Modelle sowie deren Zusammenhang nicht aufgeklärt. Diese Promotionsarbeit soll Aufschluss zu dieser Fragestellung geben anhand folgender vier spezifischer Zielesetzungen:

1) die Aufgliederung der zugrundeliegenden Mechanismen für die genetische Kontrolle der HLA-DP Expression und deren Verbindung zu strukturellen Polymorphismen
2) die Auswirkungen struktureller Polymorphismen zwischen körpereigenen und allogenen HLA-DP Antigene auf das Repertoire alloreaktiver T-Zell Rezeptoren (TZR)
3) die Untersuchung der Funktion von strukturellen Polymorphismen und des Peptid-Editors HLA-DM bezüglich seiner Funktion in der Anpassung des von HLA-DP präsentiertem Peptidrepertoires
4) die Bestimmung, inwieweit das Ausmaß der Peptiddivergenz zwischen körpereigener und allogener HLA-DP Antigene sich auf die T-Zell-Alloreaktivität auswirkt

Diese Ziele wurden mit Hilfe molekularer und biochemischer Untersuchungen der HLA-DP Expression in Zelllinien und primären Immunzellen, mit Hilfe von *Next Generation Sequening* des TZRs, durch die Analyse des Immunopeptidomes von HLA-DP mittels Tandem-Massenspektrometrie und durch die quantitative Charakterisierung der T-Zell-Alloreaktivität zu HLA-DP *in vitro* von gesunden Spendern und *ex vivo* von Patienten nach HSZT verfolgt. Die Ergebnisse zeigen, dass die genetische Kontrolle von HLA-DP Expression zwar in B-Zellen besteht, jedoch diese in anderen Zelltypen einschließlich Antigen präsentierenden Zellen nicht gezeigt werden. Unterschiedliche T-Zell-Alloreaktivitätsniveaus gegen strukturell HLA-DP-Varianten wurden unabhängig von Expressionsniveaus beobachtet (**Meurer, 2018**) und waren mit hohem Maß an TZR Diversität (**Arrieta-**

Bolanos, 2018) assoziiert. Dagegen war die T-Zell-Alloreaktivität limitiert durch das Ausmaß der Peptidabweichung zwischen körpereigenem und allogenem HLA-DP, welches wiederum abhängig von strukturellen Polymorphismen und der Aktivität des Peptid-Editors HLA-DM war. Diese Mechanismen schienen auch auf HSZT Patienten zuzutreffen (**Meurer, eingereichtes Manuskript**). Zusammenfassend konnte das Immunopeptidom und seine Regulierung durch Peptid-Editor HLA-DM als zentraler Regulator von T-Zell-Alloreaktivität zu HLA-DP in HSZT identifiziert werden. Folglich suggerieren die gemachten Beobachtungen, dass strukturelle Diversität die Basis für die HLA-DP Permissivität ist, die jedoch auch durch unterschiedliche Expressionsniveaus beeinflusst werden könnten. Diese Ergebnisse sind von potenzieller Bedeutung für die Modelle der HLA Permissivität in der klinischen Transplantation und suggerieren den Einsatz der gezielten Regulierung des Immunopeptidoms, beispielsweise durch HLA-DM, in der Zelltherapie.

3. Summary

Human leukocyte antigen (HLA)-DP is an HLA class II molecule target of T-cell alloreactivity in haematopoietic stem cell transplantation (HSCT). Reduced toxicity and improved clinical outcome are associated with limited T-cell alloreactivity to well-tolerated (permissive) donor-recipient HLA-DP mismatch combinations. Two current models for HLA-DP permissiveness are based on structural differences or differential expression levels, respectively. However, the biological basis of both models, and the relation between them, is still elusive. This thesis attempts to shed light onto this question, with the following four specific aims. 1) To dissect the mechanisms underlying genetic control of HLA-DP expression and its relation to structural polymorphisms. 2) To elucidate the effects of structural polymorphism between self and allogeneic HLA-DP on the alloreactive T-cell receptor (TCR) repertoire. 3) To investigate the role of structural polymorphism and the peptide editor HLA-DM in shaping the peptide repertoire presented by HLA-DP molecules. 4) To establish how the degree of peptide divergence between self and allogeneic HLA-DP impacts T-cell alloreactivity. These aims were pursued by molecular and biochemical investigation of HLA-DP expression in established cell lines and primary immune cells, by next generation TCR sequencing, by analysis of the HLA-DP immunopeptidome in tandem mass spectrometry, and by quantitative characterization of T-cell alloreactivity to HLA-DP *in vitro* in healthy donors and *ex vivo* in patients after HSCT. The results show that while genetic control of HLA-DP expression could be confirmed in B cells but not in other cell types including professional antigen presenting cells, differential levels of T-cell alloreactivity to structural HLA-DP variants were observed independently from expression levels (**Meurer, 2018**), and were associated with high degrees of TCR diversity (**Arrieta-Bolanos, 2018**). In contrast, T-cell alloreactivity was limited by the degree of peptide divergence between self and allogeneic HLA-DP, which in turn was dependent on structural polymorphism and on the activity of the peptide editor HLA-DM. These mechanisms appeared to be operative also in HSCT patients (**Meurer, under submission**). Taken together, these data establish the immunopeptidome, and its modulation by the peptide editor HLA-DM, as key regulator of T-cell alloreactivity to HLA-DP in HSCT. Thus, the observations suggest structural diversity as the basis for HLA-DP permissiveness, which might however be modulated by differential expression levels. These findings have potential implications for models of HLA permissiveness in clinical transplantation and suggest that immunopeptidome modulation for instance by specific targeting of HLA-DM might be exploited in cellular therapy.

4. Introduction

4.1. Human Leukocyte Antigen

4.1.1. History

HLA was first described in 1958 independently by Jean Dausset, Jon van Rood and Rose Payne. They discovered antibodies in the human serum that agglutinated with leukocytes from patients with multiple transfusions or multiparous women[1-3]. Target of these antibodies was the polymorphic HLA, first called 'MAC' (the initials of volunteers participating in the experiments), which is nowadays known as HLA-A2[1]. In 1980, Dausset (together with Snell and Benacerraf) received the Nobel Prize for physiology or medicine for his discovery of HLA[4]. Prior to that also, van Rood and Payne pursue their findings and were able to detect a diallelic system of HLA. Van Rood discovered HLA-4a (HLA-Bw4) and -4b (HLA-Bw6) by screening sera from multiparous women against donor leukocytes resulting in a number of similar agglutination patterns[5]. As well, Payne together with Julia and Walter Bodmer detected a new leukocyte isoantigen system LA1 (HLA-A1) and LA2 (HLA-A2) by testing sera from multiparous women[6]. Little by little, more new leukocyte antigens were identified. For solving the complexity of HLA, collaboration between the different laboratories around the world was required. For this, the International Histocompatibility Workshop (IHWS) was established in 1964 organized by Bernard Amos. The IHWS was of importance to uncover the relationship, polymorphisms, and genetics of the different HLA alleles. This was feasible through exchange of knowledge, techniques, patient material, and reagents[4]. Thus, on the 6th IHWS in 1975 by exchange of Lymphocyte defined determinant homozygous typing cells, HLA-Dw1-6 was identified using mixed lymphocyte culture typing[7]. Later studies discovered that the corresponding HLA-D locus consists of three different determinants – DR, DC (later DQ) and SB (later DP). The discovery of the different HLA alleles as well as the knowledge of its structure, genetics and function is the achievement of the HLA pioneers and the international network of collaboration[4]. To date the IHWS persists, where knowledge of HLA is distributed and expanded along with new technologies.

4.1.2. HLA genetics and structure

The Major Histocompatibility complex (MHC) is the most polymorphic gene locus in humans which accounts for 26,512 HLA alleles (IMGT/HLA database, release 3.39, 2020/01)[8]. It covers around 260 genes with a length of ~4 Mbp located on the short arm of chromosome 6 (6p21.3). The nine classical HLA genes are classified into two regions HLA class I locus, containing HLA-A, -B and –C and HLA class II locus which carries genes that code for HLA-DR, - DQ and –DP. Both classical HLA classes are involved in antigen presentation. The third region class III, located between class I and class II loci, mainly comprises complement genes and a group of tumour necrosis factor genes[9]. In addition to the classical HLA genes, class I and II region comprises non-classical HLA genes with low genetic diversity. The non-classical HLA genes HLA-E, -F, -G and HFE plus HLA-class I chain related MIC-A and MIC-B, involved in immune regulation, are located in the class I region. HLA-DM as well as HLA-DO take part in the antigen processing of class II and represent the non-classical HLA genes of that region[10, 11]. The inheritance of the MHC follows the Mendelian rules, with extended haplotypes being inherited in blocks due to low recombination[12]. The vast diversity of the MHC, is ensured through the polygeny and polymorphism of the MHC and its codominant gene expression including allele heterozygosity[13].

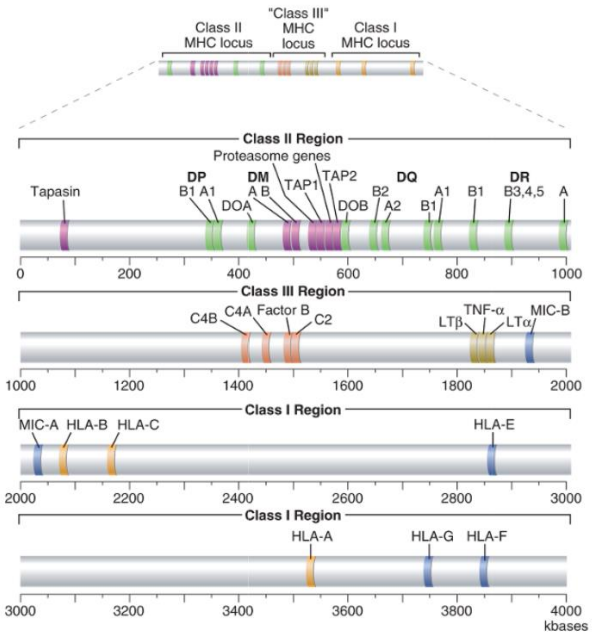

Figure 1: Map of MHC loci

Classical and Non-classical MHC genes classified into three regions: Class I, II and II region (from Abbas[14]).

The basic structure of classical HLA molecules is compared to the high variability of HLA much simpler, including many similarities between HLA class I and II. The HLA class I molecule is a heterodimer which is formed by a polymorphic α chain, and a short β2-microglobulin chain (**Figure 2A**). The 45kDa heavy α chain is MHC-encoded and composed of three hypervariable Ig-like domains. The α1 and α2 domains build up the peptide-binding groove, which accommodates peptides of 8 to 11 residues. The transmembrane region and the contact to the CD8 T cell co-receptor is assigned to the conserved α3 domain[10, 14, 15]. The α3 domain is noncovalently linked to the 12 kDa light β2-microglobulin chain. The non MHC-encoded β2 chain is not attached to the cell membrane but is able to strengthen the stability of the α chain peptide complex[14]. Unlike the class I β2 chain, the MHC class II molecule contains a polymorphic β chain attached to the cell membrane (**Figure 2B**). Similar to class I, the class II molecule is also a heterodimer. Here the heterodimer is formed by two noncovalently linked polypeptides, the α and β chain with a balanced molecular weight of about 30kDa[15]. Both chains are attached through a transmembrane region to the cell membrane and possess two domains. The α1 and β1 form together the open peptide-binding groove. Different to the closed peptide-binding groove of class I, it allows the binding of peptides with 10-30 or even more residues. The α2 and β2 domains are nonpolymorphic Ig domains, β2 domain serve as binding site for the CD4 T cell coreceptor[14].

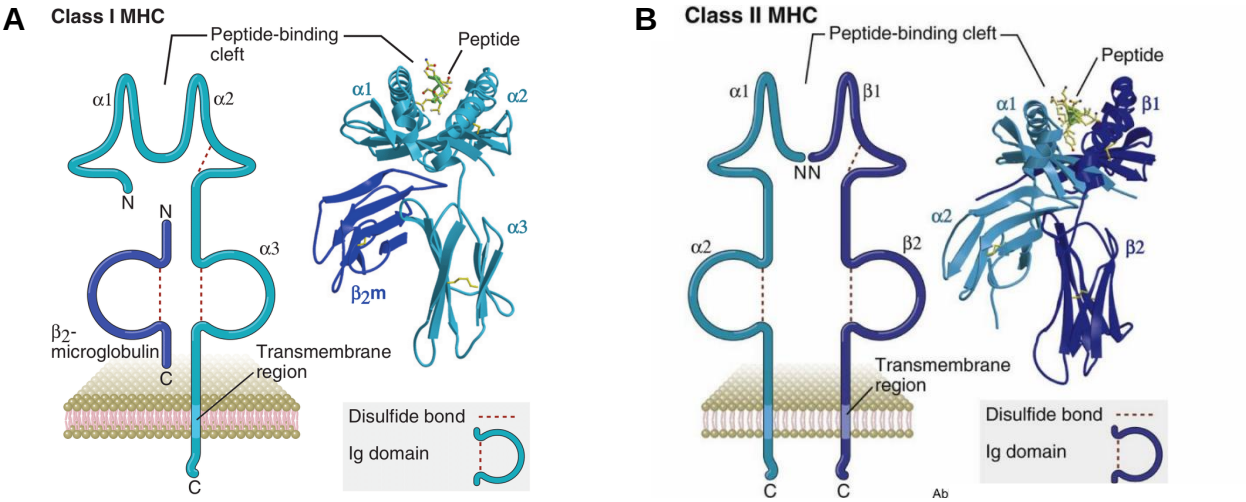

Figure 2: MHC molecule structure

Elements of the MHC molecule (A) Class I MHC structure (left). Crystallography of an HLA-B27 molecule with bound peptide (right). (B) Class II MHC structure (left). Crystallography of a HLA-DR1 molecule with bound peptide (right) (from Abbas[14]).

4.1.3. HLA antigen processing

The main function of the classical HLA class I and II is the antigen presentation to T cells that then can discriminate between self and non-self cells. Here one has to distinguish the pathway of antigen processing and presentation between HLA class I and II[16]. HLA class I molecule is expressed on all nucleated cells and presents cytosolic proteins (e.g. from viral infections or intracellular bacteria) to $CD8^+$ T cells[17]. Before the HLA is expressed on the cell surface, the presented peptide must be processed and loaded to the HLA molecule. The antigen processing pathway of HLA class I starts from a defective protein by cause of erroneous in translation or a misfolded protein (**Figure 3**). These defective proteins will then be ubiquitylated and transferred to the proteasome where the proteolysis will break them down into small fragments of 9 amino acids[18]. Subsequently the transport associated with antigen processing (TAP) complex delivers the processed peptides to the endoplasmic reticulum (ER). Here the chaperone-mediated assembly of the HLA molecule takes place. Calnexin is responsible for the right folding of the HLA α chain and ERp57 - a disulphide isomerase - mediates the binding to the β2-microglobulin chain[19]. Next, tapasin, ERp57, Calreticulin and TAP form the peptide-loading complex (PLC), which stabilizes the empty HLA molecule. Before the PLC loads the peptide to the HLA molecule, the peptide is further trimmed by endoplasmic reticulum aminopeptidase (ERAP1 and 2). Once the peptide is bound, the PLC disintegrates, and the peptide-MHC complex (pMHC) exits the ER. Finally, the Golgi complex mediated the transport to the cell surface[19, 20].

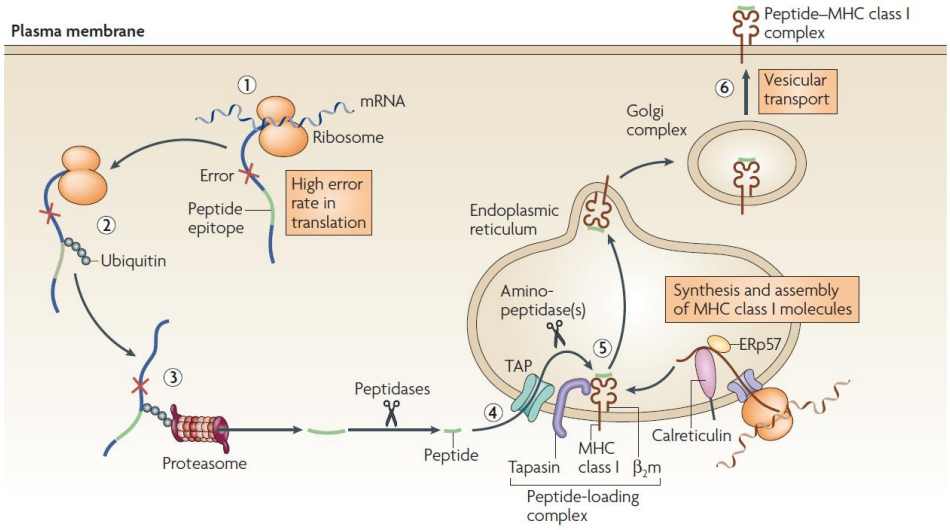

Figure 3: HLA class I pathway of antigen processing and presentation

HLA class I antigen presentation pathway in six main steps. 1) Antigen acquisition. 2) Ubiquitination. 3) Proteasome dependent proteolysis into peptides. 4) Peptide transport into the ER via TAP. 5) Peptide loading onto HLA class I molecule. 6) Cell surface expression of peptide loaded HLA (from Vyas[21]).

By reason of diverse function in adaptive immunity, HLA class I and HLA class II show different features in expression profile, antigen processing and presentation[16]. In contrast to HLA class I, HLA class II cell surface expression is restricted to some subtypes of professional antigen presenting cells (APCs) including dendritic cells, B-lymphocytes and macrophages[10]. However, under inflammatory conditions also epithelial cells and endothelial cells can express HLA class II[22, 23]. Peptides that are presented by HLA class II mostly derived from endosomal and lysosomal proteins that were internalized from the exogenous compartment. These self and non-self-derived peptides will be processed and then presented to antigen specific $CD4^+$ T cells[24]. Unlike HLA class I, the peptide loading of HLA class II does not take place in the ER, but in the late endosomal compartment, also known as MHC class II compartment (MIIC)[25]. Afore in the ER, the binding of the invariant chain (Ii), a non-polymorphic protein, to the newly synthesized HLA class II molecule takes place (**Figure 4**). The Ii not only facilitates folding of the HLA class II molecule, its binding also blocks the peptide-binding groove hence no premature peptides are able to bind[14, 26]. Besides, it is required for the trafficking through the Golgi into the late endosomal compartment. At the plasma membrane, the HLA-Ii complex is internalized by clathrin-mediated endocytosis[27]. From the early endosome the HLA-Ii complex enters the MIIC compartment. Here proteolytic degradation takes place, the result is a small fragment named class II-associated Ii chain peptide (CLIP) which is bound to the peptide-binding groove of the proteolysis resistant HLA molecule[26]. Before antigenic peptides can be loaded, the removal of CLIP is required. This process is facilitate through the chaperone HLA-DM, a HLA class II like protein, which stabilized the empty HLA molecule and allows only the binding of high affinity peptides[26, 28]. HLA-DM is expressed on a broad spectrum of professional APCs[29]. The activity of HLA-DM is pH dependent, and highest in the MIIC compartment at a pH of 4.5-6.0[28]. Additionally HLA-DM activity can be modulated by its antagonist HLA-DO[30]. Like HLA-DM, HLA-DO is as well as HLA class II like protein, whose expression is restricted to mainly B lymphocytes and a sub-group of dendritic cells[29]. Lastly, the pMHC leaves the MIIC compartment in tubulovesicular endosomes and is transported and fused with the plasma membrane, finally ready to present the peptide to $CD4^+$T cells[31].

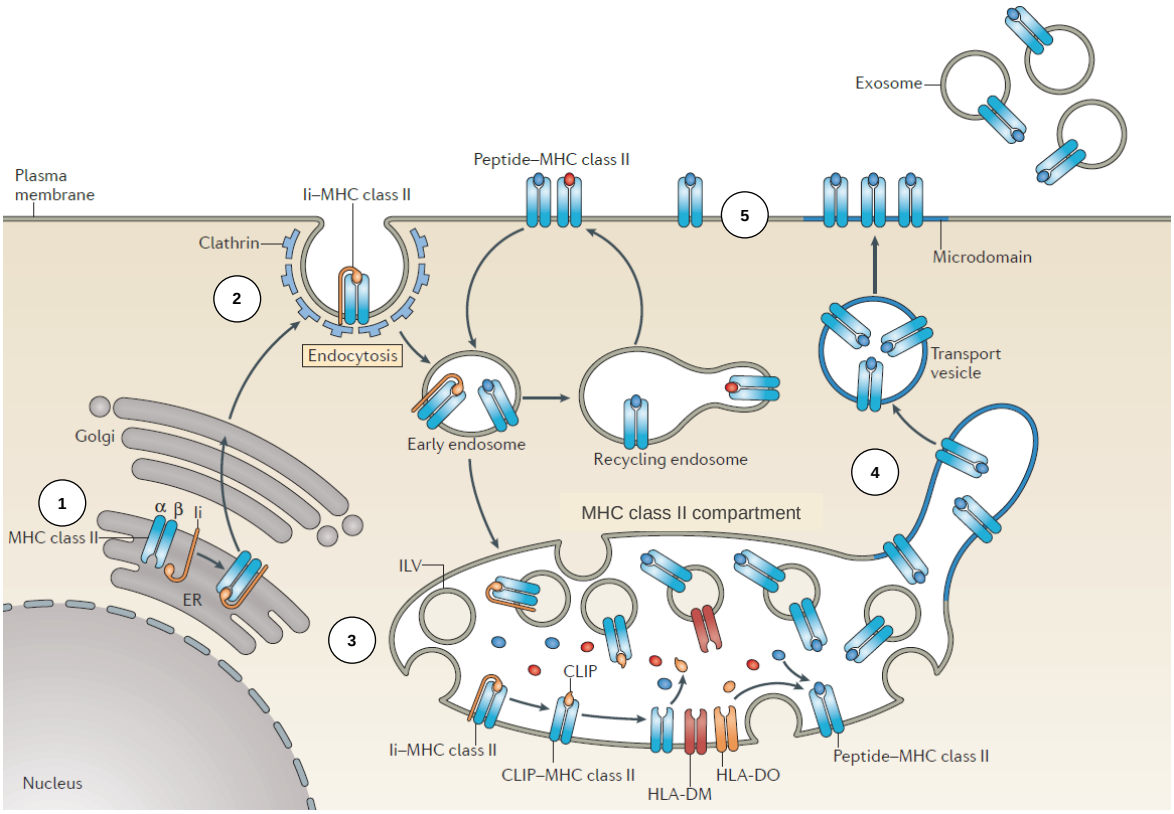

Figure 4: HLA class II pathway of antigen processing and presentation

HLA class II antigen presentation pathway in 5 main steps.1) Newly synthesized MHC class II is blocked with invariant chain in the ER. 2) Internalization of MHC-Ii complex by clathrin-mediated endocytosis. 3) Peptide loading in MIIC compartment regulated by HLA-DM and HLA-DO. 4) Transport of the MHC-peptide complex to the cell surface. 5) MHC class II antigen presentation on the cell surface (modified from Roche[31]).

Although classical antigen presentation is defined by HLA class I presenting intracellular antigens and HLA class II presenting peptides derived from exogenous antigens, still class I is capable to present exogenous peptides in a process which is called cross presentation[24]. Cross presentation is known to occur most efficiently in dendritic cells but it also includes macrophages and B lymphocytes[32]. The result of this process is the cross-priming of naïve $CD8^+$ T cells with viral or tumour antigens. Meaning exogenous peptides are presented via the HLA class I pathway, a mechanisms of great importance for the immunes system to generate self-tolerance and immunity to viruses[33].

4.2. T-cell biology and antigen recognition

4.2.1. T-cell subsets

T cells are major drivers of the immune system due to their ability to specifically recognize non-self tissue[34]. T cells can be classified according to their function, expression of cluster of differentiation (CD) and cytokine production. The expression of different CD divides $CD4^+$ T-helper cells (T_H) from $CD8^+$ cytotoxic T lymphocytes (CTL)[35]. The ontogeny of T cells comprises many maturation and differentiation steps. T cells emerge from the bone marrow as lymphocyte precursor and develop in the thymus to obtain their functional and phenotypic characteristics (see chapter 4.2.2)[14]. After maturation, T cells are released into the periphery as naïve T cells (T_N). Among peripheral T cells one distinguishes between naïve, memory and regulatory T cells (Tregs). T_N provide the recognition of new antigens while previously encountered antigens are targeted by memory T cells, maintaining long term immunity. Tregs have the capacity to regulate the immune system and maintain self-tolerance[34]. The priming of T_N and subsequent differentiation takes place in the secondary lymphoid organs (**Figure 5**). After antigen encountering, T cells proliferate and differentiate into different subpopulations of memory T cells depending on the strength of stimulatory signal. After elimination of the encountered antigen, a number of memory T cell precursors are rescued[36]. Subpopulations of memory T cells are central memory T cells (T_{CM}) and effector memory T cells (T_{EM}) classified by their combinatorial expression of distinct surface markers. Gattoni *et al* have previously identified a new distinct subpopulation of memory T cell - T memory stem cells (T_{SCM})[37].

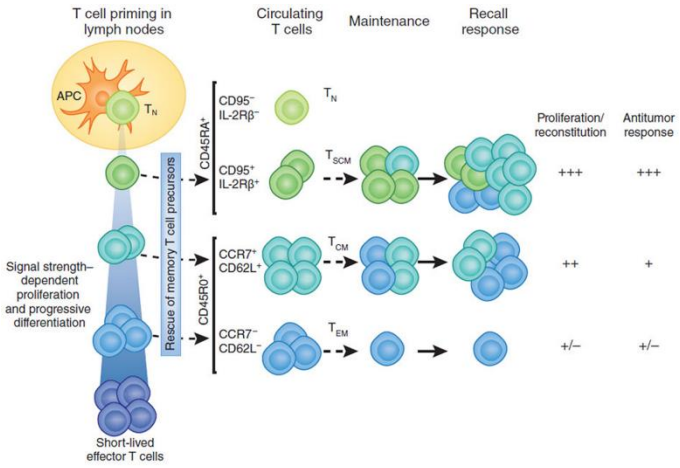

Figure 5: Naïve T cell priming

Pathway of differentiation of primed naïve T cells in the secondary lymphoid organs. Differentiation into subpopulations of memory T cells depends on signal strength. Subpopulations are divided by the combinatorial expression of distinct surface markers. T_N, naïve T cells; T_{CM}, central memory T cells; T_{EM}, effector memory T cells; T_{SCM}, T memory stem cells (From Sallusto[36]).

Besides the maturation status of T cells, the heterogeneity of $CD4^+$ T cells comprises T_H1 and T_H2 cells as firstly stated by Mossman and Coffman[38]. While T_H1 cells, involved in cell-mediated immunity, secret interferon (IFN)-γ, interleukin (IL)-2 and tumour necrosis factor (TNF)-β, T_H2 cells produce IL-4, IL-5, IL-6, IL-9, IL-10, and IL-13 and evoke mostly strong antibody responses[35] . Later, further subpopulations of T_H were discovered, including T_H9, T_H17, T_H22 and follicular T helper cells (T_{FH}), defined by their cytokine production profile (**Figure 6**). For example, are T_H17 cells able to recruit neutrophils and therefore target specific classes of pathogens. In addition this subtype is responsible for the protection of mucosal surfaces and is involved in the pathophysiology of graft versus host disease (GvHD)[39, 40]. T_{FH} are required for the germinal center formation and provide protection against pathogens via interaction with B cells[41]. Together, all different subsets are key orchestrators of the adaptive immune response and are required to maintain the human immunity.

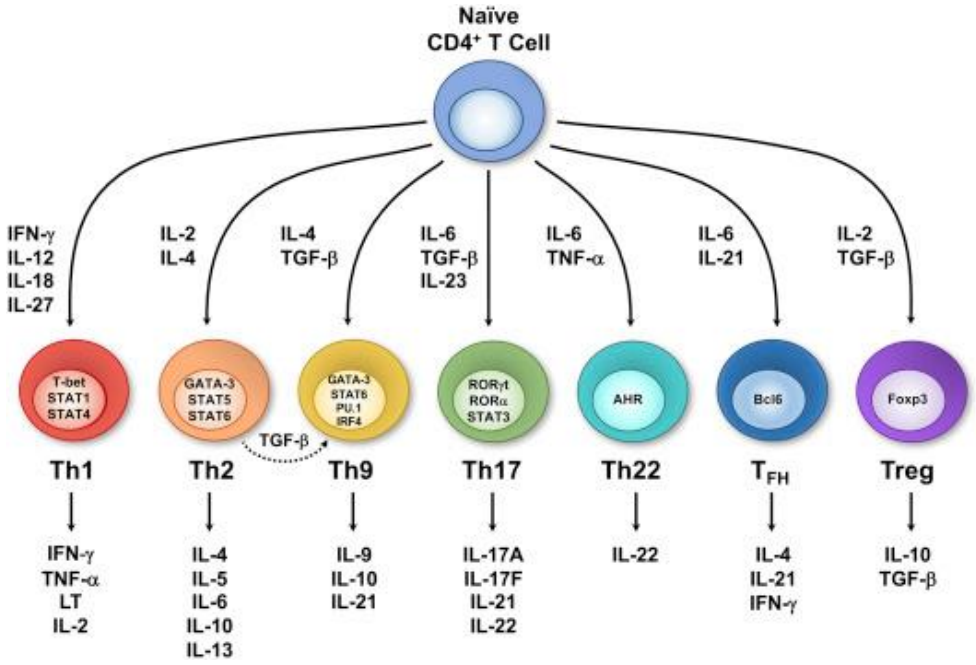

Figure 6: CD4+ T cell subsets defined by their cytokine production profile

Schematic representation of the various subsets of CD4+ T cells showing distinct cytokine production profiles (from Hayat[42]).

4.2.2. T-cell receptor genomics and education

Part of the highly efficient antigen recognition and response is the immense diversity of the T-cell receptor (TCR) repertoire. Germline organization of TCR genes and especially the TCR rearrangements contribute to this diversity[16]. The TCR is a heterodimer expressed on the cell surface of T cells. It is composed of a combination of α and β polypeptide chains (αβ TCR) or γ and δ chains (γδ TCR), the latter is less abundant[14, 43, 44]. Each TCR chain again is composed of a constant element (C) and a variable (V) element[44]. The encoding genes for the different chains are distributed on different chromosomes and three separate loci. The β and γ chain loci are located on chromosome 7 and the α, δ chain locus on chromosome 14 (**Figure 7**). The variable region, important for antigen recognition, includes several variable (V) and joining (J) genes. Exclusively the TCR β and δ loci exhibit additionally diversity (D) genes. Fewer genes are involved in the constant region, each TCR β and TCR γ includes two C genes, $C_\beta1$, $C_\beta2$ and $C_\gamma1$, $C_\gamma2$, respectively. Whereas TCR α and TCR δ each just exhibit one C gene – C_α and C_δ. The four exons of every C gene encode for a short hinge region, the cytoplasmic tail, extracellular Ig-like domain and the transmembrane segment of the TCR[14, 45].

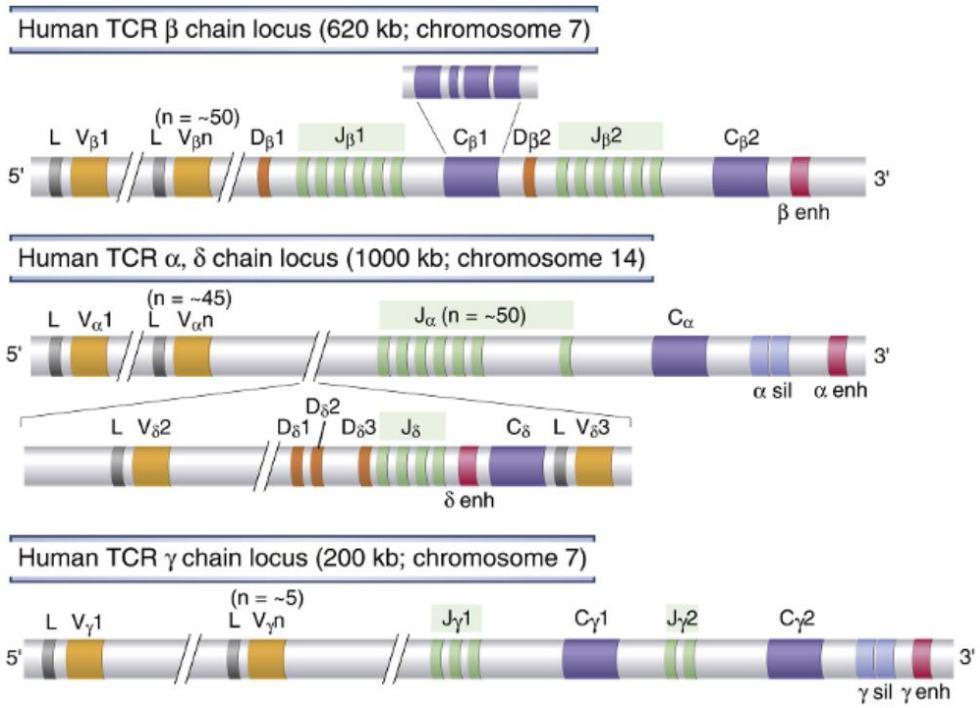

Figure 7: TCR loci organization

Simplified schematic representation of the germline organization of the TCR loci. The four different TCR chains α, β,δ and γ are distributed on two chromosomes 7 and 14 and on three different loci. V, variable; D, diversity; J, joining; C, constant; L, leader; enh, enhancer; sil, silencer (from Abbas[14]).

During thymic ontogeny the TCR genes are assembled by somatic recombination, also known as VDJ rearrangement[46]. The rearrangement of the VDJ segments is a hallmark of the immune system to create the huge diversity of TCR repertoire[47]. Thus, this mechanism is able to generate about 10^{13} T cells with a unique TCR[48]. In brief, the V and J segments are randomly selected and rearranged for the TCR α and γ. For the β and δ TCR, containing a D element, this process is split in two separate events (**Figure 8A**). The first rearrangement joins the D and J segment, subsequently the V segment is recombined to the DJ segment[14, 44]. The recombination process requires four sequential steps and is mediated by enzymes (**Figure 8B**). The first step is called synapsis, here the antigen receptor gene and the recombination machinery gather. Through chromosomal looping, the coding V segment, and its recombination signal sequence (RSS) is brought adjacent to the J segment and its RSS. The RSS are conserved heptamer and nonamer sequences which are separated by 12 or 23 random nucleotides and can be recognized by the recombination activating genes (RAG) 1 and 2[14, 49]. The chromosomal loop is enzymatically cleaved via double stranded breaks. The two recombinases work interdependent in generating a closed hairpin. RAG 1 forms a covalent hairpin by separating on one DNA strand the heptamer and the coding segment, RAG 2 generates a blunt end of double stranded DNA. For further processing RAG 1 and 2 hold the hairpin ends in position[14, 50]. In step three the endonucleases Artemis opens up the hairpins and template independent GC rich nucleotides (N) or template dependent palindromic (P) nucleotides are incorporated by the terminal deoxynucleotidyl transferase (TdT)[14, 51]. Finally, the two segments are fused by nonhomologous end joining. This process involves the ubiquitous factors Ku70 and Ku80 which are binding to the break, then a DNA-dependent protein kinase (DNA-PK) repairs the DNA double strand. The fusion of two encoding segments is mediates by the DNA ligase IV and its subunit XRCC4[14].

Not only the process of the different possibilities of recombination of the three different segments (V, D, J), also the possible insertion and deletion events at the cleavage step and later on the pairing of the TCR α and β chains or TCR γ and δ chains account for the huge heterogeneity of the T cell repertoire, essential to cover all antigen for recognition[49].

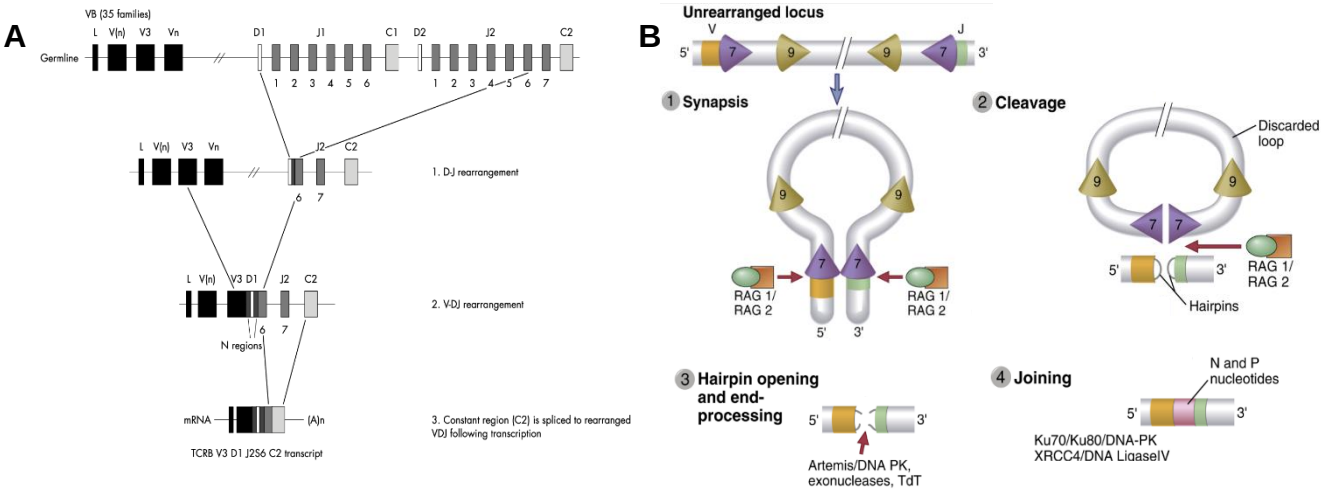

Figure 8: V(D)J rearrangement

Schematic representation of VDJ rearrangement of TCR β (from Hodges[45]). (B) Four sequential steps during VJ rearrangement. 7, heptamer sequence; 9, nonamer sequence (modified from Abbas [14]).

The protein structure of the TCR is built by the constant region, a complex of non-polymorphic proteins known as CD3, connected to the membrane via a membrane-spanning region including a short cytosolic tail (**Figure 9A**) [52]. The associated variable region is assembled by two diverse polypeptide chains, either αβ or γδ, which are linked via a disulphide bond [52, 53]. The specificity of the TCR is given by the complementarity determining regions (CDR) which interfere with the antigenic peptide and MHC (**Figure 9A, B**). The CDR is a structure of six hairpin loops connecting adjacent β-strands [53, 54]. These CDRs are mostly encoded on the V segment – CDR1 and CDR2. The hypervariable CDR3 is encoded between the V and J or D and J segment and includes N and P nucleotides[44].

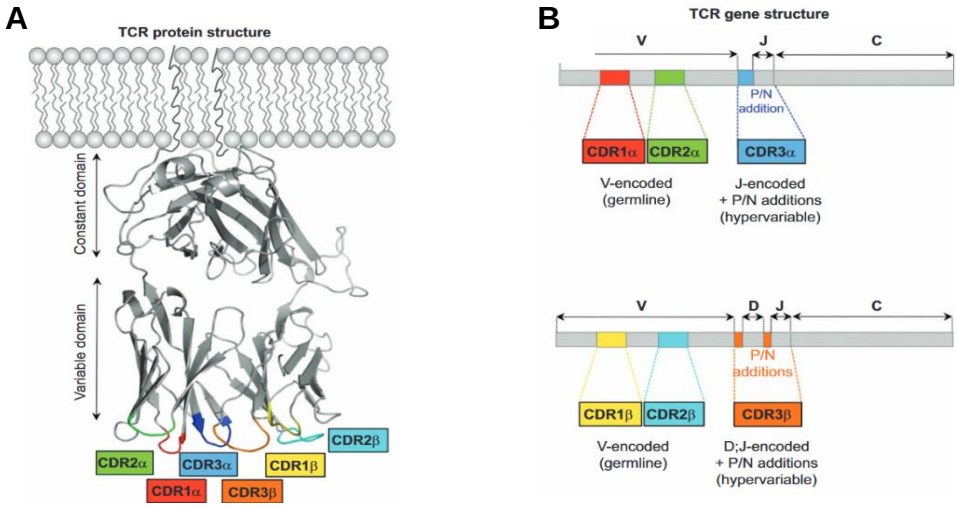

Figure 9: TCR protein and gene structure

(A) Protein structure of an αβ TCR (B) Organization of CDR genes in VDJ segments (from Attaf[53]).

The functionality of the TCR is verified by two selection mechanisms in the thymus[55](**Figure 10**). Immature thymic T cells, called thymocytes, enter the thymus as double negative cells, meaning they do not express the TCR nor CD4 or CD8[56]. At the stage of β selection a pre-TCR is generated by a TCR β chain, an invariant Tα chain, CD3 and the cytosolic subunit ζ. Pre TCR signals lead to expression and recombination with the TCR α chain[14, 57]. Subsequently the thymocytes reach their double positive stage, expressing the complete TCR and associated CD3 and ζ subunit as well as CD4 and CD8[14]. Once the αβ TCR is expressed, the expression of γδ TCR chains is no longer feasible. Since the TCR δ locus is deleted as soon as the rearrangement of the TCR α occurs[58]. To generate γδ TCR the rearrangements of their chains must occur before a productive TCR β rearrangement is generated, a rare event occurring in just 10% of the time[14]. The first selection mechanism to ensure self-tolerance of the immune system is the negative selection. Primary negative selection occurs in the cortex. Here all TCRs that strongly recognize the self-antigen or that do not recognize the self pMHC at all will be eliminated by apoptosis or neglection[59]. Double-positive cells are also able to maturate into $CD4^+$ Tregs by a non-elusive process[60]. Next, positive selection occurs in the medulla and ensures the self-MHC restriction of the T cells. Here T cells will be assigned to express either CD4 or CD8 depending on their recognition of MHC class I or II molecules[61]. Secondary negative selection events also exist in the medulla, eliminating self-reactive single-positive T cells. Result of the thymic education mature functionally T cells are released into the periphery[55].

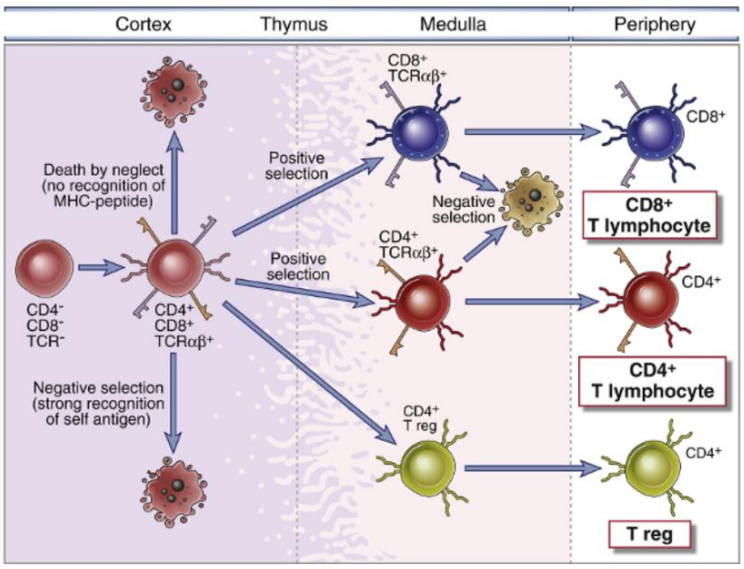

Figure 10: Thymic education

Schematic representation of T cell thymic education ensuring TCR functionality and preventing autoreactivity (from Abbas[14]).

4.2.3. T-cell receptor function

T cells are key orchestrators of the adaptive immune response, hence a balanced TCR repertoire is essential for specific TCR dependent recognition[62]. The recognized peptides are of exogenous or endogenous origin presented by MHC class I or MHC class II, respectively[63]. The MHC restriction of T cells was first discovered by Zinkernagel and Doherty in1974[64]. Hence, T cell can recognize a foreign peptide presented by a self-MHC molecule, a feature that is ensured during thymic education. Recognition of MHC class II is restricted to CD4 expressing T cells, whereas MHC class I is recognized by CD8 T cells (**Figure 11A**)[13, 65]. The diversity of the pMHC exceeds the diversity of the TCR repertoire, thus an additional feature of T cells is their poly-specificity. Meaning they are cross reactive, able to recognize more than just one antigenic pMHC[66]. Thus, the TCR discriminates even single amino acids differences between peptides, yet the binding affinity to the pMHC is relatively low [67, 68]. The structurally binding to MHC is exhibit by the CDR1 and CDR2 loops of the TCR, the highly variable CDR3 loop favours the contact with the presented peptide (**Figure 11B**)[63]. The phenomenon of cross reactivity is enabled by the conformational plasticity of the CDR loops, especially CDR3 loop [69].

For activation of the T cell the formation of the immunological synapsis (IS) is required. The IS describes the formation of a cellular complex structure at the interface of the T cell and pMHC expressing target cell, involving several molecules (**Figure 12**)[70]. The three most important signals to trigger the T cell activation are 1) the engagement of

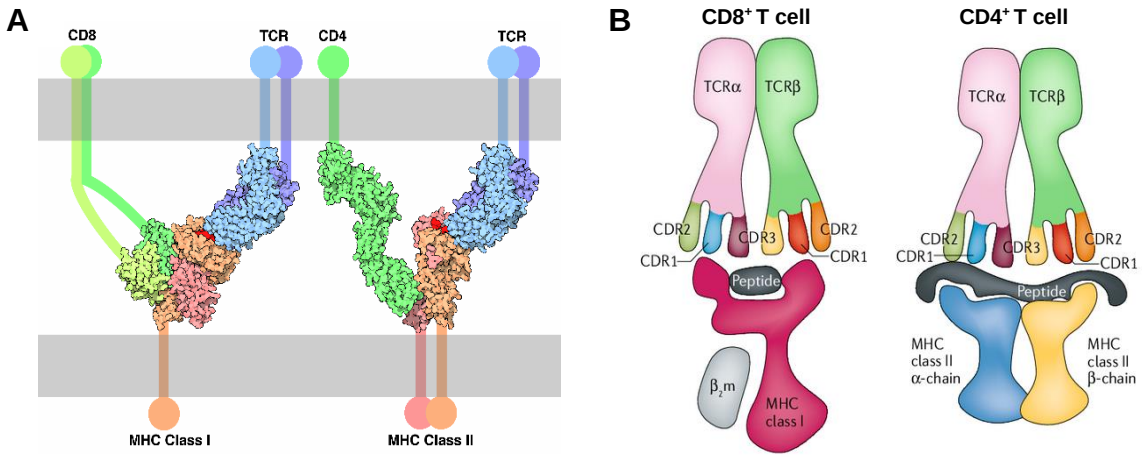

Figure 11: MHC-restricted T-cell recognition

(A) Illustration of MHC class I/II-restricted T-cell recognition strengthen by the interaction of the CD molecules (CD4, CD8) (from Goodsell[71]). (B) $CD4^+$ and $CD8^+$ T-cell recognition and the involvement of CDR loops (from La Gruta[65]).

TCR and pMHC, 2) signals from co-stimulatory molecules like CD28 and CD80/CD86 3) signals from cytokine or cell bound ligand signals such as TNFα or IL6 [72,73]. Another co-stimulatory molecule involved in T cell activation is 4-1BB (also known as CD137)[74]. TCR activation leads to several intracellular signal cascades which trigger eventually a T cell response. In brief, engagement of TCR and pMHC leads to activation of the kinase Lck. It mediates the phosphorylation of the sequence motifs on the CD3 subunits, called ITAMs. This triggers the recruitment and activation of protein kinase ZAP-70, provoking further downstream phosphorylation of scaffold proteins. Phosphorylation of ZAP-70 substrates leads to activation of further signalling pathways including the Ras pathway, cytoskeletal reorganization, and calcium mobilization. Calcium release involves the MAPK/Erk pathway, NF-κB activation, and the activation of the protein phosphatase calcineurin promoting in the end the transcription of IL-2[75]. Ras activation leads as well to the transcription of various key genes essential for T cell immune response. Negative regulation of TCR-mediated signalling is promoted via SHP2, an interacting transmembrane adaptor protein, to prevent a hyperactive immune response. Additionally, CTLA4 acts as natural inhibitor. In summary, T cell response is balanced via activation and negative regulation of the TCR signalling. So that the response only to foreign pMHC is assured and T cell activation by self-pMHC is inhibited[75, 76].

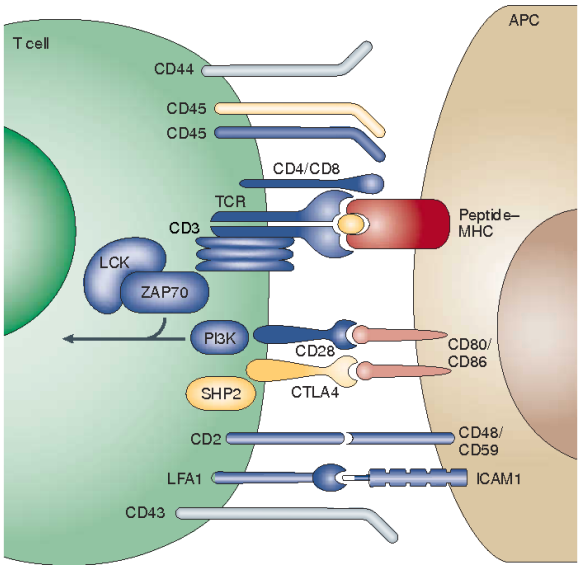

Figure 12: Immunological synapse

Schematic representation of the immunological synapse, a cellular complex structure at the interface of the T cell and pMHC expressing APC. TCR activation involves interaction with different receptors and co-stimulatory molecules leading to activation of several signalling cascades (from Huppa[70]).

Despite the self MHC-restricted T-cell recognition, many T cells can specifically recognize non-self, allogeneic MHC molecules[15]. This T cell alloreactivity especially appears in the context of transplantation involving graft rejection and GvHD[77]. Alloreactive T cells display a high precursor frequency with 1 in 10^3-10^4, 100-fold to 1000-fold higher compared to the precursor frequency of conventional recognizing T cells[66]. One differentiates T-cell alloreactivity between direct, indirect, and semi direct pathway (**Figure 13**). The ability of T cells to cross react facilitates the direct recognition of an allogeneic MHC expressed on an allogeneic target cell[78]. Resulting in T cells that are restricted by the allogeneic MHC. Via the indirect pathway of alloreactivity, peptides of a processed allogeneic MHC molecule or minor histocompatibility antigens (see chapter 4.4.1) are presented by an autologous APC on a self-MHC class II molecule. The third form of T-cell alloreactivity is the semidirect presentation, also known as cross-dressing. An autologous APC presents a peptide via an allogeneic MHC molecule, a process used by viruses during infection [79, 80]. The direct T cell alloreactivity plays a crucial role in stem cell transplantation, promoting the beneficial graft versus leukaemia (GvL) but as well GvHD and thereby destroying healthy tissue. In an HLA-matched context, minor histocompatibility antigen serves as target for indirect T-cell alloreactivity. Further indirect T cell alloreactivity can lead to enhancement of allograft immunity or allograft tolerance in tissue and cellular transplantation [81].

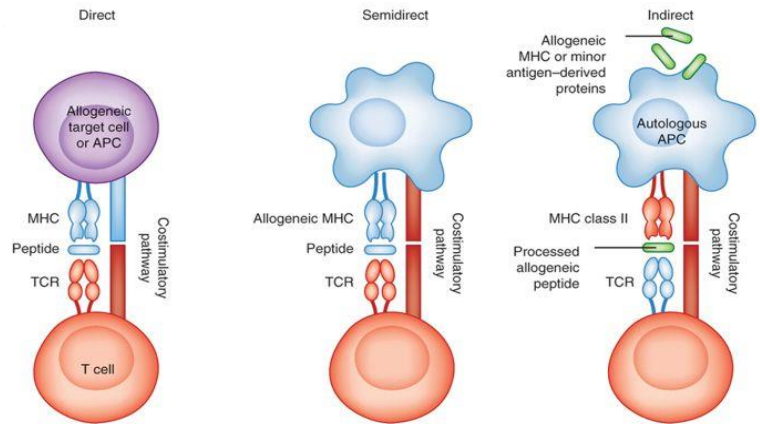

Figure 13: Forms of T-cell alloreactivity

Schematic representation of the three forms of T-cell alloreactivity. Direct T-cell alloreactivity represents a donor APC dependent recognition. Semi-direct alloreactivity is the peptide presentation via an allogeneic MHC molecule expressed by an autologous APC. Indirect T-cell alloreactivity is the recognition of an allogeneic MHC derived peptide or minor antigen peptide presented by an autologous APC (from Zakrzewski [82]).

The dependency of TCR interaction is contradictory. Some models reveal that exclusively the interaction with the allogeneic MHC molecule accounts TCR alloreactivity[83]. Other models are peptide centric in T-cell recognition of an allogeneic MHC complex (e.g. altered-self model)[84].Further studies have demonstrated a central role of the peptide for alloreactive T cells[85, 86]. Finally, T-cell allorecognition is influenced by polymorphic residues of the MHC molecule, but also indirectly by the presented peptide, which is bound by hypervariable peptide-binding groove of the MHC molecule[87].

4.3. Clinical relevance of HLA

4.3.1. Cell Therapy

Cell therapy is defined as the injection of a cell product into a patient. Among other applications, cell therapy is widely used as treatment of cancer, autoimmune diseases, and haematological malignancies. This can be either an autologous or allogeneic cell product. An autologous cell product is used for *ex vivo* manipulation and will be reinfused into the same patient. A donor allogeneic cell product, not necessarily manipulated, is infused into a recipient patient. However, cell therapy has to face many obstacles such as safety and ethical issues [88].

4.3.1.1. Haematopoietic stem cell transplantation

A well-established type of cell therapy is the haematopoietic stem cell transplantation (HSCT), a treatment for malignant and non-malignant conditions. HSCT is the transplantation of pluripotent haematopoietic stem cells (HSC). The first HSCT in humans was performed by Thomas in 1957[89], by now more than one million HSCTs have been performed, the only cell therapy carried out in a large scale[90]. There are two main types of HSCTs 1) autologous stem cell transplantation and 2) allogeneic stem cell transplantation. In the autologous setting the patients cells itself are the source of transplanted HSCs. Thus, damaged bone marrow cell after high-dose chemotherapy and radiation treatment is replaced by prior extracted autologous cells. By using autologous cells high risk factors such as GvHD and graft rejection are excluded via self-tolerance. The autologous HSCT is most often used in haematological malignancies such as plasma cell disorders (52%), Non-Hodgkin's lymphoma (28%), and Hodgkin's disease (10%)[91]. The allogeneic HSCT requires HSCs from a donor which are infused into a patient and thereby establish a donor-derived haematopoiesis. Unlike the autologous HSCT, the allogeneic HSCT must overcome the barrier of

Histocompatibility (see chapter 4.4.1) with arising risks like GvHD[92]. This treatment is applied only for high risk patients with haematological diseases such as acute myeloid leukaemia (39%), acute lymphoblastic leukaemia (16%), and Myelodysplastic syndromes (12%)[91]. Similar to the autologous setting, the patient's immune system is destroyed by chemotherapy or radiation prior to allogeneic HSCT. Thereafter donor's granulocyte-colony stimulating factor (G-CSF)-enriched $CD34^+$ HSC are transplanted into the patient. Selection of $CD34^+$ HSC can be performed either *ex vivo*, prior to HSCT or *in vivo*, post HSCT by T and B cell depleting agents like anti-thymocyte globulin (ATG)[93, 94]. Besides ATG, also other antiproliferative agents and calcineurin inhibitors are used to supress T cell proliferation, an approach used for GvHD prophylaxis[92]. While T cell depletion can prevent GvHD, the T cells can also be beneficial. They promote the eradication of residual malignant cells, an effect named graft versus leukaemia (GvL) and are also valuable in preventing opportunistic infections. Thus, for example relapsed patients benefit from the GvL effect by the administration of donor-lymphocyte infusions (DLI). However, DLI administration can lead to sever GvHD[95]. Yet, the major challenge of HSCT still remains relapse, albeit different approaches to eliminate residual malignant cells - the major source of relapse. Therefore, shifting the balance between GvHD and GVL towards GvL is the key to control the disease and prevent relapse and infections[94].

4.3.1.2. New adoptive cell therapy approaches

Adoptive cell therapy is a type of cellular immunotherapy in which the treatment of cancer is addressed by anti-tumour T cells. The treatment can be either alone or in combination with other therapies. The main types of adoptive cell therapies include the Tumour-infiltrating lymphocyte (TIL) therapy, Engineered TCR therapy, and the most emerging CAR T cell therapy[96]. The TIL Therapy promotes tumour killing by re-infusion of autologous *ex vivo* expanded and activated TILs. TIL treatment of metastatic melanoma revealed effective results in form of tumour regression [97].The engineered TCR Therapy involves autologous T cells which are re-infused into the patient after they are *ex vivo* genetically modified to express a TCR that targets a specific cancer antigen. A limiting factor of this therapy is the MHC-restriction of conventional TCRs, which restricts the applicability to patients with a specific HLA allotype[96]. Targets identified for engineered TCR Therapy are for instance MART-1 for melanoma, and NY-ESO-1 expressed by several cancers such as breast cancer, thyroid cancer and synovial cell sarcoma[98, 99]. One main risk factor of engineered TCRs is their cross-

reactivity to healthy tissue which can lead to severe complications[100]. The area of cellular therapy currently drawing most attention is CAR T cell Therapy. CAR T cells are *ex vivo* genetically modified to express a CAR, a synthetic receptor targeting a specific antigen of choice. Compared to engineered TCRs, CARs are advantageously MHC-independent resulting in broad applicability. Initially CAR T cell therapy using autologous T cells was investigated. Nowadays advanced approaches are being exploited using allogeneic, "off-the-shelf" CAR T cells[101]. The first autologous CD19 CAR T cell therapy for the treatment of B cell precursor ALL and B cell NHL was approved in 2017 in the U.S.[102]. But CAR T cell treatment also entails side effects. In particular the cytokine release syndrome (CRS) which lead to high fever and flu-like symptoms, but as well neurological toxicities and B-cell aplasia are reported[103]. Recent studies reveal NK cells as promising immune cell source for adoptive allogeneic cell therapy[104].

4.3.2. Other clinical applications

Clinical relevance of HLA is also confirmed in the field of cancer, autoimmunity, and viral infection. Thus, highly polymorphic HLA molecules can affect the outcome of infection by their ability to trigger immune responses. Associations of certain HLA class I genes have been shown for the clearance of hepatitis B virus (HBV) infection[105]. Both HLA class I and II molecules are associated with several autoimmune disease such as Graves' disease, Celiac disease, Type 1 diabetes, and Multiple sclerosis, displaying a predisposing or protective factors[106]. Also HLA class II DP disparities are associated not only with HSCT but also with solid organ transplantation[107, 108]. Additionally, HLA-DP single nucleotide polymorphisms (SNP) are involved in associations with different autoimmune diseases and the outcome of viral infections, including HIV and autoimmune thyroid disease [109, 110]. Besides HLA disease associations, HLA also influences different approaches of cancer immunotherapy. Immune checkpoint blockade represents a treatment strategy for malignant melanoma and squamous non-small cell lung cancer. Anti-tumour response was demonstrated for inhibitors of cytotoxic T-lymphocyte-associated antigen 4 and programmed cell death-1[111]. Recent results have shown that certain HLA class I supertypes or HLA class I impact the success of these inhibitors [112]. Therapy approaches using personalized neoantigen vaccines make use of T cells directed to cancer neoantigens. The binding affinity to HLA a key step in identifying neoantigens [113]. Another antibody-based immunotherapy Milatuzumab targets the invariant chain of MHC II complexes[114].

4.4. Donor selection in HSCT

The major barrier in allogeneic HSCT is the immune recognition of HLA incompatibilities, playing a major role in engraftment, GvHD severity, and overall survival. Preferably used as donor source for allogeneic HSCT are HLA-matched siblings. However, in about 70% a suitable HLA-matched sibling donor is not available[115]. Alternatives donor sources to HLA-identical sibling donors are unrelated mismatched/matched donors, haploidentical donors, and cord blood. Cord blood has a downward trend (**Figure 14**), albeit decreased association with GvHD due to a polyclonal naïve T cell repertoire, but disadvantageously displaying much slower immune reconstitution[116]. Haploidentical donor transplantation provides as high availability, donor and recipient share by inheritance one haplotype and are HLA-mismatched for the unshared haplotype[117]. In combination with GvHD prophylaxis post-transplant cyclophosphamide (PT-Cy) haploidentical HSCT has become a promising alternative[118]. Most used alternative donor source is represented by unrelated donors exhibit HLA incompatibilities. HLA mismatches are bearing a high risk of GvHD but also promote beneficial T cell alloreactivity against the residual tumour cells resulting in lower relapse rates[117]. HLA incompatibilities are determined by HLA high resolution typing. Today's gold standard defines an "HLA match" as 10/10 match including the loci HLA-A, -B, -C, -DRB1, and -DQB1[115]. Additional typing for HLA-DPB1 is recommended as results have demonstrated functional importance on HSCT outcome (see chapter 4.4.2)[119].

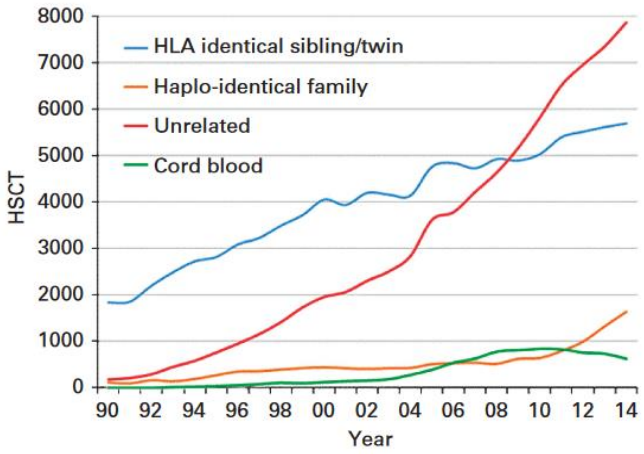

Figure 14: Numbers of HSCT by donor type from 1990-2014

Development of performed HSCTs in Europe between 1990 and 2017 using different donor types (from Passweg[120]).

4.4.1. Histocompatibility

Histocompatibility is defined as concordance of HLA between donor and recipient. As already mentioned, HLA disparity-dependent T-cell alloreactivity is the major source of complications like GvHD and graft failure. The higher the degree of HLA histocompatibility the significantly better the survival of HSCT (**Figure 15A**). An HLA-matched donor (10/10) can be found for 50% of the patients in a Caucasian population, a number that is limited by the high diversity of HLA. Therefore, the identification of well tolerated HLA mismatches is of urgent need to provide the best suitable donor for a successful HSCT outcome (see chapter 4.4.2). An adverse outcome of HSCT was already demonstrated in association with HLA-A, -B, -C, and -DRB1 mismatches[121]. In that regard, single mismatches at HLA-A or HLA-DRB1 are not tolerated as good as HLA-B or HLA-C single mismatches[122]. Since HLA-DQB1 mismatches are less common, a significant clinical relevance could not be shown. One characteristic of HLA impacting histocompatibility is the phenomenon of linkage disequilibrium (LD)[115]. Accordingly, different HLA loci exhibit a non-random association of different alleles promoted by adjacent located loci of the HLA genes[123]. By implication of the strong LD to the well-matched HLA-DRB1, the low frequency of HLA-DQB1 mismatches can be explained. Whereas HLA-A to HLA-DQ exhibit strong LD, HLA-DP is separated by at least one recombination hot spot and only demonstrate a weak LD to other class II loci. Therefore the frequency of HLA-DPB1 mismatches (>80%) is very high in HSCT[108]. Significant higher relapse rates and lower incidence of acute GvHD after HLA-DPB1-matched HSCT provide evidence of its immunogenic role (**Figure 15B**)[124].

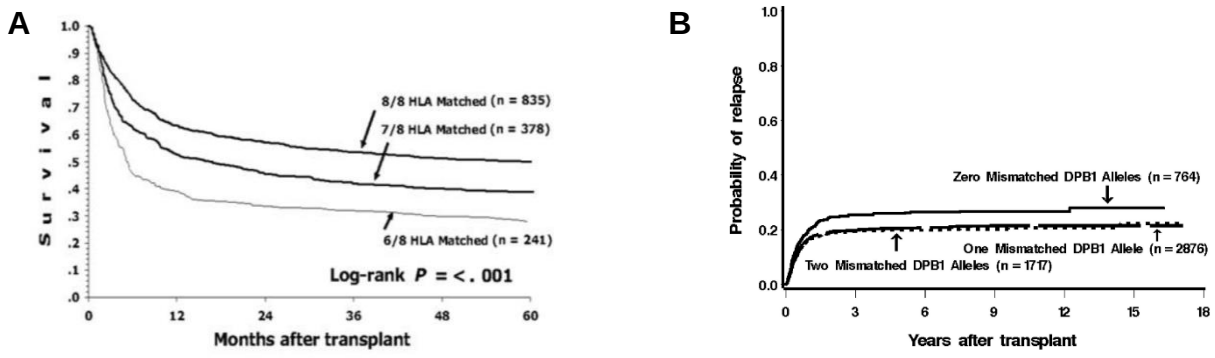

Figure 15: Impact of HLA histocompatibility on HSCT outcome

(A) Quantitative impact of HLA-A, -B, -C, and -DRB1 mismatches on survival of patients with early disease (Form Lee[122]). (B) Relapse probability (cumulative incidence) of HLA-DPB1 allele-mismatched or HLA-DBP1-matched patients (From Shaw[125]).

Histocompatibility can be also influenced by minor histocompatibility antigens (mHAgs). MHAgs are processed proteins deriving from nonsynonymous SNPs in the coding sequence that differ between donor and recipient[126]. In contrast to major mismatches that present allopeptides on the non-self HLA to donor T cells, mHAgs (host peptides) are displayed by APCs on self-HLA class I and II molecules to donor derived T cells[127]. Especially in HLA-identical allogeneic HSCT, mHAgs are target of T-cell alloreactivity able to mediate GvHD and GvL effect[128, 129]. T-cell alloreactivity against mHAgs derives from the naïve T cell subset whereas major mismatched-mediated T-cell alloreactivity can be elicited by naïve and memory T cells[127]. Since mHAgs can mediate GvHD and GvL, they are exploited as target for adoptive T cell therapy or vaccination. Interference with mHAgs presentation is a potential strategy to prevent GvHD in HLA-identical HSCT. Another approach is mHAg vaccination and thereby trigger target immunization. When mHAg expression is restricted to leukemic cells, they can be targeted and eliminated using mHAg-specific T cells clones[129].

4.4.2. Permissive mismatching for HLA-DP by T cell epitope and Expression

Modulating T-cell alloreactivity or identify well-tolerated mismatches is an objective tackled by different models. Favourable target molecule of these models is HLA-DP since it is often mismatched in allogeneic HSCT due to its weak linkage disequilibrium to other HLA loci and its clinical association with HSCT outcome. The T cell epitope (TCE) model is based on the observation that structural differences in the peptide-binding groove encoded by exon 2 SNPs of HLA-DPB1 alleles influence the strength of T-cell alloreactivity[130]. HLA-DP mismatches from different TCE groups have been associated with increased risk of mortality. It was shown that a single HLA-DPB1*09:01 mismatch in an allogeneic HSCT was target of T cell mediated-allograft rejection[119]. Several T-cell clones of this patient cross recognized structural similar HLA-DP alloantigen. Based on this observation HLA-DPB1 alleles were group into three different TCE groups, predicted of being high (TCE1), intermediate (TCE2), or low immunogenic (TCE3). These results lead to the establishment of an algorithm predicting well tolerated “permissive” HLA-DPB1 mismatches or detrimental, “non-permissive” mismatches in allogeneic HSCT. Permissive mismatches arise from HLA-DPB1 alleles within the same TCE group and non-permissive mismatches across different TCE groups (**Figure 16**). Depending on donor-recipient combination of the non-permissive HLA-DPB1 mismatch, T-cell alloreactivity can be directed either in

GvH or host versus graft (HvG) direction[130]. The TCE based algorithm predicting permissive or non-permissive HLA-DPB1 mismatches has been demonstrated to have clinical impact in allogeneic HSCT. The detrimental effect of non-permissive mismatches returns into lower probability of survival and transplant-related mortality compared to HLA-DPB1 matched or permissive mismatches (**Figure 17A**)[131, 132]. The probability of relapse has been shown to be significant higher in HLA-DPB1 matched compared to HLA-DPB1 mismatched patients (**Figure 17B**)[131]. Permissive mismatches are suggested to elicit limited alloreactivity sufficient to promote GvL and thereby shifting the balance from GvHD to GVL[108].

<table>
<tr><td colspan="2" rowspan="2"></td><td colspan="6">Recipient</td></tr>
<tr><td>1/1</td><td>1/2</td><td>1/3</td><td>2/2</td><td>2/3</td><td>3/3</td></tr>
<tr><td rowspan="6">Donor</td><td>1/1</td><td colspan="3" rowspan="3">Permissive</td><td colspan="3" rowspan="3">Non-permissive (HvG)</td></tr>
<tr><td>1/2</td></tr>
<tr><td>1/3</td></tr>
<tr><td>2/2</td><td colspan="4" rowspan="2">Non-permissive (GvH)</td><td>Permissive</td></tr>
<tr><td>2/3</td></tr>
<tr><td>3/3</td><td colspan="4">Permissive</td></tr>
</table>

Figure 16: Classification of permissive and non-permissive HLA-DP mismatches

TCE group assignment of the first allele is represented before the slash, and TCE assignment of the second allele is represented after the slash, both for donor and recipient. Mismatches can be predicted as permissive or non-permissive (GvH or HvG) mismatch (modified from Zino[130]).

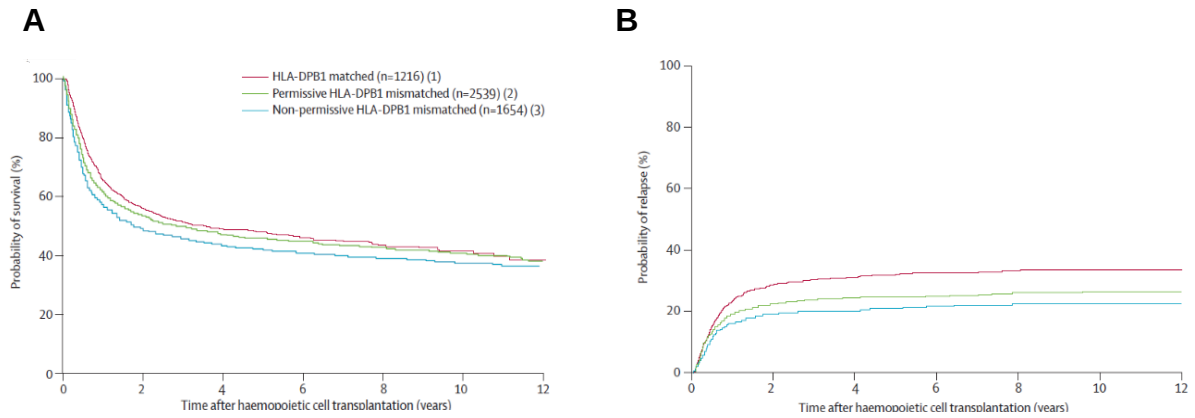

Figure 17: Clinical relevance of non-permissive HLA-DPB1 mismatches

Comparison of HLA-DPB1 matched and permissive and non-permissive HLA-DPB1 mismatches in Kaplan Meier estimates of overall survival (A) and of relapse (B) (modified from Fleischhauer[131]).

Another model predicting permissive mismatches is the Expression model. This model is based on the observation that the cell surface expression levels of HLA-DPB1 are genetically regulated by a SNP (rs9277534) in the 3'untranslated region (UTR). Rs9277534 variants of HLA-DPB1 were first described by Thomas *et al*. in relation to HBV recovery, distinguishing most protective and most susceptible HLA-DPB1 alleles. Rs9277534 A is linked to lower HLA-DPB1 expression and higher HLA-DPB1 expression is linked to rs9277534G[133]. Furthermore, a strong association with another SNP rs2281389 was shown[134]. In the clinical setting of unrelated allogeneic HSCT the expression marker demonstrated an impact on the risk of aGvHD. Thus, the risk of GvHD was higher for recipients with the high expression-linked SNP (G) in combination with a donor with low expression-linked SNP (A) (**Figure 18**). This significant association is limited to donors with rs9277534 A linked HLA-DBP1[135].

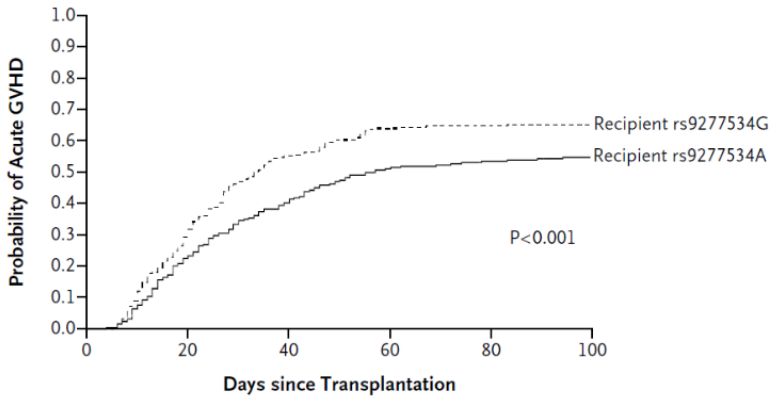

Figure 18: Clinical impact of high HLA-DPB1 expression linked SNP rs9277534

Probability of acute GvHD of recipients either with rs9277534A-linked HLA-DPB1 (solid line) or rs9277534G-linked HLA-DPB1 receiving a transplant from a donor with rs9277534A-linked HLA-DPB1 (from Petersdorf[135]).

Interestingly, HLA-DPB1 expression levels and TCE associated differences in immunogenicity show a strong overlap (**Figure 19**). Thus, high expression variant rs9277534 G is found in almost all HLA-DPB1 alleles assigned to TCE 1 and 2 associated with higher immunogenicity and accordingly worse clinical outcome. Most TCE 3 assigned HLA-DPB1 alleles are linked to the low expression SNP variant A identified as well tolerated mismatch[136].

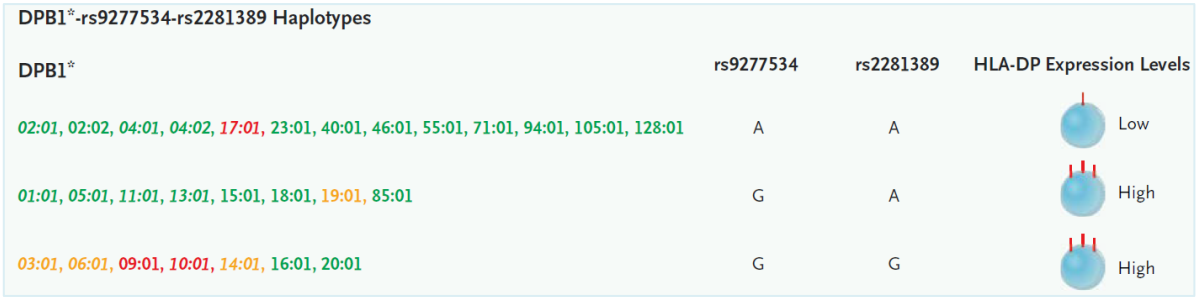

Figure 19: Overlap of TCE and Expression model

Association of HLA-DPB1 alleles and expression levels linked to SNPs rs9277534 and rs2281389. High immunogenic TCE group1 HLA-DPB1 alleles are depicted in red, intermediate immunogenic TCE group 2 alleles are depicted in orange, and low immunogenic TCE group 3 alleles are depicted in green (From Fleischhauer[136]).

5. Objective of this thesis

HLA-DP is a molecule frequently mismatched in unrelated HSCT. Interestingly, HLA-DP mismatches can induce limited T-cell alloreactivity mediating beneficial GvL and thereby lower the risk of relapse. However, the factors regulating differential T-cell alloreactivity against HLA-DPB1 are elusive.

Thus, the goal of this thesis is to determine key regulators modulating T-cell alloreactivity against HLA-DPB1 and informing the prediction of permissive mismatches in HSCT. For this, the following investigations were addressed:

(i) *In vitro* approaches to evaluate the relative role of expression vs structural variation in T-cell alloreactivity against HLA-DP molecules.

(ii) An analysis of TCR diversity in relation to structurally characteristics of HLA-DP antigens.

(iii) A comprehensive study of the HLA-DP immunopeptidome and the effect of the peptide editor HLA-DM

(iv) and how Immunopeptidome shaping impacts T-cell alloreactivity in healthy donors and transplanted patients and its relevance for permissive prediction assessment.

Altogether the results should elucidate how permissive T-cell alloreactivity could be predicted to shift the balance towards GvL effect in HSCT. Moreover, it should give rise how to harness T-cell alloreactivity in fields of cancer immunology and Autoimmunity, as well for translational applications.

6. Articles

I. Dissecting Genetic Control of HLA-DPB1 Expression and Its Relation to Structural Mismatch Models in Hematopoietic Stem Cell Transplantation.

Thuja Meurer, Esteban Arrieta-Bolaños, Maximilian Metzing, Mona-May Langer, Peter van Balen, J. H. Frederik Falkenburg, Dietrich W. Beelen, Peter A. Horn, Katharina Fleischhauer and Pietro Crivello

Published in: Frontiers in Immunology, October 2018
doi: 10.3389/fimmu.2018.02236

II. Alloreactive T Cell Receptor Diversity against Structurally Similar or Dissimilar HLA-DP Antigens Assessed by Deep Sequencing.

Esteban Arrieta-Bolaños, Pietro Crivello, Maximilian Metzing, **Thuja Meurer**, Müberra Ahci, Julie Rytlewski, Marissa Vignali, Erik Yusko, Peter van Balen, Peter A. Horn, J. H. Frederik Falkenburg and Katharina Fleischhauer

Published in: Frontiers in Immunology, February 2018
doi: 10.3389/fimmu.2018.00280

III. Immunopeptidome restriction by HLA-DM limits T-cell alloreactivity against HLA-DP 84Gly/Asp variants in clinical transplantation.

Thuja Meurer, Pietro Crivello, Maximilian Metzing, Michel G. Kester, Dominik A. Megger, Weiqiang Chen, Peter A. van Veelen, Peter van Balen, Astrid M. Westendorf, Georg Homa, Sophia E. Layer, Amin T. Turki, Marieke Griffioen, Peter A. Horn, Barbara Sitek, Dietrich W.Beelen, J. H. Frederik Falkenburg, Esteban Arrieta-Bolaños, Katharina Fleischhauer

Submitted to: PNAS, April 2020

6.1. Article I

Author contributions

Dissecting Genetic Control of HLA-DPB1 Expression and Its Relation to Structural Mismatch Models in Hematopoietic Stem Cell Transplantation

Thuja Meurer, Esteban Arrieta-Bolaños, Maximilian Metzing, Mona-May Langer, Peter van Balen, J. H. Frederik Falkenburg, Dietrich W. Beelen, Peter A. Horn, Katharina Fleischhauer and Pietro Crivello

Original Research article in Frontiers in Immunology

Impact factor: 4.716 (2018)

Status: published on 05th October 2018, Frontiers in Immunology

DOI: 10.3389/fimmu.2018.02236

PubMed-ID: 30344521

Contributions:

- Conception: 50 %
- Experimental work: 85 %
- Data analysis: 85 %
- Statistical analysis: 85 %
- Writing the manuscript: 75 %
- Revising the manuscript: 75 %

Katharina Fleischhauer ……..

(Prof. Dr. Katharina Fleischhauer)

T. Meurer ……..

(Thuja Meurer)

frontiers in Immunology

ORIGINAL RESEARCH
published: 05 October 2018
doi: 10.3389/fimmu.2018.02236

Dissecting Genetic Control of HLA-DPB1 Expression and Its Relation to Structural Mismatch Models in Hematopoietic Stem Cell Transplantation

Thuja Meurer[1], Esteban Arrieta-Bolaños[1], Maximilian Metzing[1], Mona-May Langer[2], Peter van Balen[3], J. H. Frederik Falkenburg[3], Dietrich W. Beelen[4], Peter A. Horn[2], Katharina Fleischhauer[1,5] and Pietro Crivello[1]*

[1] Institute for Experimental Cellular Therapy, University Hospital Essen, Essen, Germany, [2] Institute for Transfusion Medicine, University Hospital Essen, Essen, Germany, [3] Department of Hematology, Leiden University Medical Center, Leiden, Netherlands, [4] Department of Bone Marrow Transplantation, West German Cancer Center, University Hospital Essen, Essen, Germany, [5] Deusches Konsortium für Translationale Krebsforschung (DKTK), Heidelberg, Germany

OPEN ACCESS

Edited by:
Hermann Einsele,
Universität Würzburg, Germany

Reviewed by:
Christophe Picard,
Établissement Français du Sang, France
Reem Al-Daccak,
Institut National de la Santé et de la Recherche Médicale (INSERM), France

***Correspondence:**
Katharina Fleischhauer
katharina.fleischhauer@uk-essen.de

Specialty section:
This article was submitted to Alloimmunity and Transplantation, a section of the journal Frontiers in Immunology

Received: 02 May 2018
Accepted: 10 September 2018
Published: 05 October 2018

Citation:
Meurer T, Arrieta-Bolaños E, Metzing M, Langer M-M, van Balen P, Falkenburg JHF, Beelen DW, Horn PA, Fleischhauer K and Crivello P (2018) Dissecting Genetic Control of HLA-DPB1 Expression and Its Relation to Structural Mismatch Models in Hematopoietic Stem Cell Transplantation. Front. Immunol. 9:2236. doi: 10.3389/fimmu.2018.02236

HLA expression levels have been suggested to be genetically controlled by single nucleotide polymorphisms (SNP) in the untranslated regions (UTR), and expression variants have been associated with the outcome of chronic viral infection and hematopoietic stem cell transplantation (HSCT). In particular, the 3′UTR rs9277534-G/A SNP in HLA-DPB1 has been associated with graft-versus-host-disease after HSCT (Expression model); however its relevance in different immune cells and its mode of action have not been systematically addressed. In addition, there is a strong though not complete overlap between the rs9277534-G/A SNP and structural HLA-DPB1 T cell epitope (TCE) groups which have also been associated with HSCT outcome (TCE Structural model). Here we confirm and extend previous findings of significantly higher HLA-DPB1 expression in B cell lines, unstimulated primary B cells, and monocytes homozygous for rs9277534-G compared to those homozygous for rs9277534-A. However, these differences were abrogated by interferon-γ stimulation or differentiation into dendritic cells. We identify at least seven 3′UTR rs9277534-G/A haplotypes differing by a total of 37 SNP, also characterized by linkage to length variants of a short tandem repeat (STR) in intron 2 and TCE group assignment. 3′UTR mapping did not show any significant differences in post-transcriptional regulation assessed by luciferase assays between two representative rs9277534-G/A haplotypes for any of eight overlapping fragments. Moreover, no evidence for alternative splicing associated with the intron 2 STR was obtained by RT-PCR. In an exemplary cohort of 379 HLA-DPB1 mismatched donor-recipient pairs, risk prediction by the Expression model and the Structural TCE model was 36.7% concordant, with the majority of discordances due to non-applicability of the Expression model. HLA-DPB1 from different TCE groups expressed in the absence of the 3′UTR at similar levels by transfected HeLa cells elicited significantly different mean alloreactive CD4+ T-cell responses, as assessed by CD137 upregulation assays in 178 independent cultures. Taken together, our data provide new insights into the cell

type-specific and mechanistic basis of the association between the rs9277534-G/A SNP and HLA-DPB1 expression, and show that, despite partial overlap between both models in HSCT risk-prediction, differential alloreactivity determined by the TCE structural model occurs independently from HLA-DPB1 differential expression.

Keywords: HLA-DPB1, expression levels, SNP, rs9277534, hematopoietic stem cell transplantation, high risk non-permissive mismatches, T cell epitope, T cell alloreactivity

INTRODUCTION

Genetic control of HLA expression is a topic of increasing interest due to accumulating evidence for its relevance in different biomedical areas including infectious disease and transplantation. In particular, expression levels of HLA-A, -C and -DPB1 genes have been shown to be associated with specific single nucleotide polymorphism (SNP) variation in the untranslated regions (UTR) (1–5). The presence of high-expression variants was in turn associated with poor clearance of chronic viral infections including HIV (1, 6) and HBV (5), suggesting mechanistically increased natural killer (NK) cell inhibition and higher T cell tolerance, respectively. Interest in HLA expression was further fostered by the observation that donor-recipient HLA mismatches involving a high-expression variant in the patient are associated with the risks of developing graft-versus-host-disease (GvHD) after Hematopoietic Stem Cell Transplantation (HSCT), both for HLA-C (7) and HLA-DPB1 (8). The latter involves the bi-allelic SNP rs9277534, with the G-variant leading to high expression and the A-variant to low expression.

The mechanisms underlying the above-mentioned associations between SNP variation and HLA expression are only partly elucidated. For HLA-A, they have been suggested to be correlated with differential methylation and/or the usage of different polyadenylation sites (PAS) (2, 3). For HLA-C and HLA-DPB1, no specific mechanisms for the observed genetic control of expression levels have been postulated to date. Moreover, the association of the rs9277534-G/A SNP with HLA-DPB1 expression has been demonstrated only in a limited set of immune cells of the B cell lineage (5, 8).

Two conceptually different models of HLA-DPB1 mismatches associated with favorable or less favorable outcome of unrelated HSCT have been developed in recent years, and have been validated in independent clinical studies (8–14). The Expression model is based on the assumption that patient-specific HLA-DP antigens with high levels of cell surface expression could be recognized more efficiently by alloreactive donor T cells than patient-specific HLA-DP antigens with low levels of cell surface expression. Therefore, genetic association of HLA-DPB1 expression with the bi-allelic rs9277534 SNP in the 3′UTR is used to assign high or low expression levels to alleles carrying the G- or the A-variant, respectively (5). The TCE Structural model considers variability in the HLA-DPB1 coding sequence translating into polymorphisms in the peptide binding domain, which in turn leads to the generation of structural epitopes recognized by alloreactive T cells. Based on this, at least three different TCE groups were identified, each comprising different HLA-DPB1 alleles sharing the relevant structural epitope. TCE group assignment of HLA-DPB1 alleles was defined either by cross-reactivity of alloreactive T cells (9) or, more recently, by the combined median impact of polymorphic amino acids on T-cell alloreactivity, termed functional distance (FD) (15). The three TCE groups are not equivalent but follow a hierarchical order of immunogenicity, with TCE group 1 > TCE group 2 > TCE group 3. Interestingly, due to strong linkage disequilibrium (LD) between the HLA-DPB1 3′UTR and its coding sequence, there is a strong though not complete overlap between HLA-DPB1 alleles carrying the rs9277534 SNP and the structural TCE groups (16). The relationship between the rs9277534 SNP Expression model and the TCE structural mismatch model for high-risk non-permissive HLA-DPB1 mismatches in HSCT is currently unknown.

In this study, we have set out to fill these gaps by (i) investigating rs9277534 SNP association with transcriptional and cell surface HLA-DPB1 expression in different Antigen Presenting Cells (APC); (ii) 3′UTR haplotype mapping of different HLA-DPB1 alleles and functional testing of their regulatory activity; (iii) comparing the demographics of risk prediction based on the Expression model and the TCE Structural mismatch model for HLA-DPB1 in an exemplary cohort of unrelated HSCT; and (iv) assessment of *in vitro* T cell alloreactivity against different HLA-DPB1 TCE groups at similar transcriptional expression levels in transfected APC.

MATERIALS AND METHODS

Cells and Cell Lines

Peripheral blood mononuclear cells (PBMC) were obtained from healthy blood donors from the University Hospital Essen after informed consent under Ethical Review Board approval, in accordance with the Declaration of Helsinki. EBV-transformed B lymphoblastoid cell lines (BLCL) were generated from PBMC by standard procedures (17), or purchased from the European Collection of Authenticated Cell Cultures (ECACC). HLA-DPB1 typing of the healthy donors was performed by sequence-specific oligonucleotide probing (LABType SSO, One Lambda, Canoga Park, CA, USA) according to the manufacturer's recommendations, under accreditation by the European Federation for Immunogenetics. A list of PBMC and BLCL used in this study and their HLA-DPB1 types is presented in **Tables 1**, **2**. Typing of the rs9277534 SNP was performed by sequence-specific primer (SSP) PCR (**Table 3**), and confirmed by Sanger sequencing of the 3′UTR following published methods (5).

TABLE 1 | BLCL used in this study.

BLCL[a]	HLA-DPB1*			Application in this study[d]
	Allele	rs9277534[b]	3′UTR Haplotype[c]	
MGAR	04:01	AA	6	Exp, Hap, Luc
MOU	02:01	AA	6	Exp, Hap, Luc
SWEIG007	04:02	AA	6	Exp, Hap
OSR-6924	*02:01, 04:02*	AA	6	Exp, Luc
OSR-2674	*04:01, 17:01*	AA	6	Exp
OSR-7891	*04:01, 17:01*	AA	6	Exp
OSR-5678	*02:02, 04:01*	AA	6	Exp
OSR-1629	*02:01*	AA	6	Exp
OSR-2674	*04:01, 17:01*	AA	6	Exp
BM21	10:01	GG	1	Exp, Hap, Luc
APA	05:01	GG	1	Exp, Hap, Luc
BEL7MON	03:01	GG	1	Exp, Luc
AKIBA	09:01	GG	1	Exp, Hap
KAS116	13:01	GG	3	Exp, Hap
PLH	15:01	GG	1	Exp, Hap
SLE005	03:01	GG	1	Exp, Hap
VAVY	01:01	GG	2	Exp, Hap
H0301	05:01	GG	1	Exp

[a] *BLCL were purchased from the ECACC (regular font), or generated locally (italic).*
[b] *rs9277534-G/A as determined locally.*
[c] *3′UTR haplotypes refer to those identified in* ***Table 5****.*
[d] *Use in this study for quantification of HLA-DPB1 protein and transcript expression (Exp), 3′UTR haplotype sequencing (Hap), or Luciferase assays (Luc).*

Stable single HLA-DP HeLa cells transfectants (HeLa-II) were generated by retroviral gene transfer of HLA-DPB1 and DPA1 together with the invariant chain (Ii), HLA-DM, and CD80 as previously described (18). Monocyte-derived dendritic cells (DC) were obtained from frozen PBMC after MicroBead sorting of CD14+ cells (Miltenyi Biotec, Bergisch Gladbach, Germany) and incubation with 500 IU/mL Interleukin (IL)-4 (R&D systems, Minneapolis, MN, USA) and 1000 IU/mL Granulocyte Macrophage Colony-Stimulating Factors (GM-CSF; Miltenyi Biotec, Bergisch Gladbach, Germany) for 5 days. Immature and mature DC were subsequently obtained by incubation with medium alone or in the presence of 10 ng/mL IL-1β (Miltenyi Biotec, Bergisch Gladbach, Germany), 10 ng/mL tumor necrosis factor (TNF)-α (Miltenyi Biotec, Bergisch Gladbach, Germany), 1000 IU/mL IL-6 (Miltenyi Biotec, Bergisch Gladbach, Germany), and 1 μg/mL prostaglandin E2 (PGE2) (Sigma Aldrich, St.Louis, MO, USA) for 24 h, respectively, as described (19). Immature and mature DC were discriminated by the presence or absence of CD83 within the DC population identified as positive for CD11c and negative for CD14 (20).

Monoclonal Antibodies (mAb) and Flow Cytometry

The following mAb were used: CD3 krome orange [clone UCHT1] (Beckmann Coulter, Brea, CA, USA), CD4 phycoerythrin-cyanin 7 (PE-Cy7) [clone SK3] (BD Bioscience, Franklin Lakes, NJ, USA), CD8 pacific blue [clone B9.11] (Beckmann Coulter), CD11c PE [clone S-HCL3] (BD Bioscience), CD14 fluorescein isothiocyanate (FITC) [clone MϕP9] (BD Bioscience), CD19 allophycocyanin [clone HIB19] (BD Bioscience), CD137 allophycocyanin [clone 4B4-1] (BD Bioscience), CD83 PE [clone HB15] (Miltenyi Biotec), HLA-DP PE [clone B7/21] (21) (Leinco Technologies, Inc. St.Louis, MO, USA), HLA-DR PE [clone L243] (BD Bioscience), murine IgG2A PE [clone S43.10] (Miltenyi Biotec) and murine IgG3 PE [clone A112-3] (BD Bioscience). Flow cytometric determinations were performed on a Gallios^{TM} 10/3 cytometer (Beckman Coulter, Brea, CA, USA), using the Kaluza for Gallios Acquisition software (Version 1.0, Beckman Coulter) and the data were analyzed with Kaluza Analysis Software (Version 1.3, Beckman Coulter).

Quantification of HLA-DP and DR Cell Surface Expression Levels

HLA-DP and HLA-DR cell surface expression levels were quantified by flow cytometry staining by converting the median fluorescence intensity (MFI) observed with the relevant mAb into Molecules of Equivalent Soluble PE (MEPE) (22), using Sphero Rainbow Calibration Particles (Spherotech, Lake Forest, IL, USA) according to the manufacturer's recommendations. MEPE values were corrected for non-specific binding by subtracting the corresponding fluorescent background detected with isotype controls. Gating strategies were as follows: BLCL were analyzed as homogenous population in forward and side scatter dot plots; primary B cells and monocytes were gated in total PBMC as negative for CD4 and CD8 but positive for CD19 or CD14, respectively, before or after 48 h incubation with 200 IU/ml IFN-γ (Axxora, Farmingdale, NY, USA); immature and mature DC were analyzed by gating cells negative for CD14 and positive for CD11c after *in-vitro* differentiation.

Quantification of HLA-DPB1 Transcript Levels

HLA-DPB1 transcript levels were quantified from reverse transcribed cDNA by quantitative PCR (qPCR). Total RNA was extracted from 0.5–5 × 10^6 cells using the PureLink RNA mini kit (ThermoFisher Scientific, Waltham, MA, USA), and cDNA was synthetized from 0.5 to 2 μg total RNA with the High Capacity cDNA Reverse Transcription Kit (ThermoFisher Scientific). qPCR reactions were designed based on SYBR Green chemistry (ThermoFisher Scientific) using a previously described qPCR for GAPDH (5) as normalizer. The normalized amount of HLA-DPB1 mRNA was expressed as $2^{-\mathrm{deltaCt}}$ with delta Ct = $\mathrm{Ct_{HLA}}$-DPB1 −$\mathrm{Ct_{GAPDH}}$. qPCR primers, conditions and characteristics are shown in **Table 3**.

Identification of HLA-DPB1 3′UTR Haplotypes

HLA-DPB1 3′UTR nucleotide sequences were aligned from the IMGT/HLA database release 3.31.0 (2018-01) (23). Haplotypes were assigned according to polymorphisms located in the first

TABLE 2 | PBMC used in this study.

PBMC[a]	HLA-DPB1*			Application in this study[d]
	Allele[a]	rs9277534[b]	3′UTR Haplotype[c]	
UKE-9117	04:01, 04:02	AA	6	Exp(B,Mono,DC), T-cell culture
UKE-9149-04	02:01, 04:01	AA	6	Exp(B,Mono,DC), T-cell culture
UKE-9169-02	02:01, 04:01	AA	6	Exp(B,Mono,DC), T-cell culture
UKE-9169-03	04:01, 04:02	AA	6	Exp(B,Mono,DC), T-cell culture
UKE-9731	02:01, 04:01	AA	6	Exp(B,Mono,DC), T-cell culture
UKE-11103	02:01, 04:01	AA	6	Exp(B,Mono,DC), T-cell culture
UKE-11154	02:01, 04:01	AA	6	Exp(B,Mono,DC), T-cell culture
UKE-9068	02:01, 04:02	AA	6	Exp(B,Mono,DC)
UKE-9765	04:01, 04:02	AA	6	Exp(B,Mono,DC)
UKE-11116	02:01, 04:01	AA	6	Exp(B,Mono,DC)
UKE-9133-01	01:01, 13:01	GG	2, 3	Exp(B,Mono,DC)
UKE-9157	01:01, 03:01	GG	1, 2	Exp(B,Mono,DC)
UKE-8305B	01:01, 11:01	GG	2, 3	Exp(B,Mono,DC)
UKE-8097-A	01:01, 03:01	GG	1, 2	Exp(B,Mono,DC)
UKE-020215B	01:01, 03:01	GG	1, 2	Exp(B,Mono,DC)
UKE-8461C	01:01, 03:01	GG	1, 2	Exp(B,Mono,DC)
UKE-11012B	03:01, 13:01	GG	1, 3	Exp(B,Mono,DC)
UKE-11055A	01:01, 13:01	GG	2, 3	Exp(B,Mono,DC)
UKE-11209A	01:01, 03:01	GG	1, 2	Exp(B,Mono,DC)
UKE-11209B	03:01	GG	1	Exp(B,Mono,DC)
UKE-11177	02:01, 04:01	AA	6	Exp(B,Mono)
UKE-7547	03:01	GG	1	Exp(B,Mono)
UKE-8117A	04:01, 04:02	AA	6	T-cell culture
UKE-7595	04:01	AA	6	T-cell culture
UKE-7903-3	04:01, 04:02	AA	6	T-cell culture
UKE-020215A	04:01	AA	6	T-cell culture
UKE-8522C	04:01	AA	6	T-cell culture
UKE-7903-2	02:01, 04:02	AA	6	T-cell culture
UKE-8251C	02:01, 04:01	AA	6	T-cell culture
UKE-8360A	02:01, 04:01	AA	6	T-cell culture
UKE-8522A	02:01, 04:02	AA	6	T-cell culture
UKE-8522B	02:01, 04:02	AA	6	T-cell culture
UKE-10999	04:01	AA	6	T-cell culture
UKE-11012A	04:01, 04:02	AA	6	T-cell culture
UKE-10917	04:01, 04:02	AA	6	T-cell culture
UKE-9595	04:01, 04:02	AA	6	T-cell culture
UKE-9822	04:01	AA	6	T-cell culture
UKE-9110	02:01, 04:01	AA	6	T-cell culture
UKE-7964-2	04:01	AA	6	T-cell culture
UKE-9320B	02:01, 04:01	AA	6	T-cell culture
UKE-10294A	04:01	AA	6	T-cell culture
UKE-7713	03:01, 04:02	AG	1, 6	T-cell culture
UKE-7964-1	03:01, 04:02	AG	1, 6	T-cell culture
UKE-120315	03:01, 04:02	AG	1, 6	T-cell culture
UKE-8360B	03:01, 04:02	AG	1, 6	T-cell culture
UKE-9487	03:01, 04:01	AG	1, 6	T-cell culture
UKE-9751C	03:01, 04:02	AG	1, 6	T-cell culture
UKE-8097B	02:01, 03:01	AG	1, 6	T-cell culture
UKE-8461A	02:01, 03:01	AG	1, 6	T-cell culture
UKE-8360C	04:01, 14:01	AG	1, 6	T-cell culture
UKE-9145	04:01, 14:01	AG	1, 6	T-cell culture

[a] *PBMC were isolated from peripheral blood of 51 healthy individuals. HLA-DPB1* allele typing was performed as described in Materials and Methods.*
[b] *rs9277534-G/A typing was determined by SSP-PCR as described in Materials and Methods.*
[c] *3′UTR haplotypes were assigned based on the linkage disequilibrium to HLA-DPB1 alleles as reported in* ***Table 4****.*
[d] *PBMC samples were used for quantification of HLA-DPB1 expression (Exp) in B cells (B), monocytes (Mono) and dendritic cells (DC), and/or in functional testing of alloreactive T-cell cultures stimulated with HeLa cells expressing single HLA-DPB1 antigens (T-cell culture).*

TABLE 3 | PCR reactions used in this study.

Reaction[a]	Type[b]	Purpose	Primers[c]	Cycling conditions	Efficiency[d]
rs9277534 SSP-PCR	STD-PCR	rs9277534 SNP typing	FW-A:'ATCCATTTATGTCTCAGACCA' (rs9277534-A) FW-G:'TCCATTTATGTCTCAGACCG' (rs9277534-G) RV: 'GGTCCTATCAGGCAGATTTGCAG' (both)	95°C for 15" 60°C for 30" 72°C for 30"	N.A.
HLA-DPB1 short mRNA	qPCR	Gene expression	FW-a:'AAGAAAGTTCAACGAGGATCTGC' (exon 5) RV-b:'GAAGAAGGGAACATGGTTGGAG' (exon 6)	95°C for 15" 62°C for 1'	92%
HLA-DPB1 long mRNA	qPCR	Gene expression	FW-c:'ATGACACTCTTCTGAATTGACTG' (exon 6) RV-d:'GGTAATGATAAAACATGCTCTC' (exon 6)	95°C for 15" 62°C for 1'	97%
F1[e]	STD-PCR	Molecular cloning	FW-F1A:'ACAGGGTTCCTGAGCTC' (A-haplotype) RV-F1A:'TTGGAAGTTGAAGGTCTGTC' (A-haplotype) FW-F1G:'ACAGGGTTCCTGACCTC' (G-haplotype) RV-F1G:'TGGGAAGCTGAGGGTC' (G-haplotype)	95°C for 15" 63°C for 30" 72°C for 30"	N.A.
F2[e]	STD-PCR	Molecular cloning	FW-F2A:'TCCAGGACAGACCTTCAAC' (A-haplotype) FW-F2G:'TCCAGGACAGACCCTCAG' (G-haplotype) RV-F2:'GAAACAGTGCTTTGAATCAAAGAGC' (both)		
F3[e]	STD-PCR	Molecular cloning	FW-F3:'GCTCTTTGATTCAAAGCACTG' (both) RV-F3A: 'AAACAAACAGTCATGTTGGG' (A-haplotype) RV-F3G:'AAACAAACACTTATGTTGGGTTTTG' (G-haplotype)		
F4[e]	STD-PCR	Molecular cloning	FW-F4A:'CAAAACCCAACATGACTGTTTG' (A-haplotype) RV-F4A:'TTATTAACTCCTACTGTCTACTAAAACC' (A-haplotype) FW-F4G:'CAAAACCCAACATAAGTGTTTG' (G-haplotype) RV-F4G:'TTATTAACTCCTACTGTTTACTAAAACCC' (G-haplotype)		
F5[e]	STD-PCR	Molecular cloning	FW-F5A:'TTTAGTAGACAGTAGGAGTTAATAAAGAAG' (A-haplotype) RV-F5A:'CCATTATACAATAGTTAACATATCCCC' (A-haplotype) FW-F5G: 'TTTAGTAAACAGTAGGAGTTAATAAAGAAG' (G-haplotype) RV-F5G:' ACATTATACAATAGTTAACATATCTCCAC' (G-haplotype)		
F6[e]	STD-PCR	Molecular cloning	FW-F6A:'GGATATGTTAACTATTGTATAATGGGG' (A-haplotype) FW-F6G:'AGATATGTTAACTATTGTATAATGTGGC' (G-haplotype) RV-F6:'GAGGGCACTAAACTTGATTTG' (both)	95°C for 15" 63°C for 30" 72°C for 30"	N.A.

(Continued)

TABLE 3 | Continued

Reaction[a]	Type[b]	Purpose	Primers[c]	Cycling conditions	Efficiency[d]
F7[e]	STD-PCR	Molecular cloning	FW-F7:'CCCCCAAATCAAGTTTAGTG' (both) RV-F7A:'TGGGTCCTATCAGGCAG' (A-haplotype) RV-F7G:'CGGGTCCTATCAGGC' (G-haplotype)		
F8[e]	STD-PCR	Molecular cloning	FW-F8:'CTGCAAATCTGCCTGATAG' (both) RV-F8: 'TTCATTTAACTTCTTAATGGTAATGATAAAAC' (both)		
HLA-DPB1 exon 2-4 splicing	RT-PCR	Alternative splicing	FW-e:'GCTTCCTGGAGAGATACATC' (exon 2) RV-f:'CAGCTCGTAGTTGTGTCTGC' (exon 2) RV-g:'TTGAATGCTGCCTGGGTAG' (exon 3) RV-h: 'AGCTCCCGTCAATGTCTTAC' (exon 4)	95°C for 1' 55°C for 30" 72°C for 1'	N.A.
HLA-DPB1 exon 2	qPCR	Gene expression	FW-e:'GCTTCCTGGAGAGATACATC' (exon 2) RV-f:'CAGCTCGTAGTTGTGTCTGC' (exon 2)	95°C for 15" 62°C for 1'	100%

[a] *Reactions are reported in order of appearance.*
[b] *STD-PCR: standard PCR performed on genomic or plasmid DNA. qPCR: quantitative real-time PCR performed on cDNA obtained as described in Materials and Methods. RT-PCR: reverse transcriptase PCR performed on cDNA as described in Materials and Methods. STD-PCR and RT-PCR were performed using Amplitaq GOLD DNA polymerase and buffer (ThermoFisher Scientific), qPCR were performed using SYBR Green Real-time Mastermix (ThermoFisher Scientific).*
[c] *For each primer, name, sequence, and target region or polymorphism in HLA-DPB1 are reported. FW: forward primer; RV: reverse primer.*
[d] *Efficiency of qPCR reactions was calculated by quantifying the target template in 5-fold serial dilution of cDNA for 10 ng to 16 pg. All qPCR reactions resulted in high reaction efficiency comparable to the qPCR targeting GAPDH as reference gene (Efficiency = 93%) (5).*
[e] *F1-F8 fragments of the HLA-DPB1 3'UTR from A- or G-Haplotype were amplified by PCR and subsequently cloned downstream of luciferase gene Luc2 in pmirGLO vector (see also Figure 5). The following restriction sites were added at the 5' of each primer: NheI for forward primers and SalI for reverse primers.*

671 bp of the transcribed 3′UTR, i.e., the last 4 bp of exon 5 and the first 667 bp of exon 6. The nucleotide sequence of selected haplotypes was confirmed by direct Sanger sequencing (Seqlab, Göttingen, Germany) on both strands of a 667 bp 3′UTR PCR fragment obtained from genomic DNA according to previously described protocols (5).

Dual Luciferase Assay

HLA-DPB1 3′UTR fragments or control wild-type (WT) and mutant (mut) target sequence of hsa-miR-21 (mir21-WT and mir21-mut) were pre-amplified by PCR (primers and conditions in **Table 3**) or synthetized *in vitro* (Eurofins Genomics, Ebersberg, Germany). 3′UTR fragments and controls were cloned into the pmirGLO vector (Promega, Madison, WI, USA) downstream of the luciferase reporter gene (luc2) and transfected into HeLa cells or BLCL by electroporation with the Neon transfection system (Invitrogen, USA), according to the manufacturer's recommendations. Luciferase activity was measured after 24 h with a Dual Luciferase Reporter Assay System (Promega) using the monochromator multimode microplate reader LB 943 Mithras² (Berthold Technologies, Bad Wildbad, Germany). Luciferase activity under the control of mir21-WT or mir21-mut was used as positive and negative controls, respectively, since the expression of the relevant miRNA hsa-miR-21 was shown to be abundant in both HeLa and BLCL (24, 25). The *Renilla* luciferase gene (hRluc-neo fusion) included in the same vector was used as transfection control for normalization of the luc2 signal.

Assessment of Splicing in HLA-DPB1 mRNA by RT-PCR

Splicing between exons 2–4 of HLA-DPB1 mRNA was assessed by standard RT-PCR on total RNA extracted from BLCL; RNA and reverse-transcribed cDNA were prepared as described above. cDNA samples were used as template for 3 PCR reactions designed to target exon 2 alone, exon 2–3, and exon 2–4 with primers and PCR condition described in **Table 3**. Analysis of the PCR products was performed using standard agarose gel electrophoresis.

Alloreactive T-Cell Cultures

Alloreactive T-cell effectors were raised against individual HLA-DP alloantigens by *in vitro* stimulation of CD4+ T cells with HeLa-II cells. Briefly, CD4+ T cells were isolated from frozen PBMC of HLA-DPB1-typed healthy blood donors (**Table 2**) by MicroBeads sorting (Miltenyi Biotec, Bergisch Gladbach, Germany), and stimulated for 14 d at a 3:1 ratio with irradiated

(100 Gy) HeLa-II expressing the allogeneic HLA-DPB1 allele of interest in culture medium supplemented with 10% heat-inactivated AB human serum (Sigma-Aldrich) and 50 IU/mL IL-2 (Miltenyi Biotec, Bergisch Gladbach, Germany). After 2 weeks, T cells were re-stimulated for 24 h with fresh HeLa-II carrying the relevant allogeneic HLA-DPB1 allele or autologous HLA-DPB1 allele(s), or medium alone. The specific T-cell response was quantified by flow cytometry as the percentage of gated CD4+ T cells upregulating cell surface expression of CD137, corrected for the background response to HeLa-II expressing autologous HLA-DPB1.

Statistical Analysis

Statistical analysis was performed using the Prism 6 software (GraphPad Software, La Jolla, CA, USA), using the two-tailed unpaired *t*-test or the Wilcoxon matched-pairs signed rank Test.

RESULTS

High and Low Cell Surface Expression of HLA-DP in Relation to rs9277534 SNP in Different Cell Types

Association of the bi-allelic rs9277534-G/A SNP variants with high and low HLA-DP expression levels, respectively, was originally reported by Thomas et al. on the cell surface of primary B cells (5) and more recently observed at the transcriptional level in BLCL by Petersdorf and collaborators (8). Here we quantified HLA-DP cell surface expression on BLCL by MEPE flow cytometry, using the mAb B7/21 which recognizes a monomorphic determinant on HLA-DP (21) and was used and validated also in the previous study by Thomas et al. (5) (**Figure 1A**). Compared with rs9277534-A/A (AA), BLCL homozygous for rs9277534-G/G (GG) showed significantly higher amounts of HLA-DP molecules, while no difference was observed in HLA-DR expression (**Figure 1A**, **Table 4**). On primary B cells, we confirmed the original finding of Thomas et al. with expression levels of HLA-DP significantly higher in primary unstimulated B cells from healthy blood donors homozygous for GG in comparison to AA, while no difference was observed in HLA-DR expression (**Figure 1B**, **Table 4**). Interestingly, overnight incubation with IFN-γ to simulate inflammatory conditions abrogated these differences (**Figure 1C**, **Table 4**).

To address the question whether these observations also apply to other APC potentially relevant in allogeneic HSCT, we carried out similar analyses in primary monocytes and monocyte-derived DC. Similar to primary B cells, significant differences for HLA-DP but not HLA-DR expression were found in primary monocytes between individuals homozygous for rs9277534-A/A or rs9277534-G/G (**Figure 2A**, **Table 4**), but these differences were also abrogated after overnight incubation with IFN-γ (**Figure 2B**, **Table 4**). Importantly, no significant differences for either HLA-DP or HLA-DR expression were observed in association with rs9277534 for immature DC (**Figure 2C**, **Table 4**) or mature DC (**Figure 2D**, **Table 4**).

Genetic Control of HLA-DPB1 Transcriptional Levels in BLCL and DC

The HLA-DPB1 3′UTR is over 3000 bp in length and contains three sets of PAS, located at position 235–240, 667, and 3162, respectively (GenBank ID: NM_002121.5). The rs9277534 SNP is located at position 496 between the first and the second PAS which mediate the synthesis of at least two mRNA isoforms of different length, a short one using the more proximal and a long one using the more distal PAS. The rs9277534 SNP is contained in the long but not in the short transcript (**Figure 3A**). Transcriptional expression levels of HLA-DPB1 were comparatively determined for the short and the long transcript by qPCR in BLCL, immature and mature DC. Consistent with previous reports (5, 8) and with our findings on HLA-DP protein expression levels, BLCL homozygous for rs9277534-G/G carried significantly higher transcript levels of the short mRNA isoform lacking the rs9277534 SNP, compared with rs9277534-A/A (mean normalized expression relative to GAPDH was 0.1666 ± 0.08686 vs. 0.0665 ± 0.01387, $p < 0.01$. Transcription levels of the long mRNA isoform including the rs9277534 SNP were at least 2-log lower compared with the short, and not significantly different between the two groups of BLCL (mean normalized expression relative to GAPDH 0,0013 ± 0.00114 vs. 0.0007 ± 0.00017, $p = 0.18$; **Figure 3B**). This observation suggests that the rs9277534 SNP probably does not have a direct role in regulating mRNA transcript levels in BLCL, but that rather other, linked polymorphisms could mediate this function. Consistent with our findings on protein expression levels, no significant differences in the transcript levels of either the short or the long mRNA isoform were observed in immature and mature DC from individuals homozygous for rs9277534-G/G or rs9277534-A/A (**Figures 3C,D**).

HLA-DPB1 3′UTR Haplotypes

Polymorphic variation in HLA-DPB1 is characterized by tight LD which encompasses the entire genomic region from intron 2 to the 3′UTR (26). We aligned HLA-DPB1 3′UTR sequences from common alleles identified in Europe (27) deposited in the IMGT/HLA database (23) and found a total of 37 SNP, which gave rise to a total of 7 different haplotypes, 5 linked to rs9277534-G and 2 linked to rs9277534-A (**Figure 4A** and **Table 5**). The 5 rs9277534-G linked haplotypes 1-5 differ only by 1-3/37 SNP, while at least 28/37 SNP differences are found in the 2 rs9277534-A linked haplotypes 6 and 7, which in turn are strikingly similar to each other. Interestingly, the haplotypes are in tight LD with a STR located in intron 2 at 44 bp upstream of exon 3, with G- and A-haplotypes linked with a short and a long STR, respectively (**Table 5**). Moreover, LD also encompasses the exon sequences, with TCE groups 1 and 2 linked with the G-haplotype and TCE group 3 linked with the A-haplotype, although a number of exceptions do exist (**Table 5**).

Mapping of Regulatory Elements in the 3′UTR of HLA-DPB1 by Luciferase Assays

In order to determine whether the rs9277534 itself and/or other linked SNP might be directly involved in differential

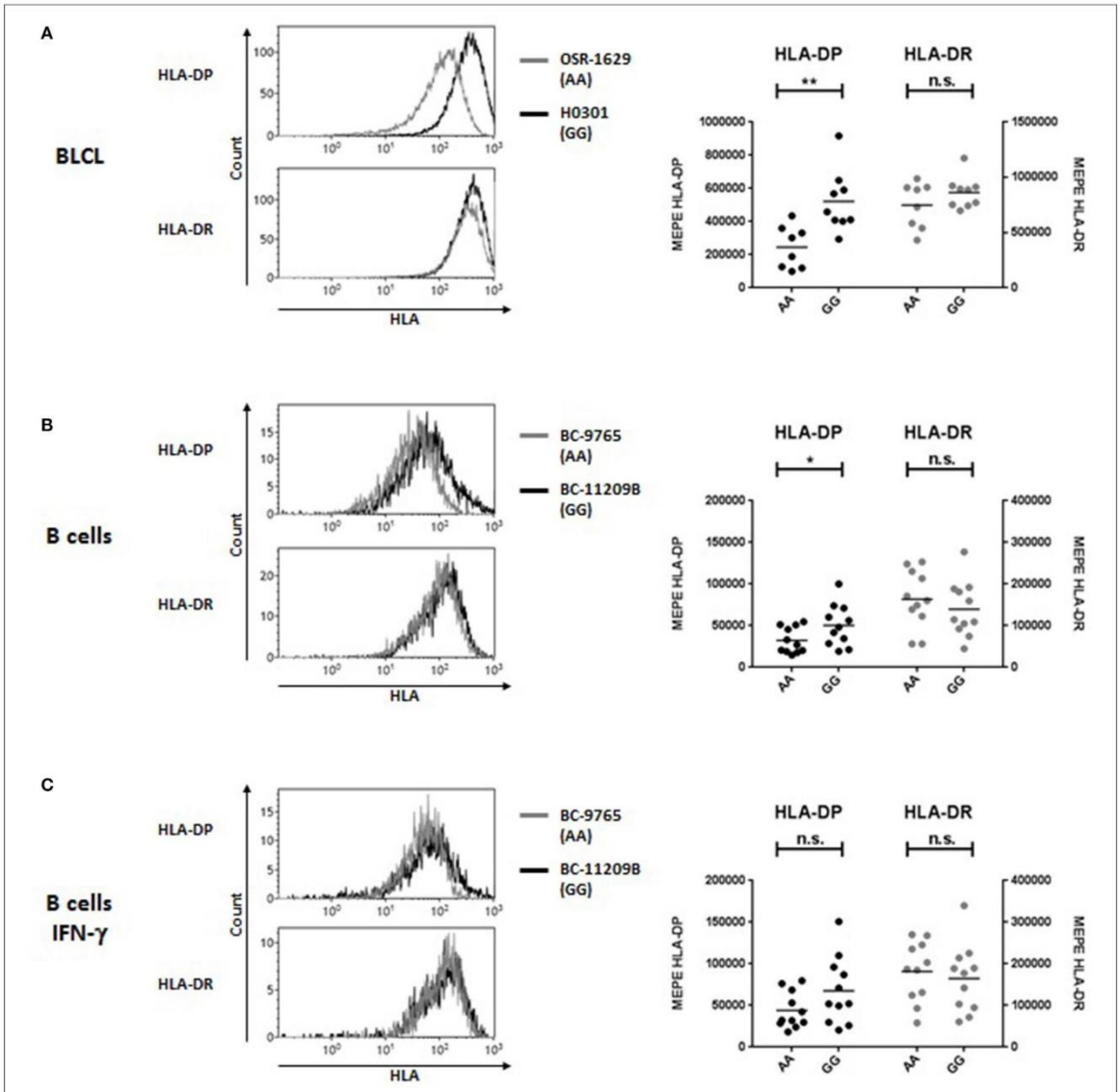

FIGURE 1 | HLA-DP and HLA-DR cell surface expression in relation with rs9277534 SNP in B cells. Cell surface staining for HLA-DP and HLA-DR was performed with the mAb B7/21 and L243, respectively, on **(A)** BLCL ($N = 17$) (**B,C**) CD19+ B cells in PBMC after 48 h incubation with medium ($N = 22$, **B**) or with 200 IU/ml IFN-γ ($N = 22$, **C**). Cells were homozygous for either rs9277534-A/A (AA) or rs9277534-G/G (GG) (**Tables 1**, **2**). Shown are two representative FACS plots (left panel) and the Molecules of Equivalent Soluble PE (MEPE) of all samples (right panels). Statistical comparisons were performed by the two-tailed unpaired *t*-test (n.s. not significant; $^{*}p < 0.05$; $^{**}p < 0.01$). Mean ± SD are reported in **Table 4**.

regulation of transcript abundance, the HLA-DPB1 3′UTR was mapped into a total of eight overlapping fragments of 100 bp each, covering the polymorphisms in the region from the stop codon to the second PAS at position 667, including rs9277534 in fragment F7 (**Figure 4B**). Fragments F1-F8 from haplotypes 1 and 6, prototypes of rs9277534-G and rs9277534-A haplotypes, respectively (**Figure 4A** and **Table 5**), were cloned downstream of a luciferase reporter gene and tested by standard luciferase assays in 4 different BLCL, a cell type in which the genetic control of HLA-DPB1 transcript levels by the rs9277534 SNP was evident. Significant differences in luciferase activity were observed between mir21-WT and

TABLE 4 | HLA-DP and HLA-DR cell surface expression in different cell types.

APC[a]	rs9277534 (N)[b]	HLA-DP[c] mean±SD	*p*	HLA-DR[c] mean±SD	*p*
BLCL	AA (8)	$2.45 \times 10^5 \pm 1.27$	**	$7.48 \times 10^5 \pm 2.06$	n.s.
	GG (9)	$5.22 \times 10^5 \pm 1.85$		$8.62 \times 10^5 \pm 1.44$	
B cell	AA (11)	$0.32 \times 10^5 \pm 0.15$	*	$1.64 \times 10^5 \pm 0.69$	n.s.
	GG (11)	$0.50 \times 10^5 \pm 0.25$		$1.40 \times 10^5 \pm 0.67$	
B cells + IFN-γ[d]	AA (11)	$0.44 \times 10^5 \pm 0.21$	n.s.	$1.82 \times 10^5 \pm 0.72$	n.s.
	GG (11)	$0.68 \times 10^5 \pm 0.40$		$1.64 \times 10^5 \pm 0.82$	
Monocytes	AA (11)	$0.17 \times 10^e \pm 0.17$	*	$1.61 \times 10^5 \pm 1.35$	n.s.
	GG (11)	$0.37 \times 10^5 \pm 0.26$		$1.83 \times 10^5 \pm 1.26$	
Monocytes + IFN-γ[e]	AA (11)	$1.02 \times 10^5 \pm 0.37$	n.s.	$4.46 \times 10^5 \pm 1.02$	n.s.
	GG (11)	$1.31 \times 10^5 \pm 0.58$		$3.81 \times 10^5 \pm 1.29$	
Immature DC	AA (10)	$1.23 \times 10^5 \pm 0.95$	n.s.	$3.73 \times 10^5 \pm 2.60$	n.s.
	GG (10)	$2.71 \times 10^5 \pm 2.20$		$3.84 \times 10^5 \pm 2.78$	
Mature DC	AA (10)	$5.56 \times 10^5 \pm 2.71$	n.s.	$10.62 \times 10^5 \pm 2.71$	n.s.
	GG (10)	$6.86 \times 10^5 \pm 5.26$		$8.36 \times 10^5 \pm 3.69$	

[a] *HLA-DP and HLA-DR expression was quantified by flow cytometry on the cell surface of different cell types as described in Materials and Methods. Lists of the APC used in this study are reported in* ***Table 1,2****.*

[b] *rs9277534-G/A as determined locally.*

[c] *Cell surface expression of HLA-DP and HLA-DR are reported as converted MEPE values as described in Materials and Methods.*

[d] *IFN-γ significantly upregulated HLA-DP and DR expression on total B cells: HLA-DP untreated $0.41x10^5 \pm 0.22$ vs. IFN-γ treated $0.56x10^5 \pm 0.34$ ($p<0.0001$); HLA-DR untreated $1.51x10^5 \pm 0.67$ vs. IFN-γ treated $1.73x10^5 \pm 0.76$ ($p<0.001$).*

[e] *IFN-γ significantly upregulated HLA-DP and DR expression on total monocytes: HLA-DP untreated $0.27x10^5 \pm 0.24$ vs. IFN-γ treated $1.17x10^5 \pm 0.50$ ($p<0.0001$); HLA-DR untreated $1.72x10^5 \pm 1.28$ vs. IFN-γ treated $4.14x10^5 \pm 1.18$ ($p<0.0001$). Statistical comparisons were performed by two-tailed unpaired t-test (n.s. not significant; $*p < 0.05$; $**p < 0.01$).*

mir21-mut used as positive and negative controls, respectively (**Figure 4C**). Compared with the positive control, none of the eight fragments, including F7 encompassing rs9277534, was able to markedly reduce luciferase activity. Moreover and importantly, no significant differences were observed when comparing luciferase activity under the control of the same fragment cloned from haplotype 1 or from haplotype 6 (**Figure 4C**). Taken together, these results did not define any major regulatory element in the 3′UTR of HLA-DPB1, suggesting that polymorphism in other regions of the gene might be involved.

Assessment of Alternative Splicing Associated With the HLA-DPB1 Intron 2 STR

We next asked whether the long isoform of the intron 2 STR, in linkage with the low expression rs9277534-A variant (**Table 5**) (28), could induce a splicing defect involving exon 3, which is in relatively close vicinity to the 3′ end of the STR. The resulting hypothetical alternatively spliced transcript would join exon 2 and exon 4, resulting in a complete loss of function (**Figure 5A**). To test this hypothesis, we designed PCR primers in exon 2, 3 and 4, which would give rise to PCR products of different sizes in the presence or absence of alternative splicing. In a total of 6 BLCL homozygous for a rs9277534-G or a rs9277534-A haplotype, no evidence for alternative splicing was observed (**Figure 5B**).

Expression Model vs. TCE Structural Model of Donor-Recipient HLA-DPB1 Mismatches in HSCT

Two currently proposed HLA-DPB1 mismatch models, i.e., the Expression model and the TCE Structural model (**Figure 6A**), take the classical concept of donor-recipient matching for polymorphic HLA-DPB1 alleles further to matching for HLA-DPB1 allele groups. For the Expression model, each of the two HLA-DPB1 alleles in patient and donor is assigned to the rs9277534-G or –A group, based on tight LD between this SNP and the different alleles (8). The Expression model is considered to be predictive only for single HLA-DPB1 mismatches in GvH direction, i.e., recipient and donor are matched for the HLA-DPB1 allele on one haplotype but mismatched for the other. These single mismatches are classified as unfavorable ("high-risk") if there is a patient-specific HLA-DPB1 allele not shared by the donor which belongs to the high expression rs9277534-G group, and as favorable ("low risk") if it belongs to the low expression rs9277534-A group. All other combinations, including those in which there is no patient-specific single mismatched allele, or in which patient and donor are mismatched for HLA-DPB1 alleles on both haplotypes, cannot be classified as favorable or unfavorable by the Expression model ("not applicable"; **Figure 6B**, left panel). For the TCE Structural model, each of the two HLA-DPB1 alleles in patient and donor is assigned to one of the three TCE groups, and mismatches are considered to be unfavorable ("non-permissive") if the TCE group of the highest order in the hierarchy is not shared between patient and donor, while all other mismatch combinations

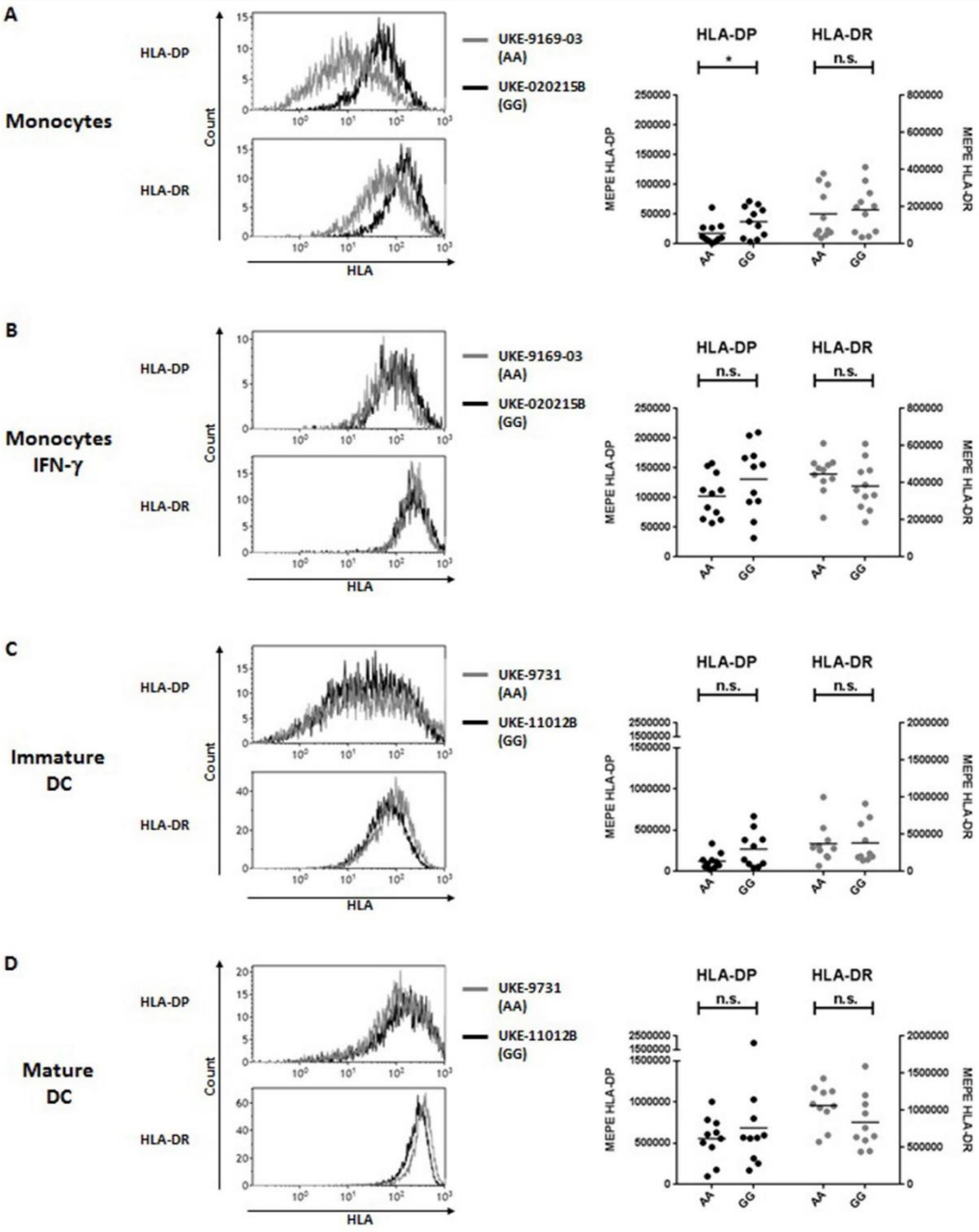

FIGURE 2 | HLA-DP and HLA-DR cell surface expression in relation with rs9277534 SNP in monocytes and DC. Cell surface staining for HLA-DP and HLA-DR was performed with the mAb B7/21 and L243, respectively, on **(A,B)** CD14+ monocytes in PBMC after 48 h incubation with medium ($N = 22$) (**A**) or with 200 IU/ml IFN-γ ($N = 22$) (**B**), and on **(C)** monocyte-derived immature DC ($N = 20$) or **(D)** mature DC ($N = 20$). Cells were homozygous for either rs9277534-A/A (AA) or rs9277534-G/G (GG) (**Table 2**). Shown are two representative FACS plots (left panel) and the Molecules of Equivalent Soluble PE (MEPE) of all samples (right panels). Statistical comparisons were performed by the two-tailed unpaired *t*-test (n.s. not significant; $^*p < 0.05$). Mean ± SD are reported in **Table 4**.

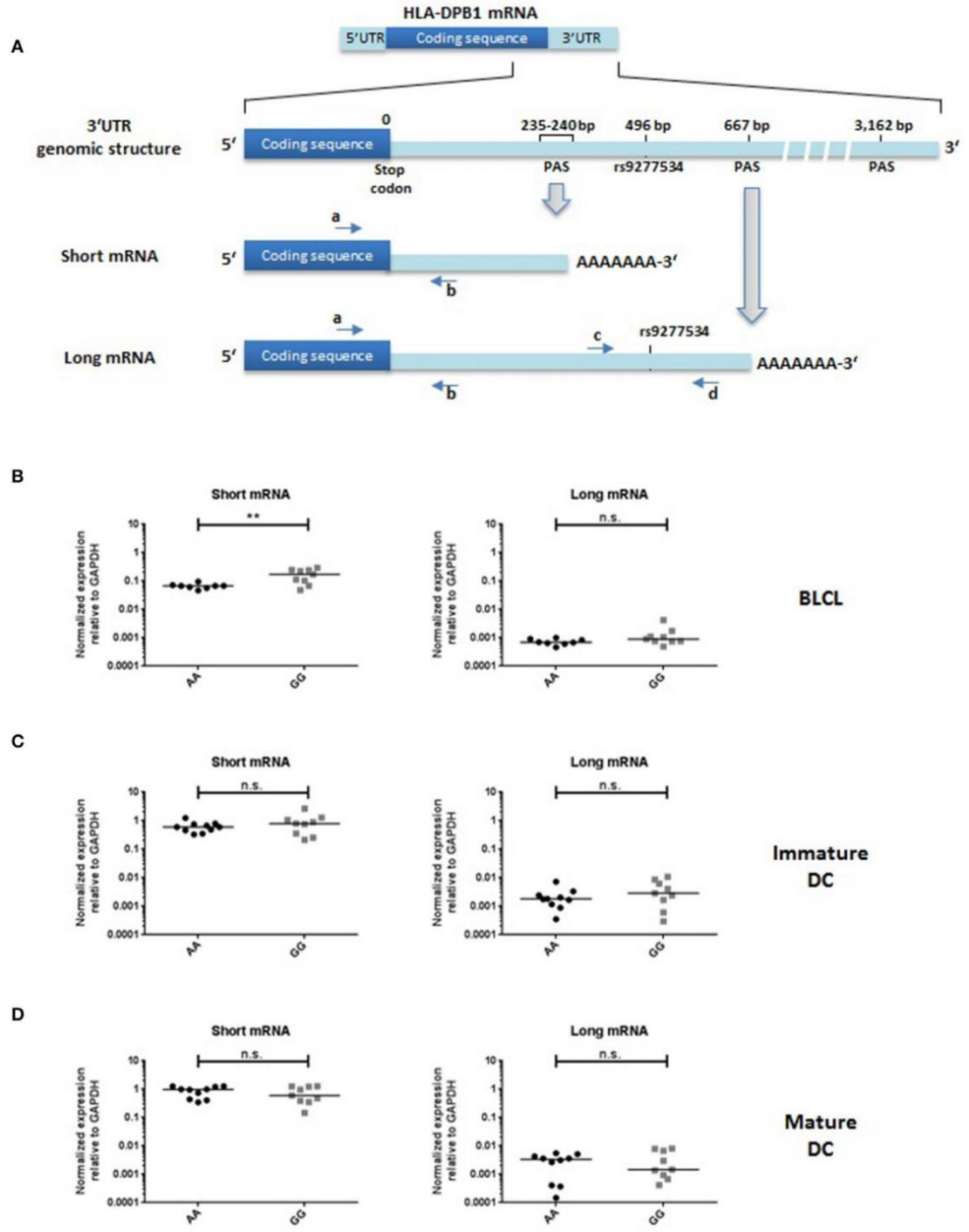

FIGURE 3 | HLA-DPB1 transcriptional expression in relation with rs9277534 SNP in BLCL and DC. **(A)** Schematic representation of the HLA-DPB1 genomic structure and a short and long form of mRNA generated by two different polyadenylation sites (PAS) about 400 bp apart, as reported in the GenBank database (ID: NM_002121.5). Note that the long but not the short mRNA includes the rs9277534 SNP. Primer locations for qPCR quantification of both transcripts are indicated as arrows a-b or c-d (see also **Table 3**). Primers "a" and "b" anneal to both the short and the long mRNA, while primers "c" and "d" are specific for the long mRNA. **(B–D)** Short (left panel) and long (right panel) HLA-DPB1 mRNA was quantified in BLCL ($N = 17$, **B**), immature DC ($N = 20$, **C**) and mature DC ($N = 20$, **D**), by qPCR relative to GAPDH as described in Materials and Methods. Cells were homozygous for either rs9277534-A/A (AA) or rs9277534-G/G (GG) (**Tables 1**,**2**). Statistical comparisons were performed by the two-tailed unpaired *t*-test (n.s. not significant; $^{**}p < 0.01$).

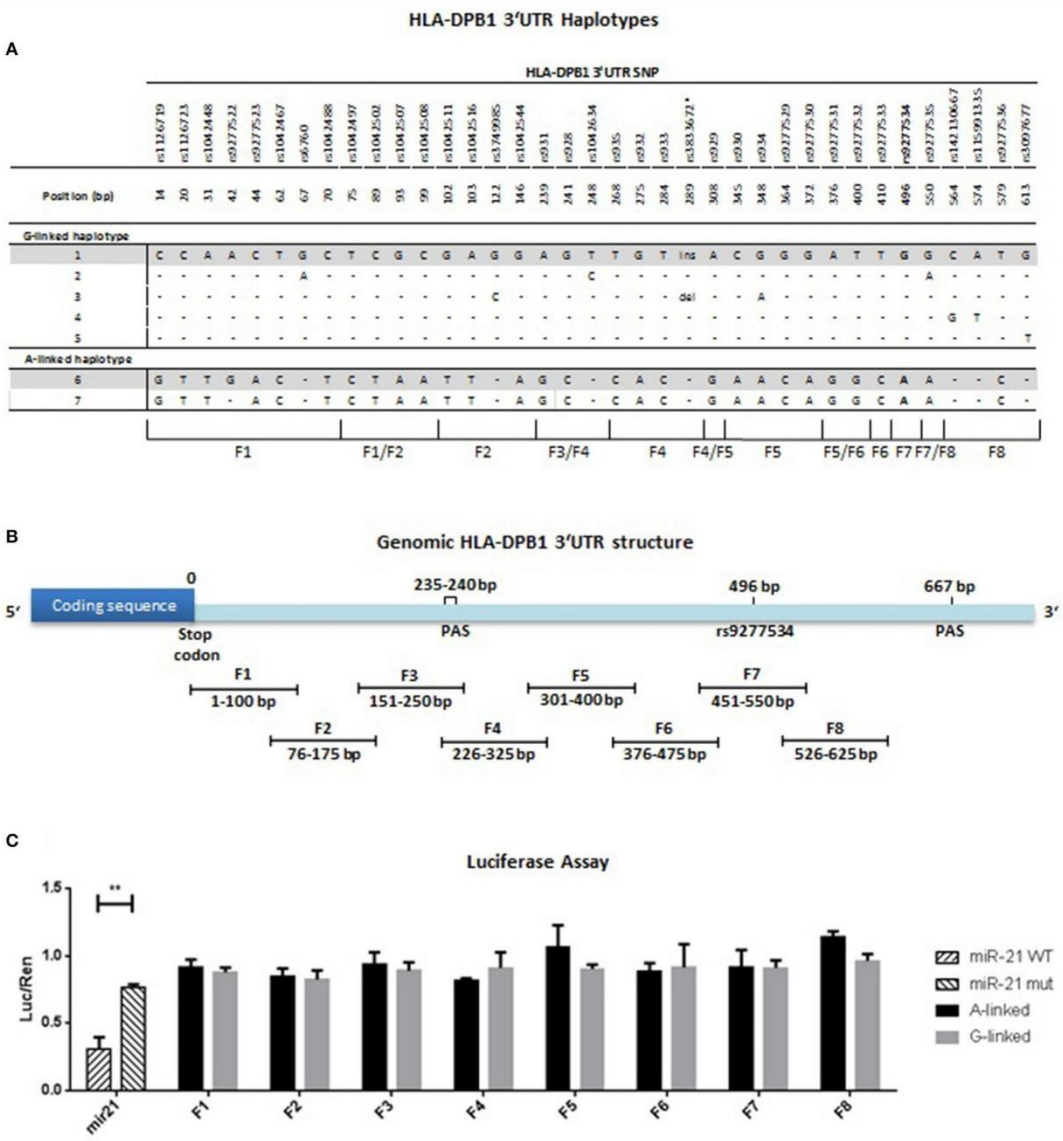

FIGURE 4 | HLA-DPB1 3′UTR haplotype identification, mapping and regulatory activity. **(A)** 671 bp of the 3′UTR (i.e., from the last 4 bp of exon 5 to the first 667 bp of exon 6) of 30 HLA-DPB1 alleles reported as common in Europe (**Table 5**) (27) were aligned from the IMGT/HLA database (23). Nucleotide polymorphism was restricted to 37 bi-allelic SNP and one insertion/deletion (ins/del), and is listed with the respective position relative to the stop codon in exon 5. The rs9277534-G/A SNP located at position 496 is indicated in bold. A total of 7 haplotypes were identified, 5 linked to rs9277534-G and 2 linked to rs9277534-A. Nucleotide polymorphism is indicated with reference to the rs9277534-G linked haplotype 1, dashes indicate sequence identity. Haplotypes 1 and 6 were chosen for further studies and are highlighted in gray. **(B)** Mapping of the HLA-DPB1 3′UTR. Eight overlapping fragments F1-F8, each 100 bp in length with an overlap of 25 bp, were PCR-amplified from haplotype 1 (BLCL AKIBA, HLA-DPB1*09:01) or haplotype 6 (BLCL MOU, HLA-DPB1*04:01) and cloned into the pmirGLO dual luciferase vector as described in Materials and Methods. Note that fragment F7 comprises rs9277534. **(C)** Gene regulation by HLA-DPB1 3′UTR fragments assessed with the dual luciferase assay. Four different BLCL (APA, MOU, BM21, OSR-6924) were transfected with pmirGLO containing F1-F8 from haplotype 1 (rs9277534-G linked, gray bars) or from haplotype 6 (rs9277534-A linked, black bars), respectively, and tested in 3 independent experiments by dual luciferase assays as described in Materials and Methods. A total of 12 independent analyses were performed for each fragment. 50 bp fragments containing the miR21 WT or mutated target sequence were used as positive and negative control, respectively (striped bars). Results are expressed as mean of fold-change of luciferase activity respect to renilla (luc/ren). Bars refer to SD between 12 independent experiments. Statistical comparisons were performed by the Wilcoxon matched-pairs signed rank Test (**$p < 0.001$).

TABLE 5 | HLA-DPB1 3′UTR haplotypes identified in this study.

		HLA-DPB1*			
3′UTR Haplotype	Frequency[a]	Allele[b]	TCE group[c]	Expression SNP[d]	Intron 2 STR[e]
1	0.191	03:01[f]	2	G	$(GGAA)_4$
		05:01	3		
		06:01	2		
		09:01[f]	1		
		10:01[f]	1		
		14:01	2		
		15:01[f]	3		
		45:01	2		
		63:01	3		
		130:01	3		
2	0.062	01:01[f]	3		
		26:01	3		
3	0.045	11:01	3		
		13:01[f]	3		
4	0.006	19:01	2		
		34:01	3		
5	n.o.	18:01	3		
6	0.677	02:01[f]	3	A	$(GGAA)_{10-16}$
		02:02	3		
		04:01[f]	3		
		04:02[f]	3		
		17:01	1		
		23:01	3		
		41:01	3		
		46:01	3		
		47:01	3		
		105:01	3		
		124:01	2		
		126:01	3		
7	n.o.	30:01	1		

[a]*Combined frequency of HLA-DPB1 alleles as reported in www.allelefrequencies.net database (England Northwest population, N=2960), n.o. not observed.*
[b]*Listed are only those HLA-DPB1 alleles reported to be common in Europe (27).*
[c]*TCE group assigned according to Crivello et al (15).*
[d]*Linked allelic variant at SNP rs9277534 associated with high (G) or low (A) HLA-DPB1 expression (8).*
[e]*Number of repeated units of the STR (AAGG)n in Intron 2 of HLA-DPB1 as reported in IMGT/HLA databank (Release 3.31.0 2018-01, http://www.ebi.ac.uk/ipd/imgt/hla).*
[f]*For this allele, the 3′UTR sequence was confirmed by direct sequencing on a homozygous BLCL as listed in* ***Table 2****.*

are considered to be favorable ("permissive"; **Figure 6B**, right panel).

Risk prediction by the Expression model and the TCE Structural model was comparatively evaluated in 379 HLA-DPB1-mismatched donor-recipient pairs from the University Hospital Essen (29). In the Expression model, 73 (19.3%) and 130 (34.3%) were classified as high or low-risk, respectively, while 176 (46.4%) pairs were "not applicable" because they did not satisfy the pre-requisite of single HLA-DPB1 allele mismatches in GvH direction (**Figure 6C**, upper left panel). In the TCE Structural model, all 379 (100%) pairs could be classified and of these, 175 (46.2%) and 204 (53.8%) fell into the non-permissive or the permissive group, respectively (**Figure 6C**, upper right panel).

The overall concordance between the two models was 36.7% with assignment as permissive/low risk in 98/379 (25.9%) and non-permissive/high risk in 41/379 (10.8%) pairs, respectively. 240/379 (63.3%) assignments were discordant. These were due to differential risk prediction in 64/379 (16.8%) pairs, with even distribution between permissive/high risk and non-permissive/low risk, each occurring in 32/379 (8.4%) pairs (**Figure 6C**, lower panel). The remaining discordances were due to non-applicability of the expression model, occurring in 176/379 (46.5%) pairs. Of these, a slightly higher number (102/176; 58%) was classified as non-permissive, compared to the remaining 74/176 (42%) pairs classified as permissive, corresponding to an overall percentage of 26.9% and 19.6%, respectively, in the cohort overall (**Figure 6C**, lower panel).

T-Cell Alloreactivity To HLA-DP Expressed in HeLa-II Cells in the Absence of the 3′UTR

The most frequent HLA-DPB1 alleles in rs9277534-G and rs9277534-A haplotypes belong to TCE groups 1/2 and TCE group 3, respectively (**Table 5**). However, a few exceptions exist, in particular HLA-DPB1*17:01 from TCE group 1, which is associated with the rs9277534-A haplotype 6, and HLA-DPB1*01:01 and *05:01, both of which are found in linkage with the rs9277534-G haplotypes 2 and 1, respectively (**Table 5** and **Figure 7A**). We expressed 5 HLA-DPB1 alleles representative of the "correct" association (HLA-DPB1*09:01, *10:01 – TCE group 1 and rs9277534-G; HLA-DPB1*02:01, *04:01, *04:02 – TCE group 3 and rs9277534-A), as well as the 3 abovementioned alleles with the "inverted" association in HeLa-II cells, under the control of a retroviral promoter (18), in the absence of the 3′UTR (**Figure 7A**). As expected, the significant differences observed in BLCL between transcript levels of HLA-DPB1 alleles from TCE group 1 (rs9277534-G) and TCE group 3 (rs9277534-A) were abrogated in transduced HeLa-II cells (**Figure 7B**).

The transduced HeLa-II cells were used in a total of 178 independent cultures for a 14-day stimulation of CD4+ T cells from healthy donors expressing at least one HLA-DPB1 allele from TCE group 3 and a second allele from either TCE group 2 or 3, for whom allogeneic HLA-DPB1 alleles from TCE group 1 and TCE group 3 represent a non-permissive and a permissive mismatch, respectively. The alloreactive response was measured after overnight re-challenging with the original target cell, compared to HeLa-II transduced with autologous HLA-DPB1 as background control, as the percentage of CD4+ T cells up-regulating the activation marker CD137, which has been shown to best describe the total pool of alloreactive T cells (30) (**Figure 8A**). In line with our previous reports (31), the mean alloresponse to HeLa-II transfected with HLA-DPB1 alleles from TCE group 1 (non-permissive mismatch) was significantly higher compared with TCE group 3 (permissive mismatch; 36.43±12.13 vs. 19.00 ± 15.58, $p < 0.0001$, **Figure 8B**). Consistent with its classification as TCE group 1, the median response to allogeneic HLA-DPB1*17:01 was also significantly higher compared with

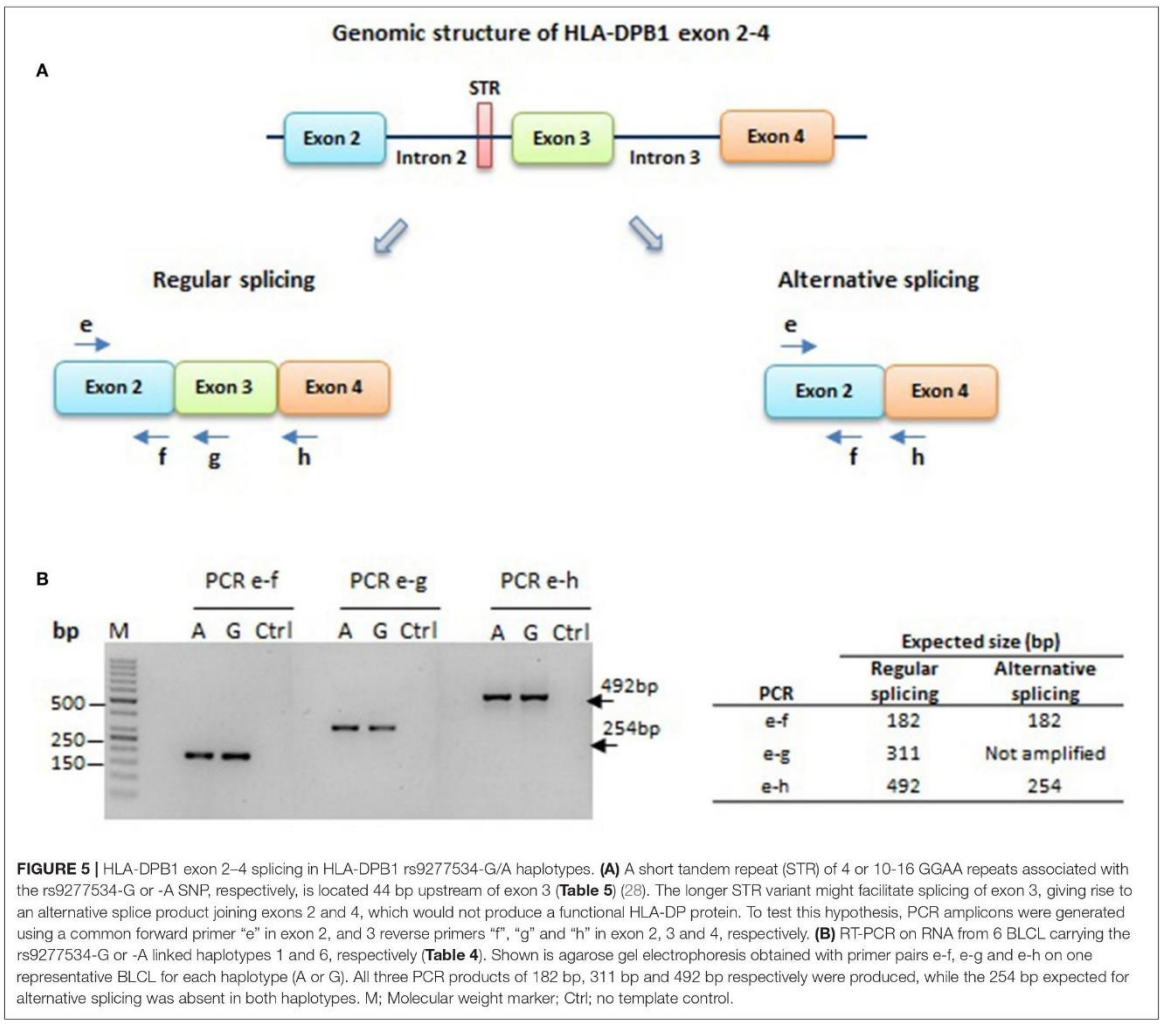

PCR	Expected size (bp) Regular splicing	Alternative splicing
e-f	182	182
e-g	311	Not amplified
e-h	492	254

FIGURE 5 | HLA-DPB1 exon 2–4 splicing in HLA-DPB1 rs9277534-G/A haplotypes. **(A)** A short tandem repeat (STR) of 4 or 10-16 GGAA repeats associated with the rs9277534-G or -A SNP, respectively, is located 44 bp upstream of exon 3 (**Table 5**) (28). The longer STR variant might facilitate splicing of exon 3, giving rise to an alternative splice product joining exons 2 and 4, which would not produce a functional HLA-DP protein. To test this hypothesis, PCR amplicons were generated using a common forward primer "e" in exon 2, and 3 reverse primers "f", "g" and "h" in exon 2, 3 and 4, respectively. **(B)** RT-PCR on RNA from 6 BLCL carrying the rs9277534-G or -A linked haplotypes 1 and 6, respectively (**Table 4**). Shown is agarose gel electrophoresis obtained with primer pairs e-f, e-g and e-h on one representative BLCL for each haplotype (A or G). All three PCR products of 182 bp, 311 bp and 492 bp respectively were produced, while the 254 bp expected for alternative splicing was absent in both haplotypes. M; Molecular weight marker; Ctrl; no template control.

TCE group 3 (38.58 ± 13.96, $p < 0.0001$, **Figure 8B**), and not significantly different from TCE group 1, despite similar cell surface expression levels (**Figure 7B**). For HLA-DPB1*01:01, responses were highly variable (27.68 ± 19.26) and significantly different from other alleles of both TCE group 1 and TCE group 3 although both with a low level of significance ($p < 0.05$ each). Similar levels of responses were also seen against HLA-DPB1*05:01 (30.75 ± 14.85), although these were significantly different ($p < 0.01$) from TCE group 3 but not from TCE group 1 (**Figure 8B**). These data suggest that HLA-DPB1*01:01 and 05:01 appear to represent a functionally distinct TCE group. Taken together, our data demonstrate that also in the absence of significant differences of transcriptional HLA-DPB1 alleles on HeLa-II cells, differential *in vitro* T-cell alloreactivity against permissive and non-permissive mismatches can be appreciated.

DISCUSSION

Our study provides new insights into the cell type-specific and mechanistic basis of the association between the rs9277534 SNP and HLA-DPB1 expression, and into the relationship between the Expression model and the TCE Structural model for HLA-DPB1 mismatch risk prediction in HSCT.

We are the first to broaden observations on the genetic control of HLA-DPB1 expression from BLCL and primary unstimulated B cells, in which this issue has been studied so far (5, 8), to other cell types likely to play a role in GvHD, such as DC and IFN-γ-stimulated B cells and monocytes. We confirm the previous data from the literature, but also show that the observed differences in HLA-DPB1 cell surface and transcriptional expression levels between the two rs9227534 variants are abrogated after IFN-γ stimulation, and could not be observed in either mature or

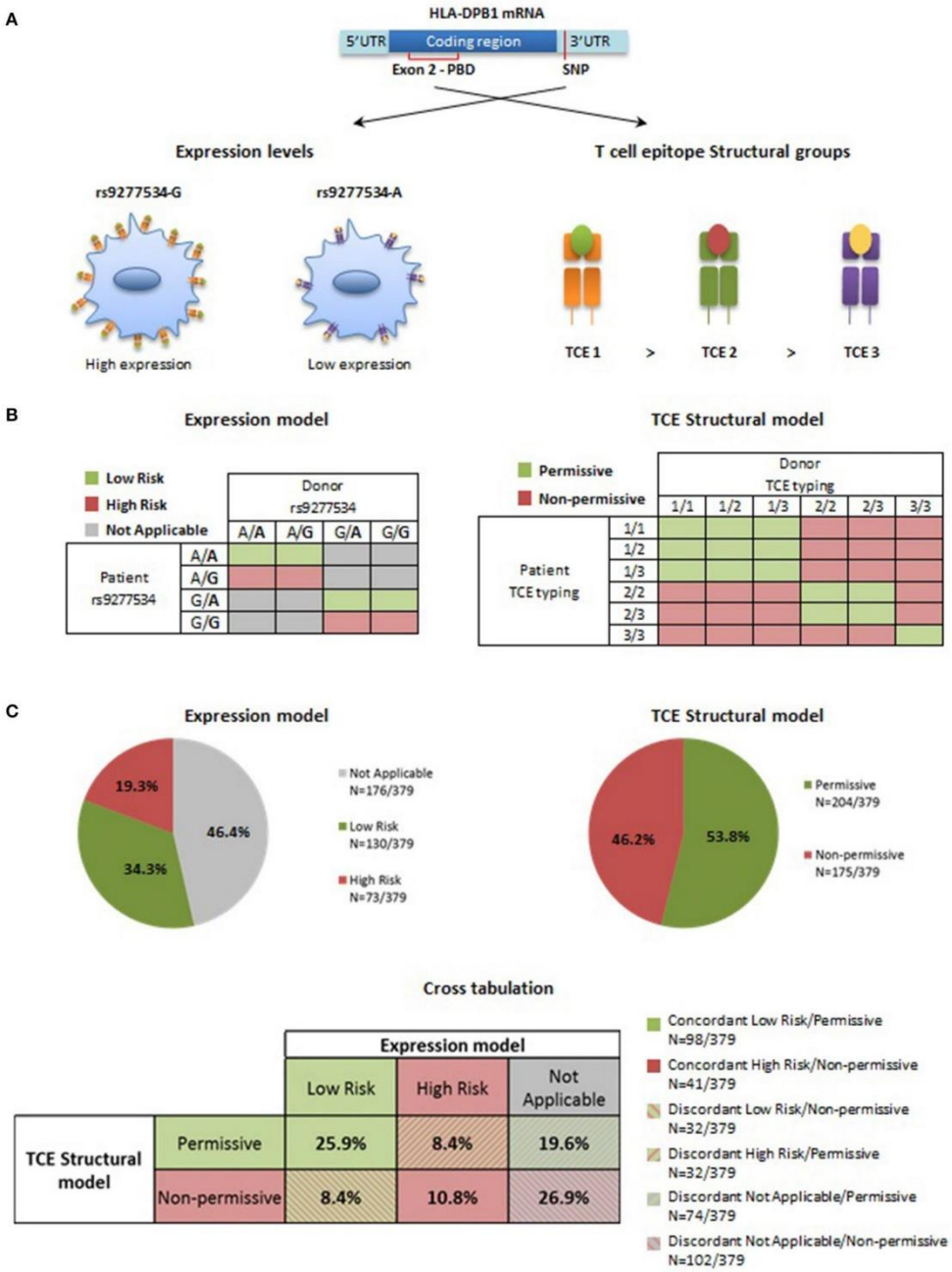

FIGURE 6 | Expression model and TCE Structural model for HLA-DPB1 mismatches in HSCT. **(A)** Genetic control of HLA-DP expression levels is mediated by the biallelic SNP rs9277534, with a high expression G- and a low expression A-variant (5). Three distinct TCE groups with decreasing immunogenicity are determined by structural amino acid variability in the peptide binding domain (PBD) encoded by exon 2 in the HLA-DPB1 coding region (9, 15). **(B)** For Expression matching, only truly single HLA-DPB1 allele mismatches in GvH direction are considered, leading to a number of combinations that cannot be classified (in gray). For the others,

(Continued)

FIGURE 6 | favorable (low risk, in green) and unfavorable (high risk, in pink) pairs are those where the mismatched allele in the patient carries the low expression rs9277534-A or the high expression rs9277534-G variant, respectively (8). For TCE Structural matching, favorable (permissive, in green) pairs are those in which patient and donor share at least one HLA-DPB1 allele from the TCE group with the highest immunogenicity; the others are predicted to be unfavorable (non-permissive, in pink) (9, 11). **(C)** Percentage of favorable and unfavorable HLA-DPB1 mismatches according to the Expression model or the TCE Structural model in 379 donor-recipient pairs from the University Hospital Essen. Pies indicate the percentage of favorable (low risk or permissive, in green) or unfavorable (high risk or non-permissive, in pink) combinations according to the two models, or of pairs that cannot be classified by the Expression model (not applicable, gray). Classification by the two models has a 36.7% concordance (filled boxes in the cross-tabulation), and 63.3% discordances (striped boxes in the cross-tabulation), either due to differential risk assignment (background green or pink) or to non-applicability of the Expression model (background gray).

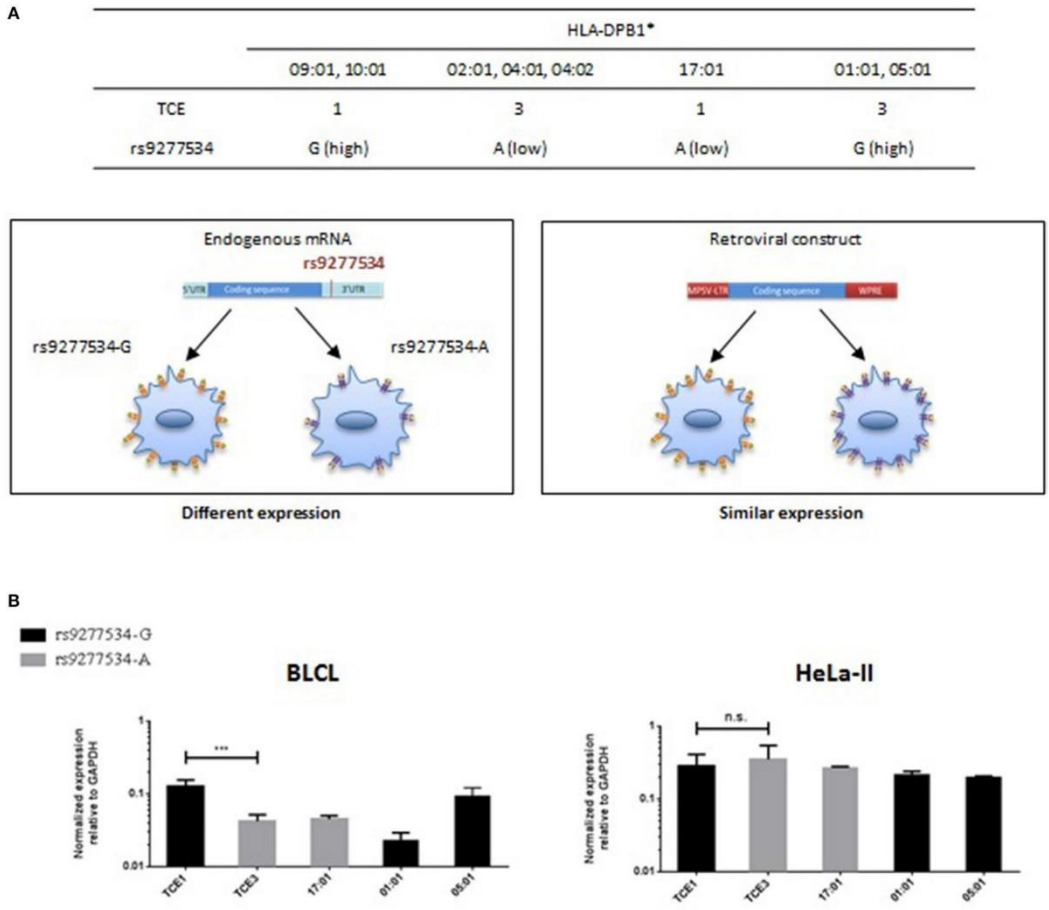

FIGURE 7 | HLA-DPB1 transcriptional expression in BLCL or transduced HeLa-II in relation with rs9277534 and TCE groups. **(A)** The most frequent HLA-DPB1 alleles from TCE group 1 and 3 are linked with rs9277534-G and -A, respectively (16). Notable exceptions are HLA-DPB1*17:01 (TCE 1), HLA-DPB1*01:01 and HLA-DPB1*05:01 (both TCE 3), in which this association is inverted. Endogenous HLA-DPB1 expression is predicted to be genetically regulated by the rs9277534-G/A SNP in the 3′UTR, while this regulation is abrogated in cells transfected with the HLA-DPB1 coding region under a retroviral promoter in the absence of the 3′UTR. **(B)** Transcriptional expression of HLA-DPB1 in BLCL or transduced HeLa-II. HLA-DPB1 mRNA was quantified by RT-qPCR relative to GAPDH in BLCL homozygous for alleles from TCE 1 (rs9277534-G) or TCE 3 (rs9277534-A) (**Table 1**), or in HeLa-II after retroviral vector transduction with the same alleles. Shown are the mean results and SD from 3 independent experiments. Statistical comparisons were performed by the two-tailed unpaired *t*-test (***$p < 0.001$).

immature DC. Although a simplistic model, IFN-γ stimulation can be seen as a simulation of an inflammatory environment that can be induced by different triggers such as the conditioning regimen or infection after HSCT, and has been described as one of the most relevant cytokines mediating toxic effects of GvHD after HSCT (32). In addition, DC are crucial APCs for inducing alloresponses particularly from naïve T cells (33, 34). The observation that genetic control of HLA-DP expression

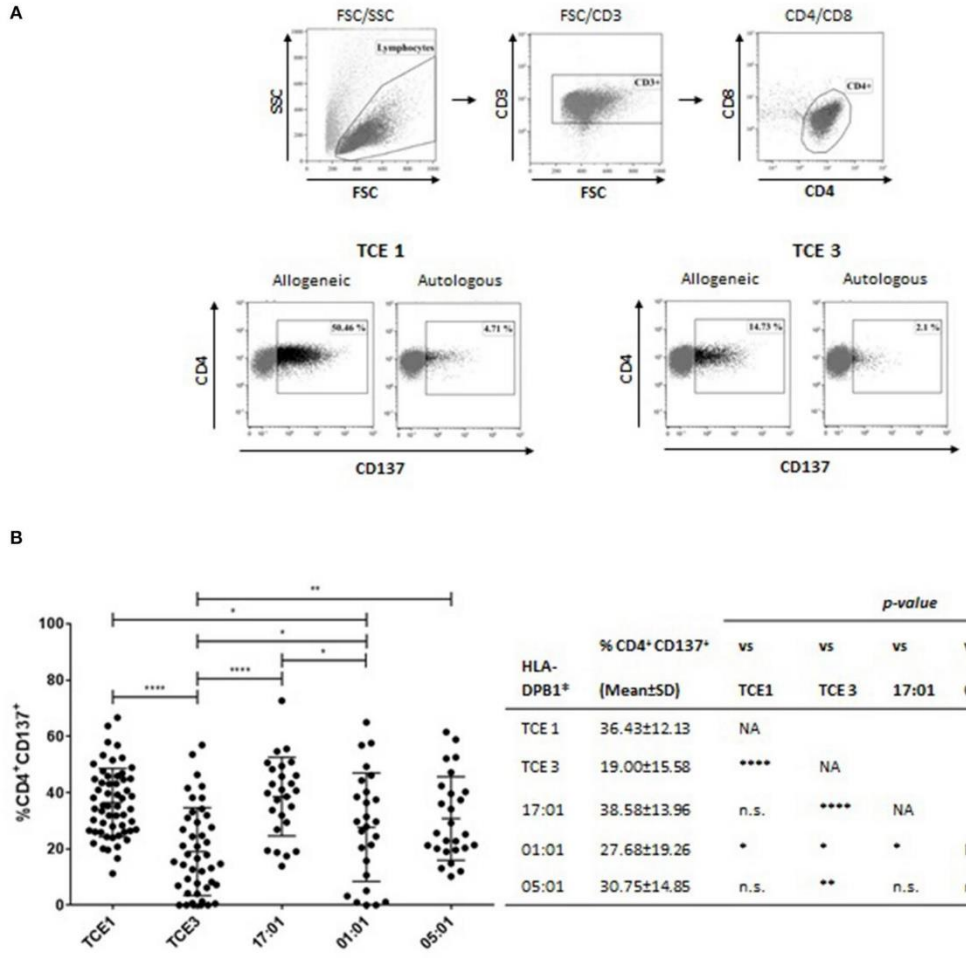

HLA-DPB1*	% CD4+ CD137+ (Mean±SD)	p-value vs TCE1	vs TCE 3	vs 17:01	vs 01:01	vs 05:01
TCE 1	36.43±12.13	NA				
TCE 3	19.00±15.58	****	NA			
17:01	38.58±13.96	n.s.	****	NA		
01:01	27.68±19.26	*	*	*	NA	
05:01	30.75±14.85	n.s.	**	n.s.	n.s.	NA

FIGURE 8 | T-cell allorecognition of HLA-DPB1 from different TCE groups expressed by HeLa-II**.** PBMC from HLA-DPB1 TCE 1-negative responders carrying at least one HLA-DPB1 TCE 3 were stimulated with irradiated HeLa-II transduced with allogeneic HLA-DPB1 TCE 1 or TCE 3 for 14 d, as described in Materials and Methods. For HLA-DPB1 typing of responders see **Table 2**. Cultures were re-stimulated for 24 h with HeLa-II expressing the original allogeneic HLA-DPB1, or with autologous HLA-DPB1, and the percentage of CD4+ T cells expressing the CD137 activation marker was assayed by flow cytometry. **(A)** Gating strategy and representative FACS plots for re-stimulation with autologous HLA-DPB1 or with allogeneic HLA-DPB1 from TCE 1 or TCE 3. Note the higher percentage of CD137+ CD4+ T cells in response to TCE 1 compared to TCE 3. **(B)** Results of CD137 assays in response to TCE 1, TCE 3 or HLA-DPB1*17:01, *01:01 or *05:01 for a total of 178 independent co-cultures. Statistical comparisons were performed by the two-tailed unpaired *t*-test (*$p < 0.05$; **$p < 0.01$; ****$p < 0.0001$).

by the rs9227534 variation appears to be dampened under these conditions challenges its relevance in the clinical setting. However, it has to be noted that ours are *in vitro* models that may not fully reflect the *in vivo* situation. Moreover and importantly, monocytes and B cells in a non-inflammatory context can have an important role in triggering alloimmunity, in particular from the memory T-cell repertoire, which is involved in direct recognition of major histocompatibility antigen mismatches (35, 36).

We are also the first to attempt a mechanistic understanding of the observed genetic control of HLA-DPB1 expression in BLCL. The data we obtained by 3′UTR mapping and analysis in luciferase assays in BLCL argue against a direct regulatory role of rs9277534 or of any other linked SNP in the 3′UTR. A limitation here is again that this *in vitro* assay might not adequately reflect the *in vivo* situation, which is likely to be considerably more complex, leaving us with the possibility that the interplay of different factors might still lead to a direct SNP regulation of expression. We also did not obtain evidence for alternative splicing associated with the linked intron 2 STR (37). An alternative role of this STR might be transcriptional

repression rather than alternative splicing, a possibility we were unable to test due to the unavailability of an appropriate *in vitro* model. In line with observations made by others for HLA-A (2), we show that also the HLA-DPB1 3′UTR contains two alternative PAS giving rise to a short and a long mRNA transcript. In contrast to their observations on HLA-A, however, the long HLA-DPB1 transcript was expressed at markedly lower levels compared to the short one. This further argues against a dominant direct role of the rs9277534 SNP in HLA-DPB1 expression, since this SNP is contained in the long but not in the majorly abundant short mRNA transcript. Nevertheless, a role of the SNP in binding factors involved in determining the stability of the long mRNA, such as described for HLA-A, cannot be ruled out.

Regarding risk prediction by the Expression model and the TCE structural model in HSCT, we show a relatively limited degree of 36.7% concordance in our exemplary cohort, which however was due in the majority of cases to non-applicability of the Expression model. It should be noted that the Expression model requires the presence of a single HLA-DPB1 mismatch in GvH direction, thereby precluding its application in almost half of the pairs under analysis. In 203 pairs where risk prediction could be performed by both models, concordance was 68.5%, with discordances evenly distributed between high risk/permissive and low risk/non-permissive pairs. These data might be useful for clinicians intending to apply either model in unrelated donor searches. The clinical cohort was too small to make any meaningful comparative outcome analysis, and future studies in large well-powered studies are clearly warranted to understand the comparative clinical validity of the two models.

From the experimental side, we confirm and extend our previous observations that non-permissive HLA-DPB1 TCE group mismatches elicit significantly stronger T-cell alloresponses compared to permissive mismatches *in vitro* (31, 38). The observation that this holds true also independently from HLA-DPB1 expression levels is in line with our unpublished evidence that permissiveness of TCE group mismatches is dependent on the HLA-DP peptidome (in preparation). This finding is of practical relevance for the 3 HLA-DPB1 alleles with inverted haplotype association studied here, i.e., HLA-DPB1*17:01, *01:01, and *05:01, which together have a 8.61% frequency in Europeans (39). While our data confirm the assignment to TCE group 1 of HLA-DPB1*17:01, they suggest that HLA-DPB1*01:01 and *05:01 belong to a yet distinct functional TCE group. Interestingly, it has recently been suggested that HLA-DPB1 alleles could be divided into two supertypes having HLA-DP2 and DP5 as respective prototypes (40). This division was based on the allele frequency profile of the Japanese population, and was correlated with the incidence of acute GvHD after unrelated HSCT. The HLA-DP2 and DP5 supertypes closely resemble our TCE group 3 and TCE group 1/2, respectively, with the main exception being HLA-DP5. The data from the present study corroborate the functional distinctness of HLA-DP5, despite its FD score of 2.97 which is clearly compatible with its assignment to TCE group 3 (FD score >2.00) (15). Based on these considerations, and on our unpublished findings on the role of peptides in determining HLA-DP permissiveness, we suggest that TCE group 3, which was coined to accommodate all alleles not included in TCE groups 1 and 2, might be more heterogeneous than expected. In line with this, we have previously suggested that HLA-DP2 might constitute a separate TCE4 group, and shown clinical associations equal to or in some cohorts superior to the 3-group TCE algorithm with clinical outcome (10, 11). Further studies are clearly needed to verify this important point.

In conclusion, the data from the present study suggest that genetic control of HLA-DPB1 expression is cell-type dependent and dampened by inflammatory conditions. While we failed to identify a mechanism for the observed association of HLA-DPB1 expression levels with rs9277534 SNP variation in certain cell types under steady state conditions, our data argue against a direct role of this SNP and in favor of indirect mechanisms mediated by linked polymorphisms. The data on clinical risk prediction by the Expression model and the TCE structural model, as well as those on significant modulation of *in vitro* T cell alloreactivity by HLA-DPB1 TCE groups in the presence of similar transcriptional expression levels, suggest that the two models are partially overlapping yet largely distinct. These findings are of both biological and potentially clinical relevance for investigators interested in unrelated stem cell donor selection.

ETHICS STATEMENT

This study was carried out in accordance with the recommendations of University Hospital Essen with written informed consent from all subjects in accordance with the Declaration of Helsinki. The protocol was approved by the local Ethics Committee of University Hospital Essen.

AUTHOR CONTRIBUTIONS

PC, TM, and KF designed the study. TM, EA-B, MM, M-ML, and PC performed experiments. PvB and JF produced the transduced HeLa cells; DB contributed HLA typings of the transplant cohort. PH contributed PBMC from healthy blood donors and their HLA typing. PC and KF wrote the manuscript. TM and EA-B proof-read the manuscript.

FUNDING

This project was supported by grants from the Deutsche José Carreras Leukämie Stiftung (DJCLS R 15/02 and DJCLS 01R-2017), the Dr. Werner Jackstädt Stiftung and the Josef-Senker Stiftung.

ACKNOWLEDGMENTS

The authors would like to thank Prof. Mirko Trilling (Institute of Virology, University Hospital Essen) for assistance in the establishment of the Dual Luciferase Assays.

REFERENCES

1. Apps R, Qi Y, Carlson JM, Chen H, Gao X, Thomas R, et al. Influence of HLA-C expression level on HIV control. *Science* (2013) 340:87–91. doi: 10.1126/science.1232685
2. Kulkarni S, Ramsuran V, Rucevic M, Singh S, Lied A, Kulkarni V, et al. Posttranscriptional regulation of HLA-A protein expression by alternative polyadenylation signals involving the RNA-binding protein syncrip. *J Immunol*. (2017) 199:3892–9. doi: 10.4049/jimmunol.1700697
3. Ramsuran V, Kulkarni S, O'Huigin C, Yuki Y, Augusto DG, Gao X, et al. Epigenetic regulation of differential HLA-A allelic expression levels. *Hum Mol Genet*. (2015) 24:4268–75. doi: 10.1093/hmg/ddv158
4. Rene C, Lozano C, Villalba M, Eliaou JF. 5' and 3′ untranslated regions contribute to the differential expression of specific HLA-A alleles. *Eur J Immunol*. (2015) 45:3454–63. doi: 10.1002/eji.201545927
5. Thomas R, Thio CL, Apps R, Qi Y, Gao X, Marti D, et al. A novel variant marking HLA-DP expression levels predicts recovery from hepatitis B virus infection. *J Virol*. (2012) 86:6979–85. doi: 10.1128/JVI.00406-12
6. Ramsuran V, Naranbhai V, Horowitz A, Qi Y, Martin MP, Yuki Y, et al. Elevated HLA-A expression impairs HIV control through inhibition of NKG2A-expressing cells. *Science* (2018) 359:86–90. doi: 10.1126/science.aam8825
7. Petersdorf EW, Gooley TA, Malkki M, Bacigalupo AP, Cesbron A, Du Toit E, et al. HLA-C expression levels define permissible mismatches in hematopoietic cell transplantation. *Blood* (2014) 124:3996–4003. doi: 10.1182/blood-2014-09-599969
8. Petersdorf EW, Malkki M, O'HUigin C, Carrington M, Gooley T, Haagenson MD, et al. High HLA-DP expression and graft-versus-host disease. *N Eng J Med*. (2015) 373:599–609. doi: 10.1056/NEJMoa1500140
9. Zino E, Frumento G, Marktel S, Sormani MP, Ficara F, Di Terlizzi S, et al. A T-cell epitope encoded by a subset of HLA-DPB1 alleles determines nonpermissive mismatches for hematologic stem cell transplantation. *Blood* (2004) 103:1417–24. doi: 10.1182/blood-2003-04-1279
10. Crocchiolo R, Zino E, Vago L, Oneto R, Bruno B, Pollichieni S, et al. Nonpermissive HLA-DPB1 disparity is a significant independent risk factor for mortality after unrelated hematopoietic stem cell transplantation. *Blood* (2009) 114:1437–44. doi: 10.1182/blood-2009-01-200378
11. Fleischhauer K, Shaw BE, Gooley T, Malkki M, Bardy P, Bignon JD, et al. Effect of T-cell-epitope matching at HLA-DPB1 in recipients of unrelated-donor haemopoietic-cell transplantation: a retrospective study. *Lancet Oncol*. (2012) 13:366–74. doi: 10.1016/S1470-2045(12)70004-9
12. Pidala J, Lee SJ, Ahn KW, Spellman S, Wang HL, Aljurf M, et al. Nonpermissive HLA-DPB1 mismatch increases mortality after myeloablative unrelated allogeneic hematopoietic cell transplantation. *Blood* (2014) 124:2596–606. doi: 10.1182/blood-2014-05-576041
13. Fleischhauer K, Shaw BE. HLA-DP in unrelated hematopoietic cell transplantation revisited: challenges and opportunities. *Blood* (2017) 130:1089–96. doi: 10.1182/blood-2017-03-742346
14. Oran B, Saliba RM, Carmazzi Y, de Lima M, Rondon G, Ahmed S, et al. Effect of nonpermissive HLA-DPB1 mismatches after unrelated allogeneic transplantation with *in vivo* T-cell depletion. *Blood* (2018) 131:1248–57. doi: 10.1182/blood-2017-07-798751
15. Crivello P, Zito L, Sizzano F, Zino E, Maiers M, Mulder A, et al. The impact of amino acid variability on alloreactivity defines a functional distance predictive of permissive HLA-DPB1 mismatches in hematopoietic stem cell transplantation. *Biol Blood Marrow Transplant*. (2015) 21:233–41. doi: 10.1016/j.bbmt.2014.10.017
16. Fleischhauer K. Immunogenetics of HLA-DP–A new view of permissible mismatches. *N Eng J Med*. (2015) 373:669–72. doi: 10.1056/NEJMe1505539
17. Hui-Yuen J, McAllister S, Koganti S, Hill E, Bhaduri-McIntosh S. Establishment of epstein-barr virus growth-transformed lymphoblastoid cell lines. *J Vis Exp*. (2011) 57:e3321. doi: 10.3791/3321
18. Rutten CE, van Luxemburg-Heijs SA, van der Meijden ED, Griffioen M, Oudshoorn M, Willemze R, et al. HLA-DPB1 mismatching results in the generation of a full repertoire of HLA-DPB1-specific CD4+ T cell responses showing immunogenicity of all HLA-DPB1 alleles. *Biol Blood Marrow Transpl*. (2010) 16:1282–92. doi: 10.1016/j.bbmt.2010.03.018
19. Dauer M, Obermaier B, Herten J, Haerle C, Pohl K, Rothenfusser S, et al. Mature dendritic cells derived from human monocytes within 48 hours: a novel strategy for dendritic cell differentiation from blood precursors. *J Immunol*. (2003) 170:4069–76 doi: 10.4049/jimmunol.170.8.4069
20. Nair S, Archer GE, Tedder TF. Isolation and generation of human dendritic cells. *Curr. Protoc. Immunol*. (2012) Chapter 7:Unit7 32. doi: 10.1002/0471142735.im0732s99
21. Robbins PA, Evans EL, Ding AH, Warner NL, Brodsky FM. Monoclonal antibodies that distinguish between class II antigens (HLA-DP, DQ, and DR) in 14 haplotypes. *Hum Immunol*. (1987) 18:301–13 doi: 10.1016/0198-8859(87)90077-2
22. Schwartz A, Wang L, Early E, Gaigalas A, Zhang YZ, Marti GE, et al. Quantitating fluorescence intensity from fluorophore: the definition of MESF assignment. *J Res Natl Inst Stand Technol*. (2002) 107:83–91. doi: 10.6028/jres.107.009
23. Robinson J, Halliwell JA, Hayhurst JD, Flicek P, Parham P, Marsh SG. The IPD and IMGT/HLA database: allele variant databases. *Nucleic Acids Res*. (2015) 43(Database issue):D423–31. doi: 10.1093/nar/gku1161
24. Wang X, Tang S, Le SY, Lu R, Rader JS, Meyers C, et al. Aberrant expression of oncogenic and tumor-suppressive microRNAs in cervical cancer is required for cancer cell growth. *PLoS ONE* (2008) 3:e2557. doi: 10.1371/journal.pone.0002557
25. Skalsky RL, Corcoran DL, Gottwein E, Frank CL, Kang D, Hafner M, et al. The viral and cellular microRNA targetome in lymphoblastoid cell lines. *PLoS Pathog*. (2012) 8:e1002484. doi: 10.1371/journal.ppat.1002484
26. Schone B, Bergmann S, Lang K, Wagner I, Schmidt AH, Petersdorf EW, et al. Predicting an HLA-DPB1 expression marker based on standard DPB1 genotyping: linkage analysis of over 32,000 samples. *Hum Immunol*. (2018) 79:20–7. doi: 10.1016/j.humimm.2017.11.001
27. Sanchez-Mazas A, Nunes JM, Middleton D, Sauter J, Buhler S, McCabe A, et al. Common and well-documented HLA alleles over all of Europe and within European sub-regions: a catalogue from the European Federation for Immunogenetics. *HLA* (2017) 89:104–13. doi: 10.1111/tan.12956
28. Barsakis K, Babrzadeh F, Chi A, Mindrinos MN, Fernandez-Vina M. OR34 Examination of HLA-DP intron/exon variation identifies two DPB1 evolutionary groups including intron 2 STR variants that may regulate DPB1 expression levels. Abstract in: The American Society for Histocompatibility and immunogenetics: 42nd annual meeting abstracts September 26 – 30, 2016 Hyatt Regency St. Louis at the Arch, St. Louis, Missouri. *Hum Immunol*. (2016) 77(Supplement):31. doi: 10.1016/j.himimm.2016.07.053
29. Crivello P, Heinold A, Rebmann V, Ottinger HD, Horn PA, Beelen DW, et al. Functional distance between recipient and donor HLA-DPB1 determines nonpermissive mismatches in unrelated HCT. *Blood* (2016) 128:120–9. doi: 10.1182/blood-2015-12-686238
30. Litjens NH, de Wit EA, Baan CC, Betjes MG. Activation-induced CD137 is a fast assay for identification and multi-parameter flow cytometric analysis of alloreactive T cells. *Clin Exp Immunol*. (2013) 174:179–91. doi: 10.1111/cei.12152
31. Sizzano F, Zito L, Crivello P, Crocchiolo R, Vago L, Zino E, et al. Significantly higher frequencies of alloreactive CD4+ T cells responding to nonpermissive than to permissive HLA-DPB1 T-cell epitope disparities. *Blood* (2010) 116:1991–2. doi: 10.1182/blood-2010-05-284687
32. Wang H, Yang YG. The complex and central role of interferon-gamma in graft-versus-host disease and graft-versus-tumor activity. *Immunol Rev*. (2014) 258:30–44. doi: 10.1111/imr.12151
33. Cherel M, Choufi B, Trauet J, Cracco P, Dessaint JP, Yakoub-Agha I, et al. Naive subset develops the most important alloreactive response among human CD4+ T lymphocytes in human leukocyte antigen-identical related setting. *Eur J Haematol*. (2014) 92:491–6. doi: 10.1111/ejh.12283
34. Distler E, Bloetz A, Albrecht J, Asdufan S, Hohberger A, Frey M, et al. Alloreactive and leukemia-reactive T cells are preferentially derived from naive precursors in healthy donors: implications for immunotherapy with memory T cells. *Haematologica* (2011) 96:1024–32. doi: 10.3324/haematol.2010.037481

35. Amir AL, D'Orsogna LJ, Roelen DL, van Loenen MM, Hagedoorn RS, de Boer R, et al. Allo-HLA reactivity of virus-specific memory T cells is common. *Blood* (2010) 115:3146–57. doi: 10.1182/blood-2009-07-234906
36. Su CA, Fairchild RL. Memory T cells in transplantation. *Curr Transplant Rep.* (2014) 1:137–46. doi: 10.1007/s40472-014-0018-5
37. Bagshaw ATM. Functional mechanisms of microsatellite DNA in eukaryotic genomes. *Genome Biol Evol.* (2017) 9:2428–43. doi: 10.1093/gbe/evx164
38. Arrieta-Bolanos E, Crivello P, Metzing M, Meurer T, Ahci M, Rytlewski J, et al. Alloreactive T cell receptor diversity against structurally similar or dissimilar HLA-DP antigens assessed by deep sequencing. *Front Immunol.* (2018) 9:280. doi: 10.3389/fimmu.2018.00280
39. Hollenbach JA, Madbouly A, Gragert L, Vierra-Green C, Flesch S, Spellman S, et al. A combined DPA1∼DPB1 amino acid epitope is the primary unit of selection on the HLA-DP heterodimer. *Immunogenetics* (2012) 64:559–69. doi: 10.1007/s00251-012-0615-3
40. Morishima S, Shiina T, Suzuki S, Ogawa S, Sato-Otsubo A, Kashiwase K, et al. Evolutionary basis of HLA-DPB1 alleles affects acute GVHD in unrelated donor stem cell transplantation. *Blood* (2018) 131:808–17. doi: 10.1182/blood-2017-08-801449

Conflict of Interest Statement: The authors declare that the research was conducted in the absence of any commercial or financial relationships that could be construed as a potential conflict of interest.

6.2. Article II

Author contributions

Alloreactive T Cell Receptor Diversity against Structurally Similar or Dissimilar HLA-DP Antigens Assessed by Deep Sequencing

Esteban Arrieta-Bolaños, Pietro Crivello, Maximilian Metzing, **Thuja Meurer**, Müberra Ahci, Julie Rytlewski, Marissa Vignali, Erik Yusko, Peter van Balen, Peter A. Horn, J. H. Frederik Falkenburg and Katharina Fleischhauer

Original Research article in Frontiers in Immunology

Impact factor: 4.716 (2018)

Status: published on 19th February 2018, Frontiers in Immunology

DOI: 10.3389/fimmu.2018.00280

PubMed-ID: 29520276

Contributions:

- Conception: 15 %
- Experimental work: 25 %
- Data analysis: 25 %
- Statistical analysis: 25 %
- Writing the manuscript: 15 %
- Revising the manuscript: 15 %

Katharina Fleischhauer ……..

(Prof. Dr. Katharina Fleischhauer)

T. Meurer ……..

(Thuja Meurer)

frontiers in Immunology

ORIGINAL RESEARCH
published: 19 February 2018
doi: 10.3389/fimmu.2018.00280

Alloreactive T Cell Receptor Diversity against Structurally Similar or Dissimilar HLA-DP Antigens Assessed by Deep Sequencing

*Esteban Arrieta-Bolaños[1], Pietro Crivello[1], Maximilian Metzing[1], Thuja Meurer[1], Müberra Ahci[1], Julie Rytlewski[2], Marissa Vignali[2], Erik Yusko[2], Peter van Balen[3], Peter A. Horn[4], J. H. Frederik Falkenburg[3] and Katharina Fleischhauer[1,5]**

[1] Institute for Experimental Cellular Therapy, University Hospital Essen, Essen, Germany, [2] Adaptive Biotechnologies, Seattle, WA, United States, [3] Department of Hematology, Leiden University Medical Center, Leiden, Netherlands, [4] Institute for Transfusion Medicine, University Hospital Essen, Essen, Germany, [5] German Cancer Consortium (DKTK), Heidelberg, Germany

OPEN ACCESS

Edited by:
Marcelo Anibal Fernandez-Vina, University of Texas MD Anderson Cancer Center, United States

Reviewed by:
Lloyd Joseph Andrew D'Orsogna, Fiona Stanley Hospital, Australia
Bjarne Kuno Møller, Aarhus University Hospital, Denmark

***Correspondence:**
Katharina Fleischhauer
katharina.fleischhauer@uk-essen.de

Specialty section:
This article was submitted to Alloimmunity and Transplantation, a section of the journal Frontiers in Immunology

Received: 06 December 2017
Accepted: 31 January 2018
Published: 19 February 2018

Citation:
Arrieta-Bolaños E, Crivello P, Metzing M, Meurer T, Ahci M, Rytlewski J, Vignali M, Yusko E, van Balen P, Horn PA, Falkenburg JHF and Fleischhauer K (2018) Alloreactive T Cell Receptor Diversity against Structurally Similar or Dissimilar HLA-DP Antigens Assessed by Deep Sequencing. Front. Immunol. 9:280. doi: 10.3389/fimmu.2018.00280

T cell alloreactivity is mediated by a self-human leukocyte antigen (HLA)-restricted T cell receptor (TCR) repertoire able to recognize both structurally similar and dissimilar allogeneic HLA molecules (i.e., differing by a single or several amino acids in their peptide-binding groove). We hypothesized that thymic selection on self-HLA molecules could have an indirect impact on the size and diversity of the alloreactive response. To test this possibility, we used TCR Vβ immunophenotyping and immunosequencing technology in a model of alloreactivity between self-HLA selected T cells and allogeneic HLA-DPB1 (DPB1) differing from self-DPB1*04:02 by a single (DPB1*02:01) or several (DPB1*09:01) amino acids in the peptide-binding groove. CD4+ T cells from three different self-DPB1*04:01,*04:02 individuals were stimulated with HeLa cells stably transduced with the relevant peptide processing machinery, co-stimulatory molecules, and HLA-DP. Flow cytometric quantification of the DPB1-specific T cell response measured as upregulation of the activation marker CD137 revealed significantly lower levels of alloreactivity against DPB1*02:01 compared with DPB1*09:01 (mean CD4+CD137+ frequency 35.2 ± 9.9 vs. 61.5 ± 7.7%, respectively, $p < 0.0001$). These quantitative differences were, however, not reflected by differences in the breadth of the alloreactive response at the Vβ level, with both alloantigens eliciting specific responses from all TCR-Vβ specificities tested by flow cytometry, albeit with higher levels of reactivity from most Vβ specificities against DPB1*09:01. In line with these observations, *TCRB*-CDR3 immunosequencing showed no significant differences in mean clonality of sorted CD137+CD4+ cells alloreactive against DPB1*02:01 or DPB1*09:01 [0.39 (0.36–0.45) and 0.39 (0.30–0.46), respectively], or in the cumulative frequencies of the 10 most frequent responding clones (55–67 and 58–62%, respectively). Most of the clones alloreactive against DPB1*02:01 (68.3%) or DPB1*09:01 (75.3%) were characterized by low-abundance (i.e., they were not appreciable among the pre-culture T cells). Interestingly, however, their cumulative frequency was lower against DPB1*02:01 compared with DPB1*09:01 (mean cumulative frequency 35.3 vs. 50.6%, respectively). Our data show that, despite lower levels

of alloreactivity, a similar clonal diversity can be elicited by structurally similar compared with structurally dissimilar HLA-DPB1 alloantigens and demonstrate the power of *TCRB* immunosequencing in unraveling subtle qualitative changes not appreciable by conventional methods.

Keywords: T-cell alloreactivity, T-cell receptor repertoire, next-generation sequencing, human leukocyte antigen-DPB1, permissive mismatches

INTRODUCTION

T cell alloreactivity against the human leukocyte antigen (HLA) system is a major barrier to successful transplantation of organs and stem cells. Alloreactivity is mediated by a T cell repertoire shaped by thymic selection to be self-HLA restricted, but at the same time capable of recognizing non-self-HLA. The fact that a large proportion of T cells is capable of recognizing previously unseen alloantigens (1, 2) remains an enigma of T cell biology. T cell alloreactivity involves a complex interplay between the polymorphic foreign HLA molecule, the peptides being presented by it, and the self T cell receptor (TCR) (3). Although the relative contribution of each of these components to alloreactivity is not completely understood, it is conceivable that amino acid changes in the peptide-binding region of a given HLA molecule may ensue changes in the biochemical and/or structural properties of the binding pockets, thereby impacting the amino acid sequence and/or conformation of peptides able to be presented by it. Alternatively, these amino acid changes could directly affect the interaction between the HLA molecule and the TCR (4). Whether the number of amino acid differences in the peptide-binding region of the HLA molecule results in higher or lower levels of alloreactivity and whether this arises from a broader or narrower alloreactive T cell response is a matter of debate.

Of note, it has been shown that even a single amino acid difference in the peptide-binding region of HLA class I molecules HLA-B*44:02 and B*44:03 can elicit a T cell response sufficient to cause allograft rejection (5) or graft-vs.-host disease (GvHD) (6) after hematopoietic stem cell transplantation (HSCT). In addition, *in vitro* measurements of the patient–donor immune response before HSCT, mainly based on direct recognition of mismatched HLA class I antigens, have suggested that the number of amino acid differences is inversely correlated with the amount of direct T cell allorecognition (7), although this concept was not supported by clinical associations with HSCT outcome (8). Our understanding, control, and capacity to harness alloreactivity in the transplantation setting are still incomplete.

HLA-DPB1 (DPB1) represents an attractive model for the study of alloreactive responses to HLA molecules. Previous work by us (9) and others (10, 11) has shown differential alloreactivity to allogeneic DPB1 according to a functional classification of its different allelic variants (12). Amino acid changes resulting in structural and functional dissimilarities between DPB1 alleles were shown to have a strong median impact on alloreactive responses to these molecules (13), allowing for the classification of DPB1 mismatches as permissive (structural similarity and low alloreactivity) or non-permissive (structural dissimilarity and higher alloreactivity) in the clinical setting (14, 15). Importantly, the classification of a mismatch as permissive or non-permissive depends on the self-HLA background of the responder, following the concepts of thymic T cell education (16). However, direct evidence for the hypothesis that thymic selection on self-alleles has an indirect impact on the size and diversity of the alloreactive response has yet to be obtained. Here, we have sought to fill this gap by characterizing the alloreactive TCR diversity from self-DPB1*04:01,*04:02 individuals against alloantigens carrying a single (DPB1*02:01) or multiple (DPB1*09:01) amino acid differences in the peptide-binding groove using a unique system of single-DPB1 allele-expressing cells, and TCR Vβ immunophenotype and deep immunosequencing of the *TCRB* gene.

MATERIALS AND METHODS

Subjects and Cells

Buffy coats from three healthy blood donors were obtained in order to isolate peripheral blood mononuclear cells (PBMC) by Ficoll centrifugation. All blood donors had been typed as self-DPB1*04:01,*04:02 by standard molecular methods and were CMV seronegative. Demographic details of each subject are presented in **Table 1**. PBMC were then used to isolate untouched CD4+ T cells *via* magnetic beads according to the manufacturer's instructions (Miltenyi Biotec GmbH, Bergisch Gladbach, Germany). Purified CD4+ T cells (average 97.7%, range: 96.7–98.3% of live cells, with a CD8+ mean content of 0.02%, range: 0.01–0.04%) were used as responders in coculture with stimulating cells as described subsequently. All participants gave informed consent, and this study was approved by the local ethics committee of University Hospital Essen.

Expansion of DPB1-Specific CD4+ Cells

In order to expand DPB1-specific alloreactive T cells, purified CD4+ cells from each donor were cocultured with HeLa cells expressing single specific HLA-DP molecules as described previously (17, 18). In brief, HeLa cells, which normally do not express HLA class II molecules, were retrovirally transduced with specific HLA-DP molecules (DPB1 and the naturally associated DPA1

TABLE 1 | HLA, CMV, and demographic data for the healthy subjects used in this study.

Subject	DPB1 typing	CMV serostatus	Age (years)	Gender
R1	*04:01,*04:02	Negative	67	Male
R2	*04:01,*04:02	Negative	56	Male
R3	*04:01,*04:02	Negative	21	Female

CMV, cytomegalovirus; HLA, human leukocyte antigen; R, responder.

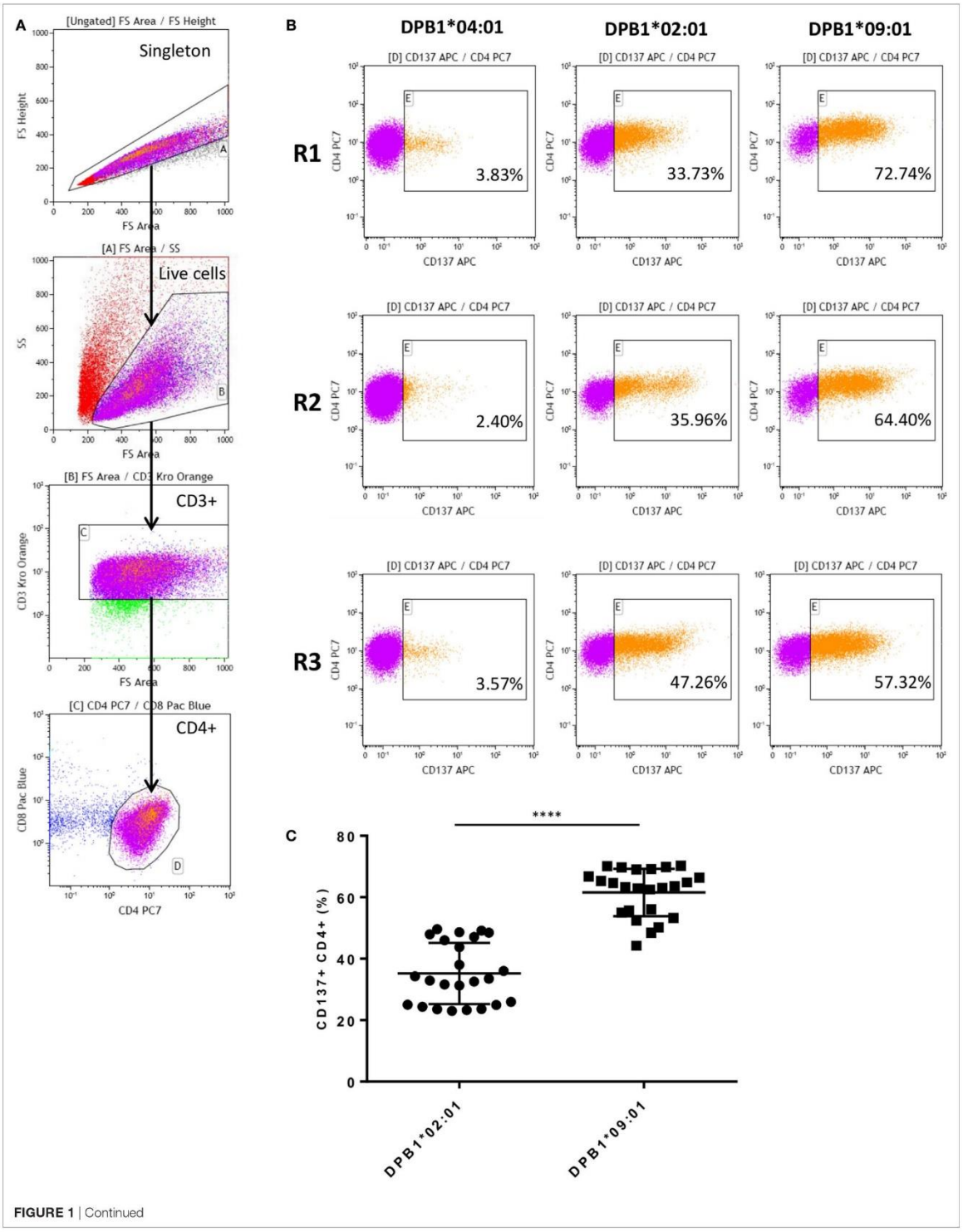

FIGURE 1 | Continued

FIGURE 1 | Alloresponses from self-DPB1*04:01,*04:02 individuals against HLA-DPB1*02:01 and DPB1*09:01 result in stronger responses against the latter. Isolated untouched CD4+ T cells from the three self-DPB1*04:01/*04:02 responders (R) were cocultured with HeLa cells expressing DPB1*02:01 or DPB1*09:01. After 2 weeks, expanded alloreactive T cells were restimulated for 24 h against HeLa cells expressing the original DPB1 alloantigen or an autologous allele, and the degree of T cell response was quantified as the proportion of CD4+CD137+ cells. **(A)** Gating strategy: cells are gated on the live cells and CD3+CD4+ cells. **(B)** Representative responses from each of the subjects. Left panels, background response of alloreactive cells against the autologous allele DPB1*04:01; middle panels, response against allogeneic DPB1*02:01; and right panels, response against allogeneic DPB1*09:01. **(C)** The specific response against each allele was quantified in parallel repeats ($n = 8$) for each subject after deduction of the background levels of CD137 positivity against HeLa expressing the autologous allele (average 4.11%). Mean response (and SD) against DPB1*02:01 and DPB1*09:01 was 35.2% (9.95) and 61.54% (7.69), respectively ($p < 0.0001$).

genes) and the necessary machinery for HLA class II antigen presentation (HLA-DM and invariant chain) and co-stimulation (CD80) and used as antigen-presenting cells. Expression of the DP heterodimer was confirmed by flow cytometry (anti-DP clone B7/21; Leinco Technologies, Inc., St. Louis, MO, USA) with comparable levels among different transduced cells (data not shown). Purified CD4+ T cells (typically 1.2 million) were cultured in RPMI (c.c.pro GmbH, Oberdorla) supplemented with L-glutamine (2 mM), penicillin–streptomycin (100 ng/mL), and 10% human AB serum at a ratio of 3:1 with irradiated (100 Gy) HeLa cells in the presence of 50 U/mL IL-2 in 24-well plates. Parallel cocultures were set up for each subject using HeLa expressing DPB1*02:01 (one peptide-binding groove amino acid difference with DPB1*04:02) or DPB1*09:01 (10 peptide-binding groove amino acid differences with DPB1*04:02). After 15 days, expanded CD4+ T cells were rechallenged for 24 h with HeLa expressing the allogeneic stimulator DPB1 at the same ratio in order to assess the alloreactive response in terms of CD137+ (i.e., activated) T cells by flow cytometry (19). HeLa cells transduced to express one of the donors' self-HLA DPB1 molecules (i.e., *04:01) were used to determine background activation levels (average 4.1%). After rechallenge, T cells were stained with fluorescently labeled antibodies against CD3 (clone UCHT1, Beckman Coulter, Marseille, France), CD4 (clone SK3, BD Biosciences, Heidelberg, Germany), CD8 (clone B9.11, Beckman Coulter, Marseille, France), and CD137 (clone 4B4-1, BD Biosciences, Heidelberg, Germany), and the proportion of CD137+CD4+ cells was measured on a Gallios flow cytometer (Beckman Coulter GmbH, Krefeld, Germany). CD137+CD4+ cells were then assessed for their TCR diversity as explained subsequently.

TCR Vβ Immunophenotype

T cell receptor diversity of anti-DPB1 T cell cultures was assessed in total and CD137+CD4+ cells at the Vβ level by flow cytometry using the IOTest® Beta Mark TCR Vβ Repertoire kit (Beckman Coulter, Marseille, France). For this, one million cultured CD4+ cells were restimulated with the specific HeLa transduced cells for 24 h. Then, the T cells were harvested and stained with subset markers as indicated earlier and the kit's eight Vβ antibody cocktails according to manufacturer's instructions. The frequency of each of the targeted Vβ specificities was recorded in the reactive (CD4+CD137+) fraction. In addition, the proportion of CD137+ cells (responsiveness) among all CD4+ cells expressing each of the Vβ specificities was quantified. Pre-culture-isolated CD4+ cells from each subject were also analyzed in parallel as baseline control.

TCR Immunosequencing

Next-generation sequencing-based high-throughput TCR analysis (TCR immunosequencing) was carried out in DPB1 alloreactive T cells. For this, two million cultured CD4+ cells were restimulated with the specific HeLa transduced cells for 24 h, after which the T cells were harvested and sorted for CD137 positivity (average purity 93.2%) using magnetic bead technology according to manufacturer's instructions (Miltenyi Biotec GmbH, Bergisch Gladbach). Enrichment for DPB1-specific alloreactive T cells was confirmed by interferon-γ Elispot assays (data not shown). Genomic DNA from sorted CD137+CD4+ cells and pre-culture-isolated CD4+ samples from each subject as baseline controls was subsequently extracted using a DNeasy Blood & Tissue Kit (QIAGEN GmbH, Hilden, Germany). DNA from each cultured and pre-culture sample was sequenced to determine *TCRB* complementarity-determining region 3 (CDR3) rearrangements using the immunoSEQ® Assay from Adaptive Biotechnologies (Seattle, WA, USA) as described previously (20, 21). Briefly, a multiplex PCR system based on forward primers targeting 54 *TRBV* segments and reverse primers targeting 13 *TRBJ* segments was used to amplify the CDR3 region of the *TCRB* locus. The PCR products were sequenced on an Illumina HiSeq System, and reads of 87 base pairs covering the CDR3 region were obtained. Sequence data were preprocessed to remove PCR and sequencing errors in the primary sequence. CDR3 regions were defined based on alignments to sequences in the international ImMunoGeneTics information system® (22). All cultured samples were analyzed at survey resolution (targeting 60,000 T cell genomes), while pre-culture samples were analyzed at deep resolution (targeting 200,000 T cell genomes). Average input DNA was 218.4 ng (range 137.9–400) for CD137+CD4+ cells and 1,200 ng for pre-culture CD4+ cells, respectively. The number of templates (total T cells) and the number of rearrangements (unique T cells) in each sample were estimated based on synthetic template pools as previously described (21).

Diversity Metrics and Statistical Analyses

Immunosequencing data generated for each sample were analyzed for their TCR diversity in terms of clonality and richness. Clonality was calculated as 1-Pielou's evenness (23), which is a measure of how uniformly distributed the repertoire is, and it is computed as normalized Shannon's Entropy. Clonality values approaching 0 indicate that every rearrangement is present at nearly identical frequency (i.e., less variation in abundance), whereas values approaching 1 indicate a very skewed distribution of frequencies (i.e., more variation in abundance).

Richness, a measure of the number of different species in a repertoire was assessed using the Daley–Smith estimate (24), a non-parametric empirical Bayes estimator of repertoire richness based on extrapolation of the rarefaction curve to 10 times the actual sample size. TCR clone sharing between samples was assessed by overlap and differential abundance analyses (25), and repertoire similarity was assessed by Morisita's index, a population overlap metric relating the dispersion of clones in the samples (26). The abundance of individual clones was defined by assessing their presence and frequency in pre-culture and cultured samples, and low abundance clones were defined as those seen in cultured samples but undetected in the pre-culture repertoire. CDR3 immunosequencing data were analyzed using custom bioinformatics tools [R version 3.3.2 (27) and RStudio version 1.0.136 (28)] and the immunoSEQ Analyzer® (Adaptive Biotechnologies, Seattle, WA, USA). Alloreactivity levels against DPB1*02:01 and DPB1*09:01 and pre-culture sample groups were compared using *t*-tests, and *p*-values < 0.01 were considered statistically significant. Statistical analyses were performed using Prism (version 6.05, GraphPad Software Inc., La Jolla, CA, USA).

RESULTS

Alloreactive Response against Similar or Dissimilar DPB1 Alleles

After coculture with DPB1-transduced HeLa cells, alloreactive T cells were obtained for all three responders studied against the stimulator alloantigen with either a single (DPB1*02:01, DPA1*01:03) or 10 (DPB1*09:01, DPA1*02:01) amino acid differences compared to self-DPB1*04:02. Levels of alloreactivity in our cultured samples were measured based on CD137 upregulation upon restimulation with the relevant alloantigen, and deduction of background levels of the marker against one of the self-alleles (i.e., DPB1*04:01, DPA1*01:03). **Figure 1** shows the gating strategy, representative CD137 upregulation plots for each responder, and overall results. The

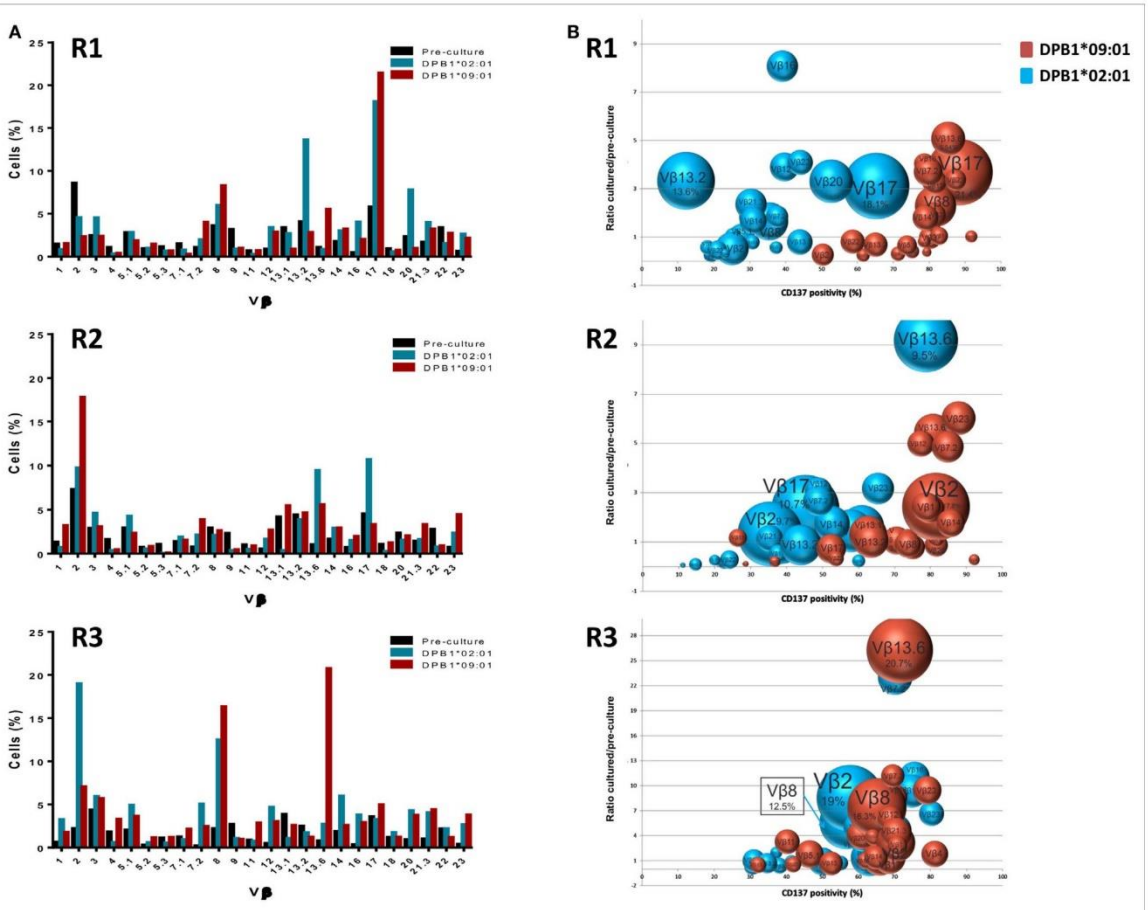

FIGURE 2 | Continued

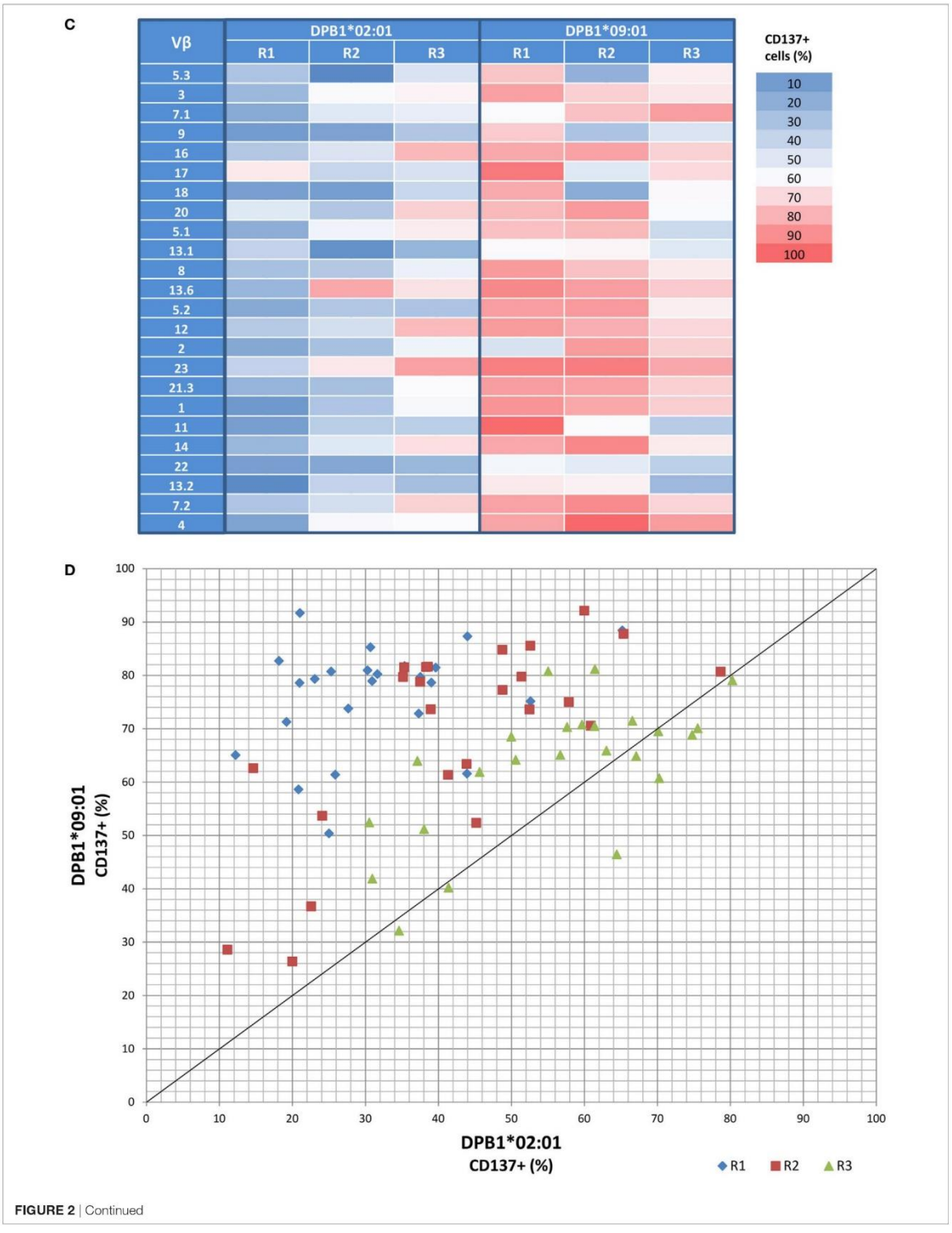

FIGURE 2 | Continued

FIGURE 2 | Alloresponses against both HLA-DPB1*02:01 and DPB1*09:01 originate from a varied repertoire at the Vβ level, but with stronger responsiveness against the latter. TCR-Vβ analysis of 24 Vβ specificities was performed by flow cytometry in CD4+ T cells from three self-DPB1*04:01,*04:02 responders (R) after 2 weeks of culture with HeLa cells expressing DPB1*02:01 or DPB1*09:01, followed by overnight reincubation with HeLa cells expressing the original alloantigen. **(A)** Percentage of cells pre-culture and in the CD137+ cultured fractions after restimulation expressing each of the targeted Vβ families against each alloantigen. **(B)** Enrichment in the CD137+ cultured fraction vs. pre-culture levels (*y* axis) of each of the Vβ specificities was quantified and plotted against CD137 positivity for all cells expressing that Vβ family after restimulation (*x* axis). The size of each circle represents the share (% cells positive) of each Vβ specificity in the CD137+ T cell receptor repertoire. Vβ family dynamics against DPB1*02:01 (blue circles) and DPB1*09:01 (red circles) are shown for each responder. **(C)** Heat map showing CD137 positivity levels among all cells expressing each Vβ specificity for each of the responders against the two DPB1 alleles. Shown in red are strongly responding Vβ specificities (>60% CD137+ cells after restimulation among all CD4+ cells expressing that specificity). **(D)** Plot showing the response (CD137 levels) of each of the targeted Vβ specificities against DPB1*02:01 (*x* axis) and DPB1*09:01 (*y* axis) for each of the three responders. Each dot represents one targeted Vβ specificity for each of the responders. The majority of the Vβ specificities respond with higher CD137 levels against DPB1*09:01 than to DPB1*02:01.

TABLE 2 | Immunosequencing data for pre-culture and cultured samples.

Sample	Responder (R)	Number of productive templates (total T cells)	Number of rearrangements (unique T cells)	Productive clonality	Maximum clonal frequency (%)
Pre-culture CD4+	R1	180,066	98,044	0.0599	0.38
	R2	167,264	116,092	0.0406	0.53
	R3	168,885	146,063	0.0122	0.04
DPB1*02:01-specific CD137+CD4+ cells	R1	7,543	720	0.3909	25.76
	R2	7,874	619	0.4512	26.35
	R3	2,530	495	0.3572	27.94
DPB1*09:01-specific CD137+CD4+ cells	R1	26,837	1,175	0.4596	22.51
	R2	1,447	251	0.2954	14.93
	R3	9,927	959	0.3905	21.80

response against DPB1*02:01 was significantly lower than that against DPB1*09:01, with mean percentages of alloreactive CD137+CD4+ of 35.2% (range 23.0–49.6%) and 61.54% (range 44.2–70.2%), respectively.

Diversity of T Cell Responses against DPB1 Alleles at the TCR-Vβ Level

We first analyzed the TCR diversity among these cells at the level of Vβ families by using flow cytometric quantification (**Figure 2**). We observed that all Vβ specificities tested could be found among the DPB1*02:01 and DPB1*09:01-reactive CD4+ cells (**Figure 2A**) and that the frequency of the majority (12–16/24 against DPB1*02:01; 12–20/24 against DPB1*09:01) of targeted Vβ specificities expanded during culture, with average fold expansions of 3.86 against DPB1*02:01 and 3.50 against DPB1*09:01. There was a correlation between CD137 positivity in each family and fold expansion from pre-culture levels, with responses against DPB1*09:01 showing a shift to higher levels of CD137 positivity (**Figure 2B**). This difference was also reflected in the number of highly reacting Vβ specificities (i.e., Vβ for which >60% of all cells expressed CD137 after restimulation) against each allele: 1–11/24 against DPB1*02:01 vs. 18–22/24 against DPB1*09:01 (**Figure 2C**). In addition, in 63/72 cases the same Vβ family responded with higher CD137 levels against DPB1*09:01 than to DPB1*02:01 (overall average 26.1% higher) (**Figure 2D**). The cumulative frequency of the top 10 Vβ specificities was similar for both alleles (63.8% against DPB1*02:01 vs. 61.7% against DPB1*09:01). Overall, these data at the Vβ level suggest that responses against a single or multiple amino acid differences in HLA-DP arise from comparable levels of diversity, albeit with overall lower levels of alloreactivity against the more similar allele.

Clonality and Richness of TCR Clones Responding against a Single or Multiple Amino Acid Differences between DPB1 Alleles

We then analyzed the diversity of alloreactive DPB1-specific CD4+ T cells at the CDR3 level by *TCRB* immunosequencing. **Table 2** shows the summary data for the immunosequencing results. As expected, clonality for the cultured CD137+CD4+ cells (mean 0.39) was higher than in pre-culture samples (average 0.04). However, the diversity among T cell clones (as defined by their CDR3 sequence at the amino acid level) responding against DPB1*02:01 was comparable to those responding against DPB1*09:01, and mean productive clonality of TCR clones responding against DPB1*02:01 (0.40, range 0.36–0.45) was similar to that of the clones responding against DPB1*09:01 (0.38, range 0.30–0.46) (**Figure 3A**). The clone richness was also markedly reduced when compared to the pre-culture samples, but did not differ substantially between clones responding against either allele (**Figure 3B**). The share for the top 10 reactive clones in the cultured samples ranged from 54.7 to 66.8%, with no substantial difference

between cultures responding against DPB1*02:01 (59.4%, range 58–62%) or DPB1*09:01 (mean 60.0%, range 55–67%) (**Figure 3C**). In accordance with these results, the frequency distribution of T-cell clones did not show any major difference between alloresponses against these two alleles (**Figure 3D**), with similar number of high-frequency clones (≥1%): 20, 19, 13 against DPB1*02:01; 11, 17, 13 against DPB1*09:01 for R1, R2, and R3, respectively. Finally, analysis of CDR3 length among alloreactive clones revealed no major skewing in the responses against either allele in comparison to pre-culture samples (**Figure 4**). Overall, these data correlate with the Vβ analyses and suggest that the responding TCR clones elicited *in vitro* against a single or multiple amino acid differences in DPB1 do not differ substantially in terms of their size and diversity.

Overlap of TCR Clones Responding against DPB1 Alleles

We then asked whether there was overlap between individual clone sets responding against either allele and between clones responding against the same allele across individuals. Overall repertoire similarity among cultured samples was low (mean Morisita's index 0.054). There was little overlap between clone sets responding against DPB1*02:01 and DPB1*09:01 within the same individual [median Morisita's index: 0.12 (0.005–0.68)] (**Figure 5A**), and almost no overlap against the same allele across individuals (**Figure 5B**). At the amino acid level, each individual's clones sets reactive against DPB1*02:01 and DPB1*09:01 shared only 38/1,204, 8/571, and 7/1,099 sequences (55/1,840, 13/857, and 7/1,447 nucleotide sequences) (**Figure 5A**). Analysis of the 10 most frequent sequences revealed almost no sharing between cultures

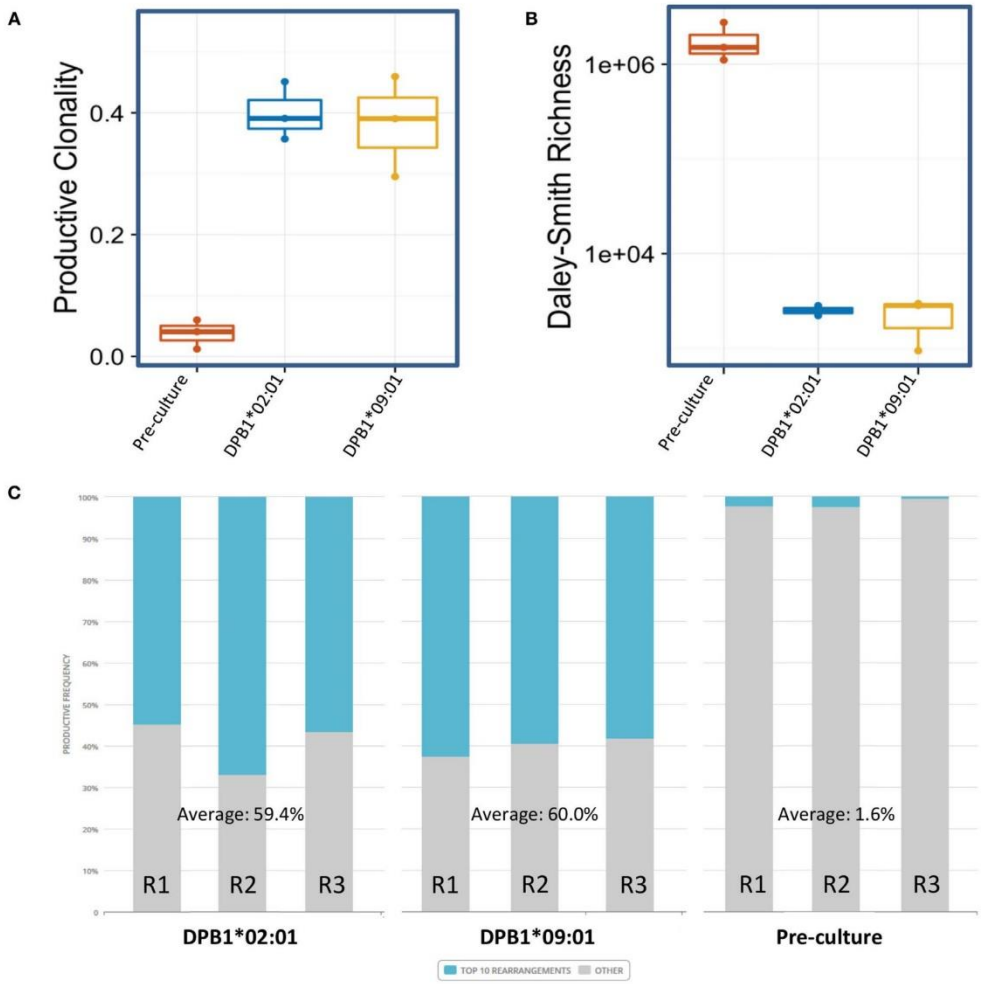

FIGURE 3 | Continued

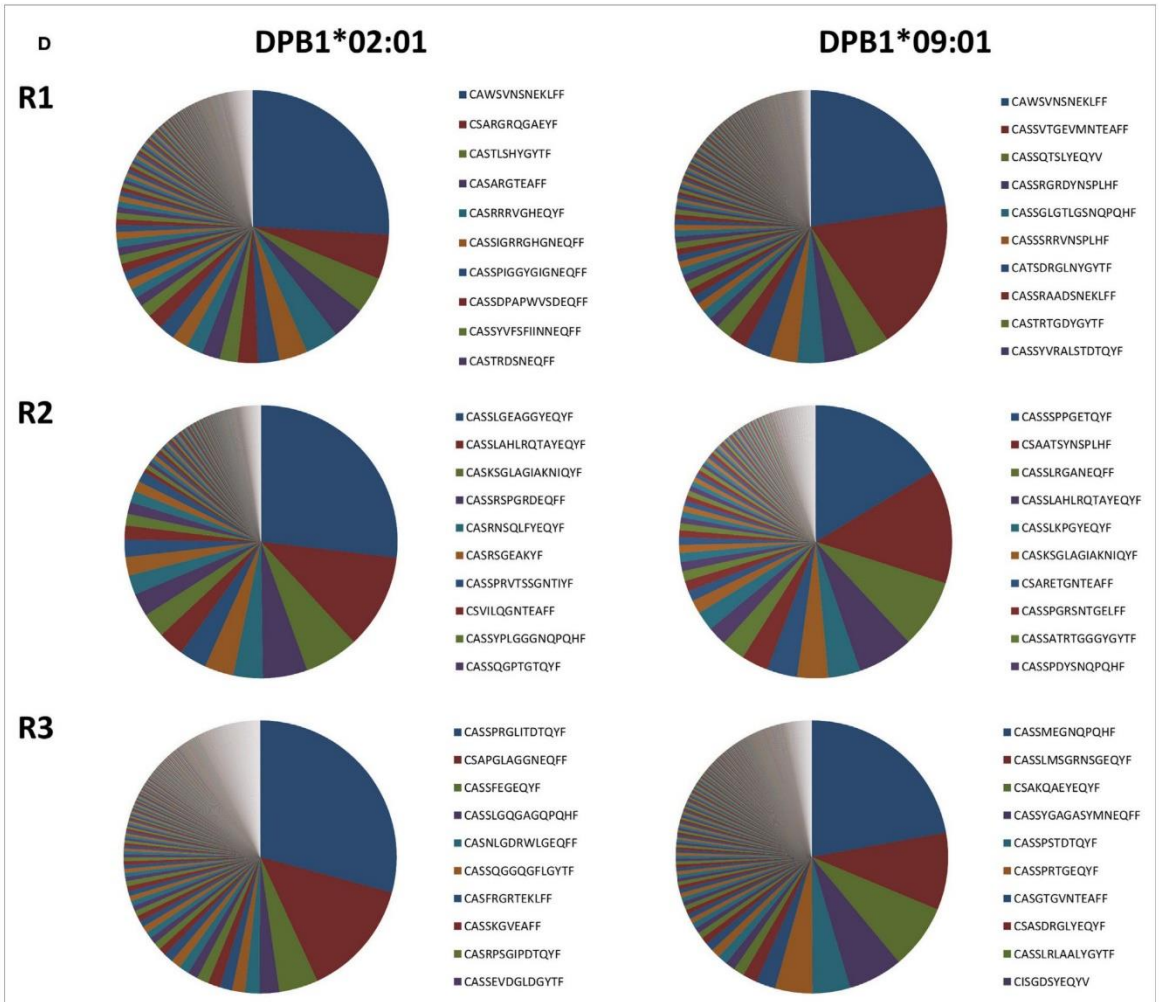

FIGURE 3 | Diversity of CD4+ T cell responses against DPB1*02:01 and DPB1*09:01 at the CDR3 level. Immunosequencing of *TCRB* of sorted CD4+CD137+ cells was performed, and the T cell receptor (TCR) repertoire diversity measures were quantified in CD4+ T cells from three self-DPB1*04:01,*04:02 responders (R) after 2 weeks of culture with HeLa cells expressing DPB1*02:01 or DPB1*09:01, followed by overnight reincubation with HeLa cells expressing the original alloantigen. Median and interquartile ranges for **(A)** productive clonality and **(B)** richness of TCR clones from each responder are plotted, including pre-culture CD4+ cells. **(C)** Cumulative frequency of the top 10 clones (blue) for each set of alloreactive clones and the pre-culture TCR repertoire is shown. Top 10 clones at the DNA (or amino acid in brackets) level accounted for 54.73% (56.04%), 66.83% (68.71%), and 56.56% (58.85%) against DPB1*02:01, and 62.5% (63.21%), 59.5% (63.99%), and 58.14% (60.80%) against DPB1*09:01 for R1, R2, and R3, respectively. Pre-culture top 10 clones at the DNA (or amino acid in brackets) level accounted for 2.14% (2.20%), 2.39% (2.45%), and 0.29% (0.31%) for R1, R2, and R3, respectively. **(D)** Pie plots showing the frequency distribution for clones at the amino acid level responding against DPB1*02:01 (left plots), and DPB1*09:01 (right plots) for each responder. Listed are the top 10 clones for each sample. The total number of clones at the amino acid level was 481, 409, and 406 against DPB1*02:01, and 761, 170, and 700 against DPB1*09:01 for R1, R2, and R3, respectively.

(**Table 3**; **Figure 3D**). Apart from a single nucleotide sequence shared between two individuals responding against DPB1*02:01 and two clones against DPB1*09:01 with the same amino acid sequence but different nucleotide sequences, no clone was shared by subjects responding against the same allele (**Figure 5B**). Overall, these data suggest that, despite showing similar repertoire size metrics, responses against these DPB1 alleles are highly divergent, while responses against the same allele are highly individualized.

Clonal Enrichment and Abundance of TCR Clones Reacting against a Single or Multiple Amino Acid Differences between DPB1 Alleles

In order to assess clone expansion against a single or multiple amino acid differences in DPB1, we examined their kinetics in terms of enrichment (25) and pre-culture abundance.

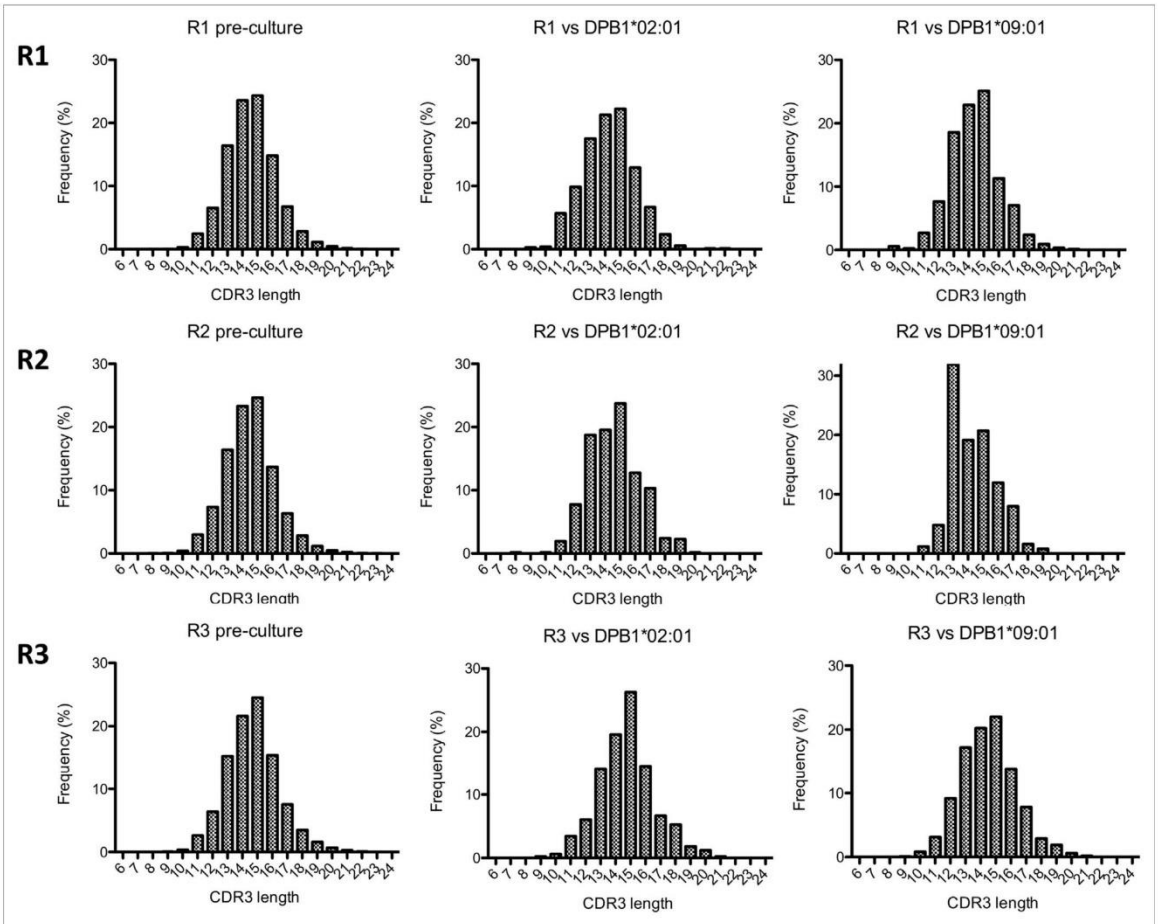

FIGURE 4 | Complementarity-determining region 3 (CDR3) length analysis of alloresponses against DPB1*02:01 and DPB1*09:01. The length of CDR3 regions (number of amino acids) as determined by immunosequencing for each responder's (R) samples was quantified. Shown are histograms for the total pre-culture CD4+ cells (left panels) and cultured CD4+CD137+ cells alloreactive against DPB1*02:01 (middle panels) and DPB1*09:01 (right panels).

Significantly enriched clones in the cultured samples with respect to the pre-culture repertoires accounted for a large part of the clones responding against DPB1*02:01 (mean cumulative frequency 82.4%, range 71.82–89.26%). This was similar against DPB1*09:01 (mean 84.2%, range 74.5–93.3%). A total of 69, 52, and 33 clones against DPB1*02:01 and 172, 26, and 105 clones against DPB1*09:01 showed statistically significant enrichment in cultured samples ($p < 0.01$). For significantly enriched clones detected in the pre-culture samples, average fold expansions against DPB1*02:01 were 866× (range 15–6,016×), 2,245× (6–14,693×), and 5,350× (49–47,194×), for R1, R2, and R3, respectively, while among clones responding against DPB1*09:01 they were 873× (2–32,260×), 2,012× (11–12,022×), and 1,396× (6–10,786×) for R1, R2, and R3, respectively. As shown in **Figure 6**, among clones detected in both the cultured and the pre-culture samples, apart from a few cases where higher frequency clones expanded strongly, those with lower pre-culture frequencies constitute a large part of the cultured clones, with no major difference between DPB1 alleles.

Due to the fact that low-abundance (i.e., rare) alloreactive T cell clones seem to constitute a major component of alloresponses (29), we evaluated their presence and cumulative frequencies among clones responding against DPB1*02:01 and compared them to responses against DPB1*09:01. We defined low-abundance pre-culture clones as those present in the cultured samples but not detectable in the respective pre-culture samples (**Figure 7A**). We found that low-abundance clones represented the majority of the clones identified against DPB1*02:01 (average 68.3%) and DPB1*09:01 (average 75.3%). However, the mean cumulative frequency of low-abundance clones expanded against DPB1*02:01 was lower in comparison to those expanded against DPB1*09:01 (average 36.3%, range 33.6–39.0% and average 50.6%, range 32.0–71.3%, respectively) (**Figure 7B**). Overall, these data show that DPB1-specific alloreactive clones arise preferentially from low-frequency

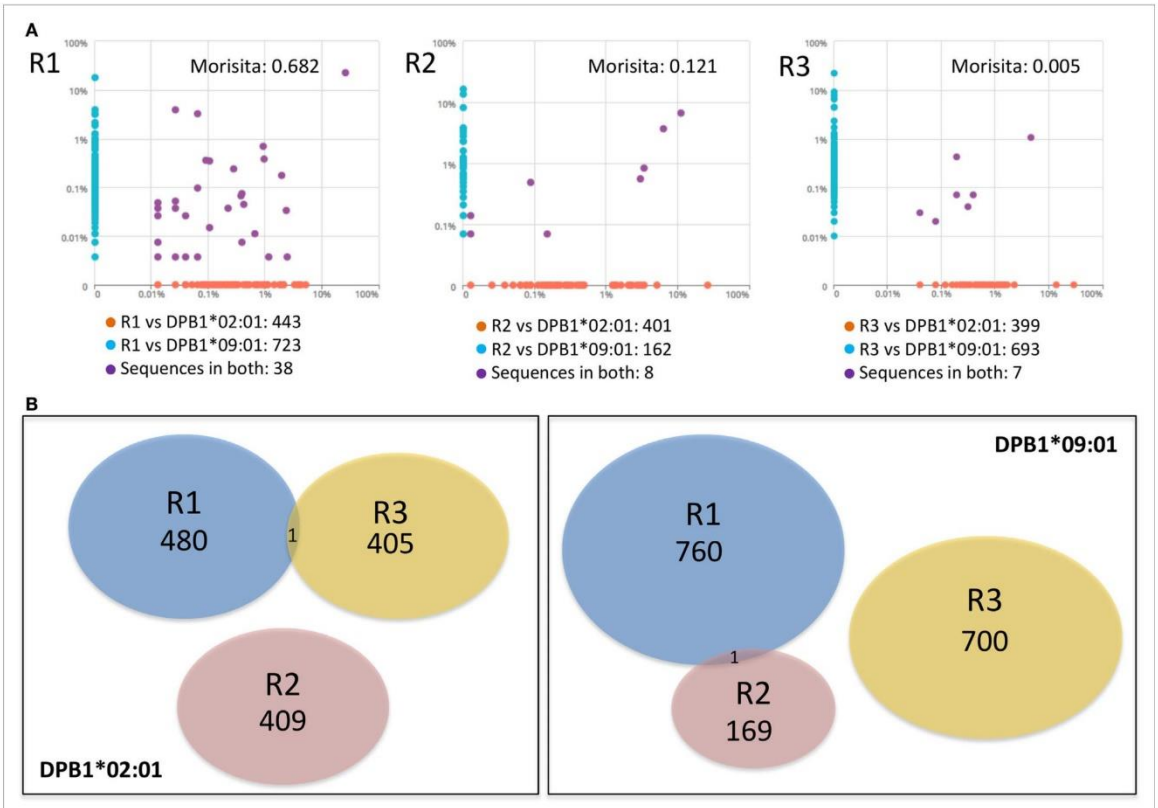

FIGURE 5 | Responses against DPB1*02:01 and DPB1*09:01 alleles are highly divergent and individualized. The sharing of *TCRB*-CDR3 amino acid sequences among CD4+CD137+ cells responding against DPB1 alleles was compared. **(A)** Pairwise scatter plots showing the frequency and sharing of clones against each allele in each of the three responders (R). Within each responding individual, there was a low sharing of clones (purple dots) between their responses against DPB1*09:01 (*y* axis) and DPB1*02:01 (*x* axis). Morisita's indexes for each pairwise T cell receptor clone set comparison are shown. **(B)** Venn diagrams show the sharing of clones across individuals against DPB1*02:01 (left panel) and DPB1*09:01 (right panel). The number of unique sequences in each clone set is depicted. Only one DPB1-alloreactive clone was shared across individuals for each allele.

clones, with undetected low-abundance pre-culture T cell clones representing a substantial part of the alloreactive repertoires against HLA-DP molecules, in particular against dissimilar DPB1.

DISCUSSION

In this study, we have characterized the self-selected (i.e., self-DPB1*04:01,*04:02) alloreactive CD4+ T cell clone sets generated against structurally similar (DPB1*02:01) or dissimilar (DPB1*09:01) HLA-DP molecules in healthy individuals using Vβ immunophenotyping and, for the first time, cutting-edge high-resolution immunosequencing of the TCR. Our analyses show that despite quantitative differences in the strength of the *in vitro* alloresponse, with higher levels of reactivity against the more dissimilar allele, a single amino acid difference in the peptide-binding groove encoded by allogeneic DPB1*02:01 compared to self-DPB1*04:02 is able to generate an array of alloreactive TCR clones of similar broadness and diversity to those elicited by 10 amino acid changes in the peptide-binding groove encoded by allogeneic DPB1*09:01, with no major differences in clonality and other diversity measures when comparing both alloantigens. In addition, we show a very low overlap between the responses against both alleles at the individual subject level, and essentially no overlap among TCRs responding against the same allele across individuals. Finally, by making use of the unique power of immunosequencing we show that clones with low pre-culture frequencies appear with high frequency among the expanded alloreactive clones and confirm previous observations regarding the relevant role of low-abundance clones in alloreactivity (30). We suggest that this compartment might play a more important role in alloreactivity to more dissimilar DPB1 alleles based on their greater share of the alloreactive clone array elicited by DPB1*09:01 compared with DPB1*02:01.

By using specific DPB1 mismatches (i.e., DPB1*04:01,*04:02 vs. DPB1*02:01 or DPB1*09:01) involving a single or multiple amino acid changes in the HLA-DP peptide-binding groove with respect to one of the self-selecting alleles (i.e., DPB1*04:02),

TABLE 3 | Top 10 CDR3 amino acid sequences for CD137+CD4+ cells.

DPB1*02:01-specific CD137+CD4+ cells	Amino acid sequence	Frequency in cultured sample (%)	Frequency in pre-culture sample (%)
R1	CAWSVNSNEKLFF	25.9446	0.0405
	CSARGRQGAEYF	5.2897	ND
	CASTLSHYGYTF	4.3219	ND
	CASARGTEAFF	3.9639	ND
	CASRRRVGHEQYF	3.9374	0.0128
	CASSIGRRGHGNEQFF	3.3674	0.0006
	CASSPIGGYGIGNEQFF	2.5321	0.0006
	CASSDPAPWVSDEQFF	2.3996	0.0017
	CASSYVFSFIINNEQFF	2.1477	0.0033
	CASTRDSNEQFF	2.1344	0.0006
R2	CASSLGEAGGYEQYF	26.8732	0.0018
	CASSLAHLRQTAYEQYF	11.2395	0.5548
	CASKSGLAGIAKNIQYF	6.4135	0.0006
	CASSRSPGRDEQFF	5.2705	ND
	CASRNSQLFYEQYF	3.4798	ND
	CASRSGEAKYF	3.4417	0.0048
	CASSPRVTSSGNTIYF	3.2512	ND
	CSVILQGNTEAFF	3.0734	0.0012
	CASSYPLGGGNQPQHF	2.9337	0.0006
	CASSQGPTGTQYF	2.7305	ND
R3	CASSPRGLITDTQYF	29.2095	0.0006
	CSAPGLAGGNEQFF	13.9130	0.0006
	CASSFEGEQYF	4.6245	0.0012
	CASSLGQGAGQPQHF	2.2925	0.0012
	CASNLGDRWLGEQFF	1.7391	ND
	CASSQGGQGFLGYTF	1.5415	ND
	CASFRGRTEKLFF	1.4625	ND
	CASSKGVEAFF	1.4625	0.0006
	CASRPSGIPDTQYF	1.3834	ND
	CASSEVDGLDGYTF	1.2253	0.0006
DPB1*09:01-specific CD137+CD4+ cells	**Amino acid sequence**	**Frequency in cultured sample (%)**	**Frequency in pre-culture sample (%)**
R1	CAWSVNSNEKLFF	22.5659	0.0405
	CASSVTGEVMNTEAFF	17.93	0.0006
	CASSQTSLYEQYV	3.9200	ND
	CASSRGRDYNSPLHF	3.8976	0.0061
	CASSGLGTLGSNQPQHF	3.2530	0.0006
	CASSSRRVNSPLHF	3.2455	0.0072
	CATSDRGLNYGYTF	3.1337	0.0028
	CASSRAADSNEKLFF	2.1426	0.0061
	CASTRTGDYGYTF	1.8556	ND
	CASSYVRALSTDTQYF	1.2632	ND
R2	CASSSPPGETQYF	16.3787	0.0036
	CSAATSYNSPLHF	13.5453	ND
	CASSLRGANEQFF	8.1548	0.0006
	CASSLAHLRQTAYEQYF	6.6344	0.5548
	CASSLKPGYEQYF	3.8010	ND
	CASKSGLAGIAKNIQYF	3.6628	0.0006
	CSARETGNTEAFF	3.5936	ND
	CASSPGRSNTGELFF	3.1790	ND
	CASSATRTGGGYGYTF	2.7643	0.0042
	CASSPDYSNQPQHF	2.2806	0.0018
R3	CASSMEGNQPQHF	22.1416	ND
	CASSLMSGRNSGEQYF	9.1468	0.0024
	CSAKQAEYEQYF	7.6760	ND
	CASSYGAGASYMNEQFF	6.4874	0.0006
	CASSPSTDTQYF	4.4525	0.0065
	CASSPRTGEQYF	4.4223	ND
	CASGTGVNTEAFF	2.3169	ND
	CSASDRGLYEQYF	1.7024	0.0006
	CASSLRLAALYGYTF	1.2894	ND
	CISGDSYEQYV	1.1685	0.0006

CDR3, complementarity-determining region 3; ND, not detected.

we sought to dissect the effect of the extent of variation in this region of the HLA-DP molecule exerted indirectly *via* thymic selection on the diversity of clones expanded from the alloreactive TCR repertoire. DPB1*09:01 and DPB1*04:01/*04:02 differ at 13 and 10 positions in exon 2, respectively. It is expected that the peptide repertoires of these molecules differ substantially, providing a plausible explanation for strong alloreactivity and diverse TCR responses observed among self-DPB1*04:01,*04:02 individuals. On the other hand, the DPB1*02:01 exon 2 differs from DPB1*04:02 only at position 69 (E69K). This makes it likely that the peptide repertoires of these two molecules overlap to a certain extent. Indeed, analysis of the peptide binding motifs for DPB1*02:01 (31) and DPB1*04:02 (unpublished data, manuscript in preparation) show that peptide position P4, which interacts with the pocket formed in part by the side chain of position 69 on the alpha-helix of the DP beta polypeptide, is the only position that seems to differ significantly between these two alleles, with DPB1*02:01 having affinity for lysine and DPB1*04:02 for glutamic acid at P4. Importantly, position 69 on the DPB1*02:01 molecule has been shown to impact the recognition of this molecule by monoclonal antibodies (32), bone marrow recipient–donor mixed-lymphocyte reactions (10), and the lysis of DPB1*02:01-expressing cells by alloreactive T cell clones (33, 34). Moreover, mutation of position 69 in DPB1*02:01 was shown to impact the class II-associated invariant chain-derived peptide binding affinities of pockets 4 and 6 (35). Interestingly, this position of the DPB1 molecule and the specific amino acid E69K change have been previously identified as having a strong impact on the generation of alloreactivity against DPB1*09:01 (13).

Of note, some studies have reported that class I HLA molecules with numerous sequence differences do not elicit an allogeneic cytotoxic lymphocyte response (36) and that such highly diverged mismatches might be acceptable in HSCT (37). We have not observed this phenomenon in our CD4+ assays, neither with DPB1*09:01 nor with other alleles having several amino acid

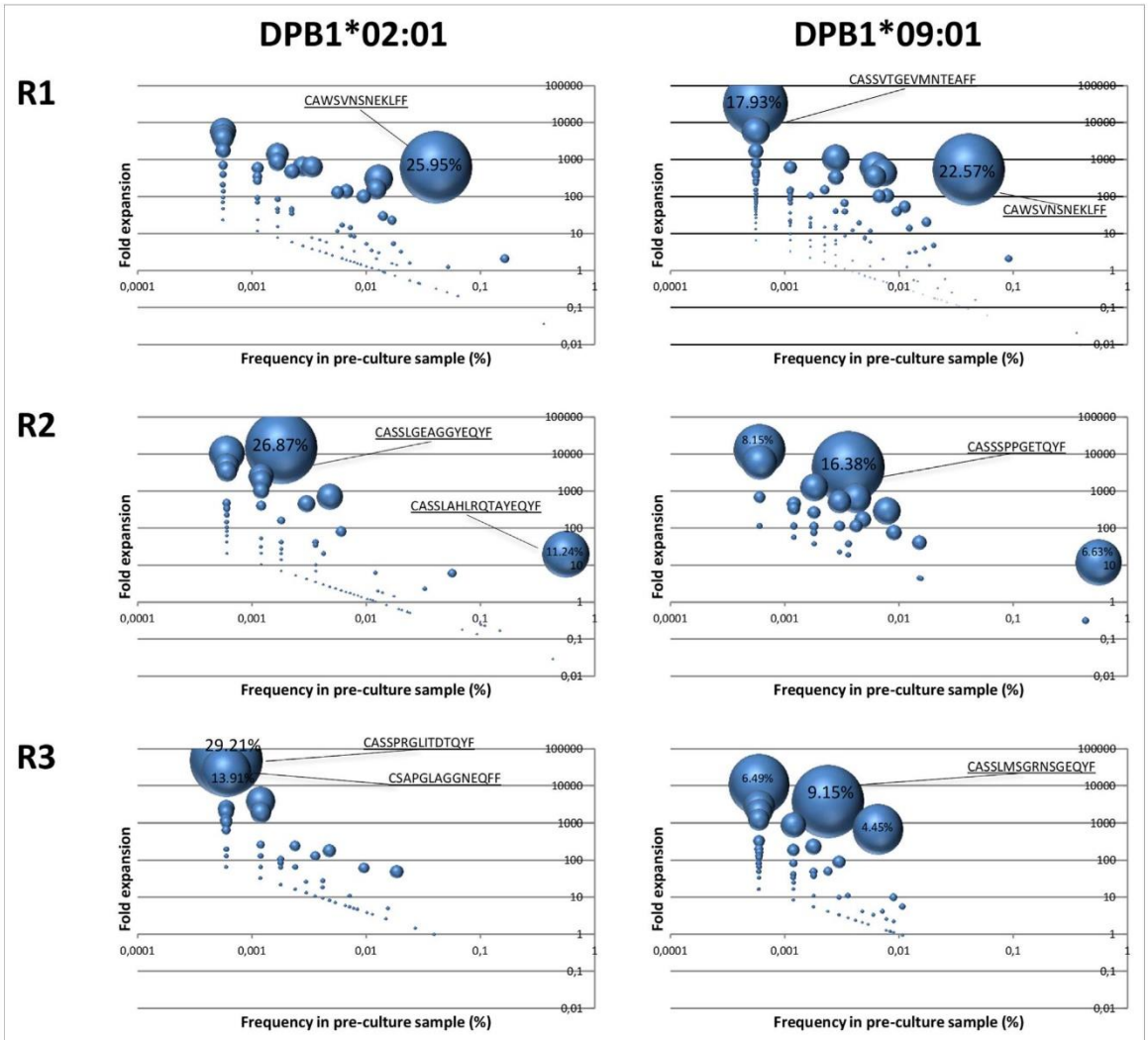

FIGURE 6 | Expansion of DPB1-specific alloreactive clones detected in pre-culture samples. Fold expansion among alloreactive T cell clones present in the cultured samples and that could be detected in the pre-culture samples for each responder (R) was quantified and plotted (*y* axis) against their frequency in the pre-culture sample (*x* axis). The size of the circle represents the share of each clone in the total cultured set. Highest values (%) are indicated for each sample. Left panels, clones responding against DPB1*02:01; right panels, clones responding against DPB1*09:01. As shown in **Figure 7A** (purple dots), 177, 146, and 92 clones against DPB1*02:01, and 249, 43, and 112 clones against DPB1*09:01 were detected in both the cultured and the pre-culture samples for R1, R2, and R3, respectively.

differences when compared to the autologous alleles (unpublished data). Intuitively, more amino acid differences in the peptide-binding grove would generate more divergent peptide repertoires resulting in a lower indirect effect of thymic selection and higher alloreactivity, something that lies at the basis of the TCE model.

In the context of allogeneic HSCT, compatibility between donor and recipient for polymorphic HLA plays a central role in the balance between the detrimental graft-vs.-host and therapeutic graft-vs.-leukemia effects (38, 39), both mediated mainly by alloreactive T cell responses. Because of this, the search of HLA permissive mismatches, which contribute to cure the patient's malignancy while reducing the toxicity of the transplant, is a major goal in HSCT (40). Permissiveness to DPB1 mismatches is now a well-established phenomenon in HSCT, both clinically (14, 15) and *in vitro* (9, 12, 41), with permissive mismatches (i.e., those involving two alleles of the same T cell epitope, TCE, group, and that share structural similarities) conferring significantly lower risks of relapse without significant increases in non-relapse mortality when compared to DPB1 allele matches after HSCT for hematologic malignancies (14, 42, 43).

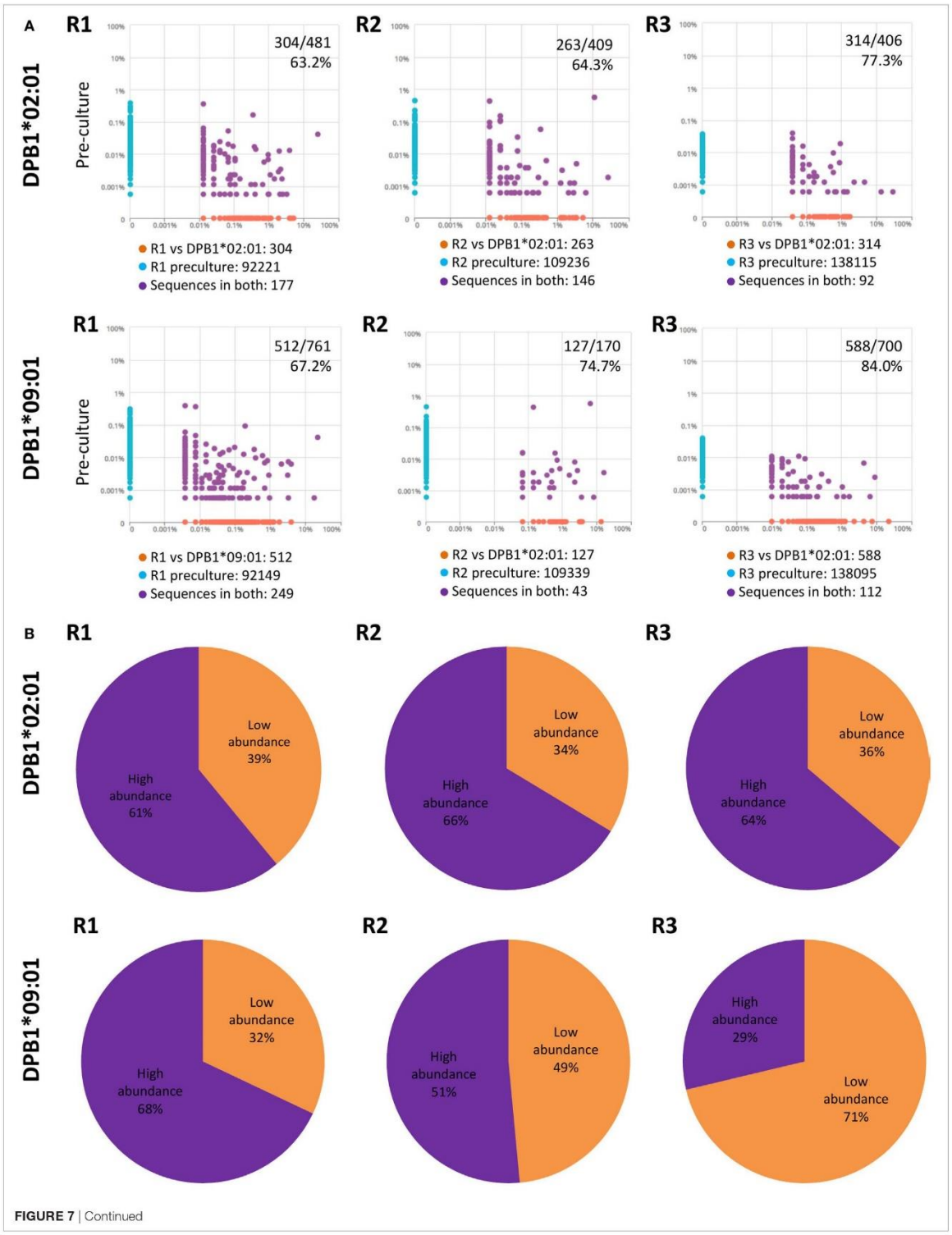

FIGURE 7 | Continued

FIGURE 7 | Low abundance pre-culture T cell clones represent a substantial part of the alloreactive clones elicited against HLA-DPB1 molecules with higher share against DPB1*09:01. **(A)** Clone (CDR3 amino acid) pairwise scatter plots between pre-culture repertoires and CD4+CD137+ cells responding against DPB1*02:01 (top panels) and DPB1*09:01 (bottom panels) are shown for each responder (R). Low-abundance DPB1-alloreactive clones (orange dots in the pairwise scatter plots) were defined as those present in the cultured sample (*x* axis) and not detected in the respective pre-culture repertoire (*y* axis). The number and percentage of low abundance clones relative to the total number of clones detected in the cultured sample are shown. **(B)** The share (cumulative frequency) of low abundance clones was quantified for clones responding against DPB1*02:01 (top panels) or DPB1*09:01 (bottom panels) in each subject. The average cumulative frequency for low-abundance clones against DPB1*02:01 and DPB1*09:01 was 36.3 and 50.6%, respectively.

Clinically, a mismatch involving a donor who is self-DPB1*04:01,*04:02 and a patient bearing DPB1*02:01 would currently be considered permissive, whereas one involving a patient with a self-DPB1*09:01 is considered non-permissive. Our data show that, contrary to the strength of the alloreactive response, the diversity of the alloreactive clones elicited by such a permissive mismatch does not seem to be impacted by the number of amino acid differences in the peptide-binding groove. This feature is desirable for the therapeutic effect of HSCT: moderate alloreactivity levels combined with a sufficiently broad repertoire maximizing the capacity of donor-derived T cells of effectively recognizing malignant patient cells while minimizing GvHD.

Since permissiveness was not predicted by significant differences in terms of the size of the set of responding TCR clones, it is possible that a qualitative characteristic of the HLA–TCR interaction influencing events downstream of TCR recognition (44, 45) and shaped by thymic selection might be responsible for this phenomenon (16, 46). Thymic education in a self-DPB1*04:01,*04:02 individual could have an indirect effect on the allogeneic repertoire capable of reacting to a structurally related molecule such as DPB1*02:01, by reducing the affinity of the binding to the allogeneic molecule. This would not result in more restricted reacting TCR repertoires but in lower activation and proliferation of the T cells. We cannot, however, rule out that TCR repertoire breadth plays a role in permissiveness to other specific allelic combinations. Moreover, DPB1*02:01 might still represent a separate TCE group (47) and hence behave differently with respect to other alleles sharing similarity to DPB1*04:02. More research into this question is warranted.

Interestingly, low-abundance T cell clones, which have been shown to constitute a significant amount of the alloreactive response *in vitro* (29) and *in vivo* (30), seem to represent a higher proportion of the TCR clone sets against DPB1*09:01 than against DPB1*02:01. A possible explanation for this observation could be that a more functionally distant allele such as DPB1*09:01 might elicit stronger TCR signaling that could help to beat the threshold to extract these specificities from the deep pre-culture repertoire thanks to better proliferative signals.

Recent reports have shown a potential effect of differential 3′UTR-controlled expression levels on permissiveness of DPB1 mismatches in the context of HSCT (48, 49). This model would not play a role in the results presented in this study since the HeLa cell system utilized does not include the 3′UTR region of this gene (18). However, we cannot dismiss a potential effect of this model on the alloreactive TCR repertoires against HLA-DP molecules in a physiological setting.

Our study is limited by the number of subjects included, the use of the HeLa system (i.e., of a non-physiological antigen presenting cell to stimulate our alloreactive T cells), and the use of total CD4+ responder T cells. Although we have been unable to identify any "public" TCR clones responding against DPB1*02:01 and/or DPB1*09:01, a larger study with a significantly larger number of subjects would be required to rule out the existence of such clones in the population. Similarly, the analysis of a potential effect of responder age and the frequency of memory CD4+ T cells in their repertoire on the clonality of HLA-DP alloreactive cells would require a larger number of samples. The use of HeLa cells transduced to express specific DPB1 alleles, although extremely useful experimentally, could skew our results due to the underlying peptidome of this non-hematopoietic tumor cell line. Moreover, we have not addressed the question whether the naïve and memory CD4+ repertoires could behave differently in alloresponses, something that has been previously suggested (50, 51). In addition, despite the high level of over 90% purity of our CD137+ samples, a confounding effect of contaminating CD137− cells especially on rare CDR3 sequences cannot be ruled out. Finally, CD4+ T cells reactive against HLA class I molecules have been described (52, 53). However, their impact on our results, if any, must be minimal, since very low levels of activation were observed when the responder cells were restimulated with the HeLa expressing the autologous DPB1 allele, which would express the same class I molecules as those transduced with the allogeneic molecules.

In conclusion, our study, the first one to comparatively address TCR diversity in responses to similar or dissimilar allogeneic HLA-DP molecules by NGS immunosequencing, shows proof-of-principle evidence for the novel concept that limited strength alloreactivity can coexist with broad TCR diversity, providing a potential platform for clinically favorable DPB1 mismatches in allogeneic HSCT. The potential role for *in vitro* pre-transplant low-abundance clones, revealed solely through the power of NGS immunosequencing, as personalized clinical biomarkers in HSCT needs to be further clarified by *in vivo* tracking of expanded clones in patients with alloreactivity against DPB1 mismatches.

ETHICS STATEMENT

This study was carried out in accordance with the recommendations of University Hospital Essen with written informed consent from all subjects in accordance with the Declaration of Helsinki. The protocol was approved by the local Ethics Committee of University Hospital Essen.

AUTHOR CONTRIBUTIONS

EA-B, PC, and KF designed the study; EA-B, PC, MM, and TM performed experiments; MA contributed advice on TCR immunosequencing experiments; PB and JF produced the transduced HeLa cells; EA-B, JR, MV, and EY performed statistical analysis;

PH contributed PBMC from healthy blood donors and their HLA typing; and EA-B and KF wrote the manuscript.

ACKNOWLEDGMENTS

The authors would like to thank Prof. Monika Lindemann (Institute for Transfusion Medicine, University Hospital Essen) for assistance with the interferon-γ Elispot assays.

FUNDING

This work was supported by grants from the Deutsche José Carreras Leukämie Stiftung (DJCLS R 15/02) to KF and PH, and the Dr. Werner Jackstädt Stiftung and the Joseph Senker Stiftung to KF, and an Adaptive Biotechnologies Young Investigator Award to EA-B.

REFERENCES

1. Ford WL, Atkins RC. The proportion of lymphocytes capable of recognizing strong transplantation antigens in vivo. *Adv Exp Med Biol* (1973) 29(0):255–62. doi:10.1007/978-1-4615-9017-0_37
2. DeWolf S, Shen Y, Sykes M. A new window into the human alloresponse. *Transplantation* (2016) 100(8):1639–49. doi:10.1097/TP.0000000000001064
3. Felix NJ, Allen PM. Specificity of T-cell alloreactivity. *Nat Rev Immunol* (2007) 7(12):942–53. doi:10.1038/nri2200
4. Wang Y, Singh NK, Spear TT, Hellman LM, Piepenbrink KH, McMahan RH, et al. How an alloreactive T-cell receptor achieves peptide and MHC specificity. *Proc Natl Acad Sci U S A* (2017) 114(24):E4792–801. doi:10.1073/pnas.1700459114
5. Fleischhauer K, Kernan NA, O'Reilly RJ, Dupont B, Yang SY. Bone marrow-allograft rejection by T lymphocytes recognizing a single amino acid difference in HLA-B44. *N Engl J Med* (1990) 323(26):1818–22. doi:10.1056/NEJM199012273232607
6. Keever CA, Leong N, Cunningham I, Copelan EA, Avalos BR, Klein J, et al. HLA-B44-directed cytotoxic T cells associated with acute graft-versus-host disease following unrelated bone marrow transplantation. *Bone Marrow Transplant* (1994) 14(1):137–45.
7. Joris MM, van Rood JJ, Roelen DL, Oudshoorn M, Claas FH. A proposed algorithm predictive for cytotoxic T cell alloreactivity. *J Immunol* (2012) 188(4):1868–73. doi:10.4049/jimmunol.1102086
8. Joris MM, Lankester AC, von dem Borne PA, Kuball J, Bierings M, Cornelissen JJ, et al. Translating in vitro prediction of cytotoxic T cell alloreactivity to hematopoietic stem cell transplantation outcome. *Transpl Immunol* (2014) 30(2–3):59–64. doi:10.1016/j.trim.2013.08.006
9. Sizzano F, Zito L, Crivello P, Crocchiolo R, Vago L, Zino E, et al. Significantly higher frequencies of alloreactive CD4+ T cells responding to nonpermissive than to permissive HLA-DPB1 T-cell epitope disparities. *Blood* (2010) 116(11):1991–2. doi:10.1182/blood-2010-05-284687
10. Nicholson I, Varney M, Kanaan C, Grigg A, Szer J, Tiedemann K, et al. Alloresponses to HLA-DP detected in the primary MLR: correlation with a single amino acid difference. *Hum Immunol* (1997) 55(2):163–9. doi:10.1016/S0198-8859(97)00091-8
11. Cesbron A, Moreau P, Milpied N, Harousseau JL, Muller JY, Bignon JD. Crucial role of the third and fourth hypervariable regions of HLA-DPB1 allelic sequences in the mixed lymphocyte reaction. *Hum Immunol* (1992) 33(3):202–7. doi:10.1016/0198-8859(92)90072-U
12. Zino E, Frumento G, Marktel S, Sormani MP, Ficara F, Di Terlizzi S, et al. A T-cell epitope encoded by a subset of HLA-DPB1 alleles determines nonpermissive mismatches for hematologic stem cell transplantation. *Blood* (2004) 103(4):1417–24. doi:10.1182/blood-2003-04-1279
13. Crivello P, Zito L, Sizzano F, Zino E, Maiers M, Mulder A, et al. The impact of amino acid variability on alloreactivity defines a functional distance predictive of permissive HLA-DPB1 mismatches in hematopoietic stem cell transplantation. *Biol Blood Marrow Transplant* (2015) 21(2):233–41. doi:10.1016/j.bbmt.2014.10.017
14. Fleischhauer K, Shaw BE, Gooley T, Malkki M, Bardy P, Bignon JD, et al. Effect of T-cell-epitope matching at HLA-DPB1 in recipients of unrelated-donor haemopoietic-cell transplantation: a retrospective study. *Lancet Oncol* (2012) 13(4):366–74. doi:10.1016/S1470-2045(12)70004-9
15. Pidala J, Lee SJ, Ahn KW, Spellman S, Wang HL, Aljurf M, et al. Nonpermissive HLA-DPB1 mismatch increases mortality after myeloablative unrelated allogeneic hematopoietic cell transplantation. *Blood* (2014) 124(16):2596–606. doi:10.1182/blood-2014-05-576041
16. Brzostek J, Gascoigne NR. Thymic origins of T cell receptor alloreactivity. *Transplantation* (2017) 101:1535–41. doi:10.1097/TP.0000000000001654
17. Rutten CE, van Luxemburg-Heijs SA, Halkes CJ, van Bergen CA, Marijt EW, Oudshoorn M, et al. Patient HLA-DP-specific CD4+ T cells from HLA-DPB1-mismatched donor lymphocyte infusion can induce graft-versus-leukemia reactivity in the presence or absence of graft-versus-host disease. *Biol Blood Marrow Transplant* (2013) 19(1):40–8. doi:10.1016/j.bbmt.2012.07.020
18. Rutten CE, van Luxemburg-Heijs SA, van der Meijden ED, Griffioen M, Oudshoorn M, Willemze R, et al. HLA-DPB1 mismatching results in the generation of a full repertoire of HLA-DPB1-specific CD4+ T cell responses showing immunogenicity of all HLA-DPB1 alleles. *Biol Blood Marrow Transplant* (2010) 16(9):1282–92. doi:10.1016/j.bbmt.2010.03.018
19. Litjens NH, de Wit EA, Baan CC, Betjes MG. Activation-induced CD137 is a fast assay for identification and multi-parameter flow cytometric analysis of alloreactive T cells. *Clin Exp Immunol* (2013) 174(1):179–91. doi:10.1111/cei.12152
20. Robins HS, Campregher PV, Srivastava SK, Wacher A, Turtle CJ, Kahsai O, et al. Comprehensive assessment of T-cell receptor beta-chain diversity in alphabeta T cells. *Blood* (2009) 114(19):4099–107. doi:10.1182/blood-2009-04-217604
21. Carlson CS, Emerson RO, Sherwood AM, Desmarais C, Chung MW, Parsons JM, et al. Using synthetic templates to design an unbiased multiplex PCR assay. *Nat Commun* (2013) 4:2680. doi:10.1038/ncomms3680
22. Lefranc MP, Giudicelli V, Duroux P, Jabado-Michaloud J, Folch G, Aouinti S, et al. IMGT(R), the international ImMunoGeneTics information system(R) 25 years on. *Nucleic Acids Res* (2015) 43(Database issue):D413–22. doi:10.1093/nar/gku1056
23. Pielou EC. Species-diversity and pattern-diversity in the study of ecological succession. *J Theor Biol* (1966) 10(2):370–83. doi:10.1016/0022-5193(66)90133-0
24. Daley T, Smith AD. Predicting the molecular complexity of sequencing libraries. *Nat Methods* (2013) 10(4):325–7. doi:10.1038/nmeth.2375
25. DeWitt WS, Emerson RO, Lindau P, Vignali M, Snyder TM, Desmarais C, et al. Dynamics of the cytotoxic T cell response to a model of acute viral infection. *J Virol* (2015) 89(8):4517–26. doi:10.1128/JVI.03474-14
26. Morisita M. Measuring of the dispersion and analysis of distribution patterns. *Mem Fac Sci Kyushu Univ Ser E Biol* (1959) 2:215–35.
27. R_Core_Team. *R: A Language and Environment for Statistical Computing*. Vienna, Austria: R Foundation for Statistical Computing (2017). Available from: https://www.R-project.org/
28. RStudio_Team. *RStudio: Integrated Development for R*. Boston, MA: RStudio, Inc (2015). Available from: http://www.rstudio.com/
29. Emerson RO, Mathew JM, Konieczna IM, Robins HS, Leventhal JR. Defining the alloreactive T cell repertoire using high-throughput sequencing of mixed lymphocyte reaction culture. *PLoS One* (2014) 9(11):e111943. doi:10.1371/journal.pone.0111943
30. Zuber J, Shonts B, Lau SP, Obradovic A, Fu J, Yang S, et al. Bidirectional intragraft alloreactivity drives the repopulation of human intestinal allografts and correlates with clinical outcome. *Sci Immunol* (2016) 1(4):eaah3732. doi:10.1126/sciimmunol.aah3732
31. Diaz G, Canas B, Vazquez J, Nombela C, Arroyo J. Characterization of natural peptide ligands from HLA-DP2: new insights into HLA-DP peptide-binding motifs. *Immunogenetics* (2005) 56(10):754–9. doi:10.1007/s00251-004-0735-5
32. Arroyo J, Alvarez AM, Nombela C, Sanchez-Perez M. The role of HLA-DP beta residue 69 in the definition of antibody-binding epitopes. *Hum Immunol* (1995) 43(3):219–26. doi:10.1016/0198-8859(95)00022-V

33. Diaz G, Catalfamo M, Coiras MT, Alvarez AM, Jaraquemada D, Nombela C, et al. HLA-DPbeta residue 69 plays a crucial role in allorecognition. *Tissue Antigens* (1998) 52(1):27–36. doi:10.1111/j.1399-0039.1998.tb03020.x
34. Diaz G, Amicosante M, Jaraquemada D, Butler RH, Guillen MV, Sanchez M, et al. Functional analysis of HLA-DP polymorphism: a crucial role for DPbeta residues 9, 11, 35, 55, 56, 69 and 84-87 in T cell allorecognition and peptide binding. *Int Immunol* (2003) 15(5):565–76. doi:10.1093/intimm/dxg057
35. Berretta F, Butler RH, Diaz G, Sanarico N, Arroyo J, Fraziano M, et al. Detailed analysis of the effects of Glu/Lys beta69 human leukocyte antigen-DP polymorphism on peptide-binding specificity. *Tissue Antigens* (2003) 62(6):459–71. doi:10.1046/j.1399-0039.2003.00131.x
36. Heemskerk MB, Roelen DL, Dankers MK, van Rood JJ, Claas FH, Doxiadis II, et al. Allogeneic MHC class I molecules with numerous sequence differences do not elicit a CTL response. *Hum Immunol* (2005) 66(9):969–76. doi:10.1016/j.humimm.2005.06.007
37. Heemskerk MB, Cornelissen JJ, Roelen DL, van Rood JJ, Claas FH, Doxiadis II, et al. Highly diverged MHC class I mismatches are acceptable for haematopoietic stem cell transplantation. *Bone Marrow Transplant* (2007) 40(3):193–200. doi:10.1038/sj.bmt.1705721
38. Weisdorf DJ. How closely related is graft-vs-leukemia to donor/recipient disparity? *Best Pract Res Clin Haematol* (2010) 23(4):525–8. doi:10.1016/j.beha.2010.09.015
39. Falkenburg JH, Jedema I. Allo-reactive T cells for the treatment of hematological malignancies. *Mol Oncol* (2015) 9(10):1894–903. doi:10.1016/j.molonc.2015.10.014
40. Fleischhauer K, Beelen DW. HLA mismatching as a strategy to reduce relapse after alternative donor transplantation. *Semin Hematol* (2016) 53(2):57–64. doi:10.1053/j.seminhematol.2016.01.010
41. Fleischhauer K, Zino E, Mazzi B, Sironi E, Servida P, Zappone E, et al. Peripheral blood stem cell allograft rejection mediated by CD4(+) T lymphocytes recognizing a single mismatch at HLA-DP beta 1*0901. *Blood* (2001) 98(4):1122–6. doi:10.1182/blood.V98.4.1122
42. Shaw BE, Marsh SG, Mayor NP, Russell NH, Madrigal JA. HLA-DPB1 matching status has significant implications for recipients of unrelated donor stem cell transplants. *Blood* (2006) 107(3):1220–6. doi:10.1182/blood-2005-08-3121
43. Shaw BE, Potter MN, Mayor NP, Pay AL, Smith C, Goldman JM, et al. The degree of matching at HLA-DPB1 predicts for acute graft-versus-host disease and disease relapse following haematopoietic stem cell transplantation. *Bone Marrow Transplant* (2003) 31(11):1001–8. doi:10.1038/sj.bmt.1704029
44. Corse E, Gottschalk RA, Allison JP. Strength of TCR-peptide/MHC interactions and in vivo T cell responses. *J Immunol* (2011) 186(9):5039–45. doi:10.4049/jimmunol.1003650
45. van Panhuys N. TCR signal strength alters T-DC activation and interaction times and directs the outcome of differentiation. *Front Immunol* (2016) 7:6. doi:10.3389/fimmu.2016.00006
46. Hogquist KA. Signal strength in thymic selection and lineage commitment. *Curr Opin Immunol* (2001) 13(2):225–31. doi:10.1016/S0952-7915(00)00208-9
47. Crocchiolo R, Zino E, Vago L, Oneto R, Bruno B, Pollichieni S, et al. Nonpermissive HLA-DPB1 disparity is a significant independent risk factor for mortality after unrelated hematopoietic stem cell transplantation. *Blood* (2009) 114(7):1437–44. doi:10.1182/blood-2009-01-200378
48. Petersdorf EW, Malkki M, O'HUiginC, Carrington M, Gooley T, Haagenson MD, et al. High HLA-DP expression and graft-versus-host disease. *N Engl J Med* (2015) 373(7):599–609. doi:10.1056/NEJMoa1500140
49. Fleischhauer K. Immunogenetics of HLA-DP – a new view of permissible mismatches. *N Engl J Med* (2015) 373(7):669–72. doi:10.1056/NEJMe1505539
50. Cherel M, Choufi B, Trauet J, Cracco P, Dessaint JP, Yakoub-Agha I, et al. Naive subset develops the most important alloreactive response among human CD4+ T lymphocytes in human leukocyte antigen-identical related setting. *Eur J Haematol* (2014) 92(6):491–6. doi:10.1111/ejh.12283
51. Distler E, Bloetz A, Albrecht J, Asdufan S, Hohberger A, Frey M, et al. Alloreactive and leukemia-reactive T cells are preferentially derived from naive precursors in healthy donors: implications for immunotherapy with memory T cells. *Haematologica* (2011) 96(7):1024–32. doi:10.3324/haematol.2010.037481
52. Flomenberg N, Russo C, Ferrone S, Dupont B. HLA class I specific T lymphocyte clones with dual alloreactive functions. *Immunogenetics* (1984) 19(1):39–51. doi:10.1007/BF00364474
53. Strassman G, Bach FH. OKT4+ cytotoxic T cells can lyse targets via class I molecules and can be blocked by monoclonal antibody against T4 molecules. *J Immunol* (1984) 133(4):1705–9.

Conflict of Interest Statement: JR, MV, and EY have employment and equity ownership with Adaptive Biotechnologies. All other authors declare that the research was conducted in the absence of any commercial or financial relationships that could be construed as a potential conflict of interest.

6.3. Article III

Author contributions

Immunopeptidome restriction by HLA-DM limits T-cell alloreactivity against HLA-DP 84Gly/Asp variants in clinical transplantation

Thuja Meurer, Pietro Crivello, Maximilian Metzing, Michel G. Kester, Dominik A. Megger, Weiqiang Chen, Peter A. van Veelen, Peter van Balen, Astrid M. Westendorf, Georg Homa, Sophia E. Layer, Amin T. Turki, Marieke Griffioen, Peter A. Horn, Barbara Sitek, Dietrich W.Beelen, J. H. Frederik Falkenburg, Esteban Arrieta-Bolaños, Katharina Fleischhauer

*These authors contributed equally

Article under submission in PNAS

Impact factor: 9.58 (2018)

Status: submitted April 2020, PNAS

DOI: NA

PubMed-ID: NA

Contributions:

- Conception: 30 %
- Experimental work: 75 %
- Data analysis: 75 %
- Statistical analysis: 75 %
- Writing the manuscript: 30 %
- Revising the manuscript: 30 %

Katharina Fleischhauer ……..

(Prof. Dr. Katharina Fleischhauer)

T. Meurer ……..

(Thuja Meurer)

Immunopeptidome restriction by HLA-DM limits T-cell alloreactivity against HLA-DP 84Gly/Asp variants in clinical transplantation

Thuja Meurer[1,9], Pietro Crivello[1,9], Maximilian Metzing[1], Michel G. Kester[2], Dominik A. Megger[3], Weiqiang Chen[3], Peter A. van Veelen[4], Peter van Balen[2], Astrid M. Westendorf[5], Georg Homa[1], Sophia E. Layer[1], Amin T. Turki[1,6], Marieke Griffioen[2], Peter A. Horn[7], Barbara Sitek[3], Dietrich W. Beelen[6], J. H. Frederik Falkenburg[2], Esteban Arrieta-Bolaños[1,9], & Katharina Fleischhauer[1,8,9*]

[1]Institute for Experimental Cellular Therapy, University Hospital Essen, Germany

[2]Department of Hematology, Leiden University Medical Center, The Netherlands

[3]Medical Proteome Center, Ruhr University Bochum, Germany

[4]Centre for Proteomics and Metabolomics, Leiden University Medical Center, The Netherlands

[5]Institute for Medical Microbiology, University Hospital Essen, Germany

[6]Department of Bone Marrow Transplantation, University Hospital Essen, Germany

[7]Institute for Transfusion Medicine, University Hospital Essen, Germany

[8]German Cancer Consortium, Heidelberg Germany

[9]These authors contributed equally

[*]Correspondence: katharina.fleischhauer@uk-essen.de

Abstract

HLA class II DP molecules are important orchestrators of the immune response, with two allotype groups defined by glycine (Gly) or aspartic acid (Asp) at position 84, which are associated with differential peptide processing and immunogenicity. The mechanistic link between these genetic and functional features is unknown. Here, we sequenced the immunopeptidome of representative HLA-DP 84Gly/Asp allotypes in the same cellular background with or without HLA-DM, showing that HLA-DM activity restricts peptide diversity across allotype groups. In contrast, HLA-DM is required to limit the magnitude and $CD4^+$ T-cell receptor diversity of alloresponses to HLA-DP disparities within the same, but less so across different 84Gly/Asp allotype groups, in healthy individuals and in patients after hematopoietic cell transplantation. Our findings provide a mechanism for previously described associations of donor-recipient HLA-DP allotype group disparity with mortality and graft-versus-host disease after clinical transplantation, and have also potential implications for autoimmunity, infection and cancer.

Introduction

HLA-DP is a classical MHC class II molecule that has emerged over the last two decades as an important orchestrator of allotype-specific immune functions in transplantation, autoimmunity, infection, and cancer. Donor-recipient HLA-DP disparity has been associated with humoral and cellular alloreactivity in solid organ[1] and hematopoietic cell transplantation (HCT)[2]. In addition, the molecular structure of HLA-DP2 is at the basis of hypersensitivity to beryllium[3], and single nucleotide polymorphisms (SNP) in the HLA-DP region have been associated with different autoimmune disorders[4, 5, 6] and with the outcome of viral infections, including hepatitis[7, 8, 9] and HIV[10]. Interestingly, certain HLA-DP allotypes have recently been reported as the only known MHC class II ligands for the activating NK cell receptor NKp44[11]. Moreover, HLA-DP polymorphism is associated with the risk of developing certain hematologic cancers[12, 13], and HLA-DP-restricted T cells are being promoted for cancer immunotherapy in melanoma[14] and leukemia[15].

HLA-DP molecules can be divided into two functionally distinct allotype groups characterized by the presence of either glycine (Gly) or aspartic acid (Asp) at polymorphic position 84 of their peptide-binding domain (PBD), which defines DP4-like (84Gly) and DP10-like (84Asp) variants, respectively. DP4-like variants have been shown to display lower affinity for cleaved invariant chain peptide (CLIP) and hence improved presentation of endogenous peptides compared to DP10-like variants[16, 17]. Moreover, HLA-DP 84Gly/Asp variants have been associated with differential immunogenicity for alloreactive $CD4^+$ T cells, which is low (permissive) when self and non-self HLA-DP variants are from the same allotype group, while it is significantly stronger (non-permissive) when involving different allotype groups[18]. In the clinical setting of HCT, these two conditions have been shown to be associated with the risks of mortality, graft-versus-host disease (GvHD), and rejection[19, 20].

As for other class II molecules, binding of high-affinity peptides to HLA-DP is facilitated by the non-classical MHC class II chaperone HLA-DM, a process at least partially inhibited by HLA-DO[21]. Interestingly, endosomal removal of CLIP is critically dependent on HLA-DM activity for HLA-DR, but less so for HLA-DQ and HLA-DP[22]. Therefore, HLA-DR but not HLA-DP complexes are predominantly loaded with CLIP in the absence of HLA-DM[23]. The mechanistic link between these locus- and allotype-specific HLA-DP-peptide processing characteristics and differential allogenicity, and the significance of HLA-DM-mediated peptide editing for $CD4^+$ T-cell recognition of HLA-DP allotypes, are currently unknown.

Here we sequenced the immunopeptidomes of representative HLA-DP molecules from the 84Gly/Asp allotype groups in the presence and absence of HLA-DM in the same cellular background, and probed into the role of HLA-DM in the magnitude and T-cell receptor (TCR) diversity of the alloreactive $CD4^+$ T-cell response in healthy individuals and patients after HCT. We show that both 84Gly/Asp allotypes are similarly susceptible to HLA-DM-mediated restriction of the peptide repertoire, and that HLA-DM is required for limiting T-cell alloreactivity, in particular against permissive HLA-DP disparities within the same 84Gly/Asp allotype group displaying partially overlapping immunopeptidomes. These findings provide a mechanism for the described associations with HCT outcomes, and have also potential implications in the aforementioned HLA-DP-associated clinical settings.

Results

Allotype-specific features of the HLA-DP immunopeptidome

We studied three HLA-DP allotypes, namely DP401, DP402 (both 84Gly), and DP10 (84Asp), representative of the 84Gly/Asp variants (Fig. 1a). These alleles were selected on the basis of their high frequency in different populations (DP401), and of their being representative of two distinct T-cell epitope (TCE) groups (DP402 and DP10) previously identified by us as being significantly associated with T-cell alloreactivity and HCT outcomes[18, 24]. Reflecting exonic linkage disequilibrium within HLA-DPB1, the 84Gly/Asp variants are linked to several other polymorphic amino acid (aa) residues in different hypervariable regions (HvR) of the HLA-DP PBD, resulting in sharing of all but three aa between the DP401 reference and DP402, as opposed to no aa sharing between DP401 and DP10 (Fig. 1a). Crystallography-based molecular structure of HLA-DP showed position 84 of the PBD to be located in HvR F, closely contacting the P1 anchor residue of the peptide (Fig. 1b). Each of the three HLA-DP allotypes was introduced along with CD80, invariant chain (Ii), and HLA-DM into HeLa cells[25], where they were expressed at comparable levels (Supplementary Fig. 1a). Tandem mass spectrometry (MS) of peptides eluted from affinity-purified HLA-DP molecules from these cells revealed a consistent correlation (>80% median shared peptides) between the peptides identified in both technical and biological replicates (Supplementary Fig. 1b). The peptides detected had mean lengths congruent with expectations for HLA class II molecules (Supplementary Fig. 1c). We found a significant overlap in the immunopeptidomes presented by the 84Gly variants DP401 and DP402, while the overlap between these two molecules and the 84Asp variant DP10 was negligible, both in terms of unique peptides (~30% and <2%, respectively) (Fig. 1c) and the cumulative abundance of core epitopes (~40% and <5%, respectively) (Fig. 1d). This observation reflected in their peptide-binding motifs,

which were largely superimposable for DP401 and DP402, but divergent for DP10 (Fig. 1e). In line with a predominant role of the 84 residue in the HLA-DP PBD predicted by molecular modeling (Fig. 1b), DP10 preferred positively charged residues at the P1 peptide anchor residue correlating with the presence of the negatively charged 84Asp, while different uncharged P1 residues were found in both 84Gly allotypes (Fig. 1e). Gene ontology (GO) analysis revealed a larger proportion of peptides from endogenous sources in the immunopeptidomes of DP401 and DP402 compared to DP10, the latter presenting predominantly peptides from exogenous sources (Fig. 1f). Together, these data show that the 84Gly/Asp variants of the PBD determine important changes in the immunopeptidome presented by HLA-DP allotypes.

HLA-DM restricts the peptide repertoire diversity of HLA-DP across 84Gly/Asp allotype groups

To understand whether HLA-DP 84Gly/Asp allotypes differed in their susceptibility to HLA-DM-mediated peptide editing, DP402 and DP10 were introduced into HeLa cells expressing CD80, Ii, but not HLA-DM, and expressed at levels comparable to their HLA-DM positive counterparts (Supplementary Fig. 1a). Tandem MS analysis of peptides eluted from these HLA-DP molecules again gave reproducible results and expected mean peptide lengths (Supplementary Fig. 1b,c). The absence of HLA-DM doubled the number of peptides eluted from both allotypes compared to its presence (Fig. 2a), with no significant change in their peptide motifs (data not shown). The peptide repertoire overlap between DP401 DM and DP402 dropped from 32% in the presence of HLA-DM to 14.4% in its absence, while it remained low with DP10 in the presence or absence of HLA-DM (0.5% for both conditions) (Supplementary Fig. 1d). In addition to quantitative differences, the absence of HLA-DM also resulted in qualitative changes, both when considering all unique peptides or only core

epitopes, with less than 25% and 40% of unique and core peptides presented in the absence of HLA-DM found also in its presence (Fig. 2a,b and Supplementary Fig. 1e). Both DP402 and DP10 presented significantly ($p<0.001$) more CLIP in the absence of HLA-DM than in its presence, but DP10 was at least ten times more efficient in CLIP presentation than DP402 (Fig. 2c). Quantitatively, twice as many peptides were significantly ($p<0.01$) more abundant in the absence compared to the presence of HLA-DM for both HLA-DP allotypes (Fig. 2d), with similar results when the analysis was restricted to core epitopes (Fig. 2e). GO analysis revealed that the origins of most peptides quantitatively upregulated in the presence of HLA-DM were also found in its absence, with only a single cellular compartment among the top 15 specifically enriched only in peptides upregulated in the presence of HLA-DM (Fig. 2f and Supplementary Fig. 1f). In contrast, peptides specifically upregulated in the absence of HLA-DM originated from a broad array of mainly intracellular compartments for both HLA-DP allotypes (Fig. 2f and Supplementary Fig. 1f). Collectively, these data demonstrate that HLA-DM restricts the peptide repertoire lodged into the PBD of HLA-DP to a similar extent in 84Gly and 84Asp allotypes.

HLA-DM regulates T-cell alloreactivity to HLA-DP in an allotype-specific manner

We have previously shown that the most important residues in the HLA-DP PBD for *in vitro* alloreactive $CD4^+$ T-cell responses are those contacting the bound peptide, which include position 84[26]. Therefore, we hypothesized that HLA-DM-mediated modulation of the peptide repertoire might have an impact on T-cell alloreactivity. To test this hypothesis, we quantified the specific *in vitro* $CD4^+$ T-cell alloresponse from $DP401^+$ (84Gly) healthy responders against allogeneic DP402 (84Gly-matched, i.e. permissive) or DP10 (84Asp-mismatched, i.e. non-permissive) in the presence or absence of HLA-DM on the same HeLa cells used for the immunopeptidomics studies above (Fig. 3a,b). For both HLA-DP allotypes,

we obtained specific alloresponses that could be inhibited by monocolonal antibody (mAb) (Supplementary Fig. 2a). We confirmed our previous results[18] that in the presence of HLA-DM, the mean specific alloresponse from DP401+ (84Gly) CD4+ T cells to permissive DP402$^+$ (84Gly-matched) stimulators was significantly ($p<0.0001$) lower than to non-permissive DP10$^+$ (84Asp-mismatched) stimulators (Fig. 4a). Strikingly, however, the absence of HLA-DM led to significantly ($p<0.0001$) increased mean levels of alloreactivity against DP402, which became similar ($p=0.77$) to those against DP10 in the presence of HLA-DM. On the contrary, the latter did not significantly increase in the absence of HLA-DM ($p=0.56$). The effect of peptide editing by HLA-DM was further demonstrated when T cells cultured against allogeneic HLA-DP in the absence of HLA-DM were re-stimulated with cells expressing the allotype with HLA-DM or vice versa. In these experiments, CD4$^+$ T cells primed against DP402 or DP10 with HLA-DM did not show increased responses to the respective allotype in the absence of HLA-DM at re-stimulation. In contrast, the presence of HLA-DM significantly reduced strong responses against DP402 and, to a lesser extent, DP10, primed in the absence of HLA-DM (Fig. 4b). For CD4$^+$ T cells primed against DP402 without HLA-DM, similar results were obtained by quenching HLA-DM activity by co-expression of its antagonist HLA-DO, which resulted in levels of response approaching those elicited in the absence of HLA-DM (Fig. 4c). HLA-DP-alloreactive CD4$^+$ T cells were mostly (<10%) negative for the cytotoxicity marker CD57[27, 28] (data not shown), and produced mainly Th1 (IFN-γ, TNF-α) and Th17 (IL-17A, IL-23) cytokines, with levels proportional to CD137 expression (Fig. 4d,e and Supplementary Fig. 2b,c). Overall, these data suggest that the restriction of the peptide repertoire by HLA-DM limits the number of primed alloreactive CD4$^+$ T cells, particularly for permissive HLA-DP disparities within the 84Gly allotype group. Moreover, a large percentage of CD4$^+$ T cells primed in the absence of HLA-DM against permissive or non-

permissive (i.e. 84Gly/Asp-matched or –mismatched) HLA-DP allotypes require peptides no longer presented in the presence of HLA-DM.

HLA-DM limits the TCR-β repertoire diversity responding to HLA-DP allotypes

To obtain evidence for the HLA-DM-mediated effects on the clonotypic repertoire of T-cells responding to HLA-DP allotypes, we investigated the TCR-β diversity from three representative self-DP401 (84Gly) responders against allogeneic permissive DP402 (84Gly, matched) or non-permissive DP10 (84Asp, mismatched) with or without HLA-DM using TCR variable region beta (Vβ) flow cytometry (Supplementary Fig. 3a) and TCR-β next-generation sequencing (NGS). At the Vβ level, alloreactive responses against both permissive and non-permissive HLA-DP were diverse, with most of the Vβ families responding against each allotype with and without HLA-DM in all three responders. However, the percentage of responding T cells within each Vβ family was limited by HLA-DM for DP402 but less so for DP10 (Fig. 5a). TCR-β NGS showed differences in the cumulative frequency of the top-10 CDR3 rearrangements (Fig. 5b) and in the number of unique clonotypes at different sampling depths (Fig. 5c and Supplementary Fig. 3b). Both features revealed higher clonality for T-cell responses against both HLA-DP allotypes in the presence of HLA-DM compared to its absence in all three responders, although this effect was more marked for DP402 (mean 0.52 vs 0.26, p=0.04) than for DP10 (mean 0.32 and 0.25, p=ns). Of note, unlike responses from parallel cultures in the presence of HLA-DM (Supplementary Fig. 4), clonotype sharing and repertoire similarity against the same HLA-DP allotype with or without HLA-DM within the same individual was only weak (Fig. 5d,e and Supplementary Fig. 5a,b). Moreover, sharing of HLA-DP-reactive clonotypes across individuals was almost non-existent (Supplementary Fig. 5b). Most HLA-DP-alloreactive clonotypes came from the deep, low-abundance repertoires (i.e. not detected in pre-culture samples) for both allotypes with and without HLA-DM

(Supplementary Fig. 6a). TCR-β responses against DP402 but not DP10 with HLA-DM were skewed toward clonotypes with shorter CDR3, which were normalized if HLA-DM was absent (Supplementary Fig. 6b). V-J rearrangement usage was different between responses across HLA-DP allotypes and against the same HLA-DP antigen with or without HLA-DM (Supplementary Fig. 6c). Taken together, these data suggest that HLA-DM-mediated restriction of the peptide repertoire limits the diversity of the broad and individualized spectrum of TCR clonotypes responding to allogeneic HLA-DP, in particular in the setting of permissive, 84Gly/Gly HLA-DP disparity.

HLA-DM-dependency of the T-cell response to allogeneic HLA-DP in transplanted patients

Non-permissive host-donor HLA-DP disparity across 84Gly/Asp allotype groups has been associated with increased risks of mortality, GvHD and rejection after leukemia immunotherapy by HCT[2]. In order to understand whether the observed HLA-DM-mediated effects are relevant also in this clinical setting, we investigated 10 patients who had reconstituted donor-derived (100% donor chimerism) $CD4^+$ T cells several months after unrelated HCT matched for all HLA class I and II alleles except for HLA-DP. All donors carried 84Gly but not 84Asp HLA-DP allotypes. The mismatched HLA-DP in the patient was either also 84Gly (permissive mismatch), or 84Asp (non-permissive mismatch) (Supplementary Table 1). $CD4^+$ T-cell recognition of the mismatched HLA-DP allotypes was tested by priming and re-stimulation in the presence or absence of HLA-DM, following the experimental design in Fig.3a. The absence of HLA-DM led to an increase in the frequency of responding $CD4^+$ T cells in 4/7 cases against permissive 84Gly HLA-DP mismatches, and in 3/4 cases against non-permissive 84GAsp HLA-DP (Fig. 6a). Two patients for whom $CD4^+$ T cells could be purified >9 months after DP402 permissive (IZTF-3) or DP10 non-permissive (IZTF-28) HCT, were studied in greater detail. Cytokine responses by the alloreactive $CD4^+$ T cells from these patients

were dominated by Th1 and Th17 patterns, with a more consistent increase in the absence of HLA-DM for DP402 than for DP10 (Fig. 6b). The TCR-β repertoire against DP402 was more skewed than for DP10, regardless of the presence or absence of HLA-DM (Fig. 6c). The TCR-β clonotypes in the $CD4^+$ T-cell cultures were also traced longitudinally in primary *ex vivo* samples after HCT, as well as in their respective donors. Progressive skewing of the T-cell repertoires was more pronounced in IZTF-3 than in IZTF-28, with top-10 clonotype cumulative frequencies reaching 78.0% and 30.1% of the repertoires >9 months after HCT, respectively (Fig. 6c). IZTF-3 experienced *in vivo* expansion in the first 6 months of a sinlge clonotype that also dominated the repertoires after *in vitro* culture against DP402 with or without HLA-DM, where it amounted to over 85% of the sequences (Fig. 6d). This clonotype might have been triggered by high-titer CMV re-activation on day 54 after HCT (Supplementary Table 1). However, also the underlying repertoire was less diverse than the one expanded *in vitro* from IZTF-28, regardless of the presence of HLA-DM (Fig. 6d). Moreover, the overlap of CDR3 sequences in $CD4^+$ T cells cultured in the presence or absence of HLA-DM was higher for DP402 in IZTF-3 (~25%) than for DP10 in IZTF-28 (~10%; Fig. 6e). Interestingly, clonotypes specific for the *in vitro*-primed $CD4^+$ T-cell cultures in the absence of HLA-DM were markedly less frequent in the *ex vivo* samples than those from the *in vitro*-primed $CD4^+$ T-cell cultures in the presence of HLA-DM, suggesting a role of $HLA\text{-}DM^+$ cells in priming alloreactive $CD4^+$ T-cell responses *in vivo* (Fig. 6d). Tracking of the top-10 clonotypes across all samples (*ex vivo* and *in vitro*) confirmed discontinuity and low similarity of the TCR-β repertoires at 1 and 6 months post-HCT in both patients (Fig. 6f,g). Taken together, these data provide evidence that both the variants at position 84 of mismatched HLA-DP allotypes, and HLA-DM-mediated editing contribute to the complex *in vivo* dynamics of T-cell alloreactive responses and TCR diversity in patients after clinical transplantation.

Discussion

$CD4^+$ T-cell responses to peptide antigens presented by HLA-DP play an important role in transplantation, autoimmunity[4, 5, 6], infection[7, 8, 9, 10], and cancer[12, 13, 14, 15]. Although HLA-DR-restricted immune responses have been most widely studied, accumulating evidence indicates a central role also for HLA-DP in these settings. Recently, 84Gly/Asp variants of HLA-DP have been shown to be associated with differential CLIP binding affinity, impacting on their preference for presentation of peptides from endogenous vs exogenous antigen sources[16, 17]. We and others have shown that in cancer immunotherapy by HCT, host 84Gly/Asp HLA-DP allotypes display differential immunogenicity for alloreactive $CD4^+$ T cells depending on the donor genetic background, and that these differences are significantly associated with the risks of mortality, GvHD, and rejection after transplantation[19, 20]. It has been unclear whether this phenomenon reflects a mechanistic link between the HLA-DP peptide repertoire shaped by allotype polymorphism and HLA-DM-mediated editing, and immunogenicity. Our data establish that HLA-DM restricts and edits the peptide repertoire displayed by the HLA-DP PBD of both 84Gly and 84Asp variants, thereby limiting the number and diversity of TCR-β clonotypes responding to allogeneic HLA-DP. This is most pronounced for permissive 84Gly/Gly responder/stimulator disparities with partially overlapping immunopeptidomes when HLA-DM is present, but can also be appreciated in the setting of non-permissive 84Gly/Asp combinations despite their essentially non-overlapping immunopeptidomes, especially in patients after clinical transplantation.

Our data show that both genetic features (i.e. the 84Gly/Asp-associated polymorphism) and HLA-DM leave important imprints on the HLA-DP immunopeptidome. The 84Gly DP401 allotype showed significantly higher peptide overlap with the 84Gly DP402 compared to the 84Asp DP10 allotype, both qualitatively and quantitatively. Moreover, the presence of HLA-

DM restricted the peptide repertoire by about 50% in both 84Gly and 84Asp HLA-DP allotypes. The latter is in stark contrast to many HLA-DR allotypes, where HLA-DM activity diversifies an immunopeptidome dominated by CLIP in its absence[22, 23, 29]. This has implications for the functional effects of HLA-DM down-modulation, either directly or through its antagonist HLA-DO, on HLA-DP vs HLA-DR-restricted immune responses. For the latter, low HLA-DM activity leading to increased presentation of CLIP is associated with lower immunogenicity for alloreactive and tumor antigen-specific T cells, with selective downregulation of HLA-DM described as a mechanism of immune evasion by HLA-DR$^+$ leukemias and lymphomas[30, 31, 32]. Our findings show that the loss or inhibition of HLA-DM activity has opposite effects for HLA-DP, where limited Ii and CLIP dependency[22] leads to a broader array of peptides from various cellular compartments presented in HLA-DM$^-$ compared to HLA-DM$^+$ cells. Interestingly, peptides up-regulated in the absence of HLA-DM were derived from predominantly endogenous sources for both 84Gly and 84Asp variants, suggesting that the limited presentation of endogenous peptides by 84Asp variants can be at least partially overruled by the absence of HLA-DM. These findings have potential implications for HLA-DP-restricted immune responses to intracellular agents such as viral or tumor antigens. These responses might be potentiated when HLA-DM activity is low, a mechanism potentially contrasting impaired antigen presentation by HLA-DR in this condition. Our findings also suggest that described loss-of-function genetic variants of HLA-DM[33] might play a yet unappreciated role in HLA-DP-linked autoimmune disease such as ANCA vasculitis[5] or aplastic anemia[6], where the combined polymorphism of HLA-DP and HLA-DM might jointly contribute to setting the genetic stage for disease onset.

Our data show that the imprints on the HLA-DP immunopeptidome by the 84Gly/Asp variants and HLA-DM-mediated peptide editing have a significant impact on CD4$^+$ T-cell

alloreactivity *in vitro* and in transplanted patients. The degree of immunopeptidome overlap between mismatched HLA-DP allotypes was reflected by the number and diversity of responding $CD4^+$ TCR-β clonotypes. These features were significantly lower in response to permissive 84Gly/Gly (DP401 vs DP402) compared to non-permissive 84Gly/Asp (DP401 vs DP10) HLA-DP mismatches in the presence of HLA-DM, and increased in the absence of HLA-DM in particular for permissive HLA-DP disparity. These findings provide mechanistic insights into previous clinical observations made by us and others, that permissive HLA-DP disparity is associated with significantly reduced risks of GvHD and mortality after leukemia immunotherapy by allogeneic HCT, compared to non-permissive HLA-DP disparity[19, 20]. In these studies, permissive HLA-DP mismatches were identified by three T-cell epitope (TCE) groups established according to alloreactive T-cell cross-reactivity patterns[24, 26]. The 84Asp variant is carried by all HLA-DP allotypes of TCE group 1 and 2, while TCE group 3 is more heterogeneous, including both the most frequent 84Gly, but also some 84Asp allotypes[35]. Hence, 84Gly/Asp variants do not define all HLA-DP mismatches previously classified as permissive or non-permissive, but a considerable fraction of them (1720/2736, i.e. 63% of HLA-DP-mismatched donor-host pairs from one of our previous studies[36]). Moreover, another algorithm developed to classify high-risk HLA-DP mismatches in HCT is based on the evolutionary relation between 2 allele clades (DP2 and DP5 groups), which are also correlated to the 84Gly/Asp variant[37]. Further investigations are thus needed to establish if the proof-of-principle findings regarding the mechanisms underlying permissive mismatches reported here for the frequent 84Gly/Asp allotypes apply also to the remaining ones, and if they represent a central feature able to reconcile different mismatch risk algorithms.

Interestingly, 84Asp is in strong, though not exclusive, linkage disequilibrium with the G-variant of the rs9277534 SNP in the 3' untranslated region (UTR) of HLA-DPB1[38], which is

associated with high HLA-DP expression levels and poor clearance of hepatitis B virus[7], as well as with GvHD in allogeneic HCT[39]. It is tempting to speculate that unique peptides displayed in the HLA-DP immunopeptidome might be presented more efficiently in high-expression variants, thereby determining an additive effect between exon and 3'UTR polymorphisms for GvHD risks after HCT.

Increasing evidence suggests an important role for $CD4^+$ T-cells responding to peptide antigens processed and presented by HLA class II in both GvHD and leukemia control after allogeneic HCT. HLA class II-expressing gut epithelial cells were shown to be involved in lethal GvHD[40], and selective downregulation of HLA-DR and HLA-DP was established as a mechanism of specific immune evasion by leukemia relapsing after allogeneic HCT[41, 42]. Comparative tracking of alloreactive $CD4^+$ T-cell clonotypes specific for $HLA\text{-}DM^+$ or $HLA\text{-}DM^-$ conditions in our study showed that the repertoire reconstituting in patients long-term after HCT contains few $HLA\text{-}DM^-$-specific clonotypes, suggesting that *in vivo* priming might occur preferentially on $HLA\text{-}DM^+$ antigen presenting cells. Thus, low HLA-DM activity in leukemia cells, either due to concomitant HLA-DO expression e.g. in B-cell tumors[43], or after targeted inhibition of HLA-DM by small molecules or RNA interference[44], might reduce toxicity but maintain therapeutic efficacy in HLA-DP-mismatched allogeneic immune therapy.

In summary, our data provide new evidence for complementary effects of the 84Gly/Asp-associated PBD polymorphism and HLA-DM-mediated peptide editing in shaping the HLA-DP immunopeptidome, which is central in determining HLA-DP immunogenicity for alloreactive $CD4^+$ T-cells in clinical transplantation. These mechanistic insights shed new light onto HLA-DP as an emerging orchestrator of immunity, whose particular locus-specific polymorphism and antigen-processing characteristics may be therapeutically exploited in different areas of life sciences.

Methods

Cell lines. Single HLA-DP antigen-expressing cells were previously generated by retroviral transduction of HeLa cells[45] with vectors encoding CD74 (component of the HLA class II processing machinery), CD80 (T-cell costimulatory molecule), and combinations of HLA-DP alpha and beta chain genes either with or without co-transduction of the peptide editor HLA-DM alpha and beta chains[25]. The following combinations of HLA-DP alpha (DPA1) and beta (DPB1) genes were used in this study: DPA1*01:03/DPB1*04:01 in the presence of HLA-DM (DP401 DM), DPA1*01:03/DPB1*04:02 either in the presence (DP402 DM) or absence (DP402) of HLA-DM, DPA1*02:01/DPB1*10:01 either in the presence (DP10 DM) or absence (DP10) of HLA-DM. Expression of HLA-DP in the presence of HLA-DM and its antagonist HLA-DO was obtained using a parental cell line expressing CD74, CD80, HLA-DM, and DO together with HLA-DQ antigens (HeLa DM/DO) previously generated by Kremer *et al*.[46] HLA-DQ expression was knocked out by CRISPR/Cas9 genome editing, and HLA-DQ-negative cells were transduced with lentiviral vectors encoding HLA-DP alpha and beta chain genes as described below. All cell lines were maintained at 37°C and 5% CO_2 in a humidified incubator in Iscove's Modified DMEM supplemented with 10% heat-inactivated fetal calf serum (FCS), 2 mM L-glutamine, 100 ng/ml penicillin-streptomycin (all from c.c.pro).

Primary blood mononuclear cells from human subjects. Peripheral blood (PBMC) or bone marrow (BMMC) mononuclear cells were isolated from healthy donors and HCT patients by standard gradient centrifugation using Lymphoprep (STEMCELL); collected cells were stored at -170°C until use. PBMC were obtained from anonymized healthy blood donors of the University Hospital Essen after informed consent and approval from the local ethics committee (14-5961-BO), in accordance with the principles of the Declaration of Helsinki. Characteristics of the healthy donors (n=18) were the following: median age 53 (range 21-

62); 11 male, 6 female, and 1 unknown; 10 CMV-seropositive and 8 CMV-seronegative. Typing of HLA-DPB1 was performed by sequence-specific oligonucleotide probing (LABType SSO, One Lambda) according to the manufacturer's recommendations in a European Federation of Immunogenetics-accredited HLA typing laboratory at the University Hospital Essen. Types were the following: 10 donors homozygous for HLA-DPB1*04:01; and 8 donors heterozygous for HLA-DPB1*04:01, *02:01. Post-transplant samples from HCT patients and their respective 10/10 HLA-matched stem cell donors were collected as part of a prospective observational clinical study of HLA-DP matching at University Hospital Essen after informed consent. This study and the collection of samples from patients and their donors was approved by the local ethics committee according to the Declaration of Helsinki (16-6769-BO). Peripheral blood and/or bone marrow aspirates from transplanted patients were obtained around days +30, +180, +365 post-transplant during their routine follow up at the Bone Marrow Transplantation Department. Stem cell donor peripheral blood cell samples were collected after mobilization with G-CSF and apheresis of $CD34^+$ enriched cellular products. Patient characteristics including comorbidity index[47] are reported in Table S1. Myeloablative conditioning was performed with cyclophosphamide and melphalan or treosulfan. Reduced intensity conditioning was performed with fludarabine/busulfan or fludarabine/total-body irradiation. GvHD prophylaxis was based on cyclosporin and methotrexate, and additional *in vivo* T-cell depletion by anti-thymocyte globulin (30 mg/kg) at transplantation for all patients.

Flow cytometry. Cell surface or intracytoplasmic expression of relevant molecules was detected using flow cytometry. For cell surface staining, cells were incubated with the relevant fluorochrome-conjugated mAb in phosphate-buffered saline (PBS, Gibco) supplemented with 2% FCS (c.c.pro) for 10 min at 4°C in the dark. For intracytoplasmic

staining, cells were firstly stained for surface antigens as described above and then fixed with PBS containing 4% paraformaldehyde (Morphisto) for 15 min at room temperature. After fixation and washing, cells were permeabilized with PBS+0.1% Saponin (Sigma) for 15 min at room temperature and incubated with the relevant mAb for additional 30 min. Characterization of the HeLa cell lines used in this study was performed using the following mAb: anti-HLA-DP-PE (clone B7/21; Leinco Technologies), anti-CD74-PE (clone LN2; BioLegend), anti-CD80-APC-Alexa Fluor 750 (clone MAB104; Beckman Coulter), and anti-CLIP-PE (clone cerCLIP.1; Santa Cruz) used in surface staining; and anti-HLA-DM-PE (clone MaP.DM1; BD Bioscience), anti-CD74-PE (clone LN2; BioLegend), and isotype control mouse IgG1-PE (clone B11/6; Abcam) for intracytoplasmic staining. Gating strategy can be found in Supplementary Fig. 1a. The following mAb were used as basic panel to identify T-cell subsets by surface staining: anti-CD3-Krome orange (clone UCHT1; Beckman Coulter), anti-CD4-Phycoerithrin-Cyanin7 (PE-Cy7) (clone SK3; BD Bioscience), anti-CD8-Pacific blue (clone B9.11; Beckman Coulter). To assess the purity of isolated $CD4^+$ T cells or immunophenotype of PBMC samples, the following mAb were additionally included: anti-CD14-Fluorescein isothiocyanate (FITC) (clone M φP9), anti-CD19-Allophycocyanin (APC) (clone HIB19, both BD Bioscience), and anti-CD56-PE (clone N901, Beckman Coulter). For quantification of the alloreacitve T-cell response, the following mAb were additionally included: anti-CD57-FITC (clone TB03; Miltenyi Biotec) and anti-CD137-APC (clone 4B4-1; BD Bioscience). Flow-cytometric measurements and data analysis were performed on a GalliosTM 10/3 cytometer (Beckman Coulter) using the software Kaluza for Gallios (Version 1.0, Beckman Coulter) and Kaluza analysis (Version 2.1, Beckman Coulter). Cells were gated as singlet events using forward scatter area/height parameters, excluding cell debris in forward/side scatter dot plots. Additional gating strategies are reported below for each relevant experimental setting.

HLA-DPB1 sequence alignment and visualization of crystal structure. Alignment of HLA-DPB1 genes was retrieved from the IMGT/HLA database[35] and visualized using the software Bioedit version 7.2 (http://www.mbio.ncsu.edu/bioedit/bioedit.html). Crystal structure of the DP2 molecule complexed with a HLA-DR alpha chain-derived peptide was retrieved from the Research Collaboratory for Structural Bioinformatics Protein Data Bank (www.rcsb.org/; RCSB-PDB identifier: 3LQZ[48, 49], and visualized using Deepview SwissPDBviewer software version 4.1[50]. All HLA-DP residues at a distance <5Å from the peptide were considered peptide contacts.

HLA-DP immunoaffinity purification and peptide elution. The HLA-DP specific monoclonal antibody B7/21 was purified by Prot A Sepharose CL-4B beads (GE Healthcare) from the supernatant of hybridoma cells expanded in serum-free Corning Hybrigro SF medium (Corning) using CELLline Bioreactor (Corning). The purified antibody was covalently coupled to Prot-A sepharose beads at a concentration of 2.5 mg/ml using dimethyl pimelimidate dihydrochloride (Sigma-Aldrich). For each biological replicate, 1 ml of B7/21-coupled beads was used to purify HLA-DP/peptide complexes from $1.2x10^9$ HeLa cells expressing the relevant HLA-DP antigen. HeLa cells were initially expanded in 175 cm^2 5-layer multi-flasks (Corning) and distributed into 15-cm diameter dishes the day before cell lysis. Cells were lysed by scraping directly in lysis buffer containing 50 mM Tris-HCl pH 8.0, 150 mM NaCl, 5 mM EDTA, and 0.5% Zwittergent 3-12 (Millipore) freshly supplemented with cOmplete protease inhibitor cocktail (Roche); 1 ml cold lysis buffer was used per $1x10^6$ cells. After 2 hours, cell lysates were pre-cleared overnight with uncoupled Prot-A sepharose beads and loaded by gravity onto glass Econo columns (Biorad) packed with B7/21-coupled beads using a flow rate of 2.5 ml/min. After washing, bound HLA-DP/peptide complexes were eluted and dissociated using 10% acetic acid, and peptides were separated from the HLA-DP molecules

via low-pH solid phase extraction in Oasis HLB 1cc extraction cartridges (Waters). Peptides were finally eluted in 500 µl water/acetonitrile (ACN)/formic acid v/v/v 70/30/0.1, freeze-dried and resuspended in 0.1% trifluoroacetic acid (TFA) prior Mass Spectrometry analysis.

LC-MS/MS analysis. Mass spectrometry analysis was carried out using an Ultimate 3000 RSLCnano liquid chromatography system online coupled to an Orbitrap Elite mass spectrometer (both Thermo Fisher Scientific, Waltham, USA). Each sample was processed in 3 technical replicates, and a total of 2 biological samples per condition were analyzed. In each run, 15 µl of each peptide sample was injected. The peptides were pre-concentrated for 7 min on a trap column (Acclaim® PepMap 100, 75 µm × 2 cm, C18, 5 µm, 100 Å) using 30 µl/min 0.1% TFA as loading solvent. Subsequent separation on an analytical column (Acclaim® PepMap RSLC, 75 µm × 50 cm, nano Viper, C18, 5 µm, 100 Å) was carried out using a gradient from 5 to 40% solvent B in solvent A over 98 min (solvent A: 0.1% formic acid; solvent B: 0.1% formic acid, 84% acetonitrile). A flow rate of 400 nl/min was used with a column oven temperature of 60°C. Data-dependent acquisition mode was used. Full scans were acquired in the Orbitrap analyzer (mass range: 350 – 2,000 m/z, resolution: 60,000). Fourier Transform Mass Spectrometry full scan Automatic Gain Control target was set to $1x10^6$ with a maximum injection time of 200 ms. Number of micro scans was set to 1. The 20 most abundant ions of a spectrum acquired at MS1 level were fragmented using CID (collision-induced dissociation) with a normalized collision energy of 35% and an isolation width of 2 m/z. Fragment mass spectra were acquired in the linear ion trap with a maximum injection time of 100 ms.

Peptide identification and quantification. Peptide identification was carried out using the Proteome Discoverer software (ver. 1.4, Thermo Fisher Scientific). The human UniProt/Swiss-Prot database (release 2016_10, number of sequences: 20,121) was searched

using Mascot (ver. 2.5.1, Matrix Science Ltd). Mass tolerances were set to 5 ppm and 0.4 Da for precursor and fragment ion masses, respectively. Proteolytic cleavage was set to unspecific with no missed cleavages. Oxidation of methionine was considered as variable modification. Confidence of peptide identifications was estimated using the target decoy Peptide Spectrum Matches (PSM) validator function implemented in Proteome Discoverer software. Only high confident peptide identifications with false discovery rates <1% were considered in the further analyses. Protein grouping function (strict maximum parsimony principle) was enabled in Proteome Discoverer. Lists of peptide spectrum matches and corresponding peptide and protein identifications were exported as Excel sheets (Microsoft) and filtered for >9 amino acids length prior subsequent analysis and import into the quantification software. Overlap between lists of unique peptides was represented by proportional Venn diagrams.

Quantitative analysis was performed with Progenesis QI for Proteomics (ver. 2.0.5, Nonlinear Dynamics Ltd). A detailed description of the quantification procedure has been previously reported[51, 52]. Briefly, LC-MS/MS runs were aligned and normalized before individual runs were assigned to respective experimental groups (with or without HLA-DM). Afterwards, quantified features were annotated with PSM. For subsequent analysis, normalized abundances of individual peptides were exported. To highlight significant differences between the experimental groups, statistical analysis of the label-free data was conducted with an in house-developed R script (R Foundation for Statistical Computing, Vienna, Austria) as previously described[53]. Briefly, normalized abundances were arcsinhyp-transformed and analyzed by means of one-way ANOVA. The generated p-values were False-discovery rate (FDR)-adjusted according to Benjamini and Hochberg[54].

Analysis of core epitopes. Raw Mass Spectrometry data were analyzed using the MaxQuant software (version 1.6.5.0) for peptide identification using the human UniProt/Swiss-Prot database mentioned above. Parameters for the analysis were the following: digestion mode was set to unspecific, fixed modification was set to none, variable modifications were Oxidation(M) and Acetyl(protein N-term), option "match between runs" was enabled, all other settings were default values. The generated evidence.txt file was submitted to the online available webtool PLAtEAU (https://plateau.bcp.fu-berlin.de/)[55] for identification and quantification of core epitopes. Minimal core length was set at 10 and data were not filtered for replicate limits. Output lists of core epitopes with the corresponding percentage of relative intensities were compared between data sets from the same HLA-DP antigens expressed in the presence or absence of HLA-DM.

Peptide-binding motifs. Both peptide lists generated by Proteome Discoverer and core epitope lists generated by PLAtEAU as described above were used for identification of peptide-binding motifs using Gibbs clustering approach[56]. List of unique peptides or core epitopes were submitted to GibbsCluster 2.0 Server (http://www.cbs.dtu.dk/services/GibbsCluster/), and analysis was performed using default parameter settings for MHC class II ligands with the only exception of “Interval between Phase shift moves” set at 1000. Up to 5 possible clusters were allowed during the analysis and accuracy of the clustering was assessed using Kullback Leibler distance (KLD) proportional to the size of each cluster. In all analysis, single clusters reached the highest KLD scores and were used to generate peptide binding motif logos by Seq2Logo[57], where the height of each represented amino acid was proportional to the frequency of the amino acid at the indicated position.

Gene ontology analysis. The origin of the identified peptides was analyzed by Gene Ontology (GO) using the software Cytoscape[58] with ClueGO plug-in[59]. Lists of protein sources identified by MS experiments were analyzed for statistically significant enrichment of cellular component GO terms by right-sided hypergeometric test corrected using Benjamini and Hochberg[54]. Parameters for the analysis were the following: analysis of cellular component annotations in the Gene Ontology Annotation Database (GOA, released 2019_09, number of annotations: 2026 terms for 19089 genes)[60, 61], the option "GO term fusion" was enabled, tree interval set from 3 to 8 minimum and maximum levels, kappa score set to 0.4, reference GO set was set to default, threshold for significant enrichment was $p<0.01$. Lists of enriched GO terms were comparatively analyzed between HLA-DP antigens expressed in the presence or absence of HLA-DM and ranked according to the number of associated genes found in each immunopeptidome.

HLA-DP-specific alloreactive T-cell cultures. *In vitro* T-cell alloreactivity was assessed by co-culturing isolated $CD4^+$ T cells or PBMC with irradiated HeLa cells expressing single HLA-DP alloantigens as previously described[62]. In brief, untouched $CD4^+$ T cells were magnetically isolated from PBMC of healthy donors or HCT patients using a $CD4^+$ T-cell isolation kit following manufacturer recommendations (Miltenyi Biotec). Purified $CD4^+$ T cells or PBMC (typically $1.2x10^6$ cells) were plated in a 3:1 ratio with irradiated (100 Gy) HeLa stimulators in 24-well plates (Falcon). T-cell cultures were maintained at 37°C and 5% CO_2 in a humidified incubator in RPMI-1640 (c.c.pro) supplemented with 10% heat-inactivated human AB serum (Sigma), 2 mM L-glutamine (c.c.pro), 100 ng/ml penicillin-streptomycin (c.c.pro), and 50 IU/ml IL-2 (Miltenyi Biotec) for 14 days before using them in the following read-out assays.

CD137 upregulation assay. The degree of *in vitro* T-cell alloreactive response was assessed by measuring the percentage of $CD4^+$ T cells expressing the activation marker CD137[63] after

re-stimulation of each T-cell culture with HeLa cells expressing the relevant HLA-DP alloantigens as previously described[62]. Briefly, 1-1.2x10^5 T cells were re-challenged with fresh HeLa stimulators at a 3:1 ratio in 96-well U-bottom plates (Falcon). After 24 hours, upregulation of CD137 was assessed by surface staining in flow cytometry gating singlet/alive cells for $CD3^+$, $CD4^+$, $CD8^-$ expression. An example of this gating strategy can be found in Fig. 3b. Specific response to each HLA-DP allotype was calculated by subtracting from the percentage of responding $CD137^+CD4^+$ T cells in each condition (stimulation with DP402, DP402 DM, DP10, or DP10 DM) the background activation measured against HeLa cells expressing the autologous HLA-DP (DP401 DM).

CD137 upregulation blocking assay. Stimulator HeLa cells expressing the relevant HLA-DP alloantigen were pre-incubated with either anti-human HLA-DP antibody (clone B7/21; Leinco Technologies), anti-human HLA-DR antibody (clone L243; BioLegend), or without antibody for 30 min at 4°C. After incubation, 1x10^5 alloreactive T cells were added to the stimulators with an effector:target ratio of 3:1 and incubated for 24h before assessment of CD137 upregulation by flow cytometry as described above. The following mAb final concentrations were tested: 0.1 µg/ml, 0.3 µg/ml, 1 µg/ml, 3 µg/ml, and 10 µg/ml. Relative response in the presence of mAb was calculated respect to the overall response in the absence of mAb using the following formula: 100 x (% $CD137^+CD4^+$ T cells with mAb) / (%$CD137^+CD4^+$ T cells without mAb).

Cytokine quantification assay. Profiles of cytokine production in alloreactive T-cell cultures were assessed by quantifying the amount of cytokines in media supernatant collected after 24-hour incubation of T cells with the relevant HeLa stimulators. Cytokine levels were determined by magnetic bead-based multiplex assay (R&D Systems, #LXSAHM) performed on a Luminex MAGPIX® system with XPonent4.2 (Luminex corporation) according to the

manufacturer recommendations. The following cytokines were quantified in the corresponding range of detection (pg/ml): IL-1b (0.65-4.26x10^3), IL-2 (1.39-9.09x10^3), IL-3 (3.36-22.06x10^3), IL-4 (0.58-3.79x10^3), IL-5 (0.23-1.53x10^3), IL-12p70 (5.26-4.41x10^3), IL-10 (0.15-1.01x10^3), IL-17A (0.48-3.15x10^3), IL-21 (1.22-8.00x10^3), IL-23 (4.42-29.02x10^3), IFN-γ (1.63-10.69x10^3), and TNF-α (0.29-1.93x10^3).

CRISPR/Cas9-mediated genome editing and fluorescence-activated cell sorting. The cell line HeLa DM/DO[46] was used as parental cell line to generate cells expressing HLA-DP antigens in the presence of HLA-DM and DO. In order to avoid interference in subsequent experiments, expression of HLA-DQ in these cells was eliminated using transient CRISPR/Cas9 genome editing approach targeting a previously described conserved region in the HLA class II beta chain genes[64]. Briefly, the published target sequence was used for the *in vitro* synthesis of the corresponding single guide RNA (sgRNA) using the Guide-it sgRNA In Vitro Transcription kit (Takara). This sgRNA was assembled at room temperature with the Guide-it Recombinant Cas9 (Takara) and the resulting ribonucleoprotein complex was transiently transfected into the above-mentioned HeLa cells. Transfection was performed via electroporation with the Neon Transfection System (Thermo Fisher Scientific) using 10-µl electrode tips and the following settings: pulse voltage 1005 V, pulse width 35 ms, number of pulses 2. Residual HLA-DQ expression was assessed after 1 week by flow cytometry using the mAb HLADQ1 (Biolegend), and the negative fraction corresponding to 71.5% of total singlet/alive cells was sorted using a FACS Aria III with BD FACSDiva Software (BD Bioscience).

Lentiviral vector transduction of HLA-DP antigens. Coding sequence of combinations of HLA-DP alpha and beta chains were introduced into a bidirectional promoter lentiviral vector adapted from Amendola *et al.*[65, 66]. In this vector, the human phosphoglycerate kinase

(hPGK) promoter fused in the opposite direction to the minimal core promoter derived from cytomegalovirus (minCMV) controlled the coordinate expression of HLA-DP beta and alpha chain, respectively. The following combinations of HLA-DP alpha and beta were used: DPA1*01:03/DPB1*04:02 and DPA1*02:01/DPB1*10:01. The identity of all plasmid constructs was verified by Sanger sequencing. VSV-pseudotyped third generation lentiviral vector particles were produced using the cell line Lenti-X 293 T (Takara) transfected with the relevant HLA-DP constructs and packaging plasmids. For each production, $7.5x10^5$ cells were seeded in a T25 culture flask (Falcon) 24h before transfection. FuGene HD Trasfection reagent (Promega) in a 3:1 ratio with 12 µg total plasmid DNA, (5 µg HLA-DP construct from this study, 2 µg pMDLg/pRRE, 1 µg pMD2.G, and 1 µg pRSV-Rev from Addgene, and 3 µg pAdVAntage from Promega) was used following manufacturer recommendations. After 48 to 60h of incubation at 37°C and 5% CO_2, media supernatant containing the viral particles was harvested and filtered through a 0.22 µm polyethersulfone (PES) membrane (Merck). Finally, 3 ml of filtered supernatant was added to $2x10^5$ HLA-DQ negative HeLa DM/DO cells in a T25 culture flask. To enhance efficiency of transduction, polybrene (Sigma) was added at final concentration of 8 µg/ml. HLA-DP expression was assessed one week after transduction, and after 2 weeks, singlet/live cells were sorted for high HLA-DP expression using FACS Aria III with BD FACSDiva Software (BD Bioscience).

TCR Vβ immunophenotype. TCR diversity of anti-DP402 or DP10 $CD4^+$ T cells at the Vβ level was assessed by flow cytometry using the IOTest® Beta Mark TCR Vβ Repertoire kit (Beckman Coulter). For this, $1x10^6$ $CD4^+$ T cells from each of three different self-DP401 responders cultured against the relevant antigen in the presence or absence of HLA-DM as explained above were re-stimulated with the specific transduced HeLa cells for 24h at a 3:1 ratio. Upon re-stimulation, the T cells were harvested and stained with subset markers as

indicated above, as well as with the kit's 8 Vβ antibody cocktails according to the manufacturer's instructions. Singlet, live, $CD3^+CD4^+$ T cells were gated for Vβ family expression and the frequency of HLA-DP-reactive cells (i.e. $CD4^+CD137^+$) in each of the 24 targeted Vβ families was recorded. An example of this gating strategy can be found in Supplementary Fig. 3a.

TCR immunosequencing. Next generation sequencing-based high-throughput TCR analysis (TCR immunosequencing) was carried out in HLA-DP-alloreactive $CD4^+$ T cells from three self-DP401 healthy responders. For this, $2x10^6$ $CD4^+$ T cells from each responder cultured against DP402 or DP10 in the presence or absence of HLA-DM were re-stimulated with the specific HeLa transduced cells for 24h, after which the T cells were harvested and enriched for CD137 positivity (average purity 91.6%) using magnetic bead technology according to manufacturer's instructions (Miltenyi Biotec). Genomic DNA from enriched $CD4^+CD137^+$ cells and pre-culture isolated $CD4^+$ T cells (purity >95%) from each subject as baseline controls was subsequently extracted using a Qiamp DNA Blood mini Kit (QIAGEN GmbH). In addition, $CD4^+$ T cells from HCT patients approximately 1 year post-transplant cultured against DP402 or DP10 in the presence or absence of HLA-DM were harvested and their DNA as well as DNA from PBMC and BMMC post-HCT and from PBMC from their respective donors was extracted as explained above. DNA from each cultured, pre-culture, and *ex vivo* sample was sequenced to determine TCRB complementarity-determining region 3 (CDR3) rearrangements using the ImmunoSEQ™ Assay (Adaptive Biotechnologies) as previously described[67, 68]. Briefly, a multiplex PCR system based on forward primers targeting 54 TRBV segments, and reverse primers targeting 13 TRBJ segments was used to amplify the CDR3 region of the TCRB locus. The PCR products were sequenced on an Illumina HiSeq System, and reads of 87 base pairs covering the CDR3 region were obtained. Sequence data were preprocessed to remove PCR

and sequencing errors in the primary sequence. CDR3 regions were defined based on alignments to sequences in the international ImMunoGeneTics (IMGT) database®[69]. All cultured samples were analyzed at survey resolution (targeting 30,000 T-cell genomes), while pre-culture and *ex vivo* samples were analyzed at deep resolution (targeting 200,000 T-cell genomes). Input DNA was ~200, 1200, 2000, and 3600 ng for cultured $CD4^+$ and $CD4^+CD137^+$ T cells, pre-culture $CD4^+$ T cells, *ex vivo* PBMC, and *ex vivo* BMMC, respectively. The number of templates (total T cells) and the number of rearrangements (unique T cells) in each sample were estimated based on synthetic template pools as previously described[68]. Detailed information on the number of templates, number of rearrangements, clonality, and productivity for all samples sequenced for TCRB can be found in Tables S2 and S3.

TCR diversity metrics and statistical analyses. Immunosequencing data generated for each sample were analyzed for their TCR diversity in terms of clonality and number of unique rearrangements. Clonality, ranging from 0 (indicating even distribution of frequencies) to 1 (indicating an asymmetric distribution in which a few clonotypes are present at high frequencies) was calculated as 1-Pielou's evenness[70]. Rarefaction analysis of TCR repertoires was performed by plotting the diversity (i.e. number of unique clonotypes) observed under a given sampling depth (number of TCR molecules sampled). Solid and dashed lines in rarefaction curves indicate diversity estimates computed using a multinomial model by inter and extrapolation, respectively[71, 72]. All samples are extrapolated up to the size of largest sample in the comparison. TCR repertoire similarity was assessed by Morisita's index, a population overlap metric relating the dispersion of clonotypes in the samples[73]. The abundance of individual clonotypes was defined by assessing their presence and frequency in pre-culture and cultured samples, and low abundance clonotypes were defined as those seen in cultured samples but undetected in the pre-culture repertoire. Post-analysis of CDR3

immunosequencing data was performed with the ImmunoSEQ Analyzer® 3.0 (Adaptive Biotechnologies, Seattle), VDJtools v.1.1.10[72], and VDJviz[74].

Other statistical analysis. Additional statistical analysis were performed using the software Prism 6.0 (GraphPad Software) and Excel (Microsoft Corporation). Details about the statistical tests used, sample nature and size, and thresholds for statistical significance are indicated in figures and figure legends.

Data availability

All immunopeptidomics data generated and analyzed in this study are freely available at the Proteomic Identification Database (PRIDE) Archive under the accession number PXD017154. TCR immunosequencing data are available at the ImmuneACCESS Database (Adaptive Biotechnologies) under the ImmuneAccess DOI https://doi.org/10.21417/TM2020I.

Reporting summary

Further information on research design is available in the Nature Research Reporting Summary linked to this paper.

Acknowledgments

The authors thank Prof. Mirko Trilling (Essen), Dr. Luca Vago (Milan), and Prof. James P. Di Santo (Paris) for critically reading the manuscript. The Imaging Center Essen (IMCES) cell sorting facility and the Biochip Laboratory of UK-Essen are gratefully acknowledged for their support with the relevant experiments. This work was supported by grants from the Deutsche Forschungsgemeinschaft (DFG FL 843/1-1), the Deutsche José Carreras Leukämie Stiftung (DJCLS R 15-02; DJCLS 01R-2017), and the Joseph-Senker Stiftung to K.F., the Deutsche Knochenmarkspendedatei (DKMS-SLS-MHG-2018-01) to P.C., Adaptive Biotechnologies to E.A-B., and an Investment Grant NOW Medium from ZonMw (No. 91116004) to P.A.vV.

Author contributions

K.F., E.A-B., and P.C. designed the study; T.M., P.C., E.A-B., and K.F. wrote the manuscript; T.M., P.C., M.M., M.G.K., D.A.M., W.C., P.A.vV., G.H., S.E.L., and E.A-B. performed experiments; A.T. provided clinical patient data; P.A.H. provided access to healthy donor material; P.vB., A.W., M.G., P.A.H., B.S., D.W.B, and J.H.F.F. provided significant advice throughout the study.

Declaration of Interests

The authors declare no competing interests.

References

1. Filippone, E.J. & Farber, J.L. Humoral immunity in renal transplantation: epitopes, Cw and DP, and complement-activating capability--an update. *Clin Transplant* **29**, 279-287 (2015).

2. Fleischhauer, K. & Shaw, B.E. HLA-DP in unrelated hematopoietic cell transplantation revisited: challenges and opportunities. *Blood* **130**, 1089-1096 (2017).

3. Clayton, G.M. *et al.* Structural basis of chronic beryllium disease: linking allergic hypersensitivity and autoimmunity. *Cell* **158**, 132-142 (2014).

4. Shin, D.H. *et al.* HLA alleles, especially amino-acid signatures of HLA-DPB1, might contribute to the molecular pathogenesis of early-onset autoimmune thyroid disease. *PloS one* **14**, e0216941 (2019).

5. Gregersen, J.W. *et al.* PR3-ANCA-associated vasculitis is associated with a specific motif in the peptide-binding cleft of HLA-DP molecules. *Rheumatology (Oxford)* **58**, 1942-1949 (2019).

6. Savage, S.A. *et al.* Genome-wide Association Study Identifies HLA-DPB1 as a Significant Risk Factor for Severe Aplastic Anemia. *Am J Hum Genet* **106**, 264-271 (2020).

7. Thomas, R. *et al.* A novel variant marking HLA-DP expression levels predicts recovery from hepatitis B virus infection. *Journal of virology* **86**, 6979-6985 (2012).

8. Zhang, Q. *et al.* HLA-DP polymorphisms affect the outcomes of chronic hepatitis B virus infections, possibly through interacting with viral mutations. *Journal of virology* **87**, 12176-12186 (2013).

9. Xu, X. *et al.* Genetic variants in human leukocyte antigen-DP influence both hepatitis C virus persistence and hepatitis C virus F protein generation in the Chinese Han population. *Int J Mol Sci* **15**, 9826-9843 (2014).

10. Prentice, H.A. *et al.* HLA class II genes modulate vaccine-induced antibody responses to affect HIV-1 acquisition. *Sci Transl Med* **7**, 296ra112 (2015).

11. Niehrs, A. *et al.* A subset of HLA-DP molecules serve as ligands for the natural cytotoxicity receptor NKp44. *Nature immunology* **20**, 1129-1137 (2019).

12. Urayama, K.Y. *et al.* HLA-DP genetic variation, proxies for early life immune modulation and childhood acute lymphoblastic leukemia risk. *Blood* **120**, 3039-3047 (2012).

13. Sud, A. *et al.* Genome-wide association study of classical Hodgkin lymphoma identifies key regulators of disease susceptibility. *Nat Commun* **8**, 1892 (2017).

14. Lu, Y.C. *et al.* Treatment of Patients With Metastatic Cancer Using a Major Histocompatibility Complex Class II-Restricted T-Cell Receptor Targeting the Cancer Germline Antigen MAGE-A3. *J Clin Oncol* **35**, 3322-3329 (2017).

15. Herr, W. *et al.* HLA-DPB1 mismatch alleles represent powerful leukemia rejection antigens in CD4 T-cell immunotherapy after allogeneic stem-cell transplantation. *Leukemia* **31**, 434-445 (2017).

16. Anczurowski, M. *et al.* Mechanisms underlying the lack of endogenous processing and CLIP-mediated binding of the invariant chain by HLA-DP(84Gly). *Sci Rep* **8**, 4804 (2018).

17. Yamashita, Y. *et al.* HLA-DP(84Gly) constitutively presents endogenous peptides generated by the class I antigen processing pathway. *Nat Commun* **8**, 15244 (2017).

18. Sizzano, F. *et al.* Significantly higher frequencies of alloreactive CD4+ T cells responding to nonpermissive than to permissive HLA-DPB1 T-cell epitope disparities. *Blood* **116**, 1991-1992 (2010).

19. Fleischhauer, K. *et al.* Effect of T-cell-epitope matching at HLA-DPB1 in recipients of unrelated-donor haemopoietic-cell transplantation: a retrospective study. *Lancet Oncol* **13**, 366-374 (2012).

20. Pidala, J. *et al.* Nonpermissive HLA-DPB1 mismatch increases mortality after myeloablative unrelated allogeneic hematopoietic cell transplantation. *Blood* **124**, 2596-2606 (2014).

21. Mellins, E.D. & Stern, L.J. HLA-DM and HLA-DO, key regulators of MHC-II processing and presentation. *Curr Opin Immunol* **26**, 115-122 (2014).

22. van Lith, M., McEwen-Smith, R.M. & Benham, A.M. HLA-DP, HLA-DQ, and HLA-DR have different requirements for invariant chain and HLA-DM. *J Biol Chem* **285**, 40800-40808 (2010).

23. Abelin, J.G. *et al.* Defining HLA-II Ligand Processing and Binding Rules with Mass Spectrometry Enhances Cancer Epitope Prediction. *Immunity* **51**, 766-779 e717 (2019).

24. Zino, E. *et al.* A T-cell epitope encoded by a subset of HLA-DPB1 alleles determines nonpermissive mismatches for hematologic stem cell transplantation. *Blood* **103**, 1417-1424 (2004).

25. Rutten, C.E. *et al.* HLA-DP as specific target for cellular immunotherapy in HLA class II-expressing B-cell leukemia. *Leukemia* **22**, 1387-1394 (2008).

26. Crivello, P. *et al.* The impact of amino acid variability on alloreactivity defines a functional distance predictive of permissive HLA-DPB1 mismatches in hematopoietic

stem cell transplantation. *Biology of blood and marrow transplantation : journal of the American Society for Blood and Marrow Transplantation* **21**, 233-241 (2015).

27. Kared, H., Martelli, S., Ng, T.P., Pender, S.L. & Larbi, A. CD57 in human natural killer cells and T-lymphocytes. *Cancer Immunol Immunother* **65**, 441-452 (2016).

28. Phetsouphanh, C. *et al.* Maintenance of Functional CD57+ Cytolytic CD4+ T Cells in HIV+ Elite Controllers. *Frontiers in immunology* **10**, 1844 (2019).

29. Lee, D.S., Ahn, C., Ernst, B., Sprent, J. & Surh, C.D. Thymic selection by a single MHC/peptide ligand: autoreactive T cells are low-affinity cells. *Immunity* **10**, 83-92 (1999).

30. van den Ancker, W. *et al.* High class II-associated invariant chain peptide expression on residual leukemic cells is associated with increased relapse risk in acute myeloid leukemia. *Leuk Res* **38**, 691-693 (2014).

31. van Luijn, M.M., van den Ancker, W., van Ham, S.M. & van de Loosdrecht, A.A. Class II-associated invariant chain peptide as predictive immune marker in minimal residual disease in acute myeloid leukemia. *Oncoimmunology* **3**, e941737 (2014).

32. Nijland, M. *et al.* HLA dependent immune escape mechanisms in B-cell lymphomas: Implications for immune checkpoint inhibitor therapy? *Oncoimmunology* **6**, e1295202 (2017).

33. Alvaro-Benito, M. *et al.* Distinct editing functions of natural HLA-DM allotypes impact antigen presentation and CD4(+) T cell activation. *Cell Mol Immunol* **17**, 133-142 (2020).

34. Illing, P.T. *et al.* HLA-B57 micropolymorphism defines the sequence and conformational breadth of the immunopeptidome. *Nat Commun* **9**, 4693 (2018).

35. Robinson, J. *et al.* IPD-IMGT/HLA Database. *Nucleic Acids Res* **48**, D948-D955 (2020).

36. Arrieta-Bolanos, E. *et al.* In silico prediction of nonpermissive HLA-DPB1 mismatches in unrelated HCT by functional distance. *Blood Adv* **2**, 1773-1783 (2018).

37. Morishima, S. *et al.* Evolutionary basis of HLA-DPB1 alleles affects acute GVHD in unrelated donor stem cell transplantation. *Blood* **131**, 808-817 (2018).

38. Fleischhauer, K. Immunogenetics of HLA-DP--A New View of Permissible Mismatches. *The New England journal of medicine* **373**, 669-672 (2015).

39. Petersdorf, E.W. *et al.* High HLA-DP Expression and Graft-versus-Host Disease. *The New England journal of medicine* **373**, 599-609 (2015).

40. Koyama, M. & Hill, G.R. The primacy of gastrointestinal tract antigen-presenting cells in lethal graft-versus-host disease. *Blood* **134**, 2139-2148 (2019).

41. Toffalori, C. *et al.* Immune signature drives leukemia escape and relapse after hematopoietic cell transplantation. *Nat Med* **25**, 603-611 (2019).

42. Christopher, M.J. *et al.* Immune Escape of Relapsed AML Cells after Allogeneic Transplantation. *The New England journal of medicine* **379**, 2330-2341 (2018).

43. Kremer, A.N. *et al.* Human leukocyte antigen-DO regulates surface presentation of human leukocyte antigen class II-restricted antigens on B cell malignancies. *Biology of blood and marrow transplantation : journal of the American Society for Blood and Marrow Transplantation* **20**, 742-747 (2014).

44. Afridi, S., Hoessli, D.C. & Hameed, M.W. Mechanistic understanding and significance of small peptides interaction with MHC class II molecules for therapeutic applications. *Immunol Rev* **272**, 151-168 (2016).

45. Scherer, W.F., Syverton, J.T. & Gey, G.O. Studies on the propagation in vitro of poliomyelitis viruses. IV. Viral multiplication in a stable strain of human malignant epithelial cells (strain HeLa) derived from an epidermoid carcinoma of the cervix. *J Exp Med* **97**, 695-710 (1953).

46. Kremer, A.N. *et al.* Endogenous HLA class II epitopes that are immunogenic in vivo show distinct behavior toward HLA-DM and its natural inhibitor HLA-DO. *Blood* **120**, 3246-3255 (2012).

47. Sorror, M. *et al.* Hematopoietic cell transplantation-comorbidity index and Karnofsky performance status are independent predictors of morbidity and mortality after allogeneic nonmyeloablative hematopoietic cell transplantation. *Cancer* **112**, 1992-2001 (2008).

48. Berman, H.M. *et al.* The Protein Data Bank. *Nucleic Acids Res* **28**, 235-242 (2000).

49. Dai, S. *et al.* Crystal structure of HLA-DP2 and implications for chronic beryllium disease. *Proceedings of the National Academy of Sciences of the United States of America* **107**, 7425-7430 (2010).

50. Guex, N. & Peitsch, M.C. SWISS-MODEL and the Swiss-PdbViewer: an environment for comparative protein modeling. *Electrophoresis* **18**, 2714-2723 (1997).

51. Megger, D.A. *et al.* Proteomic differences between hepatocellular carcinoma and nontumorous liver tissue investigated by a combined gel-based and label-free quantitative proteomics study. *Mol Cell Proteomics* **12**, 2006-2020 (2013).

52. Padden, J. *et al.* Identification of novel biomarker candidates for the immunohistochemical diagnosis of cholangiocellular carcinoma. *Mol Cell Proteomics* **13**, 2661-2672 (2014).

53. Naboulsi, W. *et al.* Quantitative proteome analysis reveals the correlation between endocytosis-associated proteins and hepatocellular carcinoma dedifferentiation. *Biochim Biophys Acta* **1864**, 1579-1585 (2016).

54. Benjamini, Y. & Hochberg, Y. Controlling the False Discovery Rate: A Practical and Powerful Approach to Multiple Testing. **57**, 289-300 (1995).

55. Alvaro-Benito, M., Morrison, E., Abualrous, E.T., Kuropka, B. & Freund, C. Quantification of HLA-DM-Dependent Major Histocompatibility Complex of Class II Immunopeptidomes by the Peptide Landscape Antigenic Epitope Alignment Utility. *Frontiers in immunology* **9**, 872 (2018).

56. Andreatta, M., Alvarez, B. & Nielsen, M. GibbsCluster: unsupervised clustering and alignment of peptide sequences. *Nucleic Acids Res* **45**, W458-W463 (2017).

57. Thomsen, M.C. & Nielsen, M. Seq2Logo: a method for construction and visualization of amino acid binding motifs and sequence profiles including sequence weighting, pseudo counts and two-sided representation of amino acid enrichment and depletion. *Nucleic Acids Res* **40**, W281-287 (2012).

58. Shannon, P. *et al.* Cytoscape: a software environment for integrated models of biomolecular interaction networks. *Genome Res* **13**, 2498-2504 (2003).

59. Bindea, G. *et al.* ClueGO: a Cytoscape plug-in to decipher functionally grouped gene ontology and pathway annotation networks. *Bioinformatics* **25**, 1091-1093 (2009).

60. Ashburner, M. *et al.* Gene ontology: tool for the unification of biology. The Gene Ontology Consortium. *Nature genetics* **25**, 25-29 (2000).

61. The Gene Ontology, C. The Gene Ontology Resource: 20 years and still GOing strong. *Nucleic Acids Res* **47**, D330-D338 (2019).

62. Arrieta-Bolanos, E. *et al.* Alloreactive T Cell Receptor Diversity against Structurally Similar or Dissimilar HLA-DP Antigens Assessed by Deep Sequencing. *Frontiers in immunology* **9**, 280 (2018).

63. Litjens, N.H., de Wit, E.A., Baan, C.C. & Betjes, M.G. Activation-induced CD137 is a fast assay for identification and multi-parameter flow cytometric analysis of alloreactive T cells. *Clin Exp Immunol* **174**, 179-191 (2013).

64. Crivello, P. *et al.* Multiple Knockout of Classical HLA Class II beta-Chains by CRISPR/Cas9 Genome Editing Driven by a Single Guide RNA. *Journal of immunology* **202**, 1895-1903 (2019).

65. Crivello, P. *et al.* Effects of transmembrane region variability on cell surface expression and allorecognition of HLA-DP3. *Hum Immunol* **74**, 970-977 (2013).

66. Amendola, M., Venneri, M.A., Biffi, A., Vigna, E. & Naldini, L. Coordinate dual-gene transgenesis by lentiviral vectors carrying synthetic bidirectional promoters. *Nat Biotechnol* **23**, 108-116 (2005).

67. Robins, H.S. *et al.* Comprehensive assessment of T-cell receptor beta-chain diversity in alphabeta T cells. *Blood* **114**, 4099-4107 (2009).

68. Carlson, C.S. *et al.* Using synthetic templates to design an unbiased multiplex PCR assay. *Nat Commun* **4**, 2680 (2013).

69. Lefranc, M.P. *et al.* IMGT(R), the international ImMunoGeneTics information system(R) 25 years on. *Nucleic Acids Res* **43**, D413-422 (2015).

70. Pielou, E.C. Species-diversity and pattern-diversity in the study of ecological succession. *J Theor Biol* **10**, 370-383 (1966).

71. Colwell, R.K. *et al.* Models and estimators linking individual-based and sample-based rarefaction, extrapolation and comparison of assemblages. *Journal of Plant Ecology* **5**, 3-21 (2012).

72. Shugay, M. *et al.* VDJtools: Unifying Post-analysis of T Cell Receptor Repertoires. *PLoS Comput Biol* **11**, e1004503 (2015).

73. Morisita, M. Measuring of the dispersion and analysis of distribution patterns. *Memoires of the Faculty of Science, Kyushu University, Series E. Biology* **2**, 215–235 (1959).

74. Bagaev, D.V. *et al.* VDJviz: a versatile browser for immunogenomics data. *BMC Genomics* **17**, 453 (2016).

Figure legends

Fig. 1. Allotype-specific features of the HLA-DP immunopeptidome in the presence of HLA-DM. a, aa sequence alignment of the PBD (DPB1 exon 2, aa 5-92) of HLA-DP allotypes analyzed in this study. Conserved and polymorphic aa are shown in gray and red, respectively; dots indicate identity to the reference (i.e. DP401). **b,** Crystallography-based structure of the HLA-DP alpha (blue) and beta (red) chain PBD shown in ribbons, with peptide depicted in gray. Position 84 and the corresponding P1 peptide residue are highlighted. **c,** Peptide repertoire overlap and percentage of non-shared peptides (>9 aa length) between the three HLA-DP allotypes. Numbers correspond to unique peptides in each dataset. **d,** Relative abundance of core epitopes shared/not shared between HLA-DP allotypes. Epitopes found in all three or in less than three of the allotypes are indicated in gray or with colors, respectively. **e,** Peptide binding motifs of HLA-DP allotypes. The height of each aa is proportional to its frequency at the indicated position. **f,** Cellular component GO analysis of peptides from the three allotypes. Shown are the top 15 most significantly enriched GO terms ranked by the number of associated genes found per term. GO terms from the endogenous (endo, in green), exogenous (exo, in red), or any (in gray) pathway of antigen presentation are indicated. *p*-values were calculated by FDR-corrected, right-sided hypergeometric test.

Fig. 2. HLA-DM restricts the peptide repertoire diversity of HLA-DP across allotype groups. **a,** Peptide repertoire overlap and percentage of non-shared peptides (>9 aa) identified in the absence and presence of HLA-DM for DP402 and DP10. Numbers correspond to unique peptides in each dataset. The size of each Venn diagram reflects the number of identified peptides in the respective condition. **b,** Relative abundance of shared/non-shared core epitopes in the DP402 and DP10 immunopeptidomes with or without HLA-DM. Epitopes

found in one or more conditions are indicated with colors. **c,** Relative abundance of CLIP core epitopes in the immunopeptidomes of DP402 or DP10 with or without HLA-DM. ****p<0.0001 by unpaired t test. **d,** Unique peptides significantly enriched in the absence (red) or presence (green) of HLA-DM for DP402 or DP10. Significant enrichment was defined as ≥2-fold significant (p<0.01 in FDR-adjusted, one-way ANOVA) variation of relative abundance in the presence vs absence of HLA-DM. **e,** Relative abundance of core epitopes in DP402 and DP10 in the absence (red) or presence (green) of HLA-DM, or in both (gray). **f,** Cellular component GO analysis of peptides significantly enriched in DP402 and DP10 in the absence (left; red fraction in panel d) or presence (right; green fraction in panel d) of HLA-DM. Shown are the top 15 GO terms specifically enriched in the absence (red) or presence (green) of HLA-DM, or in both conditions (gray). p-values were calculated by FDR-corrected, right-sided hypergeometric test.

Fig. 3: Experimental strategy for probing the effect of HLA-DM activity on T-cell allorecognition of HLA-DP allotypes. a, Experimental design. Irradiated HeLa cells expressing CD80, Ii, and HLA-DP (either DP402 or DP10) in the presence or absence of HLA-DM, or in the presence of HLA-DM and HLA-DO, were used for 14-day *priming* with purified $CD4^+$ T cells from $DP401^+$ responders. Subsequently, a 24-hour *re-stimulation* was performed with HeLa cells expressing allogeneic HLA-DP with or without the HLA-DM/DO combinations as indicated, and separately with HeLa cells expressing autologous HLA-DP and HLA-DM as background control. After re-stimulation, a *read-out* of T-cell alloreactivity was performed by measurement of surface CD137 up-regulation and/or cytokine release using flow cytometry or multiplex bead assays, respectively. **b,** Representative FACS results of a CD137 read-out with gating strategy and relevant dot plots. HLA-DP/HLA-DM combinations on top of the FACS plots refer to the HeLa cells used for priming and allogeneic read-out; HeLa cells used

for the autologous control read-out carried DP401 DM. The percent $CD4^+CD137^+$ T cells in the allogeneic and autologous read-out cultures, and the resulting percent specific allogeneic response, are also shown.

Fig. 4: HLA-DM regulates T-cell alloreactivity to HLA-DP in an allotype specific manner. a, Specific $CD4^+$ T-cell alloresponse from healthy $DP401^+$ individuals (N=18) to the indicated HLA-DP allotypes in the presence or absence of HLA-DM. $CD4^+$ T cells were primed and re-stimulated with the same allogeneic HLA-DP/HLA-DM combination. Mean background response to autologous HLA-DP was 16.6 ± 9.5% (DP402 DM); 7.1 ± 4.8% (DP402); 4.5 ± 3.0% (DP10 DM); and 2.3 ± 1.3% (DP10). Statistical comparison by one-way ANOVA. **** $p<$ 0.0001. **b,** Specific alloresponse from healthy $DP401^+$ individuals (N=6), primed against the indicated HLA-DP/HLA-DM combinations and re-stimulated with the same HLA-DP allotype in the presence (blue rhombus) or absence (red triangles) of HLA-DM. Mean background response to autologous HLA-DP was 18.7 ± 7.4% (DP402 DM priming); 8.4 ± 3.5% (DP402 priming); 4.3 ± 1.3% (DP10 DM priming); 2.8 ± 1.4% (DP10 priming). Statistical comparison by two-way ANOVA. ***p<0.001, ****p<0.0001. **c,** Specific alloresponse from healthy $DP401^+$ individuals (N=6), primed against DP402 without HLA-DM, and re-stimulated with DP402 in the absence or presence of HLA-DM, or with HLA-DM and HLA-DO, as indicated. Mean background response to autologous HLA-DP was 16.0 ± 9.6%. Statistical comparison by one-way ANOVA. ***p<0.001. **d** and **e,** Heatmaps of cytokine production from 4 representative responders in panel a (d) or in panel c (e) after subtraction of background levels. For cultures with high (>1000pg/ml) responses to allogeneic HLA-DP, the background response to autologous HLA-DP is shown in Supplementary Fig. 2b,c.

Fig. 5: HLA-DM limits the TCR-β repertoire diversity responding to HLA-DP allotypes. $CD4^+$ T cells from 3 healthy $DP401^+$ individuals (R1-R3) were primed and re-stimulated against

DP402 or DP10 in the presence or absence of HLA-DM, as indicated. **a,** Heatmap of percent $CD4^+CD137^+$ T cells in 24 TCR-Vβ families at re-stimulation. **b,** Frequency of top-10 TCR-β rearrangements in purified $CD4^+CD137^+$ T cells at re-stimulation, or in pre-culture $CD4^+$ T cells. Color-coding refers to the size of each of the top-10 clonotypes in each sample; the remaining repertoire is shown in gray. **c,** Rarefaction curves showing the number of unique clonotypes (in brackets) with increasing sample size in R1 (R2 and R3 in Supplementary Fig. 3b). Curves (with 95% CI in gray) are interpolated from 0 to the size of each sample (solid lines), and extrapolated (dashed lines) to the size of the largest sample (i.e. DP402 DM) as indicated in the panel legend. **d,** Overlap and percentage of non-shared TCR-β CDR3 nucleotide sequences in R1 (R2 and R3 in Supplementary Fig. 5a). Numbers correspond to unique clonotypes in each dataset. **e,** Pair-wise frequency scatter plots of shared CDR3 sequences and Morisita similarity index heatmap between $CD4^+$ T cells at re-stimulation or pre-culture from R1 (R2 and R3 in Supplementary Fig. 5b). Morisita index ranges from 0 to 1 (no vs complete repertoire overlap).

Fig. 6: HLA-DM dependency of the T-cell response to HLA-DP allotypes in transplanted patients. a, $CD4^+$ T-cell alloresponses against HLA-DP from patients >5 months after permissively (84Gly/Gly; N=7) or non-permissively (84Gly/Asp; N=4) mismatched HCT (see **Supplementary Table S1**). PBMC collected were primed and re-stimulated with the relevant mismatched allotype with or without HLA-DM. Mean background response to autologous HLA-DP was 8.0 ± 6.3% (84Gly DM); 3.6 ± 2.6% (84Gly); 5.2 ± 2.3% (84Asp DM); and 3.4 ± 1.8% (84Asp). **b,** Cytokine production by purified $CD4^+$ T cells from patients IZTF-3 and IZTF-28 after priming and re-stimulation with the relevant mismatch with or without HLA-DM. Background response to autologous HLA-DP was <100pg/ml. **c,** Top-10 TCR-β clonotypes (in color) and underlying repertoire (gray) in alloreactive $CD4^+$ T-cell cultures from panel b, and

in *ex vivo* BMMC/PBMC samples at different time points after HCT and their respective donors. **d,** Cumulative frequency of TCR-β clonotypes responding *in vitro* to the relevant mismatched HLA-DP allotype with (blue) or without (purple) HLA-DM, or both (green), and their proportion in *ex vivo* and donor samples for each patient. **e,** Overlap and percentage of non-shared TCR-β clonotypes in $CD4^+$ T cells from panel b. **f,** Tracking of all clonotypes found among the top-10 in at least one of the samples analyzed for each patient (N=49 for IZTF3; N=47 for IZTF28) across all samples from that patient. **g,** Pair-wise frequency scatter plots of shared clonotypes and Morisita index heatmaps across all cultured and *ex vivo* samples from each patient.

Fig. 1

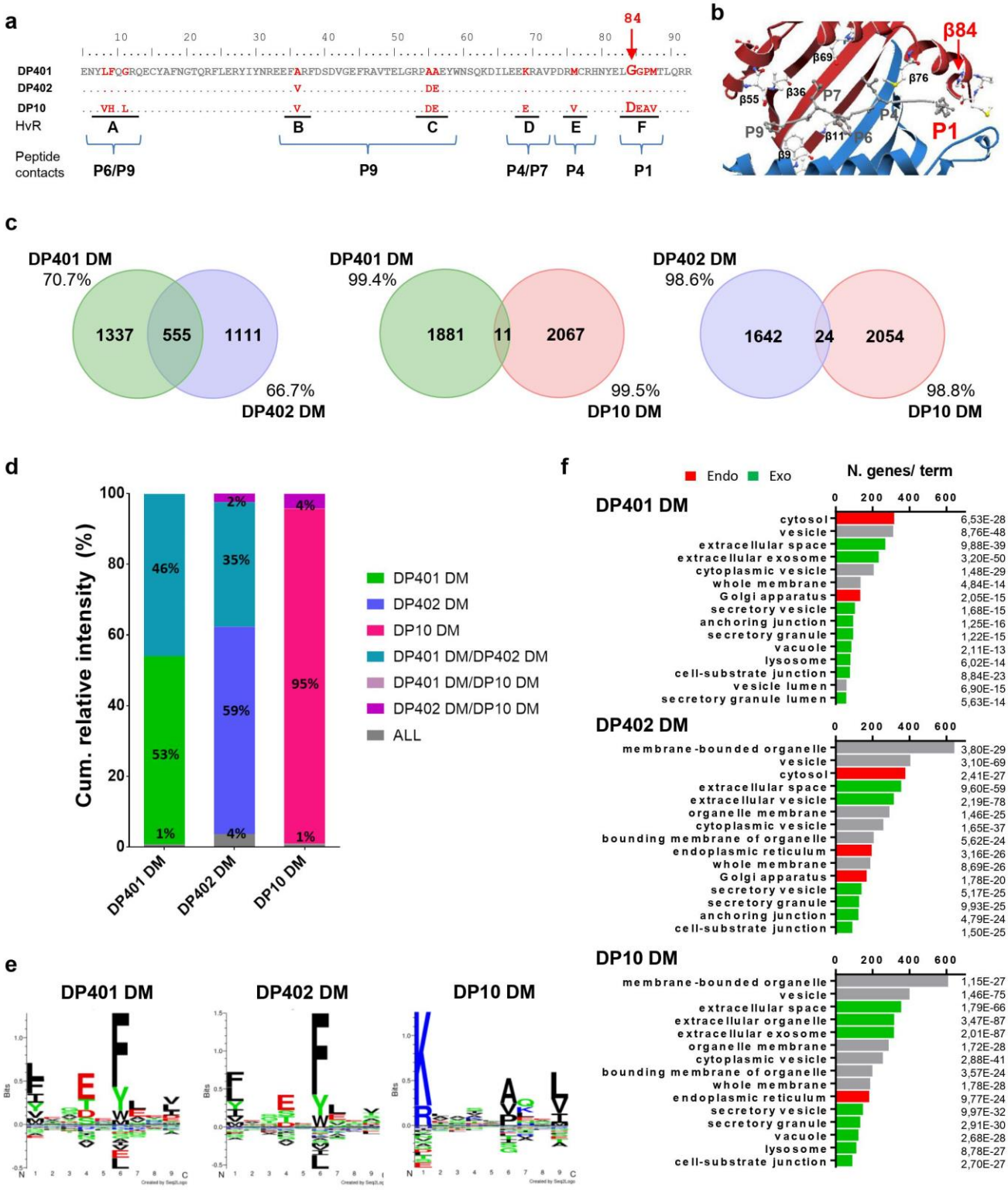
a
84
10 20 30 40 50 60 70 80 90
DP401 ENYLFQGRQECYAFNGTQRFLERYIYNREEFARFDSDVGEFRAVTELGRPAAEYWNSQKDILEEKRAVPDRMCRHNYELGGPMTLQRR
DP402 V DE
DP10 VH.L V DE E V DEAV
HvR
A B C D E F
Peptide contacts
P6/P9 P9 P4/P7 P4 P1
b
β84
β69
β76
β55
β36
P7
P4
P9
β11
P6
β9
P1
c
DP401 DM
70.7%
1337 555 1111
66.7%
DP402 DM
DP401 DM
99.4%
1881 11 2067
99.5%
DP10 DM
DP402 DM
98.6%
1642 24 2054
98.8%
DP10 DM
d
Cum. relative intensity (%)
100 80 60 40 20 0
46% 53% 1%
2% 35% 59% 4%
4% 95% 1%
DP401 DM
DP402 DM
DP10 DM
DP401 DM
DP402 DM
DP10 DM
DP401 DM/DP402 DM
DP401 DM/DP10 DM
DP402 DM/DP10 DM
ALL
e
DP401 DM
DP402 DM
DP10 DM
f
Endo Exo
N. genes/ term
DP401 DM
0 200 400 600
cytosol 6,53E-28
vesicle 8,76E-48
extracellular space 9,88E-39
extracellular exosome 3,20E-50
cytoplasmic vesicle 1,48E-29
whole membrane 4,84E-14
Golgi apparatus 2,05E-15
secretory vesicle 1,68E-15
anchoring junction 1,25E-16
secretory granule 1,22E-15
vacuole 2,11E-13
lysosome 6,02E-14
cell-substrate junction 8,84E-23
vesicle lumen 6,90E-15
secretory granule lumen 5,63E-14
DP402 DM
0 200 400 600
membrane-bounded organelle 3,80E-29
vesicle 3,10E-69
cytosol 2,41E-27
extracellular space 9,60E-59
extracellular vesicle 2,19E-78
organelle membrane 1,46E-25
cytoplasmic vesicle 1,65E-37
bounding membrane of organelle 5,62E-24
endoplasmic reticulum 3,16E-26
whole membrane 8,69E-26
Golgi apparatus 1,78E-20
secretory vesicle 5,17E-25
secretory granule 9,93E-25
anchoring junction 4,79E-24
cell-substrate junction 1,50E-25
DP10 DM
0 200 400 600
membrane-bounded organelle 1,15E-27
vesicle 1,46E-75
extracellular space 1,79E-66
extracellular organelle 3,47E-87
extracellular exosome 2,01E-87
organelle membrane 1,72E-28
cytoplasmic vesicle 2,88E-41
bounding membrane of organelle 3,57E-24
whole membrane 1,78E-28
endoplasmic reticulum 9,77E-24
secretory vesicle 9,97E-32
secretory granule 2,91E-30
vacuole 2,68E-28
lysosome 8,78E-27
cell-substrate junction 2,70E-27

Fig. 2

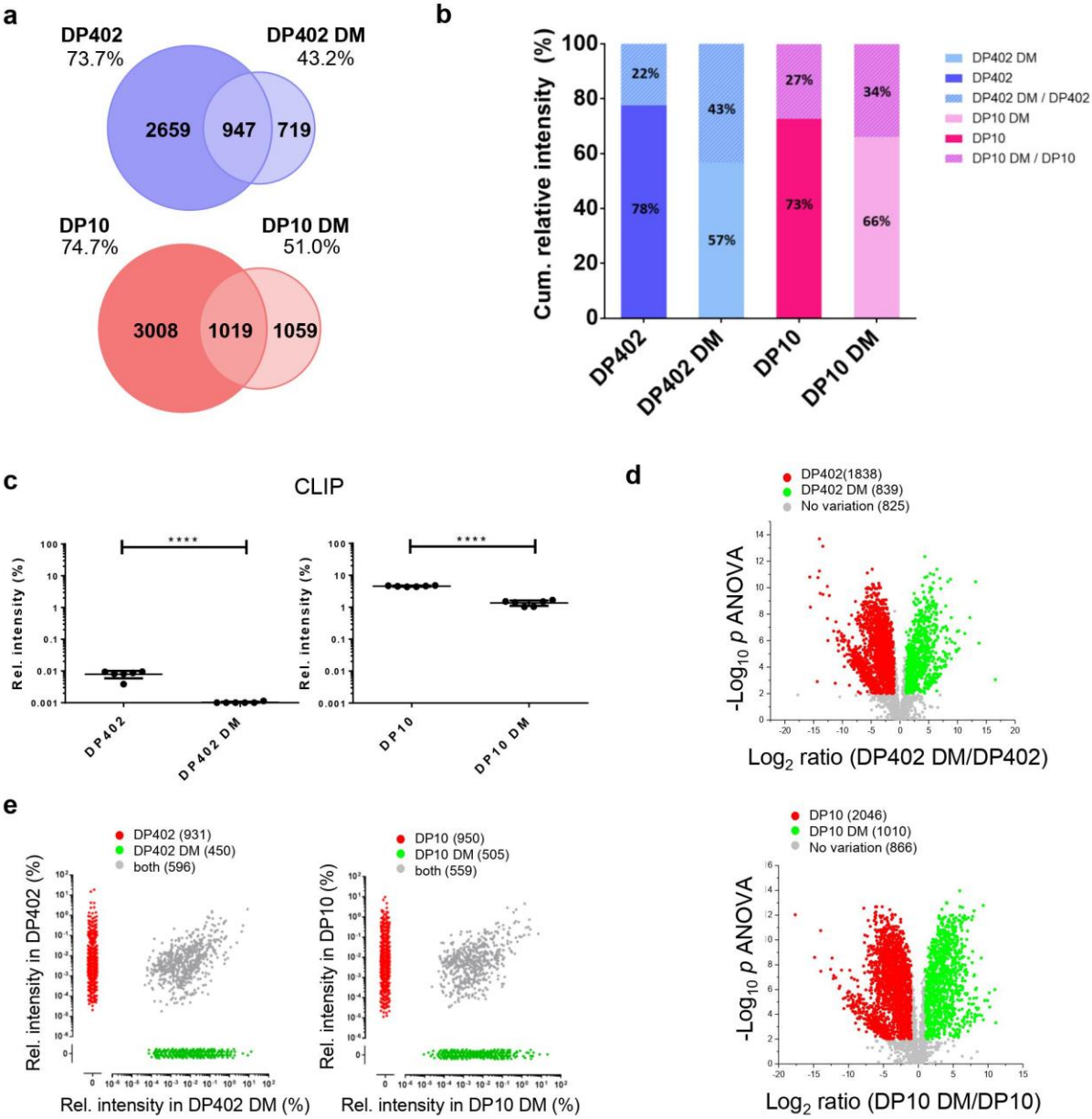
a
DP402
73.7%
DP402 DM
43.2%
2659
947
719
DP10
74.7%
DP10 DM
51.0%
3008
1019
1059
b
Cum. relative intensity (%)
DP402 DM
DP402
DP402 DM / DP402
DP10 DM
DP10
DP10 DM / DP10
22%
78%
43%
57%
27%
73%
34%
66%
DP402
DP402 DM
DP10
DP10 DM
c
CLIP
Rel. intensity (%)
****
DP402
DP402 DM
DP10
DP10 DM
d
DP402(1838)
DP402 DM (839)
No variation (825)
-Log10 p ANOVA
Log2 ratio (DP402 DM/DP402)
e
DP402 (931)
DP402 DM (450)
both (596)
Rel. intensity in DP402 (%)
Rel. intensity in DP402 DM (%)
DP10 (950)
DP10 DM (505)
both (559)
Rel. intensity in DP10 (%)
Rel. intensity in DP10 DM (%)
DP10 (2046)
DP10 DM (1010)
No variation (866)
-Log10 p ANOVA
Log2 ratio (DP10 DM/DP10)
f
DP402
N. genes/ term
cytoplasm 2.7E-35
cytoplasmic part 4.2E-56
intracellular membrane-bounded organelle 1.8E-17
intracellular organelle part 9.1E-23
vesicle 1.5E-82
endomembrane system 3.7E-60
cell periphery 1.1E-24
plasma membrane 1.9E-24
extracellular space 4.7E-66
intrinsic component of membrane 4.2E-17
cytosol 3.0E-20
integral component of membrane 4.2E-15
extracellular vesicle 1.7E-85
intracellular organelle lumen 1.1E-11
cytoplasmic vesicle 4.1E-50
DP402 DM
N. genes/ term
extracellular vesicle 2.1E-23
cytoplasmic vesicle 8.0E-13
cytoplasmic vesicle part 1.4E-11
endoplasmic reticulum part 1.3E-07
secretory vesicle 7.5E-10
secretory granule 1.7E-06
endoplasmic reticulum membrane 4.9E-09
perinuclear region of cytoplasm 5.2E-07
vesicle membrane 5.2E-05
adherens junction 1.8E-07
cytoplasmic vesicle membrane 1.3E-04
Golgi membrane 7.4E-05
cytoplasmic vesicle lumen 3.9E-10
focal adhesion 6.6E-08
secretory granule lumen 5.3E-09
DP10
cytoplasm 8.8E-29
cytoplasmic part 6.2E-45
intracellular organelle part 1.7E-21
vesicle 8.4E-86
endomembrane system 8.1E-66
extracellular space 8.1E-83
intrinsic component of membrane 2.8E-19
cell periphery 2.3E-18
plasma membrane 1.8E-17
integral component of membrane 3.6E-16
extracellular exosome 4.4E-93
intracellular organelle lumen 4.0E-10
cytosol 5.5E-07
cytoplasmic vesicle 2.0E-45
organelle membrane 2.9E-18
DP10 DM
vesicle 1.1E-36
extracellular exosome 5.5E-40
cytoplasmic vesicle 3.2E-19
cytoplasmic vesicle part 4.3E-18
secretory vesicle 4.4E-14
secretory granule 7.0E-14
endosome 6.4E-09
vacuole 6.8E-10
vesicle membrane 2.9E-07
lysosome 2.1E-08
vacuolar part 1.8E-09
adherens junction 6.1E-09
vesicle lumen 1.2E-11
focal adhesion 9.4E-10
cell body 2.0E-05

Fig. 3

a

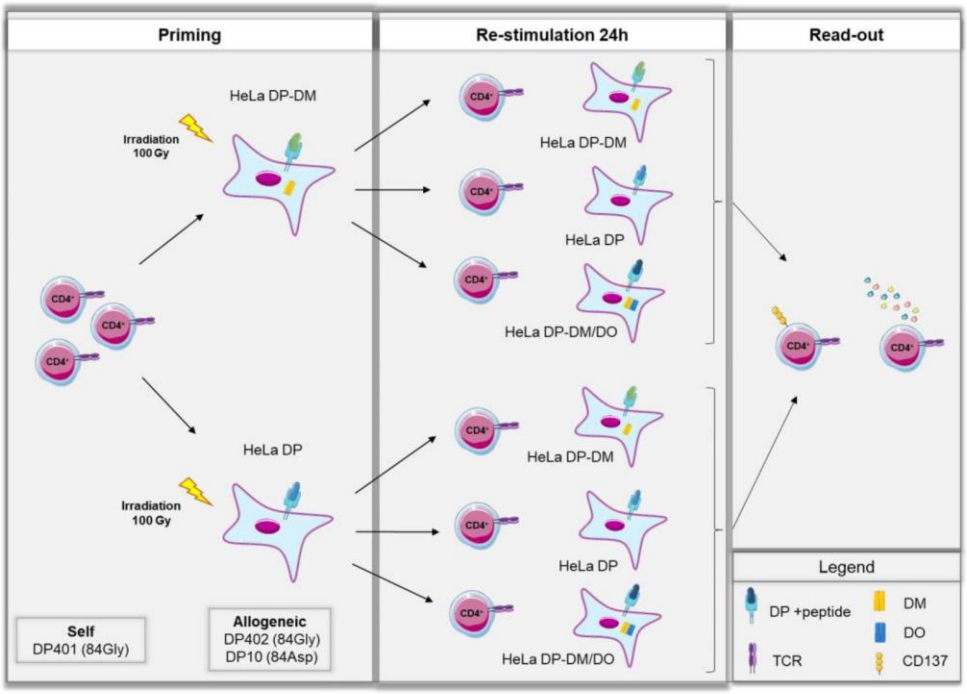

b

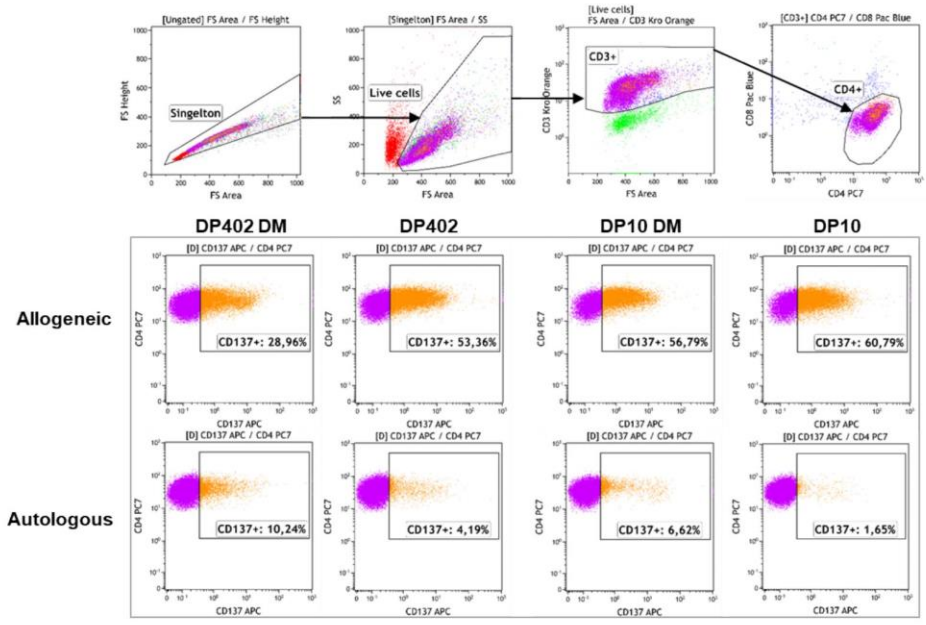

CD4⁺CD137⁺	DP402 DM	DP402	DP10 DM	DP10
Allogeneic (%)	28.96	53.36	56.79	60.79
Autologous (%)	10.24	4.19	6.62	1.65
Specific (%)	**18.72**	**49.17**	**50.17**	**59.14**

Fig. 4

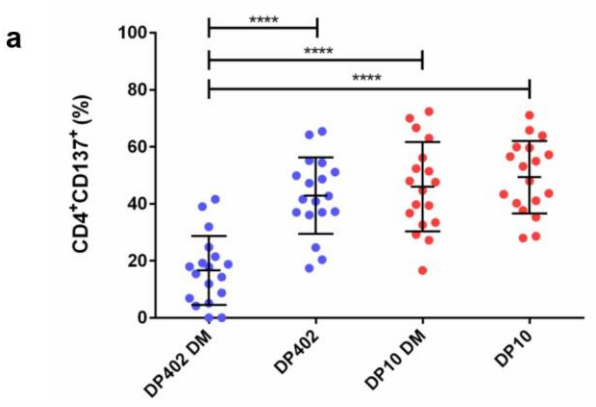

Allogeneic DP	CD4⁺CD137⁺ (%) (Mean± SD)	p-value vs DP402 DM	DP402	DP10 DM	DP10
DP402 DM	16.62 ± 12.10	NA			
DP402	42.81 ± 13.40	<0.0001	NA		
DP10 DM	45.94 ± 15.65	<0.0001	0.7657	NA	
DP10	49.32 ± 12.76	<0.0001	0.0744	0.5637	NA

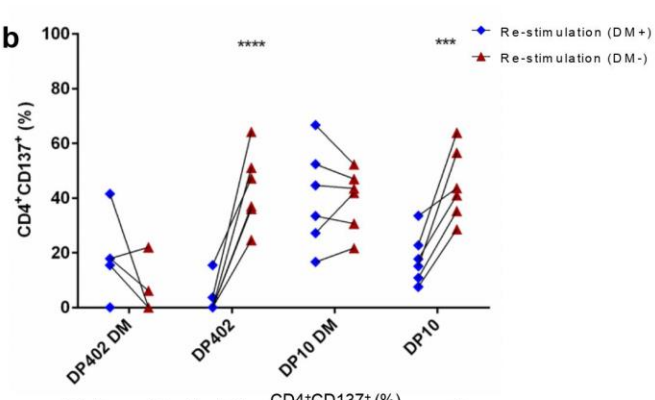

Priming	Re-stimulation	CD4⁺CD137⁺ (%) (Mean± SD)	p-value
DP402 DM	DP402 DM	15.47 ± 15.32	0.2214
	DP402	4.7 ± 8.84	
DP402	DP402	43.36 ± 13.80	<0.0001
	DP402 DM	3.20 ± 6.20	
DP10 DM	DP10 DM	40.15 ± 18.09	>0.999
	DP10	39.51 ± 11.28	
DP10	DP10	44.84 ± 13.17	0.0003
	DP10 DM	17.91± 9.30	

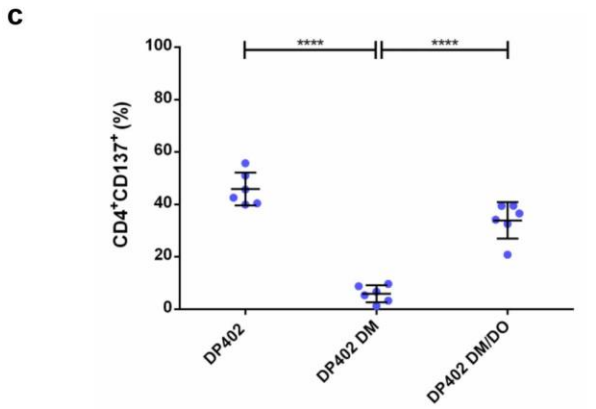

HLA-DP	CD4⁺CD137⁺ (%) (Mean± SD)	p-value vs DP402	DP402 DM	DP402 DM/DO
DP402	45.88 ± 6.30	NA		
DP402 DM	5.85 ± 3.25	<0.0001	NA	
DP402 DM/DO	33.85 ± 6.95	0.0529	<0.0001	NA

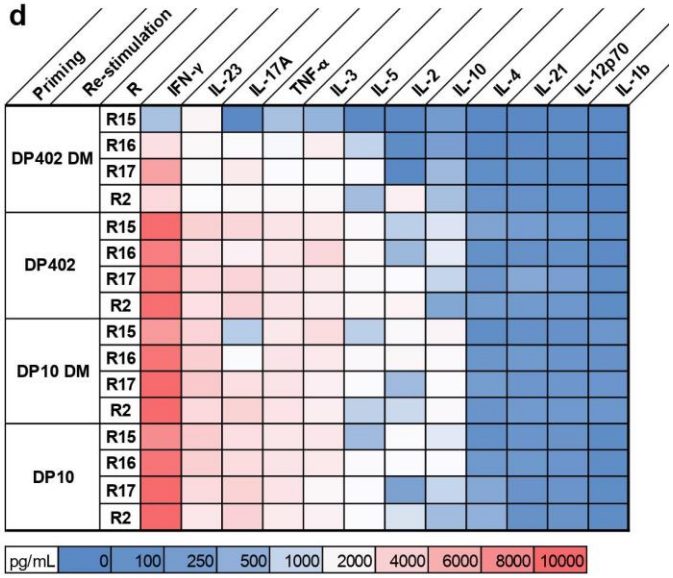

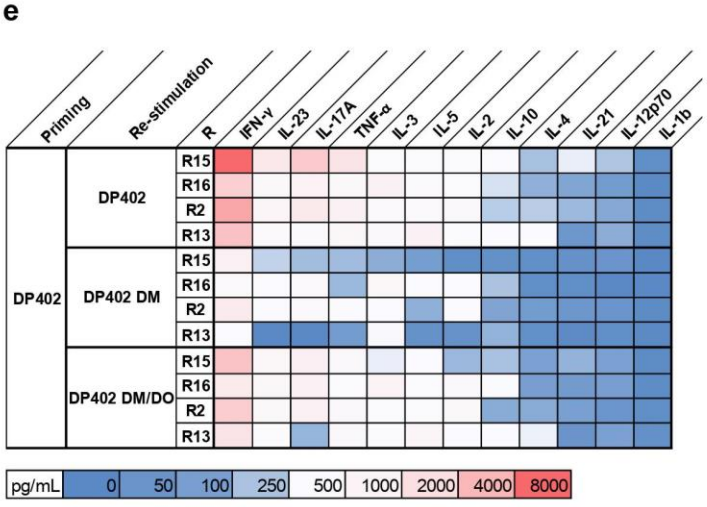

Fig. 5

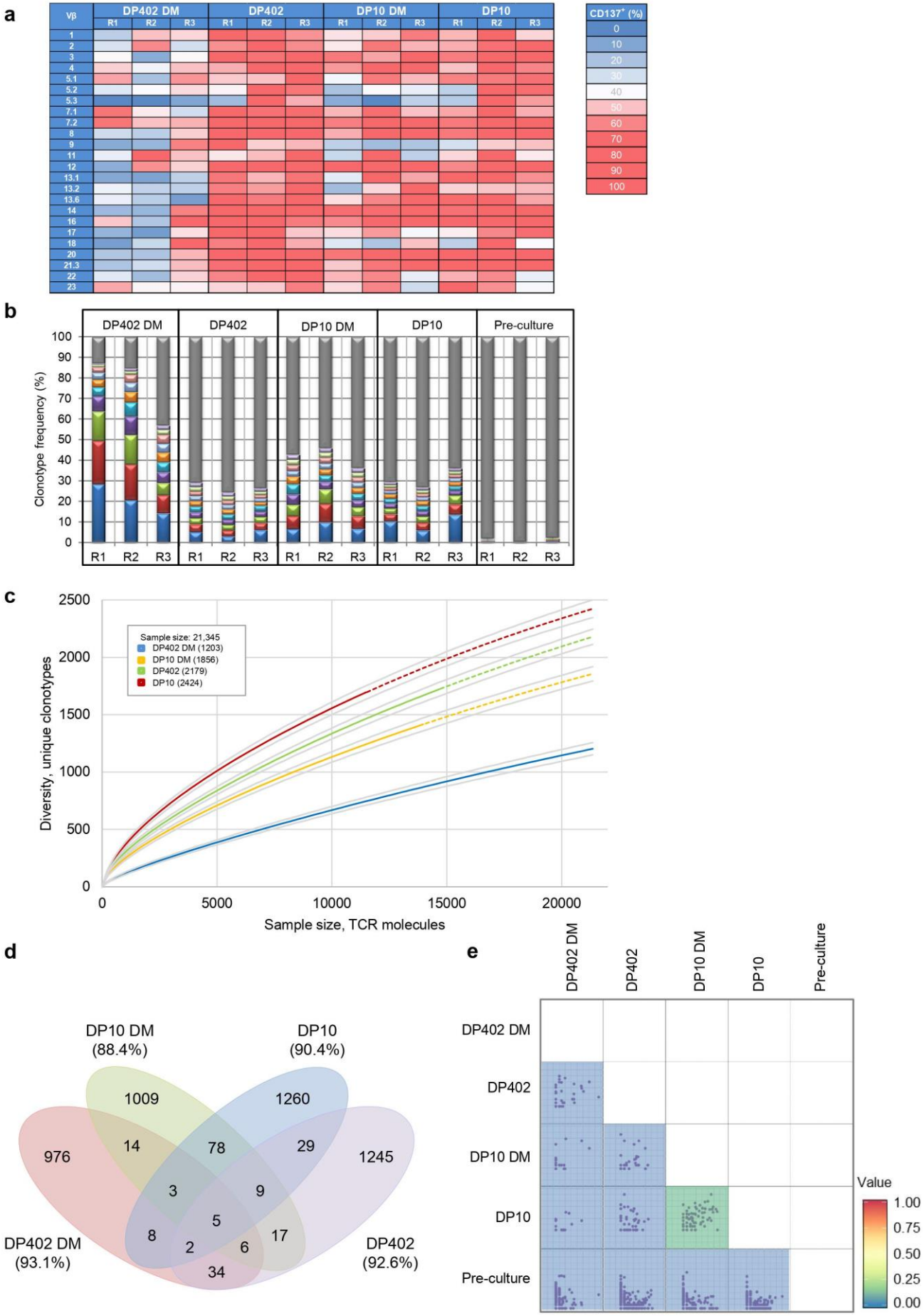
a
Vβ
DP402 DM
DP402
DP10 DM
DP10
R1
R2
R3
CD137+ (%)
0
10
20
30
40
50
60
70
80
90
100
b
DP402 DM
DP402
DP10 DM
DP10
Pre-culture
Clonotype frequency (%)
c
Sample size: 21,345
DP402 DM (1203)
DP10 DM (1856)
DP402 (2179)
DP10 (2424)
Diversity, unique clonotypes
Sample size, TCR molecules
d
DP10 DM
(88.4%)
DP10
(90.4%)
DP402 DM
(93.1%)
DP402
(92.6%)
1009
1260
976
1245
14
78
29
3
9
5
8
2
6
17
34
e
DP402 DM
DP402
DP10 DM
DP10
Pre-culture
Value
1.00
0.75
0.50
0.25
0.00

Fig. 6

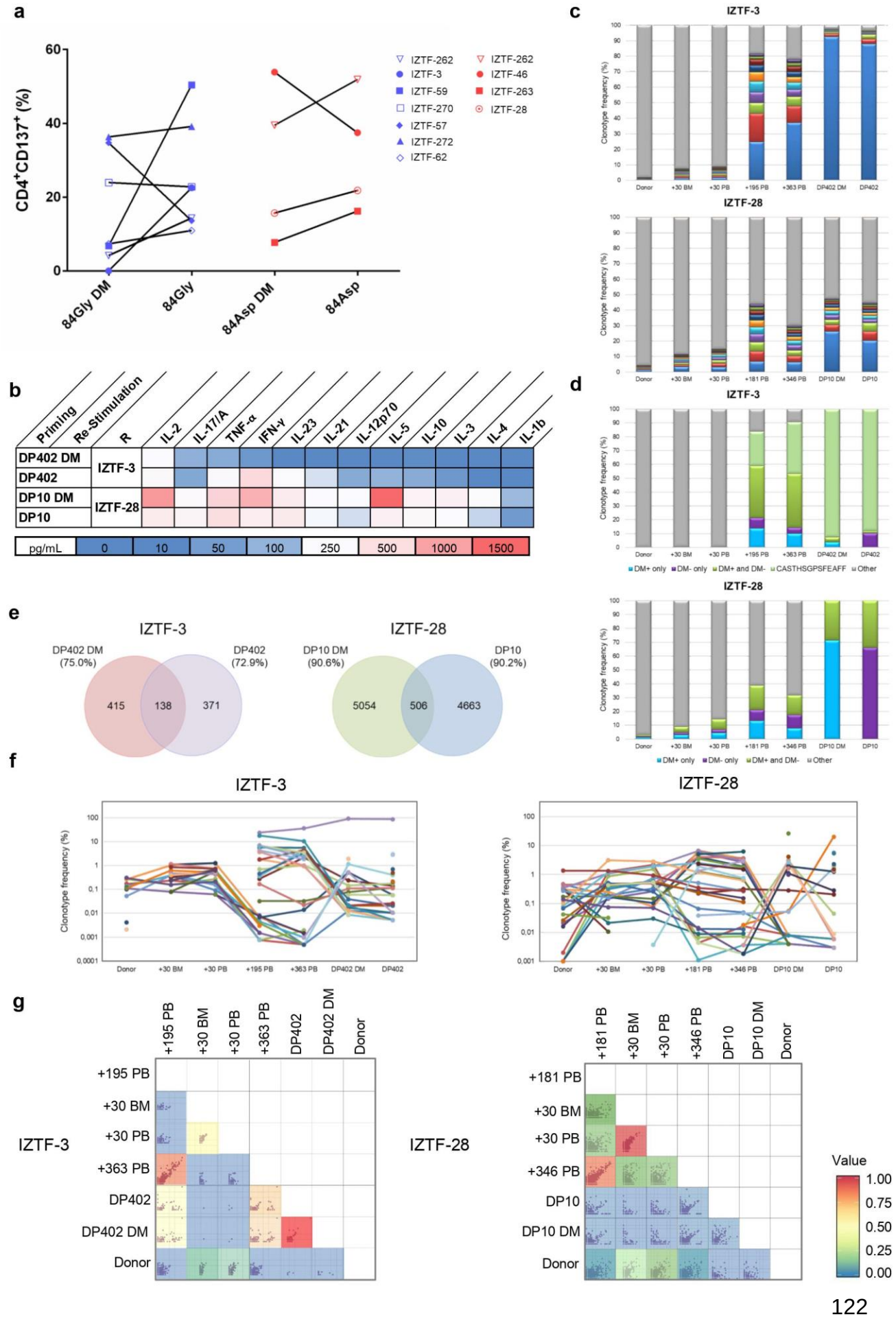
a
CD4+CD137+ (%)
84Gly DM
84Gly
84Asp DM
84Asp
IZTF-262
IZTF-3
IZTF-59
IZTF-270
IZTF-57
IZTF-272
IZTF-62
IZTF-262
IZTF-46
IZTF-263
IZTF-28
b
Priming
Re-Stimulation
R
IL-2
IL-17/A
TNF-α
IFN-γ
IL-23
IL-21
IL-12p70
IL-5
IL-10
IL-3
IL-4
IL-1b
DP402 DM
DP402
DP10 DM
DP10
IZTF-3
IZTF-28
pg/mL
0
10
50
100
250
500
1000
1500
c
IZTF-3
IZTF-28
Clonotype frequency (%)
Donor
+30 BM
+30 PB
+195 PB
+363 PB
DP402 DM
DP402
+181 PB
+346 PB
DP10 DM
DP10
d
IZTF-3
IZTF-28
DM+ only
DM- only
DM+ and DM-
CASTHSGPSFEAFF
Other
e
IZTF-3
DP402 DM
(75.0%)
DP402
(72.9%)
415
138
371
IZTF-28
DP10 DM
(90.6%)
DP10
(90.2%)
5054
506
4663
f
IZTF-3
IZTF-28
Clonotype frequency (%)
g
IZTF-3
IZTF-28
Value
1.00
0.75
0.50
0.25
0.00

Supplementary Fig. 1

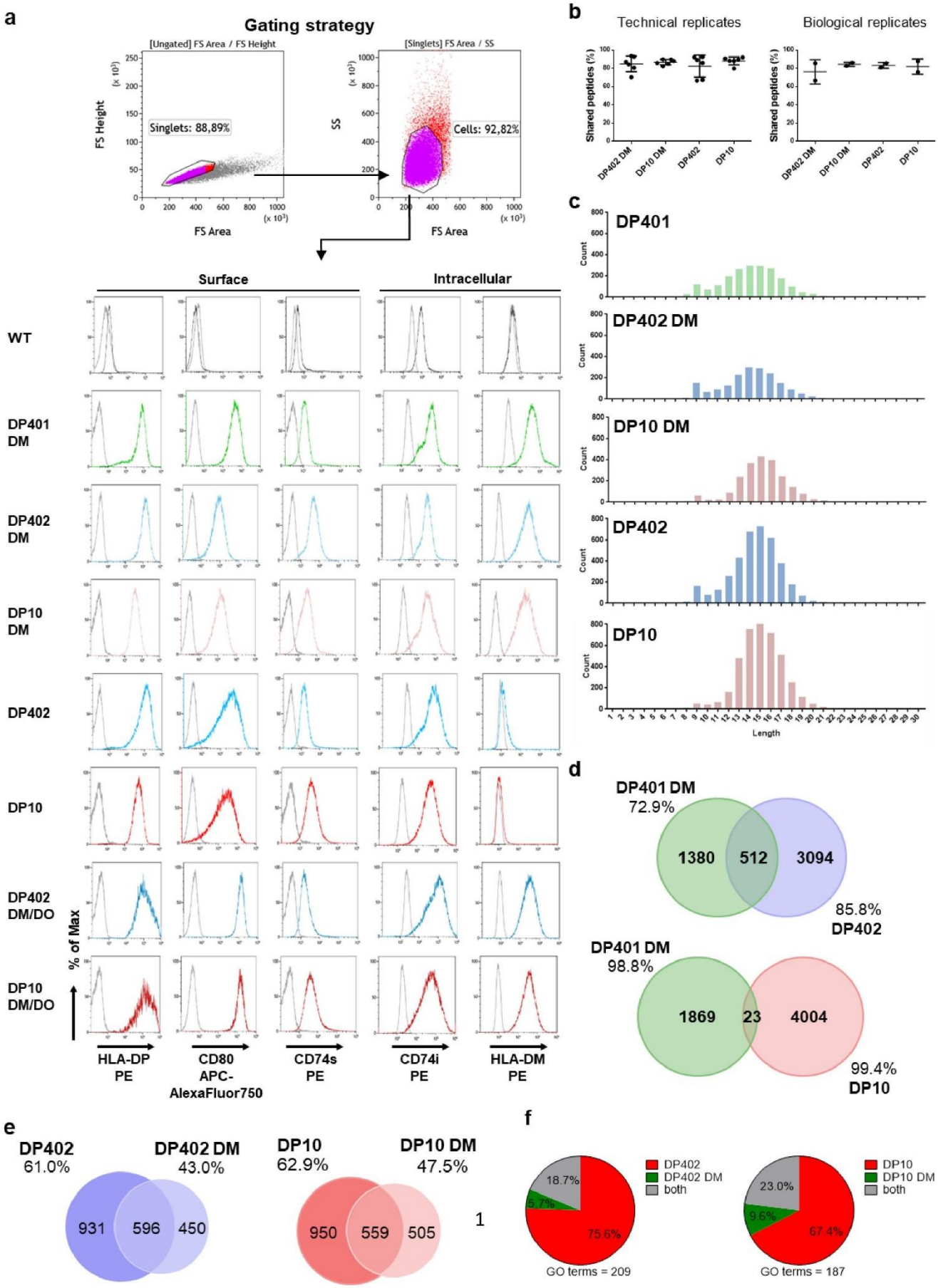

Supplementary Fig. 1: Characterization of HeLa transductants and their immunopeptidomes. **a,** Gating strategy and histograms of HeLa cell surface (three left panels) and intracytoplasmic (two right panels) expression of the molecules indicated below each column. Unstained (surface) or isotype (intracytoplasmic) controls and mAb stainings are shown in grey and color, respectively, the latter different for WT and each transductant. **b,** Percentage of peptides shared with at least one of 6 technical (left panel) or 2 biological (right panel) replicates of the indicated HLA-DP immunopeptidomes. The mean ± SD number of identified peptides was 917 ± 226, 2031 ± 467, 1303 ± 126, 2547 ± 234 for technical replicates; and 1333 ± 166, 3088 ± 84, 1797 ± 34, 3394 ± 252 for biological replicates of HeLa DP402 DM, DP402, DP10 DM, and DP10, respectively. **c,** Peptide length distribution in the indicated HLA-DP immunopeptidomes. Peptides ≤9 aa were excluded from further analysis. **d,** Peptide repertoire overlap and percentage of non-shared peptides (>9 aa) between DP401 (green) in the presence of HLA-DM and DP402 (blue) or DP10 (pink) in the absence of HLA-DM. Numbers correspond to unique peptides in each dataset. **e,** Percentage of non-shared core epitopes in DP402 (blue) and DP10 (pink) in the presence or absence of HLA-DM. Numbers correspond to unique core epitopes in each sample. The size of the Venn plots reflects the reduction of the unique epitope numbers in the presence of HLA-DM. **f,** Distribution of GO cellular components giving origin to peptides enriched in DP402 and DP10 in the presence (green) or absence (red) of HLA-DM, or present in both (grey).

Supplementary Fig. 2

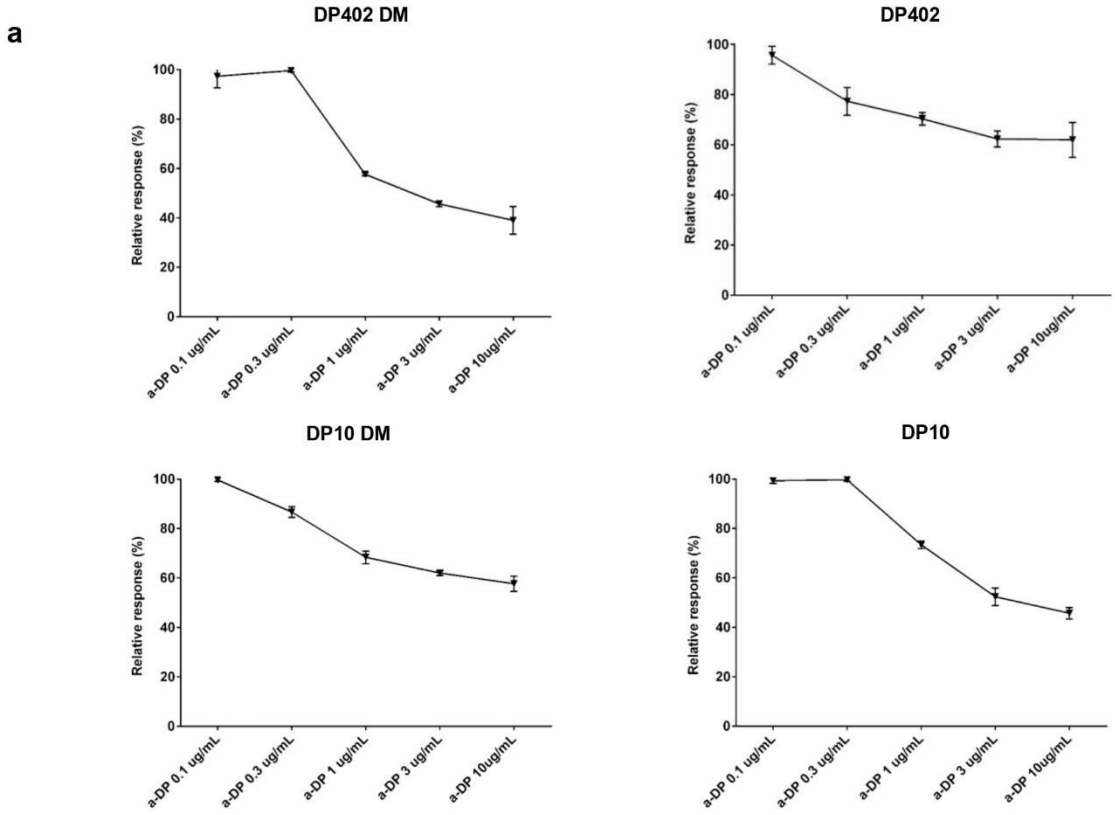

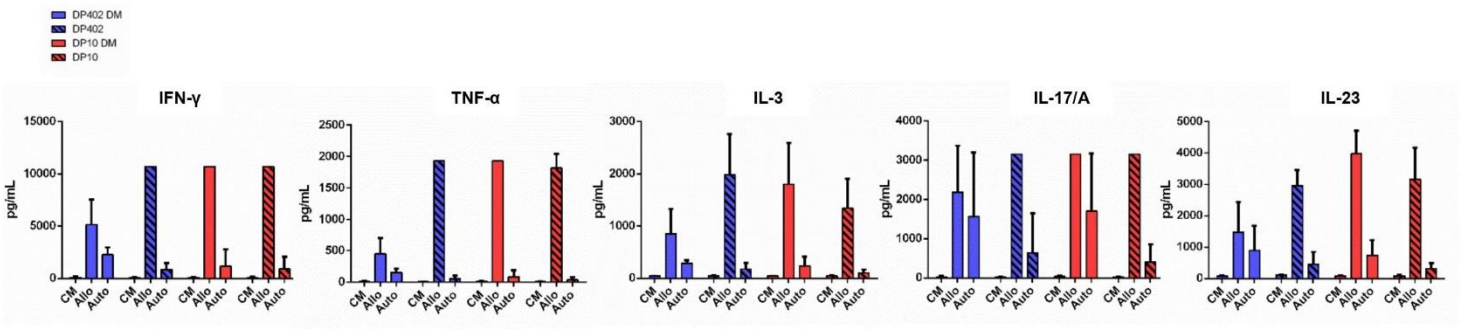

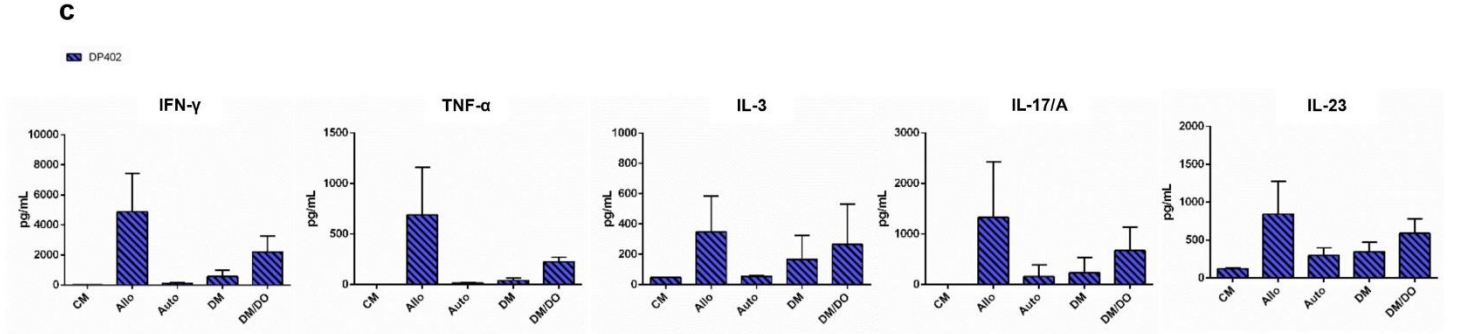

Supplementary Fig. 2: Functional characterization of alloreactive CD4$^+$ T-cell cultures. a, Antibody inhibition of *in vitro* CD4$^+$ T-cell alloreactivity to DP402 or DP10 with or without HLA-DM from a representative responder (R15) in Fig. 4a. CD137 assays were performed in the presence of the indicated concentrations of an HLA-DP-specific or an irrelevant HLA-DR-specific mAb, or no mAb. Data are shown as percent response relative to the unblocked condition (no mAb), and expressed as mean ± SD of three independent experiments. The mean relative response in the presence of irrelevant mAb was 92.0 ± 7.2% (DP402 DM), 86.7 ± 4.2% (DP402), 98.3 ± 2.9% (DP10 DM), 92.0 ± 5.3% (DP10). **b,** Cytokine production by the 4 responders in Fig. 4d, in response to culture media (CM), or HeLa expressing allogeneic (Allo) DP402 (blue bars) or DP10 (red bars), in the presence (full bars) or absence (striped bars) of HLA-DM, or autologous (Auto) DP401 with HLA-DM. Only cytokines released at >1000 pg/mL in response to allogeneic HLA-DP are shown. Data are represented as mean ± SD; cytokine levels exceeding the detection limit lack error bars. **c,** Cytokine production by the 4 responders from Fig. 4E, in response to culture media (CM), or HeLa expressing allogeneic DP402 in the absence of HLA-DM (Allo), or in the presence of HLA-DM and/or HLA-DO as indicated, or autologous (Auto) DP401 with HLA-DM. Only cytokines released at >1000 pg/mL in response to allogeneic HLA-DP are shown. Data are represented as mean ± SD.

Supplementary Fig. 3

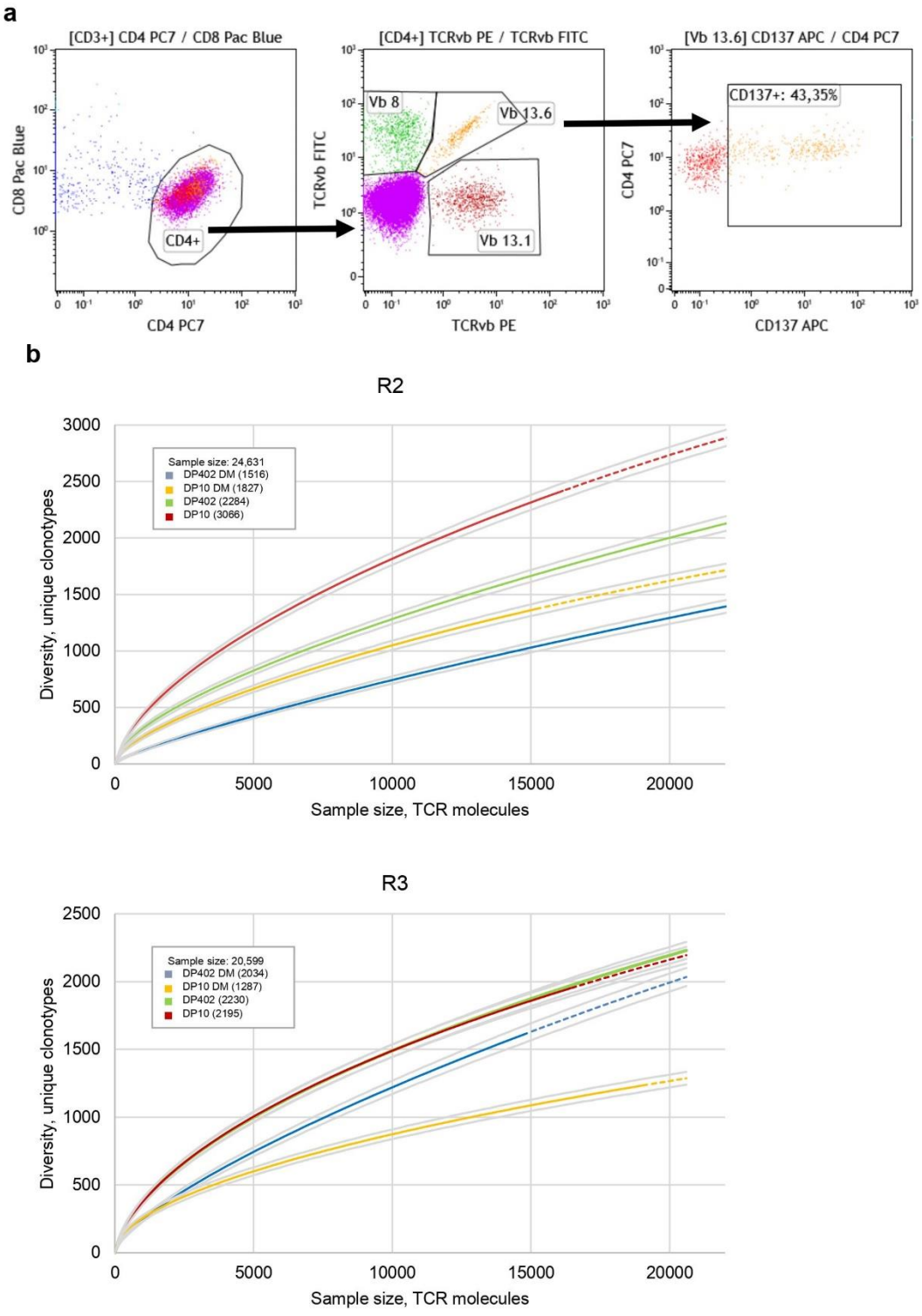

Supplementary Fig. 3: TCR-β diversity of alloreactive CD4$^+$ T-cell cultures. a, Flow cytometry gating strategy for the assessment of CD137-positivity in different CD4$^+$ TCR Vβ families upon re-stimulation. Cells were stained for CD3, CD4, CD137, and a panel of 24 TCR-Vβ-specific antibody combinations (three specificities per sample for a total of eight stainings per sample). CD3$^+$CD4$^+$ were gated as in Fig. 3b, and CD137$^+$ cells were measured in each of the three TCR-Vβ families per sample. **b,** Rarefaction curves showing the number of unique clonotypes with increasing sample sizes against DP402 or DP10 with or without HLA-DM in R2 and R3 from Fig. 5. Curves are interpolated from 0 to the size of each sample (solid lines), and extrapolated (dashed lines) to the size of the largest sample (i.e. DP402 and DP402 DM for R2, and DP402 for R3; 24,631 and 20,599 TCR molecules sampled, respectively). Numbers in brackets in the legend indicate the number of unique clonotypes in each repertoire at the maximum sample size. Curves in gray represent the lower and upper bounds of the 95% confidence interval for each modeled curve.

Supplementary Fig. 4

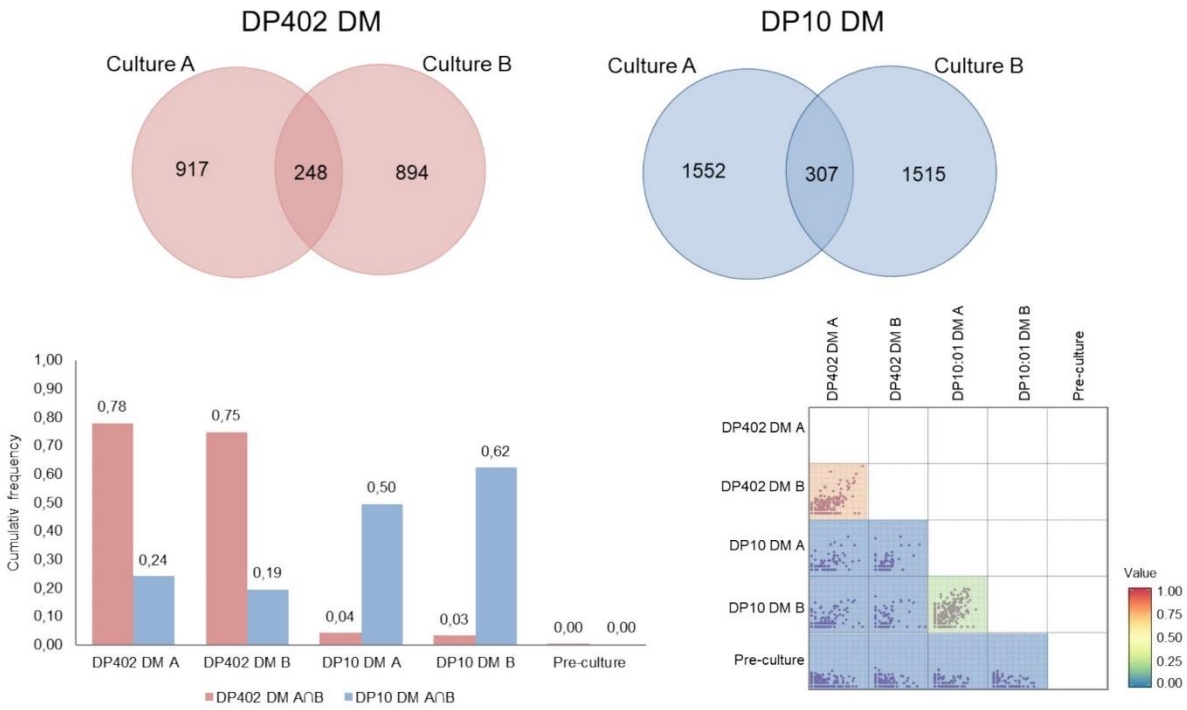

Supplementary Fig. 4: TCR-β clonotype sharing and repertoire similarity in replicate alloreactive CD4$^+$ T-cell cultures. TCR-β clonotype overlap between 2 parallel cultures (A and B) from the same healthy DP401-homozygous responder against allogeneic DP402 DM or DP10 DM. Top panels: Venn diagrams depicting the number of clonotypes shared or not shared between cultures A and B. Bottom left panel: cumulative frequency of TCR-β clonotypes shared by cultures A and B for DP402 DM (pink) or DP10 DM (blue) in each of the cultures, and in the pre-culture. Bottom right panel: TCR-β repertoire similarity among cultures A and B against both HLA-DP allotypes as indicated, and the pre-culture repertoire, shown as pair-wise frequency scatter plots of shared CDR3 aa sequences (represented as dots) and heatmap of Morisita index-based repertoire similarity between each pair of samples. Morisita repertoire similarity index ranges from 0 (no overlap) to 1 (full repertoire overlap).

Supplementary Fig. 5

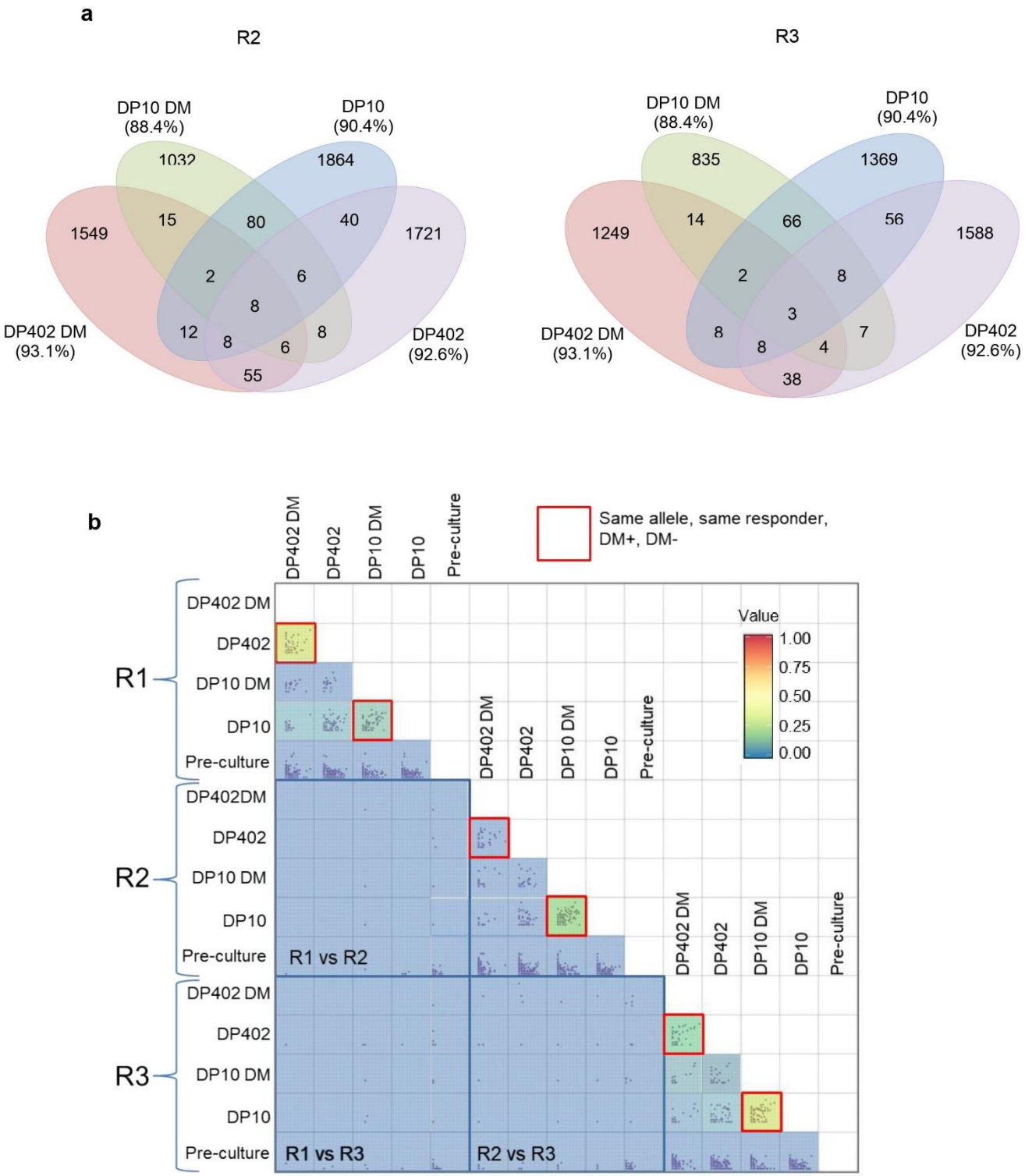

Supplementary Fig. 5: TCR-β clonotype sharing and repertoire similarity in alloreactive CD4$^+$ T-cell cultures. a, Overlap and percentage of non-shared TCR-β CDR3 nucleotide sequences responding to DP402 or DP10 with or without HLA-DM in R2 and R3 from Fig. 5. Numbers correspond to unique clonotypes in each dataset. **b**, TCR-β repertoire similarity among CD4$^+$ T cells responding to DP402 or DP10 in the presence or absence of HLA-DM, as well as in pre-culture CD4$^+$ T cells from 3 different responders (R1-R3 from Fig 5). Shown are pair-wise frequency scatter plots of shared CDR3 aa sequences (represented as dots) and heatmap of Morisita index-based repertoire similarity between each pair of samples. Morisita repertoire similarity index ranges from 0 (no overlap) to 1 (full repertoire overlap).

Supplementary Fig. 6

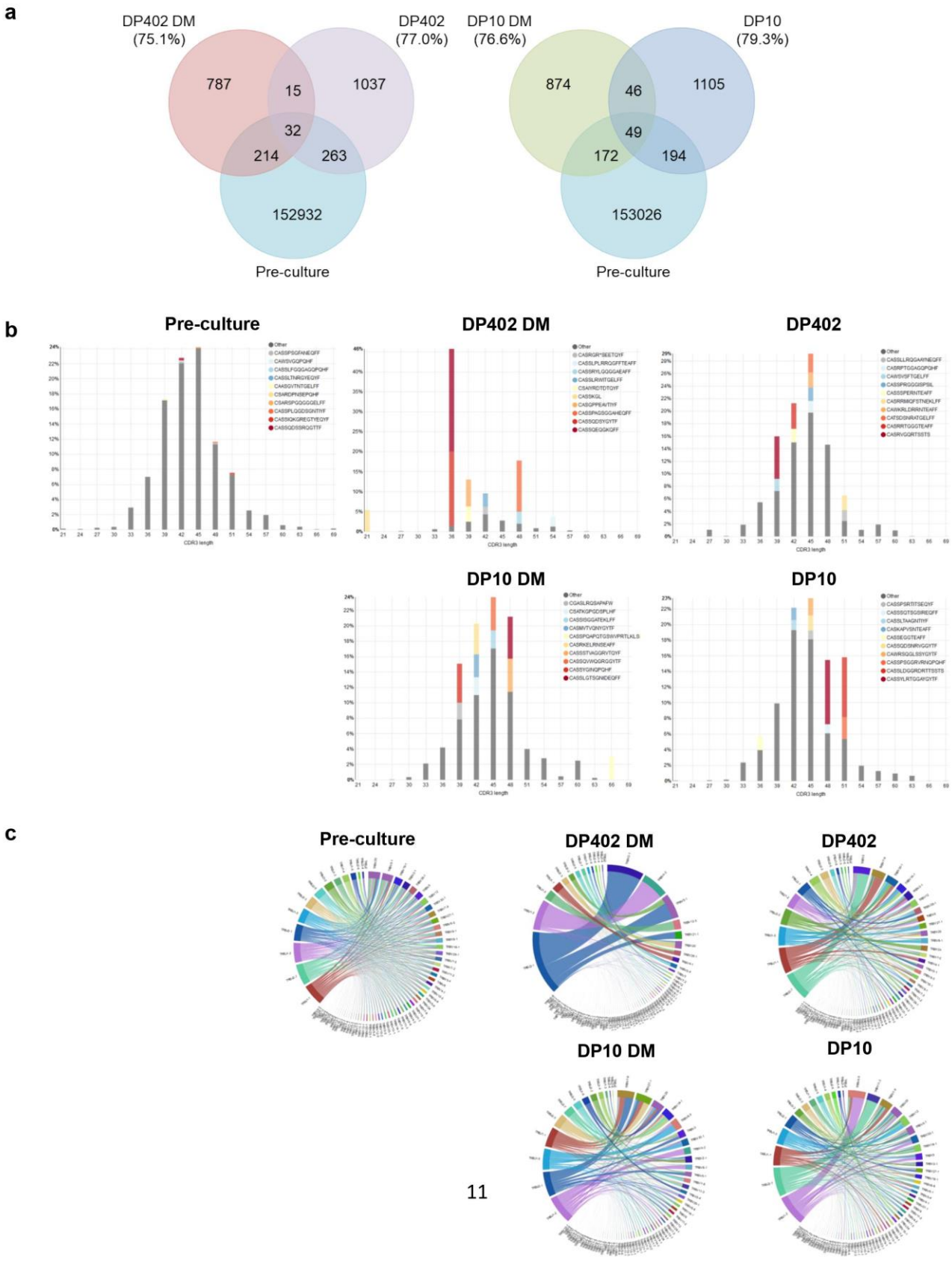

Supplementary Fig. 6: Molecular features of TCR-β clonotypes in alloreactive CD4⁺ T-cell cultures. Data are representatively shown for R1, similar data were obtained also for R2 and R3 from Fig. 5a, Origin of CD4⁺ T cell clonotypes responding against allogeneic DP402 or DP10 with or without HLA-DM. Venn diagrams show the overlap at the DNA level between samples cultured against each allele and the pre-culture repertoire. Percentages indicate the proportion of clonotypes found in the cultured samples but not in the pre-culture repertoire (i.e. low abundance). **b-c,** CDR3 length (**b**) and V-J rearrangement distributions (**c**) for CD4⁺ T cells against allogeneic DP402 or DP10 with or without HLA-DM. Histograms show the frequency distribution of CDR3 length with the top-10 clonotypes for each sample and their respective frequency. Circos plots show all V and J segments and their specific rearrangement pattern. Band width is proportional to the rearrangement frequency in each sample. CD4⁺ pre-culture T cells are also included for comparison.

Supplementary Table 1. Patient, donor, clinical, and sample characteristics related to Fig.6.

IZTF No.	pt DPB1[a]	don DPB1[b]	DP mismatch residue 84[c]	DP status[d]	CMV pt/don[e]	Age-sex pt/don[f]	HCT-CI[g]	Diagnosis[h]	Conditioning[i]	CMV peak titer[j]	aGvHD grade	cGvHD	Sampled after HCT[k]	$CD4^{+l}$ (%)
3	*04:01, ***04:02**	*04:01	Gly	P	+/+	66M/24M	7	MDS	RIC	632.000[m]	II	mild	30, 195, 327, 363[n]	44.7, ND, 42.3
28	*04:02, ***10:01**	*04:01, *04:02	Asp	NP	+/-	26F/26F	2	ALL	MAC	11.000[m]	I	no	30 ,181, 263, 346[n]	16.8, ND, 25.6
46	*02:01, ***03:01**	*02:01, *04:01	Asp	NP	-/-	63M/48M	4	NHL	RIC	<40	I	severe	279	7.0
57	*04:01, ***04:02**	*04:01	Gly	P	+/+	55F/18F	5	AML	MAC	7.000	I	mild	272	11.4
59	*04:01, ***04:02**	*04:01	Gly	P	+/+	33M/21M	6	AML	RIC	700	I	mild	278	14.0
62	***04:01**, *04:02	*02:01, *04:02	Gly	P	+/-	55M/26M	5	MDS	RIC	6.000	I	mild	475	12.7
262	***04:02, *17:01**	*02:01, *04:01	Gly, Asp	P, NP	-/-	50M/19M	3	AML	MAC	<40	I	severe	347	15.7
263	*02:01, ***03:01**	*04:01, *04:02	Gly, Asp	P, NP	+/+	59F/48F	7	AML	RIC	10.000	II	mild	170	5.6
270	***04:01**	*02:01	Gly	P	+/+	57F/50M	2	AML	MAC	38.200	I	no	283	17.1
272	***04:01**	*02:01, *04:02	Gly	P	-/-	52M/30M	4	NHL	MAC	<40	I	mild	392	53.4

[a]Patient (pt) and [b]donor (don) DPB1 types; mismatched pt DPB1 allele in bold. [c]Shown is the aa at position 84 in the mismatched HLA-DP of the pt. None of the donor HLA-DP allotypes carried 84Asp. [d]P, permissive; NP, non-permissive, as in[2]. [e]CMV IgG serology. [f]F, female; M, male. [g]HCT-CI, comorbidity index[47]. [h]MDS, myelodysplastic syndrome; ALL, acute lymphoblastic leukemia; AML, acute myeloid leukemia; NHL, non-Hodgkin lymphoma. [i]RIC, reduced-intensity conditioning; MAC, myeloablative conditioning. GvHD prophylaxis was based on cyclosporine, methotrexate, and *in vivo* T-cell depletion by anti-T-lymphocyte globulin (30 mg/kg). [j]Copies/ml by qPCR. [k]All patients had full donor chimerism by qPCR at the day of sampling. [l]Percentage of all $CD3^+$ cells from PBMC. ND, not determined. [m]Peak titer reached at d54 and d57 post-HCT in patient IZTF-3 and IZTF-28, respectively, [n]Used for co-culture experiments with $CD4^+$ T cells, amounting to 38.5% and 92.9% (IZTF-3), and 18.6% and 71.2% (IZTF-28) of $CD3^+$ before and after purification, respectively.

Supplementary Table 2. Summary statistics for TCRB immunosequencing of CD4⁺ T cells from healthy responders.

Sample	Total templates	Productive templates	Fraction productive	Total rearrangements	Productive rearrangements	Productive clonality	Maximum productive frequency	Input DNA (ng)
R1-DP10	11485	9220	0.8028	1787	1394	0.2383	0.1024	248.3
R1-DP10 DM	13978	11709	0.8377	1497	1141	0.3271	0.0649	154.2
R1-DP402	14679	11688	0.7962	1820	1347	0.2708	0.0512	177.3
R1-DP402 DM	21345	19260	0.9023	1347	1048	0.5995	0.2836	190.7
R1-pre-culture	241005	205054	0.8508	181039	153441	0.0318	0.0052	1200.0
R2-DP10	16148	14316	0.8865	2566	2020	0.2353	0.0573	178.6
R2-DP10 DM	15341	14062	0.9166	1499	1157	0.3513	0.1003	170.2
R2-DP402	24631	19762	0.8023	2446	1852	0.2774	0.0299	249.9
R2-DP402 DM	24537	19660	0.8012	1976	1655	0.5634	0.2058	191.0
R2-pre-culture	177292	151267	0.8532	150550	128131	0.0141	0.0006	1000.0
R3-DP10	16435	13473	0.8198	2082	1520	0.2806	0.1365	177.6
R3-DP10 DM	19184	15648	0.8157	1300	939	0.2931	0.0675	170.9
R3-DP402	20599	16568	0.8043	2353	1712	0.2465	0.0612	209.6
R3-DP402 DM	14849	12795	0.8617	1743	1326	0.3936	0.1433	201.0
R3-pre-culture	193567	155176	0.8017	162087	129989	0.0225	0.0097	1000.0

Supplementary Table 3. Summary statistics for TCRB immunosequencing from HCT patients and donors.

Sample	Total templates	Productive templates	Fraction productive	Total rearrangements	Productive rearrangements	Productive clonality	Maximum productive frequency	Input DNA (ng)
IZTF3-DP402 DM	24620	23355	0.9486	725	553	0.9026	0.9195	272.3
IZTF3-DP402	20244	19217	0.9493	667	509	0.8603	0.8715	209.1
IZTF3-donor	60536	47803	0.7897	54830	43420	0.0126	0.0030	1998.8
IZTF3-30-BM	1808	1269	0.7019	1481	1074	0.0191	0.0118	3641.0
IZTF3-30-PB	4415	3256	0.7375	3237	2437	0.0393	0.0129	1997.1
IZTF3-195-PB	158638	132418	0.8347	3457	2525	0.6169	0.2395	1997.5
IZTF3-363-PB	235195	207723	0.8832	4408	3282	0.6394	0.3609	1995.2
IZTF28-DP10 DM	31072	25362	0.8162	6891	5560	0.3767	0.2594	269.0
IZTF28-DP10	39576	34195	0.8640	6388	5169	0.3869	0.2030	239.4
IZTF28-donor	120672	99816	0.8272	103063	85741	0.0293	0.0135	1995.4
IZTF28-30-BM	11984	9539	0.7960	8035	6443	0.0730	0.0313	3641.7
IZTF28-30-PB	34094	27095	0.7947	16412	13115	0.1411	0.0284	1998.3
IZTF28-181-PB	123129	91572	0.7437	15411	12397	0.4077	0.0671	1996.6
IZTF28-346-PB	71239	55394	0.7776	22656	18350	0.2760	0.0622	914.9

7. Discussion

In this thesis, I have used different approaches to investigate the fundamental features of T-cell alloreactivity to HLA-DP in order to unravel the basis of mismatch permissiveness in HSCT and to identify targets to modulate its strength and that can be used translationally. We tried to dissect the effects of structural differences and SNP-linked expression levels of HLA-DPB1 to assess the relative role of these factors in differential T-cell alloreactivity. Interestingly, differential T-cell alloreactivity could be determined also in independently of differential expression levels, suggesting that structural features of HLA-DP play a predominant role over expression levels in eliciting T-cell alloreactivity. By means of deep TCR sequencing of alloreactive T cells against structurally similar and dissimilar HLA-DPB1 alleles, we showed that TCR repertoire diversity can be high, despite differences in the strength of T-cell alloreactivity. Lastly, I investigated the impact of the HLA-DP immunopeptidome on T-cell alloreactivity through the peptide editor HLA-DM. Results of mass spectrometry analysis and functional assays showed evidence for a central role of the peptide that is presented by HLA-DP in regulating T-cell alloreactivity.

For most patients undergoing HSCT, an unrelated donor is required since a matched related donor is not always available, especially in ethnic minorities. HLA-DP is very often mismatched in 9/10 or 10/10 matched unrelated donors. Thus, the definition of well-tolerated HLA mismatches is needed to achieve successful HSCT outcome. For that, HLA mismatch permissiveness prediction has been extensively sought by various groups to tackle the challenge of matching of the highly polymorphic HLA. Several proposed prediction models for HLA in general or specific for HLA-DPB1 have emerged. Apart from the expression levels-based models, which are based on differential SNP-associated expression levels[135, 137], most of the current models such as HistoCheck[138], PIRCHE[139], HLAMatchmaker[140], and the HLA-DP TCE[130] and functional distance (FD) models[141] are based on structural features of HLA molecules. HistoCheck is a sequence dissimilarity matching score originally based on HLA class I molecules taking into account amino acid relevance for antigen presentation and number of amino acid differences[138]. Its internet-based software tool claims it can predict allogenicity of HLA class I and II mismatches[142]. Epitope-based matching algorithms include the PIRCHE (Predicted Indirectly Recognizable HLA Epitopes) and the HLAMatchmaker (eplet) models. The PIRCHE model considers epitopes that are target for indirect T-cell allorecognition[139], whereas HLAMatchmaker is based on direct

recognition of so-called eplets, i.e. polymorphic key residues of HLA epitopes[140]. However, assessment of the clinical relevance of most of these models showed weaknesses characterized by studies with limited size, retrospective design, lack of validation assessment, and inconsistent association with improved clinical outcome prediction[143-145]. Other models focused on HLA-DPB1 mismatches, such as the TCE, FD, and Expression models estimate the allogenic potential of HLA-DPB1 disparities. Correlation for the 3'UTR high HLA-DPB1 expression level marker rs9277534 with higher risk of GvHD was demonstrated in clinical studies[135]. However, functional testing of the SNP association with HLA-DPB1 expression levels was not performed, so it remains unclear whether differential expression levels are the direct cause of the observed association. The high overlap (80%)[136] between HLA-DPB1 allele classification according to the Expression and TCE models does not exclude that expression levels are a surrogate for structural differences. The TCE model was experimentally proven to predict different strengths of T-cell alloreactivity initially explained via T-cell cross-recognition patterns and allowing for the classification of 72 HLA-DPB1 alleles into three T-cell epitope groups determining permissive or non-permissive HLA-DPB1-mismatches associated with clinical outcome of unrelated HSCT[108, 130]. Further investigation into the basis of the TCE model led to the conception of the FD model, which integrated the impact of single amino acids at specific positions of the HLA-DP peptide-binding groove on T-cell alloreactivity patterns. The FD risk prediction was also demonstrated to be associated with GvHD and mortality after unrelated HSCT[146, 147]. By means of *in silico* FD prediction, the quantitative limitation of TCE HLA-DPB1 allele classification was solved and shown to predict outcome in HSCT for all described alleles[141]. However, these two models still have some limitations since they are based only on one reference allele (HLA-DPB1*09:01) and only single amino acid changes were investigated for the establishment of the FD scoring, missing potential effects of additive amino acid changes.

Overall, one fundamental aspect to generate clinically informative models that can effectively predict permissiveness of HLA mismatches and clinical outcome after HSCT is a thorough understanding of the biological principles of alloreactive responses against HLA. The results of my thesis shed light onto some of these unknown aspects for alloreactivity against HLA-DP.

First, we aimed to dissect the relative role of HLA-DPB1 expression levels and TCE on T-cell alloreactivity. Although we confirmed previous data regarding rs9277534 SNP-

linked differences in HLA-DPB1 expression levels in B cells and BLCLs, we demonstrated that this effect was abrogated under *in vitro*-simulated inflammatory conditions (Article II, Figure 1). According to our *in vitro* data we could not find evidence for a direct impact of HLA-DPB1 expression levels on differential T-cell alloreactivity. On the contrary, despite similar HLA-DP expression levels, distinct strengths of T-cell alloreactivity were elicited due to structural variation across HLA-DPB1 alleles (Article II, Figure 8B). Since functional studies showing evidence for the direct impact of the rs9277534 SNP on differential expression levels are missing, we performed a thorough testing of the SNP and its direct relationship to HLA-DPB1 expression levels. Our data could not confirm a direct impact of the 3'UTR SNP on HLA-DPB1 RNA expression levels. Furthermore, we could exclude a role for alternative splicing mechanisms (Article II, Figure 4C and 5B, respectively). These results suggest that the SNP could be a surrogate for another SNP outside of the 3'UTR or for another mechanism impacting expression levels. For instance, post-transcriptional mechanisms could play a role since the 3'UTR contains many regulatory regions that can influence gene expression. Hence, non-coding RNAs such as microRNAs (miRNA) could modulate expression levels of HLA-DPB1. Recently, miRNA binding to the rs9277534 A/G SNP in the 3'UTR of HLA-DPB1 was computationally assessed showing that the A-variant linked to low HLA-DPB1 expression was associated with higher miRNA interaction. Furthermore, miRNAs targeting other polymorphisms that are in linkage disequilibrium with rs9277354 A/G[148] have been identified. These findings hint to a dynamic process impacting differential expression levels. However, our observations suggest a predominant role of the structural characteristics defined by the TCE model, which also shows even greater applicability in unrelated allogeneic HSCT compared to the Expression model (Article II, Figure 6C). Hence, expression levels might be a surrogate of structural variations of the TCE model as both models have a significant overlap[136] as explained above. We were not able to fully separate these two models, but others have directly and indirectly addressed this association. Morishima *et al.* reconstructed the evolutionary relationship of HLA-DPB1 alleles based on next-generation sequencing data of the HLA-DPB1 gene region and multi-SNP data of 19 HLA-DPB1 alleles[149]. Their results provide a new classification that separated DP2-like and DP5-like polymorphism patterns supported by the SNP-linked expression levels but showing discrepancies in association with the structural based TCE model. For example, HLA-DPB1*05:01 classified in TCE group 3 exhibits structural similarities to the DP5-like group and not the DP2-like group, which contains most TCE group 3 alleles. These

findings point to the limitations of the TCE model as TCE group 3 is an exclusion group including structurally divergent alleles. Recently, another study from Al Malki *et al.* addressed the combined impact of TCE permissive and non-permissive mismatches and expression levels of HLA-DP in a retrospective study[150]. They could demonstrate that in patients that were matched 11/12 with a permissive mismatch combined with low HLA-DP expression levels had the best outcome in allogeneic HSCT. This suggests that both models contribute to better outcome in HSCT. More importantly, however, these findings might reflect the fact that mismatches involving alleles from TCE group 3, some of which differ structurally and which are associated with the high-expression variant, could have to be reclassified as less permissive. Whether or not and to what extent the Expression model complements or refines the TCE model warrants further investigation.

Second, we addressed the influence of structural differences between HLA-DP allotypes on alloreactive TCR diversity. Despite quantitative differences in T-cell alloreactivity against structurally similar and dissimilar HLA-DPB1 alleles, the diversity of T-cell clones from healthy subjects able to respond to these mismatches was comparably high in both cases (Article I, Figure 3A). A limited T-cell response but with the presence of a diverse TCR repertoire is a desirable combination for effective malignant disease control, as it is for efficient immune responses against viral infections and other pathogens. Taken together, these data illustrate one of the possible mechanisms by which permissive mismatches according to the TCE model confer better HSCT outcome, since these kinds of mismatches confer lower relapse rate with comparable overall survival when compared to HLA-DPB1 allele matches[131, 132].

Third, we pursued a comprehensive study of the HLA-DP immunopeptidome and the effect of the peptide editor HLA-DM and their role for T-cell alloreactivity and permissive mismatch prediction assessment in healthy donors and transplanted patients. A role for the immunopeptidome for T-cell alloreactivity is supported by the fact that crucial amino acid changes that impact T-cell alloreactivity are known to be peptide contacts in the peptide-binding groove[146], potentially representing a biological basis responsible for permissiveness and a possible approach for T-cell alloreactivity modulation. Our analysis of the peptide repertoires revealed a significant overlap between structurally similar compared to structurally divergent HLA-DPB1 alleles showing distinct immunopeptidomes (Article III, Figure 1C) suggesting that structural

differences of HLA-DPB1 are reflected in the similarity of their immunopeptidomes. Furthermore, we could verify our hypothesis that HLA-DM-mediated shaping of the immunopeptidome modulates T-cell alloreactivity with strong effects in the context of permissive mismatches in healthy individuals and patients after allogeneic HSCT (Article III, Figure 4A, 6A). In responses against structurally very similar HLA-DPB1 alleles the alloreactive TCR diversity is reduced if HLA-DM is active (Article III, Figure 5B, C). Moreover, inhibition of HLA-DM via antagonist HLA-DO also increased T-cell alloreactivity in the permissive situation (Article III, Figure 4C).

In summary these findings suggest a central role of the immunopeptidome presented by HLA-DPB1, able to modulate T-cell alloreactivity in an allotype-specific manner. This observation could be transferred to a novel permissive mismatch and outcome prediction model in unrelated HSCT. More precisely, a high immunopeptidome overlap between two HLA-DPB1 alleles predicts permissiveness, whereas mismatches involving alleles with low immunopeptidome overlap would represent non-permissive mismatches. In addition, such an immunopeptidome-based prediction model (**Figure 20**) would be able to integrate existing models such as FD scoring, TCE, DP2-DP5, and Expression levels. According to this proposed model, decreasing immunopeptidome similarity caused by structural differences in the HLA-DP peptide-binding groove would lead to increasing levels of alloreactive response and alloreactive TCR diversity. For instance, HLA-DPB1*05:01, currently classified as a TCE group 3 allele, would be classified as a permissive mismatch for an individual homozygous for allele HLA-DPB1*04:01 according to the current TCE algorithm. However, classification according to the immunopeptidome-based prediction model would take the structural divergence (presence of 84DEAV87 motif) and the strength of T-cell alloreactivity into account. T-cell alloreactivity to HLA-DPB1*05:01 was shown to be significantly higher compared to other TCE 3 alleles (Article II, Figure 8B). Moreover HLA-DPB1*05:01 shows a distinct peptide binding motif compared to of HLA-DPB1*04:01 (unpublished data – Peter van Balen, personal communication), indicating that also the immunopeptidome will be different with reduced overlap. Showing strong alloreactivity, small immunopeptidome overlap with different peptide binding motifs and likely higher alloreactive TCR diversity, HLA-DPB1*05:01 would probably be classified as a non-permissive HLA-DPB1 allele for DPB1*04:01-homozygous responders according to the immunopeptidome prediction model. The Expression model also predicts HLA-DPB1*05:01 as high expression allele[135] and

hence non-permissive for DPB1*04:01 responders. The same occurs with the evolutionary based Japanese model, where DP5 is even the representative allele of one of the allele groups, with DPB1*04:01 being classified within the DP2 group[149]. Taken together, an immunopeptidome overlap-based classification of HLA-DP mismatches would represent an integral, direct approach for gradual identification of permissiveness in unrelated HSCT capable of consolidating all present algorithms. The data presented in this thesis would support a rationale for intelligent HLA-DP mismatching that combines controlled levels of alloreactivity with sufficient TCR diversity to maximise the anti-leukaemia therapeutic effects of HSCT.

In addition to their relevance for HSCT outcome prediction models, our results hold a potential for translational impact of T-cell alloreactivity modulation. HLA-DP is an interesting target for immunotherapy due its capability of eliciting leukaemia-specific T-cell alloreactivity. Earlier an *ex vivo* study demonstrated the anti-leukemic response against HLA-DP expressing B cell leukaemia[151]. Moreover, it was shown that the repertoire of HLA-DP-specific T cells exhibits restricted recognition of haematopoietic cells[152] and AML blasts[153], supporting the applicability of HLA-DP as a target for adoptive T-cell therapy. Furthermore, our results demonstrated the modulation abilities of HLA-DM impacting the strength of alloreactivity. Targeting of the immunopeptidome could be used to modulate T-cell alloreactivity against HLA-DP. Thus HLA-DM could be used as a target for pharmacological inhibition (e.g. via small molecules) to increase the strength of alloreactive T cells against DM positive leukemic cells. Modulation of HLA-DM activity using small molecules was earlier demonstrated for HLA-DR[154]. In addition, the ability of a drug mediating structural changes in the peptide-binding groove was demonstrated for HLA-B*57:01 and abacavir treatment[155]. A similar approach could potentially be applied to HLA-DP, which could produce immunopeptidome changes, mimicking HLA-DM negative conditions and allowing the induction of harnessed, cell-specific T-cell alloresponses. Alternatively, HLA-DM could be knock-out using CRISPR/Cas technology[156].

Moreover, the results presented in this thesis regarding the regulation of T-cell alloreactivity by HLA-DM could also have implications in the field of tumour immunology. Intuitively, the same immunotherapy approaches for leukaemia could also be applied for the treatment of solid tumours. Several tumour-specific antigens are used for TCR immunotherapy providing encouraging results for instance for the treatment of melanoma[157, 158]. As suggested above, alteration of the immunopeptidome

via HLA-DM could modulate T-cell alloreactivity against the tumour cells. The knockout of HLA-DM in tumour cells could lead to enhanced T-cell allorecognition and thereby improve autologous immune responses and eradication of the tumour. Another report identified HLA class II-restricted peptides as a potential therapeutic reagent (vaccine) for cancer patients showing that unique peptides presented by invariant chain-negative cancer cells can activate tumour specific T cells [159]. In this context and in view of the data presented in this thesis, HLA-DM-negative cancer cells could have the same effect for anti-cancer immunization strategies.

Our results are not only of importance in cancer therapy but also have implications for autoimmunity as antigen presentation is an essential process triggering autoimmunity. HLA-DP has been associated with autoimmune diseases like Graves Disease[160] or multiple sclerosis[161]. In contrast to other HLA class II loci, HLA-DP provides special features for antigen presentation. In particular, it is able to present a broader array of peptides in the absence of HLA-DM, whereas many HLA-DR allotypes are highly dependent HLA-DM activity for the exchange of CLIP[162]. This might mean for example that peptide changes due to inflammatory conditions might lead to a distinct peptide repertoire allowing the presentation of HLA-DM independent peptides in the periphery that were not presented in the thymus before and thus lead to auto-reactive T cells activation[163]. Beside the reported association of HLA-DM[164] and HLA-DO with autoimmune disease, the relevant role of HLA-DM and HLA-DO and their influence on self-peptide presentation on HLA class II molecules in the pathogenesis of autoimmune disease has been experimentally shown[165, 166].

In conclusion, the results presented in this thesis shed light onto the mechanism of modulation of T-cell alloreactivity against HLA-DP, providing the basis for the establishment of a refined model for permissiveness prediction in unrelated HSCT. Despite the fact that we used an *in vitro* HeLa cell system as artificial APC to assess the impact of the immunopeptidome on T-cell alloreactivity, strong evidence supports a central role of the presented peptides and their editing by HLA-DM and DO in this process. These results must be confirmed in haematopoietic APCs, and beyond the representative HLA-DPB1 alleles tested, something which would very likely enlighten the classification of alleles, especially within the heterogeneous TCE group 3, and contribute to solve the discrepancies regarding HLA-DPB1 allele and mismatch classification across the various available models in HSCT. Finally, the findings

regarding the regulation of T-cell alloreactivity against HLA-DPB1 summarized in this thesis are also of potential importance for cancer immunotherapy and autoimmunity.

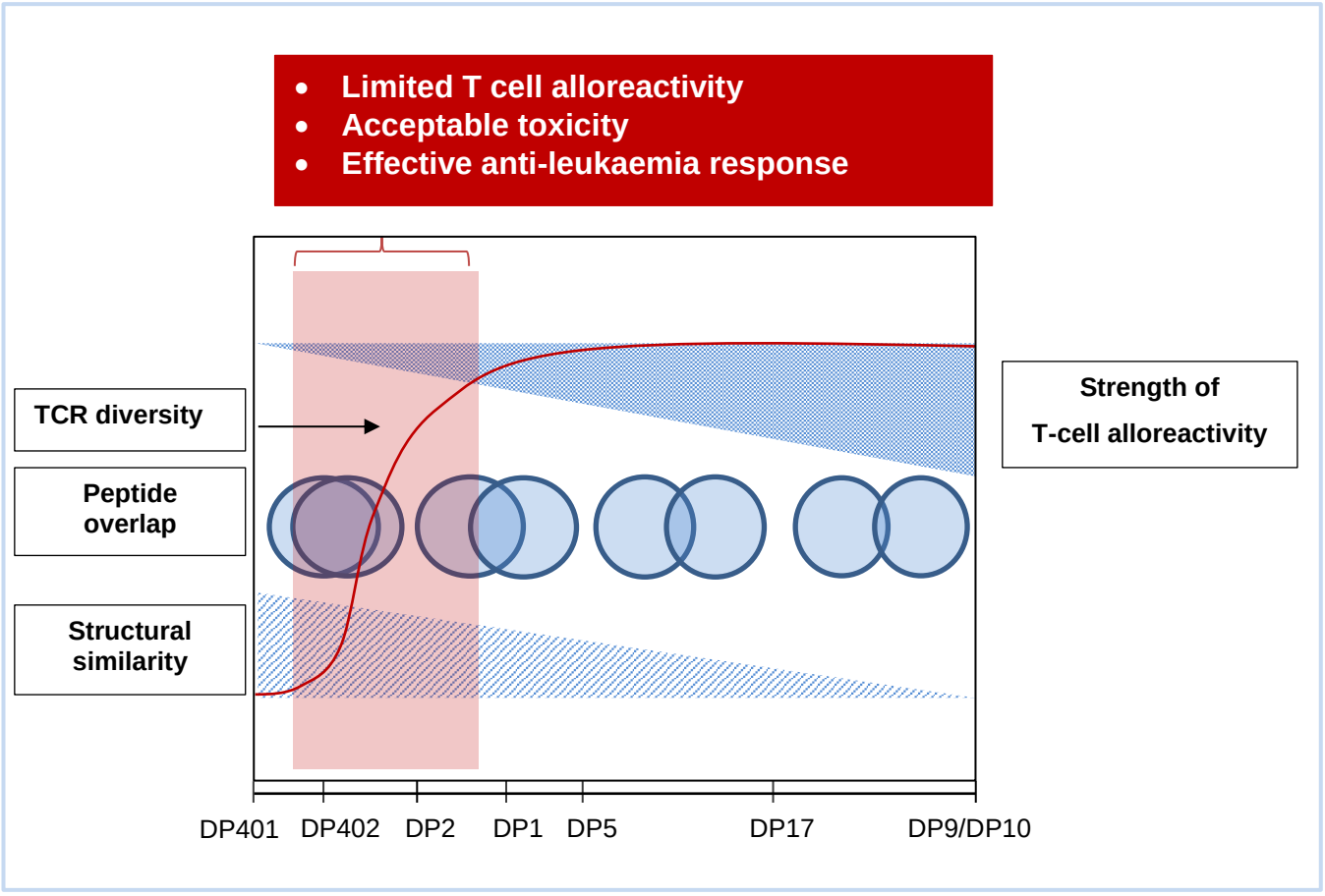

Figure 20: Immunopeptidome-based prediction model for permissiveness

A peptide repertoire similarity-based model unites immunopeptidome with TCR diversity (red curve) and structural similarities, which all together impact the strength of T-cell alloreactivity. Red box shows theoretical optimal conditions for limited T-cell alloreactivity (i.e. harnessed response with sufficient TCR diversity). Bar on the bottom presents HLA-DPB1 alleles according to their increasing immunogenicity for a self-DPB1*04:01 reference allele. Model is based experimental observation of two model alleles HLA-DPB1*04:02 and HLA-DPB1*10:01. Absence of HLA-DM modulates immunopeptidome overlap, hence could be used to achieve the range of optimal conditions.

8. References

1. Dausset, J., *[Iso-leuko-antibodies].* Acta Haematol, 1958. **20**(1-4): p. 156-66.
2. Van Rood, J.J., J.G. Eernisse, and A. Van Leeuwen, *Leucocyte antibodies in sera from pregnant women.* Nature, 1958. **181**(4625): p. 1735-6.
3. Payne, R. and M.R. Rolfs, *Fetomaternal leukocyte incompatibility.* J Clin Invest, 1958. **37**(12): p. 1756-63.
4. Thorsby, E., *A short history of HLA.* Tissue Antigens, 2009. **74**(2): p. 101-16.
5. Van Rood, J.J. and A. Van Leeuwen, *Leukocyte Grouping. A Method and Its Application.* J Clin Invest, 1963. **42**: p. 1382-90.
6. Payne, R., et al., *A New Leukocyte Isoantigen System in Man.* Cold Spring Harb Symp Quant Biol, 1964. **29**: p. 285-95.
7. Thorsby, E.P.A., *Joint report from the sixth international histocompatibility workshop conference . II. Typing for HLA-D (LD-a or MLC) determinants. .* Histocompatiblity Testing 1975.Copenhagen: Munksgaard, 1978: p. 414-58.
8. Robinson, J., et al., *The IPD and IMGT/HLA database: allele variant databases.* Nucleic Acids Res, 2015. **43**(Database issue): p. D423-31.
9. Trowsdale, J. and J.C. Knight, *Major histocompatibility complex genomics and human disease.* Annu Rev Genomics Hum Genet, 2013. **14**: p. 301-23.
10. Goldberg, A.C. and L.V. Rizzo, *MHC structure and function - antigen presentation. Part 1.* Einstein-Sao Paulo, 2015. **13**(1): p. 153-156.
11. Horton, R., et al., *Gene map of the extended human MHC.* Nat Rev Genet, 2004. **5**(12): p. 889-99.
12. Blomhoff, A., et al., *Linkage disequilibrium and haplotype blocks in the MHC vary in an HLA haplotype specific manner assessed mainly by DRB1*03 and DRB1*04 haplotypes.* Genes Immun, 2006. **7**(2): p. 130-40.
13. Janeway, C.T., P.; Walport, M.; Shlomchik M., *Immunobiology: The Immune System in Health and Disease* Garland Science, 2001. **5th edition**: p. 172-173.
14. Abbas, A.K.L., A.H.; Pillai, S. , *Cellular and Molecular Immunology.* Elsevier 2012. **Seventh Edition**.
15. Spierings, E. and K. Fleischhauer, *Histocompatibility*, in *The EBMT Handbook: Hematopoietic Stem Cell Transplantation and Cellular Therapies*, th, et al., Editors. 2019: Cham (CH). p. 61-68.
16. Goldberg, A.C. and L.V. Rizzo, *MHC structure and function - antigen presentation. Part 2.* Einstein-Sao Paulo, 2015. **13**(1): p. 157-162.
17. Jensen, P.E., *Recent advances in antigen processing and presentation.* Nat Immunol, 2007. **8**(10): p. 1041-8.
18. Rock, K.L., et al., *Protein degradation and the generation of MHC class I-presented peptides.* Adv Immunol, 2002. **80**: p. 1-70.
19. Wearsch, P.A. and P. Cresswell, *The quality control of MHC class I peptide loading.* Curr Opin Cell Biol, 2008. **20**(6): p. 624-31.
20. Spee, P. and J. Neefjes, *TAP-translocated peptides specifically bind proteins in the endoplasmic reticulum, including gp96, protein disulfide isomerase and calreticulin.* Eur J Immunol, 1997. **27**(9): p. 2441-9.
21. Vyas, J.M., A.G. Van der Veen, and H.L. Ploegh, *The known unknowns of antigen processing and presentation.* Nat Rev Immunol, 2008. **8**(8): p. 607-18.
22. Hershberg, R.M., et al., *Highly polarized HLA class II antigen processing and presentation by human intestinal epithelial cells.* J Clin Invest, 1998. **102**(4): p. 792-803.
23. Turesson, C., *Endothelial expression of MHC class II molecules in autoimmune disease.* Curr Pharm Des, 2004. **10**(2): p. 129-43.

24. Trombetta, E.S. and I. Mellman, *Cell biology of antigen processing in vitro and in vivo.* Annu Rev Immunol, 2005. **23**: p. 975-1028.
25. Neefjes, J., *CIIV, MIIC and other compartments for MHC class II loading.* Eur J Immunol, 1999. **29**(5): p. 1421-5.
26. Cresswell, P., *Invariant chain structure and MHC class II function.* Cell, 1996. **84**(4): p. 505-7.
27. McCormick, P.J., J.A. Martina, and J.S. Bonifacino, *Involvement of clathrin and AP-2 in the trafficking of MHC class II molecules to antigen-processing compartments.* Proc Natl Acad Sci U S A, 2005. **102**(22): p. 7910-5.
28. Kropshofer, H., et al., *HLA-DM acts as a molecular chaperone and rescues empty HLA-DR molecules at lysosomal pH.* Immunity, 1997. **6**(3): p. 293-302.
29. Kremer, A.N., et al., *Endogenous HLA class II epitopes that are immunogenic in vivo show distinct behavior toward HLA-DM and its natural inhibitor HLA-DO.* Blood, 2012. **120**(16): p. 3246-55.
30. Poluektov, Y.O., A. Kim, and S. Sadegh-Nasseri, *HLA-DO and Its Role in MHC Class II Antigen Presentation.* Front Immunol, 2013. **4**: p. 260.
31. Roche, P.A. and K. Furuta, *The ins and outs of MHC class II-mediated antigen processing and presentation.* Nat Rev Immunol, 2015. **15**(4): p. 203-16.
32. Ackerman, A.L. and P. Cresswell, *Cellular mechanisms governing cross-presentation of exogenous antigens.* Nat Immunol, 2004. **5**(7): p. 678-84.
33. Heath, W.R. and F.R. Carbone, *Cross-presentation in viral immunity and self-tolerance.* Nat Rev Immunol, 2001. **1**(2): p. 126-34.
34. Kumar, B.V., T.J. Connors, and D.L. Farber, *Human T Cell Development, Localization, and Function throughout Life.* Immunity, 2018. **48**(2): p. 202-213.
35. Romagnani, S., *T-cell subsets (Th1 versus Th2).* Ann Allergy Asthma Immunol, 2000. **85**(1): p. 9-18; quiz 18, 21.
36. Sallusto, F. and A. Lanzavecchia, *Memory in disguise.* Nat Med, 2011. **17**(10): p. 1182-3.
37. Gattinoni, L., et al., *T memory stem cells in health and disease.* Nat Med, 2017. **23**(1): p. 18-27.
38. Mosmann, T.R., et al., *Two types of murine helper T cell clone. I. Definition according to profiles of lymphokine activities and secreted proteins.* J Immunol, 1986. **136**(7): p. 2348-57.
39. Geginat, J., et al., *Plasticity of human CD4 T cell subsets.* Front Immunol, 2014. **5**: p. 630.
40. Normanton, M. and L.C. Marti, *Current data on IL-17 and Th17 cells and implications for graft versus host disease.* Einstein (Sao Paulo), 2013. **11**(2): p. 237-46.
41. Crotty, S., *T follicular helper cell differentiation, function, and roles in disease.* Immunity, 2014. **41**(4): p. 529-42.
42. Hayat, M.A.e., *Immunology. Volume 1, Immunotoxicology, immunopathology, and immunotherapy*.
43. Dechanet, J., et al., *Implication of gammadelta T cells in the human immune response to cytomegalovirus.* J Clin Invest, 1999. **103**(10): p. 1437-49.
44. Rosati, E., et al., *Overview of methodologies for T-cell receptor repertoire analysis.* BMC Biotechnol, 2017. **17**(1): p. 61.
45. Hodges, E., et al., *Diagnostic role of tests for T cell receptor (TCR) genes.* J Clin Pathol, 2003. **56**(1): p. 1-11.
46. Alcover, A., B. Alarcon, and V. Di Bartolo, *Cell Biology of T Cell Receptor Expression and Regulation.* Annu Rev Immunol, 2018. **36**: p. 103-125.
47. Alt, F.W., et al., *VDJ recombination.* Immunol Today, 1992. **13**(8): p. 306-14.

48. Laydon, D.J., C.R. Bangham, and B. Asquith, *Estimating T-cell repertoire diversity: limitations of classical estimators and a new approach.* Philos Trans R Soc Lond B Biol Sci, 2015. **370**(1675).
49. Davis, M.M. and P.J. Bjorkman, *T-cell antigen receptor genes and T-cell recognition.* Nature, 1988. **334**(6181): p. 395-402.
50. Oettinger, M.A., et al., *RAG-1 and RAG-2, adjacent genes that synergistically activate V(D)J recombination.* Science, 1990. **248**(4962): p. 1517-23.
51. Alt, F.W. and D. Baltimore, *Joining of immunoglobulin heavy chain gene segments: implications from a chromosome with evidence of three D-JH fusions.* Proc Natl Acad Sci U S A, 1982. **79**(13): p. 4118-22.
52. Clevers, H., et al., *The T cell receptor/CD3 complex: a dynamic protein ensemble.* Annu Rev Immunol, 1988. **6**: p. 629-62.
53. Attaf, M., E. Huseby, and A.K. Sewell, *alphabeta T cell receptors as predictors of health and disease.* Cell Mol Immunol, 2015. **12**(4): p. 391-9.
54. Chothia, C., D.R. Boswell, and A.M. Lesk, *The outline structure of the T-cell alpha beta receptor.* EMBO J, 1988. **7**(12): p. 3745-55.
55. Stritesky, G.L., S.C. Jameson, and K.A. Hogquist, *Selection of self-reactive T cells in the thymus.* Annu Rev Immunol, 2012. **30**: p. 95-114.
56. Klein, L., et al., *Positive and negative selection of the T cell repertoire: what thymocytes see (and don't see).* Nat Rev Immunol, 2014. **14**(6): p. 377-91.
57. von Boehmer, H., et al., *Thymic selection revisited: how essential is it?* Immunol Rev, 2003. **191**: p. 62-78.
58. Carpenter, A.C. and R. Bosselut, *Decision checkpoints in the thymus.* Nat Immunol, 2010. **11**(8): p. 666-73.
59. Surh, C.D. and J. Sprent, *T-cell apoptosis detected in situ during positive and negative selection in the thymus.* Nature, 1994. **372**(6501): p. 100-3.
60. Itoh, M., et al., *Thymus and autoimmunity: production of CD25+CD4+ naturally anergic and suppressive T cells as a key function of the thymus in maintaining immunologic self-tolerance.* J Immunol, 1999. **162**(9): p. 5317-26.
61. Taniuchi, I. and W. Ellmeier, *Transcriptional and epigenetic regulation of CD4/CD8 lineage choice.* Adv Immunol, 2011. **110**: p. 71-110.
62. Nikolich-Zugich, J., M.K. Slifka, and I. Messaoudi, *The many important facets of T-cell repertoire diversity.* Nat Rev Immunol, 2004. **4**(2): p. 123-32.
63. Clambey, E.T., et al., *Molecules in medicine mini review: the alphabeta T cell receptor.* J Mol Med (Berl), 2014. **92**(7): p. 735-41.
64. Zinkernagel, R.M. and P.C. Doherty, *Restriction of in vitro T cell-mediated cytotoxicity in lymphocytic choriomeningitis within a syngeneic or semiallogeneic system.* Nature, 1974. **248**(5450): p. 701-2.
65. La Gruta, N.L., et al., *Understanding the drivers of MHC restriction of T cell receptors.* Nat Rev Immunol, 2018. **18**(7): p. 467-478.
66. Felix, N.J. and P.M. Allen, *Specificity of T-cell alloreactivity.* Nat Rev Immunol, 2007. **7**(12): p. 942-53.
67. Morris, G.P. and P.M. Allen, *How the TCR balances sensitivity and specificity for the recognition of self and pathogens.* Nat Immunol, 2012. **13**(2): p. 121-8.
68. Germain, R.N. and I. Stefanova, *The dynamics of T cell receptor signaling: complex orchestration and the key roles of tempo and cooperation.* Annu Rev Immunol, 1999. **17**: p. 467-522.
69. Gagnon, S.J., et al., *T cell receptor recognition via cooperative conformational plasticity.* J Mol Biol, 2006. **363**(1): p. 228-43.
70. Huppa, J.B. and M.M. Davis, *T-cell-antigen recognition and the immunological synapse.* Nat Rev Immunol, 2003. **3**(12): p. 973-83.
71. Goodsell, D., *T-Cell Receptor.* PDB - Protein Data Bank 2005.

72. Sharpe, A.H., *Mechanisms of costimulation.* Immunol Rev, 2009. **229**(1): p. 5-11.
73. Croft, M., *The role of TNF superfamily members in T-cell function and diseases.* Nat Rev Immunol, 2009. **9**(4): p. 271-85.
74. DeBenedette, M.A., et al., *Role of 4-1BB ligand in costimulation of T lymphocyte growth and its upregulation on M12 B lymphomas by cAMP.* J Exp Med, 1995. **181**(3): p. 985-92.
75. Huse, M., *The T-cell-receptor signaling network.* J Cell Sci, 2009. **122**(Pt 9): p. 1269-73.
76. Kane, L.P., J. Lin, and A. Weiss, *Signal transduction by the TCR for antigen.* Curr Opin Immunol, 2000. **12**(3): p. 242-9.
77. Perkey, E. and I. Maillard, *New Insights into Graft-Versus-Host Disease and Graft Rejection.* Annu Rev Pathol, 2018. **13**: p. 219-245.
78. Archbold, J.K., et al., *T-cell allorecognition: a case of mistaken identity or deja vu?* Trends Immunol, 2008. **29**(5): p. 220-6.
79. Herrera, O.B., et al., *A novel pathway of alloantigen presentation by dendritic cells.* J Immunol, 2004. **173**(8): p. 4828-37.
80. Yewdell, J.W. and B.P. Dolan, *Immunology: Cross-dressers turn on T cells.* Nature, 2011. **471**(7340): p. 581-2.
81. Lin, C.M. and R.G. Gill, *Direct and indirect allograft recognition: pathways dictating graft rejection mechanisms.* Curr Opin Organ Transplant, 2016. **21**(1): p. 40-4.
82. Zakrzewski, J.L., M.R. van den Brink, and J.A. Hubbell, *Overcoming immunological barriers in regenerative medicine.* Nat Biotechnol, 2014. **32**(8): p. 786-94.
83. Bevan, M.J., *High determinant density may explain the phenomenon of alloreactivity.* Immunol Today, 1984. **5**(5): p. 128-30.
84. Matzinger, P. and M.J. Bevan, *Hypothesis: why do so many lymphocytes respond to major histocompatibility antigens?* Cell Immunol, 1977. **29**(1): p. 1-5.
85. Weber, D.A., et al., *Requirement for peptide in alloreactive CD4+ T cell recognition of class II MHC molecules.* J Immunol, 1995. **154**(10): p. 5153-64.
86. Whitelegg, A.M., et al., *Investigation of peptide involvement in T cell allorecognition using recombinant HLA class I multimers.* J Immunol, 2005. **175**(3): p. 1706-14.
87. Lombardi, G., et al., *The specificity of alloreactive T cells is determined by MHC polymorphisms which contact the T cell receptor and which influence peptide binding.* Int Immunol, 1991. **3**(8): p. 769-75.
88. Mount, N.M., et al., *Cell-based therapy technology classifications and translational challenges.* Philos Trans R Soc Lond B Biol Sci, 2015. **370**(1680): p. 20150017.
89. Thomas, E.D., et al., *Intravenous infusion of bone marrow in patients receiving radiation and chemotherapy.* N Engl J Med, 1957. **257**(11): p. 491-6.
90. Gratwohl, A., et al., *One million haemopoietic stem-cell transplants: a retrospective observational study.* Lancet Haematol, 2015. **2**(3): p. e91-100.
91. Passweg, J.R., et al., *Use of haploidentical stem cell transplantation continues to increase: the 2015 European Society for Blood and Marrow Transplant activity survey report.* Bone Marrow Transplant, 2017. **52**(6): p. 811-817.
92. Singh, A.K. and J.P. McGuirk, *Allogeneic Stem Cell Transplantation: A Historical and Scientific Overview.* Cancer Res, 2016. **76**(22): p. 6445-6451.
93. Tamari, R., et al., *CD34-Selected Hematopoietic Stem Cell Transplants Conditioned with Myeloablative Regimens and Antithymocyte Globulin for*

Advanced Myelodysplastic Syndrome: Limited Graft-versus-Host Disease without Increased Relapse. Biol Blood Marrow Transplant, 2015. **21**(12): p. 2106-2114.
94. Kekre, N. and J.H. Antin, *ATG in allogeneic stem cell transplantation: standard of care in 2017? Counterpoint.* Blood Adv, 2017. **1**(9): p. 573-576.
95. Kolb, H.J., et al., *Donor leukocyte transfusions for treatment of recurrent chronic myelogenous leukemia in marrow transplant patients.* Blood, 1990. **76**(12): p. 2462-5.
96. Feldman, S.A., et al., *Adoptive Cell Therapy--Tumor-Infiltrating Lymphocytes, T-Cell Receptors, and Chimeric Antigen Receptors.* Semin Oncol, 2015. **42**(4): p. 626-39.
97. Goff, S.L., et al., *Tumor infiltrating lymphocyte therapy for metastatic melanoma: analysis of tumors resected for TIL.* J Immunother, 2010. **33**(8): p. 840-7.
98. Morgan, R.A., et al., *Cancer regression in patients after transfer of genetically engineered lymphocytes.* Science, 2006. **314**(5796): p. 126-9.
99. Robbins, P.F., et al., *Tumor regression in patients with metastatic synovial cell sarcoma and melanoma using genetically engineered lymphocytes reactive with NY-ESO-1.* J Clin Oncol, 2011. **29**(7): p. 917-24.
100. Cameron, B.J., et al., *Identification of a Titin-derived HLA-A1-presented peptide as a cross-reactive target for engineered MAGE A3-directed T cells.* Sci Transl Med, 2013. **5**(197): p. 197ra103.
101. Yang, Y., E. Jacoby, and T.J. Fry, *Challenges and opportunities of allogeneic donor-derived CAR T cells.* Curr Opin Hematol, 2015. **22**(6): p. 509-515.
102. *First-Ever CAR T-cell Therapy Approved in U.S.* Cancer Discov, 2017. **7**(10): p. OF1.
103. Park, J.H., M.B. Geyer, and R.J. Brentjens, *CD19-targeted CAR T-cell therapeutics for hematologic malignancies: interpreting clinical outcomes to date.* Blood, 2016. **127**(26): p. 3312-20.
104. Rezvani, K., *Adoptive cell therapy using engineered natural killer cells.* Bone Marrow Transplant, 2019. **54**(Suppl 2): p. 785-788.
105. Wang, L., Z.Q. Zou, and K. Wang, *Clinical Relevance of HLA Gene Variants in HBV Infection.* J Immunol Res, 2016. **2016**: p. 9069375.
106. Gough, S.C. and M.J. Simmonds, *The HLA Region and Autoimmune Disease: Associations and Mechanisms of Action.* Curr Genomics, 2007. **8**(7): p. 453-65.
107. Filippone, E.J. and J.L. Farber, *Humoral immunity in renal transplantation: epitopes, Cw and DP, and complement-activating capability--an update.* Clin Transplant, 2015. **29**(4): p. 279-87.
108. Fleischhauer, K. and B.E. Shaw, *HLA-DP in unrelated hematopoietic cell transplantation revisited: challenges and opportunities.* Blood, 2017. **130**(9): p. 1089-1096.
109. Prentice, H.A., et al., *HLA class II genes modulate vaccine-induced antibody responses to affect HIV-1 acquisition.* Sci Transl Med, 2015. **7**(296): p. 296ra112.
110. Shin, D.H., et al., *HLA alleles, especially amino-acid signatures of HLA-DPB1, might contribute to the molecular pathogenesis of early-onset autoimmune thyroid disease.* PLoS One, 2019. **14**(5): p. e0216941.
111. Villadolid, J. and A. Amin, *Immune checkpoint inhibitors in clinical practice: update on management of immune-related toxicities.* Transl Lung Cancer Res, 2015. **4**(5): p. 560-75.
112. Chowell, D., et al., *Patient HLA class I genotype influences cancer response to checkpoint blockade immunotherapy.* Science, 2018. **359**(6375): p. 582-587.

113. Peng, M., et al., *Neoantigen vaccine: an emerging tumor immunotherapy.* Mol Cancer, 2019. **18**(1): p. 128.
114. Stein, R., et al., *CD74: a new candidate target for the immunotherapy of B-cell neoplasms.* Clin Cancer Res, 2007. **13**(18 Pt 2): p. 5556s-5563s.
115. Tiercy, J.M., *How to select the best available related or unrelated donor of hematopoietic stem cells?* Haematologica, 2016. **101**(6): p. 680-7.
116. Garderet, L., et al., *The umbilical cord blood alphabeta T-cell repertoire: characteristics of a polyclonal and naive but completely formed repertoire.* Blood, 1998. **91**(1): p. 340-6.
117. Ballen, K.K., et al., *Selection of optimal alternative graft source: mismatched unrelated donor, umbilical cord blood, or haploidentical transplant.* Blood, 2012. **119**(9): p. 1972-80.
118. Ruggeri, A., et al., *Post-transplant cyclophosphamide versus anti-thymocyte globulin as graft- versus-host disease prophylaxis in haploidentical transplant.* Haematologica, 2017. **102**(2): p. 401-410.
119. Fleischhauer, K., et al., *Peripheral blood stem cell allograft rejection mediated by CD4(+) T lymphocytes recognizing a single mismatch at HLA-DP beta 1*0901.* Blood, 2001. **98**(4): p. 1122-6.
120. Passweg, J.R., et al., *Hematopoietic stem cell transplantation in Europe 2014: more than 40 000 transplants annually.* Bone Marrow Transplant, 2016. **51**(6): p. 786-92.
121. Furst, D., et al., *High-resolution HLA matching in hematopoietic stem cell transplantation: a retrospective collaborative analysis.* Blood, 2013. **122**(18): p. 3220-9.
122. Lee, S.J., et al., *High-resolution donor-recipient HLA matching contributes to the success of unrelated donor marrow transplantation.* Blood, 2007. **110**(13): p. 4576-83.
123. Slatkin, M., *Linkage disequilibrium--understanding the evolutionary past and mapping the medical future.* Nat Rev Genet, 2008. **9**(6): p. 477-85.
124. Shaw, B.E., et al., *The degree of matching at HLA-DPB1 predicts for acute graft-versus-host disease and disease relapse following haematopoietic stem cell transplantation.* Bone Marrow Transplant, 2003. **31**(11): p. 1001-8.
125. Shaw, B.E., et al., *The importance of HLA-DPB1 in unrelated donor hematopoietic cell transplantation.* Blood, 2007. **110**(13): p. 4560-6.
126. Kaushansky, K.e., *Williams hematology*. Ninth edition. ed.
127. Chabannon, C., et al., *Hematopoietic stem cell transplantation in its 60s: A platform for cellular therapies.* Sci Transl Med, 2018. **10**(436).
128. Goulmy, E., et al., *A minor transplantation antigen detected by MHC-restricted cytotoxic T lymphocytes during graft-versus-host disease.* Nature, 1983. **302**(5904): p. 159-61.
129. Chao, N.J., *Minors come of age: Minor histocompatibility antigens and graft-versus-host disease.* Biol Blood Marrow Transplant, 2004. **10**(4): p. 215-23.
130. Zino, E., et al., *A T-cell epitope encoded by a subset of HLA-DPB1 alleles determines nonpermissive mismatches for hematologic stem cell transplantation.* Blood, 2004. **103**(4): p. 1417-24.
131. Fleischhauer, K., et al., *Effect of T-cell-epitope matching at HLA-DPB1 in recipients of unrelated-donor haemopoietic-cell transplantation: a retrospective study.* Lancet Oncol, 2012. **13**(4): p. 366-74.
132. Pidala, J., et al., *Nonpermissive HLA-DPB1 mismatch increases mortality after myeloablative unrelated allogeneic hematopoietic cell transplantation.* Blood, 2014. **124**(16): p. 2596-606.

133. Thomas, R., et al., *A novel variant marking HLA-DP expression levels predicts recovery from hepatitis B virus infection.* J Virol, 2012. **86**(12): p. 6979-85.
134. Petersdorf, E.W., et al., *MHC-resident variation affects risks after unrelated donor hematopoietic cell transplantation.* Sci Transl Med, 2012. **4**(144): p. 144ra101.
135. Petersdorf, E.W., et al., *High HLA-DP Expression and Graft-versus-Host Disease.* N Engl J Med, 2015. **373**(7): p. 599-609.
136. Fleischhauer, K., *Immunogenetics of HLA-DP--A New View of Permissible Mismatches.* N Engl J Med, 2015. **373**(7): p. 669-72.
137. Petersdorf, E.W., et al., *HLA-C expression levels define permissible mismatches in hematopoietic cell transplantation.* Blood, 2014. **124**(26): p. 3996-4003.
138. Elsner, H.A. and R. Blasczyk, *Sequence similarity matching: proposal of a structure-based rating system for bone marrow transplantation.* Eur J Immunogenet, 2002. **29**(3): p. 229-36.
139. Otten, H.G., et al., *Predicted indirectly recognizable HLA epitopes presented by HLA-DR correlate with the de novo development of donor-specific HLA IgG antibodies after kidney transplantation.* Hum Immunol, 2013. **74**(3): p. 290-6.
140. Duquesnoy, R.J., *HLAMatchmaker: a molecularly based algorithm for histocompatibility determination. I. Description of the algorithm.* Hum Immunol, 2002. **63**(5): p. 339-52.
141. Crivello, P., et al., *The impact of amino acid variability on alloreactivity defines a functional distance predictive of permissive HLA-DPB1 mismatches in hematopoietic stem cell transplantation.* Biol Blood Marrow Transplant, 2015. **21**(2): p. 233-41.
142. Elsner, H.A., et al., *HistoCheck: rating of HLA class I and II mismatches by an internet-based software tool.* Bone Marrow Transplant, 2004. **33**(2): p. 165-9.
143. Shaw, B.E., et al., *Scoring for HLA matching? A clinical test of HistoCheck.* Bone Marrow Transplant, 2004. **34**(4): p. 367-8; author reply 369.
144. Spellman, S., et al., *Scoring HLA class I mismatches by HistoCheck does not predict clinical outcome in unrelated hematopoietic stem cell transplantation.* Biol Blood Marrow Transplant, 2012. **18**(5): p. 739-46.
145. Huo, M.R., et al., *Predicted indirectly recognizable HLA epitopes are not associated with clinical outcomes after haploidentical hematopoietic stem cell transplantation.* Hum Immunol, 2018. **79**(2): p. 117-121.
146. Crivello, P., et al., *Functional distance between recipient and donor HLA-DPB1 determines nonpermissive mismatches in unrelated HCT.* Blood, 2016. **128**(1): p. 120-9.
147. Arrieta-Bolanos, E., et al., *In silico prediction of nonpermissive HLA-DPB1 mismatches in unrelated HCT by functional distance.* Blood Adv, 2018. **2**(14): p. 1773-1783.
148. Shieh, M., et al., *Computational assessment of miRNA binding to low and high expression HLA-DPB1 allelic sequences.* Hum Immunol, 2019. **80**(1): p. 53-61.
149. Morishima, S., et al., *Evolutionary basis of HLA-DPB1 alleles affects acute GVHD in unrelated donor stem cell transplantation.* Blood, 2018. **131**(7): p. 808-817.
150. Malki, M.M.A., et al., *Protective effect of HLA-DPB1 mismatch remains valid in reduced-intensity conditioning unrelated donor hematopoietic cell transplantation.* Bone Marrow Transplant, 2020. **55**(2): p. 409-418.
151. Rutten, C.E., et al., *HLA-DP as specific target for cellular immunotherapy in HLA class II-expressing B-cell leukemia.* Leukemia, 2008. **22**(7): p. 1387-94.

152. Laghmouchi, A., et al., *The allogeneic HLA-DP-restricted T-cell repertoire provoked by allogeneic dendritic cells contains T cells that show restricted recognition of hematopoietic cells including primary malignant cells.* Haematologica, 2019. **104**(1): p. 197-206.
153. Herr, W., et al., *HLA-DPB1 mismatch alleles represent powerful leukemia rejection antigens in CD4 T-cell immunotherapy after allogeneic stem-cell transplantation.* Leukemia, 2017. **31**(2): p. 434-445.
154. Nicholson, M.J., et al., *Small molecules that enhance the catalytic efficiency of HLA-DM.* J Immunol, 2006. **176**(7): p. 4208-20.
155. Illing, P.T., et al., *Immune self-reactivity triggered by drug-modified HLA-peptide repertoire.* Nature, 2012. **486**(7404): p. 554-8.
156. Crivello, P., et al., *Multiple Knockout of Classical HLA Class II beta-Chains by CRISPR/Cas9 Genome Editing Driven by a Single Guide RNA.* J Immunol, 2019. **202**(6): p. 1895-1903.
157. Rosenberg, S.A. and N.P. Restifo, *Adoptive cell transfer as personalized immunotherapy for human cancer.* Science, 2015. **348**(6230): p. 62-8.
158. Rapoport, A.P., et al., *NY-ESO-1-specific TCR-engineered T cells mediate sustained antigen-specific antitumor effects in myeloma.* Nat Med, 2015. **21**(8): p. 914-921.
159. Chornoguz, O., et al., *Major histocompatibility complex class II+ invariant chain negative breast cancer cells present unique peptides that activate tumor-specific T cells from breast cancer patients.* Mol Cell Proteomics, 2012. **11**(11): p. 1457-67.
160. Okada, Y., et al., *Construction of a population-specific HLA imputation reference panel and its application to Graves' disease risk in Japanese.* Nat Genet, 2015. **47**(7): p. 798-802.
161. Patsopoulos, N.A., et al., *Fine-mapping the genetic association of the major histocompatibility complex in multiple sclerosis: HLA and non-HLA effects.* PLoS Genet, 2013. **9**(11): p. e1003926.
162. van Lith, M., R.M. McEwen-Smith, and A.M. Benham, *HLA-DP, HLA-DQ, and HLA-DR have different requirements for invariant chain and HLA-DM.* J Biol Chem, 2010. **285**(52): p. 40800-8.
163. Kim, A. and S. Sadegh-Nasseri, *Determinants of immunodominance for CD4 T cells.* Curr Opin Immunol, 2015. **34**: p. 9-15.
164. Alvaro-Benito, M., et al., *Human leukocyte Antigen-DM polymorphisms in autoimmune diseases.* Open Biol, 2016. **6**(8).
165. Clement, C.C., et al., *The Dendritic Cell Major Histocompatibility Complex II (MHC II) Peptidome Derives from a Variety of Processing Pathways and Includes Peptides with a Broad Spectrum of HLA-DM Sensitivity.* J Biol Chem, 2016. **291**(11): p. 5576-95.
166. Welsh, R.A., et al., *Lack of the MHC class II chaperone H2-O causes susceptibility to autoimmune diseases.* PLoS Biol, 2020. **18**(2): p. e3000590.

9. Appendix

9.1. Abbreviations

A	
APC	Antigen presenting cell
C	
C	Constant
CAR	Chimeric antigen receptor
CD	Cluster of differentiation
CDR	Complementary determining region
CLIP	class II-associated Ii chain peptide
CRS	Cytokine release syndrome
CTL	Cytotoxic T lymphocytes
D	
D	Diversity
DLI	Donor-lymphocyte infusions
DNA-PK	DNA-dependent protein kinase
E	
ER	Endoplasmic reticulum
ERAP	Endoplasmic reticulum aminopeptidase
G	
G-CSF	Granulocyte-colony stimulating factor
GvHD	Graft versus host disease
GvL	Graft versus leukaemia
H	
HBV	Hepatitis B virus
HLA	Human leukocyte antigen
HSC	Haematopoietic stem cell
HSCT	Haematopoietic stem cell transplantation
HvG	Host versus graft
I	
IFN	Interferon
IHWs	International Histocompatibility Workshop
Ii	Invariant chain
IL	Interleukin
IS	Immunological synapse
J	
J	Joining
K	
kDa	Kilo Dalton
L	
LD	Linkage disequilibrium

M	
Mbp	Mega base pairs
mHAg	Minor histocompatibility antigens
MHC	Major histocompatibility complex
miRNA	MicroRNA
MIIC	MHC class II compartment
MMUD	Mismatched unrelated donors
N	
N	GC rich nucleotides
NA	Not applicable
NK	Natural killer
P	
P	Palindromic nucleotides
PLC	Peptide-loading complex
pMHC	Peptide/MHC complex
PT-Cy	Post-transplant cyclophosphamide (
R	
RAG	Recombination activating genes
RSS	Recombination signal sequence
T	
T_{CM}	Central memory T cells
T_{EM}	Effector memory T cells
T_H	T helper cells
T_N	Naïve T cells
T_{SCM}	T memory stem cell
TAP	Transporter associated with Antigen Processing
TCE	T cell epitope
TdT	Terminal deoxynucleotidyl transferase
TIL	Tumour-infiltrating lymphocyte
Tregs	Regulatory T cells
TCR	T-cell receptor
TNF	Tumour necrosis factor
U	
UTR	Untranslated region
V	
V	Variable

9.2. List of Figures

9.3. Danksagung

Zu Beginn möchte ich mich bei meiner Betreuerin Frau Prof. Dr. med. Katharina Fleischhauer bedanken für Ihre: intensive Betreuung, Ratschläge, Unterstützung, Wissensweitergabe, sowie für die vielen Weiterbildungsmöglichkeiten wie der Besuch von Konferenzen, Vorträgen und Workshops, die Sie immer befürwortet und ermöglicht haben und die meinen Wissenshorizont erweitert haben.

Des Weiteren gilt mein Dank meiner weiteren Gutachtern Prof. Dr. med. Monika Lindemann und Prof. Dr. med. Johannes Schetelig, denn es kostet nicht nur viel Zeit die Dissertation anzufertigen, sondern auch kostbare Zeit sie zu lesen und zu begutachten.

Mein weiterer Dank gilt Prof. Dr. med. Beelen, Prof. Dr. med. Horn und all den Studienteilnehmern der KMT, sowie den Blutspendern der Transfusionsmedizin, ohne die meine Experimente nicht möglich gewesen wären.

Nicht zu vergessen, schulde ich meinen Dank meiner Arbeitsgruppe, in der TEAMWORK immer großgeschrieben wird. Ich danke euch Allen für die tolle Zusammenarbeit. Danke an Frau Stempelmann und Frau Stratmann für die großartige Einarbeitungszeit, die mir den Einstieg leichtgemacht hat und Ihr umfangreiches Wissen als langjährige Mitarbeiterinnen des Universitätsklinikums. Ein "*mille grazie"* geht an meinen Betreuer Herrn Dr. Pietro Crivello für sein umfangreiches Wissen, seine Geduld und Hilfsbereitschaft in jeder Lage, wenn's mal wieder nicht klappt mit der PCR oder keine Kolonien auf der Agarplatte zu sehen waren und man am Rande der Verzweiflung stand. Danke an Joana, Luisa, Fabienne, Sophia und den ehemaligen Kollegen Müberra und Maximilian Frederik für die immer harmonische Atmosphäre, die motivierende Zusprache, euer Verständnis und eure Unterstützung in zahlreichen „Monster" Experimenten, die ohne euch nicht machbar gewesen wären.

Ein besonderer Dank gilt ausdrücklich meinen Eltern, Beate Meurer und Dieter Zöllner-Meurer, für all eure Unterstützung, motivierenden Worte, euren Rückhalt und für die vielen „Du schaffst das"! Ebenso gilt mein Dank meiner besten Freundin, meiner Schwester im Herzen Julia Meyer: Ich danke dir für deine ewige Freundschaft, die keine Grenzen kennt, für dein für mich Dasein in jeder Lebenslage! Das Beste kommt bekanntlicherweise zum Schluss: ¡muchísimas gracias! - A mi novio Esteban no solo por tu extenso conocimiento, sino también por tu paciencia, tu fe en mí y tu palabras motivacionales en momentos diffíciles, tu apoyo mental y tu amor.

9.4. Curriculum vitae

“Der Lebenslauf ist in der Online-Version aus Gründen des Datenschutzes nicht enthalten.“

“Der Lebenslauf ist in der Online-Version aus Gründen des Datenschutzes nicht enthalten.“

9.5. Stellungnahmen

Bestätigung Eigenanteil an Publikationen

Hiermit bestätige ich die Darstellung zu den Anteilen von Frau Thuja Meurer an Konzeption, Durchführung und Abfassung jeder Publikation (Chapter 6 – Articles) gemäß der Promotionsordnung der Fakultät für Biologie zur Erlangung des Doktorgrades Dr. rer. nat.

Essen, den 09.04.2020 ……

Prof. Dr. Katharina Fleischhauer

Erklärung Urheberrechte der Publikationen

Hiermit erkläre ich, Thuja Meurer, dass ich mit der Veröffentlichung der Publikationen (Chapter 6 – Articles) im Rahmen dieser Dissertation keine Urheberrechte verletze.

Essen, den 09.04.2020 ……

Thuja Meurer

9.6. Eidesstattliche Erklärung

Hiermit erkläre ich, gem. § 6 Abs. (2) g) der Promotionsordnung der Fakultät für Biologie zur Erlangung der Dr. rer. nat., dass ich das Arbeitsgebiet, dem das Thema **„Modulation of T-cell alloreactivity by molecular and biochemical effects of HLA-DPB1 in haematopoietic stem cell transplantation“** zuzuordnen ist, in Forschung und Lehre vertrete und den Antrag von **Thuja Meurer** befürworte und die Betreuung auch im Falle eines Weggangs, wenn nicht wichtige Gründe dem entgegenstehen, weiterführen werde.

Essen, den 09.04.2020 Katharina Fleischhauer ……

Prof. Dr. Katharina Fleischhauer

Hiermit erkläre ich, gem. § 7 Abs. (2) d) + f) der Promotionsordnung der Fakultät für Biologie zur Erlangung des Dr. rer. nat., dass ich die vorliegende Dissertation selbstständig verfasst und für mich keiner anderen als der angegebenen Hilfsmittel bedient, bei der Abfassung der Dissertation nur die angegebenen Hilfsmittel benutzt und alle wörtlich oder inhaltlich übernommenen Stellen als solche gekennzeichnet habe.

Essen, den 09.04.2020 ……

Thuja Meurer

Hiermit erkläre ich, gem. § 7 Abs. (2) e) + g) der Promotionsordnung der Fakultät für Biologie zur Erlangung des Dr. rer. nat., dass ich keine anderen Promotionen bzw. Promotionsversuche in der Vergangenheit durchgeführt habe und dass diese Arbeit von keiner anderen Fakultät/Fachbereich abgelehnt worden ist.

Essen, den 09.04.2020 ……

Thuja Meurer